

**AN INVESTIGATION INTO THE ROLE OF
RECEPTOR TYROSINE KINASES IN CHILDHOOD
ACUTE LYMPHOBLASTIC LEUKAEMIA**

by

Shaun Robert Wilson

**A thesis submitted to
The University of Birmingham
for the Degree of
DOCTOR OF PHILOSOPHY**

**School of Cancer Sciences
University of Birmingham**

July 2013

Abstract

Deregulation of tyrosine kinases has been implicated in Philadelphia chromosome negative Acute Lymphoblastic Leukaemia (ALL) with a higher risk of relapse. The studies in this thesis sought to identify potential receptor tyrosine kinase targets and to explore the use of tyrosine kinase inhibitors (TKIs) in childhood ALL.

Initial work describes the baseline receptor tyrosine kinase profiles of 18 primary ALLs. Alterations in the phosphorylation signals of Axl, EphA2, EphB2, FGFR2, FLT3, Mer and PDGFR β were identified and associated with clinical and biological features.

Subsequently, 5 ALL cell lines and a panel of 20 primary samples representative of common biological features were screened for sensitivity to a library of TKIs. Significant heterogeneity in sensitivity was observed in the panel of leukaemia cells. No correlation was evident between response to TKIs and current clinical or biological stratification parameters in the primary cell panel.

Two candidate inhibitors, dovitinib and foretinib, were taken forward for further preclinical work. Potent nanomolar activity was demonstrated in cell lines and primary ALL. The combination of dovitinib or foretinib with conventional cytotoxics demonstrated significant synergy and sensitised steroid – resistant cell lines to dexamethasone. Objective responses were not identified to single agent TKI therapy in a murine primagraft model.

Acknowledgements

I would like to thank my supervisors, Professor Pamela Kearns, Professor Tatjana Stankovic and Dr Victoria Weston for their patience, understanding and expertise. Thank you for helping me realise oncology is more than tilted heads.

To my darling wife and my beautiful book – end children, thank you putting up with my anxieties, late nights, missed parties and moving around the country to indulge my obsession with childhood cancer.

Finally, I would like to thank Leukaemia and Lymphoma Research for funding the research.

1 Acute Lymphocytic Leukaemia of Childhood

| | |
|---|---|
| 1.1 Incidence and prevalence of childhood malignancies | 1 |
| 1.2 Presentation, investigation and diagnosis of childhood ALL | 1 |
| 1.2.1 Presentation | 1 |
| 1.2.2 Diagnostic investigations | 2 |
| 1.3 Risk assessment of ALL and prognostic implications | 4 |
| 1.3.1 Age and white cell count | 4 |
| 1.3.2 Recurrent cytogenetic abnormalities and translocations | 5 |
| 1.3.2.1 Philadelphia chromosome – positive t(9;22)(q23;q11) | 6 |
| 1.3.2.2 <i>ETV6</i> – <i>RUNX 1</i> t(12;21) | 6 |
| 1.3.2.3 <i>E2A</i> – <i>PBX</i> t(1;19) | 6 |
| 1.3.2.4 Mixed Lineage Leukemia (<i>MLL</i>) gene rearrangements | 7 |
| 1.3.2.5 Intrachromosomal amplification of chromosome 21 (iAMP21) | 7 |
| 1.3.3 DNA context | 8 |
| 1.3.3.1 Hyperdiploid | 8 |
| 1.3.3.2 Hypodiploidy | 8 |
| 1.4 Response to treatment | 8 |
| 1.4.1 Assessment of early morphological response | 8 |
| 1.4.2 Assessment of sub – microscopic disease | 9 |
| 1.4.3 Assessment of antigen – receptor gene rearrangements | 9 |

| | | |
|--------|--|----|
| 1.4.4 | Flow cytometry assessment of MRD | 10 |
| 1.5 | Current treatment strategies | 11 |
| 1.6 | Relapsed/Refractory ALL | 13 |
| 1.7 | Signal transduction pathways associated with chemoresistance | 14 |
| 1.7.1 | PI3K/Akt/mTOR Pathway | 14 |
| 1.7.2 | Ras/Raf/MAPK | 15 |
| 1.8 | Role of Receptor Tyrosine Kinases (RTK) in malignancies | 16 |
| 1.8.1 | Classification and structure of Tyrosine Kinases | 16 |
| 1.8.2 | Activation of RTK | 18 |
| 1.9 | Negative regulation of the RTK | 22 |
| 1.9.1 | Protein tyrosine Phosphatases | 22 |
| 1.9.2 | Ubiquitination | 22 |
| 1.10 | Role of TK in B – cell physiology | 23 |
| 1.10.1 | Tyrosine kinases in normal B – cell development | 23 |
| 1.10.2 | RTK in B – cell development | 23 |
| 1.11 | RTK deregulation in cancer | 24 |
| 1.11.1 | Epidermal Growth Factor (EGFR) | 25 |
| 1.11.2 | Insulin Growth Factor – 1 receptor (IGF-1R) | 25 |
| 1.11.3 | Anaplastic lymphoma kinase (ALK) | 25 |
| 1.12 | Review of involvement of Tyrosine Kinases in ALL | 26 |

| | |
|--|----|
| 1.12.1 Philadelphia positive ALL | 26 |
| 1.12.2 CLRF2/JAK in Down Syndrome and High Risk ALL | 26 |
| 1.12.3 Fms – like tyrosine kinase 3 (FLT3) | 27 |
| 1.12.4 Mer in childhood ALL | 28 |
| 1.12.5 Tropomyosin – receptor kinase (Trk) in ALL | 29 |
| 1.12.6 c – Met/Hepatocyte Growth Factor Receptor in leukaemia | 30 |
| 1.12.7 Novel chimeric tyrosine kinase – containing oncogenes | 30 |
| 1.13 Discovery of targets and novel agents for the treatment in cancer | 31 |
| 1.13.1 Rationale for molecular targeted therapy | 31 |
| 1.13.2 Small molecule tyrosine kinase inhibitors | 31 |
| 1.14 Role of TKI in paediatric ALL | 33 |
| 1.15 Aims of study | 34 |

2 Materials and Methods

| | |
|--|----|
| 2.1 Cell culture | 35 |
| 2.1.1 ALL primary samples | 35 |
| 2.1.2 Separation of mononuclear cells from bone marrow | 35 |
| 2.1.3 Maintenance of cell lines | 35 |
| 2.1.4 Recovery of cryopreserved cells | 36 |
| 2.1.5 Cell counting | 37 |

| | | |
|--------|--|----|
| 2.1.6 | Characteristics of primary ALL samples | 38 |
| 2.2 | Cell lysis and protein extraction | 39 |
| 2.3 | Protein determination/quantification | 40 |
| 2.4 | Sodium dodecyl sulphate polyacrylamide gel electrophoresis | 41 |
| 2.5 | Protein transfer | 41 |
| 2.6 | Western blotting with antibodies | 42 |
| 2.7 | Model for assessing apoptosis response to IR – induced damage | 43 |
| 2.8 | Assessment of phospho – tyrosine kinase status by array systems | 44 |
| 2.8.1 | Principle of phospho – tyrosine kinase array kits | 44 |
| 2.8.2 | Protocol for preparation of phospho – array membranes | 46 |
| 2.9 | Treatment of cells with Tyrosine Kinase Inhibitors (TKIs) and cytotoxics | 47 |
| 2.10 | Cell viability assays | 49 |
| 2.10.1 | Promega CellTiter-Glo® luminescence ATP – based viability assay | 49 |
| 2.10.2 | Assessment of activity of TKIs, cytotoxics and combination therapy | 49 |
| 2.10.3 | Interaction of TKI and conventional cytotoxic combination therapy | 50 |
| 2.11 | Cell cycle profiling with Propidium Iodide (PI) | 51 |
| 2.12 | Assessment of apoptosis | 51 |
| 2.12.1 | Assess of Apoptosis by DNA fragmentation | 51 |
| 2.12.2 | Assessment of Annexin V – PI staining by flow cytometry | 52 |
| 2.13 | Immunofluorescence staining | 53 |

| | | |
|--------|--|----|
| 2.14 | Confirmation of polypoidy by DAPI staining | 54 |
| 2.15 | Nucleic acid work | 54 |
| 2.15.1 | Primer design for Real Time Quantitative Polymerase Chain Reaction | 54 |
| 2.15.2 | Purification of RNA | 55 |
| 2.15.3 | Synthesis of complementary DNA (cDNA) | 55 |
| 2.15.4 | FAST SYBR® Green Real time quantitative PCR of cDNA | 55 |
| 2.15.5 | Agarose gel electrophoresis of PCR products | 56 |
| 2.15.6 | Gel extraction and purification | 56 |
| 2.15.7 | Sequencing of primer products to confirm target | 58 |
| 2.16 | Xenograft model methods | 58 |
| 2.16.1 | Analysis of engraftment patterns of leukaemic populations | 58 |
| 2.16.2 | Primagraft model | 59 |
| 2.16.3 | Preparation and treatment protocols of TKIs for primagraft experiments | 60 |
| 2.16.4 | Taqman molecular analysis of VDJ rearrangement | 61 |
| 2.17 | Statistical analysis | 61 |
| 2.17.1 | Analysis of groups | 61 |
| 2.17.2 | Survival comparison | 61 |

3 Baseline phosphorylation tyrosine kinase profiles of Childhood ALL

| | |
|--|------------|
| 3.1 Introduction | 62 |
| 3.2 Stratification of primary ALL samples with clinical, genetic features and response to apoptotic induction by IR – induced apoptosis | 65 |
| 3.3 Evaluation of Phospho – RTK arrays with human cell lines | 68 |
| 3.3.1 Raybio® Human RTK array | 68 |
| 3.3.2 R&D Systems® Proteome Profiler™ Human Phospho-RTK array | 70 |
| 3.4 Screening of primary ALL cells for baseline phosphorylation profiles with Phospho – RTK arrays | 72 |
| 3.4.1 Baseline phosphorylation profiles of 8 leukaemias with Raybiotech | 73 |
| 3.4.2 Baseline phosphorylation profiles of 18 leukaemias with R&D array | 75 |
| 3.4.3 Baseline phosphorylation of 6 samples analysed on both arrays | 77 |
| 3.5 Association of apoptotic phenotype with baseline phosphorylation signal | 78 |
| 3.6 Association of cytogenetic groups with RTK phosphorylation profiles | 85 |
| 3.7 Association of NCI/Rome risk criteria with RTK phosphorylation profiles | 92 |
| 3.8 Association of blast clearance and MRD status with RTK profiles | 96 |
| 3.9 Discussion | 102 |

4 Screening of cell line panel and primary ALL cells with library of RTK inhibitors

| | |
|---|------------|
| 4.1 Introduction | 107 |
| 4.2 Generation and optimisation of RTK library screen assay | 108 |
| 4.3 Proof of principle of TKI screen in a primary Acute Myeloid Leukaemia | 113 |
| 4.4 Screen of B – precursor ALL cell lines with expanded TKI library | 114 |
| 4.4.1 Characteristics of ALL cell line panel for TKI library screen | 116 |
| 4.4.2 Sensitivity of cell lines to TKIs at 1 μ M and 10 μ M | 117 |
| 4.4.3 Sensitivity of cell lines to TKIs with activity in all cell lines at 10 μ M | 121 |
| 4.4.4 Sensitivity of cell lines with defective apoptotic responses to IR – induced DNA damage to TKIs | 124 |
| 4.4.5 TKI sensitivity in Philadelphia positive cell lines | 128 |
| 4.5 RT q-PCR analysis of expression of putative targets of active TKIs | 130 |
| 4.6 Screen of primary B – precursor ALL cohort with expanded TKI library | 134 |
| 4.6.1 Sensitivity of primary ALLs to TKIs at 1 μ M and 10 μ M | 136 |
| 4.6.2 Resistance of primary ALLs to TKI at 1 μ M and 10 μ M | 143 |
| 4.6.3 Comparison of putative targets of most and least active TKIs in primary ALLs | 145 |
| 4.6.4 Sensitivity of primary ALLs to TKIs with activity at 10 μ M alone | 146 |
| 4.6.5 Association of clinical features of ALLs sensitive to TKI | 147 |
| 4.6.5.1 Association of MRD status with proportion of ALLs sensitive to TKIs | 147 |
| 4.6.5.2 Association of cytogenetic findings with sensitivity to TKIs | 148 |
| 4.6.5.3 Association with NCI/Rome criteria with TKI sensitivity | 150 |
| 4.7 Discussion | 152 |

5 Preclinical investigations of the multikinase inhibitors, foretinib and dovitinib

| | |
|--|-----|
| 5.1 Introduction | 159 |
| 5.2 Assessment of responses of ALL cell lines and primary cells to TKIs | 160 |
| 5.2.1 Foretinib dose response assessment in cell lines | 161 |
| 5.2.2 Dovitinib dose response assessment in cell lines | 162 |
| 5.2.3 TKI responses in ALL primary cells (ALL – 20) | 163 |
| 5.3 Effects of TKIs on cell cycle profiles of ALL cell lines | 165 |
| 5.3.1 Effects of foretinib on cell cycle profiles | 165 |
| 5.3.1.1 Emergent population in Nalm 6 and TOM - 1 confirms polyploidy | 172 |
| 5.3.2 Effects of dovitinib on cell cycle profiles | 173 |
| 5.4 Characterisation of changes in cyclin B1 after foretinib – treatment | 177 |
| 5.5 Accumulation of p53 is not due to foretinib – induced DNA damage | 180 |
| 5.6 Foretinib inhibits the pro-survival Akt pathway | 184 |
| 5.7 TKIs mediate anti – leukaemic effect via apoptosis | 185 |
| 5.7.1 Foretinib induces apoptosis in cell lines | 185 |
| 5.7.2 Dovitinib induces apoptosis in SupB15 t(9;22) cell line | 187 |
| 5.8 TKIs demonstrate synergy in combination with chemotherapy | 187 |
| 5.8.1 Foretinib combinations with cytotoxics demonstrate synergy | 188 |
| 5.8.1.1 Foretinib in combination with dexamethasone | 190 |
| 5.8.1.2 Foretinib in combination the anti – metabolites | 193 |
| 5.8.1.3 Foretinib in combination with DNA – damaging agents | 199 |
| 5.8.1.4 Foretinib in combination with vincristine | 202 |
| 5.8.2 Assessment of combination of foretinib and cytotoxics in ALL – 20 | 204 |
| 5.8.3 Dovitinib combinations with cytotoxics demonstrate synergy | 206 |
| 5.8.4 Steroid sensitisation induced by foretinib in REH cell line | 209 |
| is not due to apoptosis | |
| 5.9 Assessment of <i>in vivo</i> efficacy of TKIs in primagraft model | 211 |

| | |
|--|-----|
| 5.9.1 Engraftment kinetic experiments for ALL – 20 | 211 |
| 5.9.2 Assessment of <i>in vivo</i> efficacy of foretinib | 217 |
| 5.9.3 Assessment of <i>in vivo</i> efficacy of dovitinib | 221 |
| 5.10 Discussion | 225 |

6 Conclusions and future work

| | |
|---|-----|
| 6.1 Validation of phosphorylated RTK identified by phospho – RTK arrays | 235 |
| 6.2 Genomic characterisation of primaries at baseline and in response to TKIs | 235 |
| 6.3 Identification of protein targets: Target Deconvolution | 236 |
| 6.4 Xenograft Modelling | 238 |
| 6.4.1 Identification of dexamethasone – resistant primary sample | 238 |
| 6.4.2 Combination of dexamethasone and foretinib/dovitinib in dexamethasone – resistant murine model | 239 |

| | |
|--------------|-----|
| 7 References | 240 |
|--------------|-----|

8 Appendices

| | |
|--|-----|
| 8.1 American Society of Hematologists (ASH) Annual Meeting Blood 2011; 118: Abstract 1509 | 289 |
| 8.2 International Society of Paediatric Oncologists (SIOP) Annual Meeting Pediatric Blood Cancer 2012; 59(6): Abstract O136 | 291 |

FIGURES LIST

| | |
|--|----|
| 1.1 B – cell precursor ALL mirrors B – cell development | 3 |
| 1.2 Representation of Epidermal Growth Factor Receptor | 17 |
| 1.3 Classification of the 20 families of RTK | 18 |
| 1.4 Activation of EGFR monomers by binding of EGF – ligand | 19 |
| | |
| 2.1 Coordinates of kinase antibodies RayBio® Human RTK Array | 44 |
| 2.2 Coordinates of kinase antibodies R&D Human Phospho – RTK Array | 45 |
| | |
| 3.1 Representative apoptotic phenotypes in response to 5Gy IR | 66 |
| 3.2 Phosphorylation signal of (R)TKs in ALL cell lines (Raybiotech array) | 69 |
| 3.3 Differential phosphorylation signal of IGF – 1R in ALL cell lines | 70 |
| 3.4 R&D Phospho – RTK arrays hybridised to lysates from HB2 cell line | 71 |
| 3.5 Validation of Phospho – RTK findings in HB2 cell line | 72 |
| 3.6 Restricted repertoire of (R)TKs identified with Raybiotech array | 74 |
| 3.7 Heterogeneous repertoire of RTKs identified with R&D array | 76 |
| 3.8 Comparison of Axl and FGFR2 derived from different array systems | 77 |
| 3.9 Representative Raybiotech arrays of different apoptotic phenotypes | 79 |
| 3.10 Increased Axl and Txk signals are associated with apoptosis proficient leukaemias assayed on Raybiotech arrays | 80 |
| 3.11 Comparison of RTK signal intensity by apoptotic phenotype (R&D) | 81 |
| 3.12 Phosphorylation signals of ALL cytogenetic subgroup assayed by Raybiotech arrays | 84 |
| 3.13 Comparison of RTK phosphorylation by cytogenetic subgroups (R&D) | 86 |
| 3.14 Comparison of phosphorylation for EphA2 by cytogenetic subgroup | 90 |
| 3.15 Comparison of signals for FLT3 by cytogenetic subtypes | 91 |
| 3.16 Comparison of signals for EphB2 by cytogenetic subtypes | 92 |
| 3.17 JAK2 phosphorylation is associated with low WCC at presentation | 93 |

| | |
|--|-----|
| 3.18 Association of NCI/Rome WCC criteria with RTK phosphorylation | 94 |
| 3.19 Phosphorylation of FGFR2 and Mer correlate with adverse WCC | 94 |
| 3.20 Association of NCI/Rome age criteria with RTK phosphorylation | 95 |
| 3.21 Increased Axl and JAK2 phosphorylation present in leukaemias with positive molecular MRD status in Raybiotech arrays | 96 |
| 3.22 Association of blast clearance with individual RTK signals(R&D array) | 97 |
| 3.23 Association of molecular MRD status with RTK signals (R&D array) | 98 |
| 3.24 PDGFR β signal associates with flow MRD (R&D array) | 101 |
| | |
| 4.1 Incubation of Kasumi – 1 cell line with Kit – inhibitors | 109 |
| 4.2 Selective response to Kit – inclusive inhibitors in Kasumi – 1 | 111 |
| 4.3 Relative luminescence of ALL-36 by cell density and culture media | 112 |
| 4.4 Activity of TKIs against AML – 2 at 1 and 10 μ M | 114 |
| 4.5 Summary of response of cell lines to individual TKIs | 119 |
| 4.6 Common putative targets of bosutinib, CEP-701, dovitinib, and foretinib | 120 |
| 4.7. TKIs which induced cell death in all 5 cell lines at 10 μ M | 122 |
| 4.8 Comparison of possible targets of TKIs with activity at 10 μ M and those with no activity at 10 μ M in cell lines | 123 |
| 4.9 Response to quinazoline inhibitors by apoptotic defective cell lines | 125 |
| 4.10 Nanomolar activity of BIBW – 2992 and CI – 1033 limited to apoptotic defective cell lines | 127 |
| 4.11 Dose dependent reduction in cell viability with 10 μ M treatment | 139 |
| 4.12 Comparison of possible targets of TKIs with activity at 1 μ M to those with no significant activity at 10 μ M in primary ALL samples | 145 |
| 4.13 Comparison of possible targets of TKIs with activity only at 10 μ M to those with no significant activity at 10 μ M in primary ALL samples | 147 |
| | |
| 5.1 Dose response curves of cell lines against foretinib | 162 |
| 5.2 Dose response curves of cell lines against dovitinib | 163 |

| | |
|---|-----|
| 5.3 Dose response curves for DMSO, dovitinib and foretinib in ALL – 20 | 164 |
| 5.4 Foretinib induces alterations in cell cycle profile of the REH t(12;21) | 166 |
| 5.5 Foretinib induces alterations in cell cycle profile of SupB15 t(9;22) | 167 |
| 5.6 Foretinib induces alterations in cell cycle profile of SD – 1 t(9;22) | 168 |
| 5.7 Foretinib reduces G1 and S – phase of Nalm 17 cell line | 168 |
| 5.8 Foretinib induced alterations in cell cycle profile of TOM – 1 t(9;22) | 169 |
| 5.9 Foretinib induced alterations in cell cycle profile of Nalm 6 t(5;12) | 170 |
| 5.10 Foretinib (5µM) impacts differently on the Nalm 6 and TOM – 1 | 171 |
| 5.11 Foretinib alters nuclear size and aggregation in Nalm 6 and TOM-1 | 173 |
| 5.12 Dovitinib induced alterations in cell cycle profile of Nalm 17 and REH | 174 |
| 5.13 Dovitinib induced alterations in cell cycle profile SD -1 and SupB15 | 175 |
| 5.14 Dovitinib induced alterations in cell cycle profile Nalm 6 and TOM – 1 | 176 |
| 5.15 Dovitinib does not induce polyploidy in Nalm 6 or TOM – 1 | 177 |
| 5.16 Foretinib reduces cyclin B1 and induces p53 accumulation in cell lines | 178 |
| 5.17 Foretinib 1µM induces the variable responses in cyclin B1 and p53 | 179 |
| 5.18 Foretinib 1µM induces cyclinB1 in Nalm6 and TOM -1. | 179 |
| 5.19 Foretinib treatment induces p21 in REH and SupB15 | 180 |
| 5.20 Foretinib does not induce accumulation of γH2AX foci | 182 |
| 5.21 2Gy IR induces alterations in γH2AX foci but not foretinib | 183 |
| 5.22 Foretinib reduces p – Akt status in Nalm 17 and REH | 184 |
| 5.23 Foretinib – induced DNA fragmentation in SD -1 and SupB15 | 185 |
| 5.24 Foretinib induced PARP – 1 in pre – B ALL cell lines | 186 |
| 5.25 Dovitinib dose course in the SupB15 t(9;22) cell line | 187 |
| 5.26 Dose finding response curves for foretinib | 189 |
| 5.27 Foretinib sensitises the steroid – resistant cell lines to dexamethasone | 192 |
| 5.28 Combination of foretinib with anti – metabolites in SD – 1 | 196 |
| 5.29 Combination of foretinib and cytarabine demonstrates variable responses in the REH cell line. | 197 |
| 5.30 Combination of foretinib and anti – metabolite combination in TOM -1 | 198 |

| | |
|---|---------|
| 5.31 Combination of foretinib and DNA – damaging agents | 200 |
| 5.32 Combination of foretinib with vincristine demonstrates synergy | 203 |
| 5.33 Methotrexate resistance in ALL -20 is abrogated by foretinib | 204 |
| 5.34 Dovitinib sensitises steroid – resistant cell lines to dexamethasone | 208 |
| 5.35 Foretinib and dexamethasone in REH does not potentiate apoptosis | 210 |
| 5.36 Immunophenotype of ALL – 20 cells with the fluorochrome panel | 213 |
| 5.37 Initial engraftment kinetics of ALL – 20 | 214 |
| 5.38 Xenograft demonstrates the hepatotropic nature of ALL – 20 | 216 |
| 5.39 Stability of VDJ rearrangements in ALL – 20 xenograft | 216 |
| 5.40 Peripheral engraftment of hCD45 cells for foretinib in 2 mouse cohorts | 218 |
| 5.41 Kaplan – Meier curve for foretinib cohorts | 219 |
| 5.42 Peripheral engraftment of hCD45 cells for dovitinib in 2 mouse cohorts | 221 |
| 5.43 Kaplan – Meier curve for dovitinib cohorts | 222 |
| 5.44 Dovitinib reduces splenic infiltration in primagraft model | 223 |
| 5.45 FACS analysis of organs at terminal cull for dovitinib | 224 |
| 6.1 Changes in phosphorylation are identified in response to foretinib | 236 |

TABLES LIST

| | |
|---|------------|
| 1.1 List of antigens to identify acute leukaemias | 3 |
| 1.2 Impact of genetic abnormalities on overall survival | 5 |
| 1.3 Summary of results of Cooperative trials | 13 |
| 1.4 Mechanisms of RTK dysregulation in malignancies | 24 |
| | |
| 2.1 Summary of cell lines | 36 |
| 2.2 Clinical features of primary ALLs for phospho – RTK arrays | 38 |
| 2.3 Clinical features of primary Acute Leukaemias for TKI screen | 39 |
| 2.4 List of antibodies | 43 |
| 2.5 Similarities and differences between array systems | 46 |
| 2.6 List of tyrosine kinase inhibitors (TKIs) | 48 |
| 2.7 Symbols for description of Combination Studies | 51 |
| 2.8 List of Primers | 57 |
| 2.9 List of fluorochrome – conjugated antibodies | 60 |
| | |
| 3.1 RTK antibodies imprinted on the membrane arrays for each system | 64 |
| 3.2 Clinical features of primary ALLs | 67 |
| 3.3 Comparison of Axl and FGFR2 signals derived from 2 arrays | 77 |
| 3.4 Mean RTK signals in apoptosis proficient and defective primary ALLs | 82 |
| 3.5 Comparison of cytogenetic groupings in 8 ALLs assayed with Raybiotech | 85 |
| 3.6 Comparison of RTK phosphorylation signals in 3 cytogenetic groups | 87 |
| 3.7 Analysis comparing individual cytogenetic groups to the remaining leukaemias | 88 |
| 3.8 Comparison of EphA2 phosphorylated leukaemias | 90 |
| 3.9 Association of blast clearance and MRD status with RTK profiles | 99 |
| 3.10 Association of flow MRD status with RTK profiles | 100 |

| | |
|--|-----|
| 4.1 TKI library with putative targets | 115 |
| 4.2 Characteristics of B – cell precursor ALL cell lines | 116 |
| 4.3 TKIs which demonstrated activity at 1 μ M in cell lines | 118 |
| 4.4 TKIs which demonstrated activity in Ph+ ALL cell lines | 128 |
| 4.5 Transcript levels for RTKs expressed in cell lines | 131 |
| 4.6 Clinical features for primary ALL panel for TKI screen | 135 |
| 4.7a Responses of primary ALLs to TKI panel at 1 μ M | 137 |
| 4.7b Responses of primary ALLs to TKI panel at 1 μ M | 138 |
| 4.8 TKIs which demonstrated activity in primary ALLs at 1 μ M | 140 |
| 4.9 Association of TKI responses to clinical features of primary ALL | 142 |
| 4.10 TKIs which did not induce reduction in cell viability at 10 μ M | 143 |
| 4.11 Association of MRD status with response to TKIs | 148 |
| 4.12 Association of cytogenetic with response to TKIs | 149 |
| 4.13 Association of NCI/Rome age criteria with response to TKIs | 150 |
| 4.14 Association of NCI/Rome WCC criteria with response to TKIs | 151 |
| 5.1 Kinase targets of foretinib and dovitinib | 160 |
| 5.2 Increased γ H2AX foci were induced by IR but not foretinib | 183 |
| 5.3 Combination Indices for foretinib and dexamethasone | 191 |
| 5.4a Combination Indices for foretinib and the anti – metabolites | 194 |
| 5.4b Combination Indices for foretinib and the anti – metabolites | 195 |
| 5.5 Combination Indices for foretinib and DNA – damaging agents | 201 |
| 5.6 Combination Indices for foretinib and vincristine | 202 |
| 5.7 Combination Indices for foretinib and cytotoxics in ALL – 20 | 205 |
| 5.8a Combination Indices for dovitinib and cytotoxics | 206 |
| 5.8b Combination Indices for dovitinib and cytotoxics | 207 |
| 5.9 Assessment of apoptotic cells in response to steroid, TKI or combination | 211 |
| 5.10 Kinetics of engraftment of murine blood and organs for ALL – 20 | 215 |
| 5.11 Percentage of engraftment in response to DMSO or foretinib | 219 |
| 5.12 Percentage of engraftment in response to DMSO or dovitinib | 223 |

LIST OF ABBREVIATIONS

| | |
|----------------|---|
| μM | Micromolar |
| Abl | Abelson murine leukemia viral oncogene homolog 1 |
| ALK | anaplastic lymphoma kinase |
| ALL | Acute Lymphoblastic Leukemia |
| AML | Acute Myeloid Leukaemia |
| Bcr | breakpoint cluster region protein |
| Bcr/Abl | Breakpoint cluster region - Abelson oncoprotein |
| BFM | Berlin Frankfurt Munster |
| BME | β-mercaptoethanol |
| BSA | bovine serum albumin |
| CCG | Children's Cancer Group |
| CD | cluster differentiation |
| Cdc | cell division cycle kinase |
| CI | combination indices |
| CML | Chronic Myeloid Leukaemia |
| CNS | central nervous system |
| CRLF2 | cytokine receptor - like factor 2 |
| CSF-1R | Colony Stimulating Factor - 1 Receptor |
| DMSO | dimethyl sulphoxide |
| DNA | deoxyribonucleic acid |
| DSB | double strand break |
| EFS | Event Free Survival |
| EGFR | Epidermal Growth Factor Receptor |
| Eph | Ephrin Receptor Tyrosine kinase |
| FACS | fluorescent - activated cell sorting |
| FCS | fetal calf serum |
| FGFR | fibroblast growth factor receptor |

| | |
|------------------------|--|
| FLT3 | fms-related tyrosine kinase 3 |
| FLT3-ITD | FLT3 - internal tandem duplication |
| γH2AX | gamma histone H2A (phosphorylated at serine 139) |
| Gy | gray (unit of radiation) |
| HER/ErbB | human epidermal growth factor receptor |
| IC₅₀ | half maximal inhibitory concentration |
| Ig | immunoglobulin |
| IR/IGF - 1R | Insulin Receptor/Insulin Growth Factor - 1 Receptor |
| IR | ionising radiation |
| JAK | janus kinase |
| Kit | v-kit Hardy-Zuckerman 4 feline sarcoma viral oncogene homolog |
| Mer | Tyrosine-protein kinase Mer |
| Met | Tyrosine protein kinase Met |
| MLL | Mixed Lineage Leukemia |
| MRD | minimal residual disease |
| NOD/Scid | non - obese diabetic, severe combined immunodeficiency |
| NOG | non – obese diabetic, severe combined Immunodeficiency, interleukin 2 receptor null |
| OS | Overall Survival |
| PARP | poly - ADP ribose polymerase |
| PBS | phosphate buffered saline |
| PDGFR | Platelet derived growth factor receptor |
| Ph+ | Philadelphia chromosome positive |
| Phospho - RTK | Phosphorylated receptor tyrosine kinase |
| PI | Propidium iodide |
| R&D | Research & Development Incorporated |

| | |
|-----------------|---|
| RNA | Ribonucleic acid |
| RON | Receptor d'origine nantais |
| RT - PCR | Reverse transcriptase polymerise chain reaction |
| RTK | Receptor tyrosine kinase |
| STAT | signal transducer and activator of transcription |
| Tdt | terminal deoxynucleotidase |
| TK | tyrosine kinase |
| TKI | Tyrosine Kinase Inhibitor |
| Trk | Tropomyosin - receptor kinase/neurotrophin |
| VEGFR | Vascular Endothelial Growth factor Receptor |
| WCC | Diagnostic white cell count |

1 Acute Lymphoblastic Leukaemia of Childhood

1.1 Incidence and prevalence of childhood malignancies

Childhood cancer is an uncommon event, affecting approximately 1 in 600 children in the United Kingdom (1). Despite its infrequency, cancer is an important cause of morbidity and mortality in children under 16. In 2008, malignancy was the second most common cause of death, following trauma, accounting for approximately 20% of childhood deaths (2).

Of the estimated 1500 children suffering from cancer in the United Kingdom (UK) each year, acute leukaemia accounts for 25 – 30%, of which acute lymphoblastic leukaemia (ALL) is most common. The reported incidence of ALL was 46.1 cases per million children per year in England and Wales for the period 1996 – 2000, with an international incidence of 12 – 59 cases per million (3, 4). While the incidence of childhood malignancy is relatively constant throughout Europe (4), studies from Europe and the United States of America (USA) have demonstrated annual increases of up to 1.4% for ALL (5, 6). In Europe, this increase has coincided with the westernisation of previous Eastern Bloc societies (7). In the Czech Republic a 1.5 fold increase was described in the age group 1 – 4 years for the period 1980 – 1999 (8). A corresponding increase has not been demonstrated in many non – European developing countries, which may be a spurious finding due to under – reporting and the lack of robust cancer registries (9).

The distribution of acute leukaemia varies with age. The peak incidence of ALL is around the third and fourth years, rapidly rising from birth and decreasing dramatically after 5 years of age (10).

1.2 Presentation, investigation and diagnosis of childhood ALL

1.2.1 Presentation

ALL is characterised by a combination of generalised systemic illness, haematological complications from replacement of normal haematopoietic tissue with non – functional malignant cells and invasion of extramedullary tissue. Leukaemic blasts may infiltrate intra

– abdominal and/or thoracic structures (thymus or thoracic lymph nodes), leading to life – threatening compression of the airways and great vessels. Patients with extensive systemic spread may develop central nervous system (CNS) invasion, presenting with the signs and symptoms of raised intracranial pressure from meningeal infiltration, focal neurological involvement (such as invasion of cranial nerves) or intracranial bleeds due to thrombocytopenia.

1.2.2 Diagnostic investigations

The baseline investigations required for diagnosis, classification and stratification of leukaemia include a peripheral blood film to demonstrate lymphoblasts, a bone marrow aspiration for morphology and immunophenotyping and a lumbar puncture to assess CNS involvement (11, 12).

Morphological examination of bone marrow confirms the presence of abnormal cells, with lymphoid blasts generally small, uniform cells with homogenous chromatin. The French – American – British (FAB) classification system of acute leukaemias was based on assessment of cell size, nuclear shape, cytoplasmic amount and consistency, describing leukaemia cells as L1, 2 and 3 (13). The FAB classification system has been superseded by classification systems based combining morphology, immunophenotype, leukaemic cytogenetics and assessment of treatment response. The one exception is L3 morphology, in which cells express the surface immunoglobulin M (sIgM) and demonstrates similar behaviour to the more mature Burkitt's Non – Hodgkin's Lymphoma, requiring a different treatment strategy.

Morphological examination is complemented by immunophenotyping of the leukaemic blasts by flow cytometry. Panels of monoclonal antibodies to antigens associated with leukaemias are used to determine lineage (see table 1.1 and fig 1.1), antibodies to CD3 or 7 to identify T – cell ALL, CD19 (B – cell leukaemia), cytoplasmic myeloperoxidase (myeloid lineage).

| Antigen | Maturity | Lineage |
|---|----------|---------------------------|
| CD45 (Common Leukocyte Antigen) | - | Myeloid/Lymphoblastic |
| CD34 | Immature | Myeloid/Lymphoblastic |
| | | |
| CD19 | Pan – B | B – cell precursor ALL |
| CD10 (common ALL antigen) | Immature | B – cell precursor ALL |
| Tdt (Terminal deoxynucleotidyl transferase) | Immature | Precursor B – and T – ALL |
| Cytoplasmic Immunoglobulin (cyIg) | Immature | B – cell precursor ALL |
| Surface Marker Immunoglobulin (smIg) | Mature | B – cell Mature ALL |
| | | |
| Cytoplasmic CD3 | Mature | T – cell ALL |
| Surface marker CD3 | Mature | T – cell ALL |
| CD7 | Mature | T – cell ALL |
| | | |
| Cytoplasmic MPO | - | Myeloid |

Table 1.1 List of antigens commonly used to identify lineage and maturity of acute leukaemias (14).

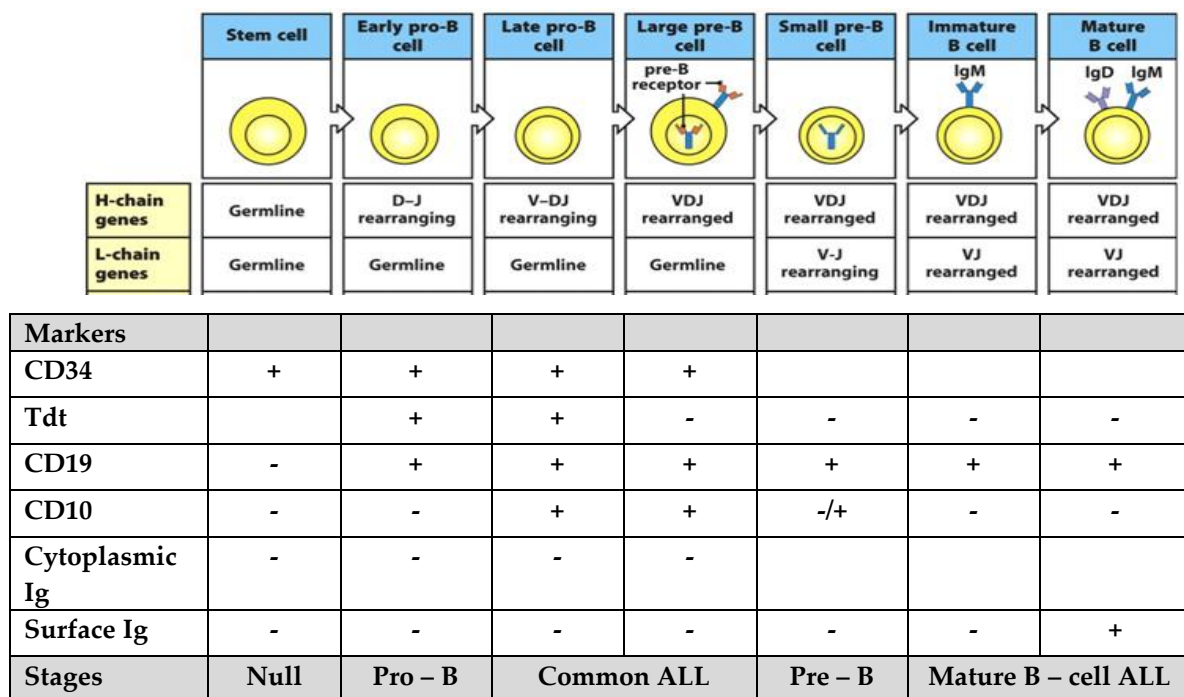


Figure 1.1 B – cell precursor ALL mirrors the stages identified in normal B – cell development. The maturity of both normal B – cells and B – cell lineage leukaemias can be determined by the expression of cell surface and intracellular antigens. Reproduced from Janeway's Immunobiology (15).

1.3 Risk assessment of ALL and prognostic implications

The heterogeneous nature of ALL has led to the understanding that a generic therapeutic strategy is not optimal. Current protocols stratify the intensity of treatment on the basis of potential relapse risk. An unfortunate consequence of this focus on relapse risk is that a significant number of children may be over – treated on current intensive strategies. Current stratification strategies combine clinical and biological risk factors with the aim to balance the burden of chemotherapy with the intention of a favourable outcome.

1.3.1 Age and white cell count

The first attempts to establish a uniform system of stratification used age and diagnostic white cell count (WCC) as the stratification tools (16, 17). Although the value of these continuous variables has been questioned, comparisons of the hazard ratios of relapse are borne out when the highest and lowest quintiles of risk categorisation have been compared (18).

The Rome/NCI classification defined WCC greater than 50×10^9 blasts/litre as the threshold to intensify therapy (16) and has been adopted by the UK Medical Research Council (MRC), US Children's Oncology Group (COG) and German – based Berlin – Frankfurt – Münster (BFM) trial cooperatives. High WCC is associated with an increased risk of bone marrow relapse in B – cell precursor, but not T – cell ALL (19). WCC greater than $100 \times 10^9/L$ is associated with increased CNS relapse in T – cell ALL (20).

The standard risk category for age defined by the Rome/NCI workshops is between 1 and 10 years, which has been widely adopted. Patients outside of this range have a poorer prognosis (21), with particularly high rates of relapse in infant ALL (<1yr) (22, 23). Similarly, adolescents and young adults (AYA) have increased rates of relapse (21, 24, 25) although outcomes can be improved by intensifying treatment (26). Reasons for the lower survival rates in AYA are thought to relate a reduced frequency of leukaemias sensitive to current treatment strategies (27, 28) and higher treatment – related toxicity (29, 30)

1.3.2 Recurrent cytogenetic abnormalities and translocations

Approximately 80% of ALL demonstrate recurrent chromosomal alterations, predominantly translocations, deletions, aneuploidy or amplifications (11, 31, 32). In general, the primary chromosomal abnormality occurs in isolation (33). More detailed molecular assessment of B – precursor ALL has revealed sub-microscopic abnormalities in cytogenetic subtypes. On average a leukaemic blast has 6.46 molecular abnormalities (34), with the copy number alteration (CNA) related to the cytogenetic subtype. *MLL* – rearranged leukaemias usually demonstrate only 1 CNA per cell, while TEL/AML1 and Philadelphia – chromosome positive (Ph+) leukaemias have been revealed to possess 6 or more CNA per case. The inference is the fewer the copy number alterations the more oncogenic the mutation. Leukaemic karyotype is a prognostic indicator independent of age and white cell count (35), with not only the total copy number but specific recurrent cytogenetic translocations impacting on the response to therapy (36).

| Translocation | Frequency | Impact on survival Hazard Ratios (95% CI) | Survival for trial |
|---|------------------------------------|--|--|
| Favourable cytogenetics: | | | |
| TEL/AML (ETV6-RUNX1) t(12;21)(p13;q22) | 22% | 0.51 (0.38 - 0.7) | EFS 89% OS 96% |
| Hyperdiploid Chromosomes >50 | 25% | 0.6 (0.47 – 0.78) | EFS 84% OS 93% |
| Unfavourable cytogenetics: | | | |
| E2A-PBX1 t(1;19)(q23;p13.3) | 5% | 0.6 (0.27 – 1.35) | EFS 80% OS 84% |
| <i>MLL</i> rearrangements 11q23 (4;11;8;11,11;19) | 8% (Infants 70%) > 1 year 2% | 2.98 (1.71 – 5.2) | EFS 50% OS 60% |
| Bcr/Abl t(9;22)(q34;q11.1) | 3% | 3.55 (2.21 – 5.72) | EFS 44% OS 58% |
| t(17;19) | <1 | - | - |
| iAMP21 | 1 – 3% | 6.04(3 – 9.35) Improved with increased intensity HR 2.246 | EFS 26% OS 69% COG trials (37): 4yr EFS 70.2±7% 4yr OS 84.7±5.6% |

Table 1.2 Summary of the impact of chromosomal abnormalities and cytogenetic variation on 5yr overall survival for the United Kingdom ALL97/99 trial. The 5yr survival for the ALL97/99 trial was 87% (86 – 89%). Five year overall survival rates for childhood ALL range between 85 – 95% in large cooperative trials (33, 35, 37).

1.3.2.1 Philadelphia chromosome – positive t(9;22)(q23;q11)

Only 3 – 5% of childhood leukaemia express t(9;22) (38); the frequency increases with age, up to 30% in adult ALL (39). The Philadelphia chromosome was initially identified in CML (40) and the molecular detail of the reciprocal translocation of the long arm of 9 (q34-ter) and long arm 22 (q11-ter), t(9;22)(q43;q11) was defined later (41). The minutiae of the translocation sites differ in the acute and chronic form of the disease. In acute leukaemia the breakpoint is upstream of the BCR (minor – BCR) and encodes for a smaller fusion oncoprotein, the p190 variant (42). The classic adult variant (p210) is rare in paediatric Philadelphia disease, usually described in CML, AML or biphenotypic leukaemia.

1.3.2.2 *ETV6/RUNX1* t(12;21)

The cryptic *ETV6/RUNX1* translocation is the most frequent recurrent abnormality (25 – 30%) in childhood B – precursor ALL (43, 44), most commonly occurring between 1 – 10yr of age (45). The translocation is less frequent in adult ALL and is very rare in T – cell ALL (46, 47).

The t(12;21) translocation results from the juxtaposition of exons 1 – 4 of *TEL/ETV6* on 12p13 and the coding region (21q22) of *RUNX1/AML1/CBFA2* (44). Both *TEL/ETV6* and *RUNX1* encode for transcription factors, and the latter is part of the core binding factor alpha – 2 complex, which is important in normal haematopoiesis. The resultant fusion oncogene interferes with the differentiation of normal lymphoid precursors, by converting *RUNX1* to a transcriptional repressor (48).

1.3.2.3 *E2A – PBX1* t(1;19)

The *E2A – PBX1* translocation occurs in all B – cell lineage leukaemias, but most commonly in pre – B ALL (49). The *E2A* gene is located on 19p13.3 and encodes 2 transcription factors, E12 and E47, which bind the *IGK* gene promoter and regulates downstream target genes. The homeodomain family gene *PBX1* (1q23) encodes a transcription factor important in lymphoid haematopoiesis. The precise mechanism of leukaemogenesis is uncertain, but

transcriptional activation by the fusion oncoprotein of genes which are normally repressed in the lymphoid compartment may explain its action.

1.3.2.4 Mixed Lineage Leukemia (*MLL*) gene rearrangements

The *MLL* gene is located on chromosome 11q23 and mutations are involved in 2 – 5% paediatric (50, 51), 10% adult (52) and 65 – 70% infant ALL (53). In comparison with global incidence, a significantly higher frequency of *MLL* – rearranged leukaemias have been described in Mexico, up to 65% of childhood ALL, possibly related to the in utero exposure to toxins (54, 55).

MLL encodes for a transcriptional factor which regulates embryonic and haematopoietic development and differentiation; downstream targets include the homeobox family of genes and *IKZF1*. A significant number of translocation partners have been described most commonly chromosomes 4, 6, 9 and 19. These patients demonstrate a progenitor B (pro – B) CD10 negative immunophenotype with biphenotypic characteristics, co – expressing the myeloid marker myeloperoxidase.

1.3.2.5 Intrachromosomal amplification of chromosome 21 (iAMP21)

The MRC UK cytogenetic group described an intrachromosomal amplification of chromosome 21, in leukaemias which demonstrated increased *RUNX1* signals but were negative for the *ETV6/RUNX1* fusion using a FISH probe (56-58). The abnormality has been associated with poor prognosis and is more commonly described in older children with low WCC at presentation (37, 56, 59-61). Intensification of therapy has diminished the unfavourable implication of this finding (62).

1.3.3 DNA context

The number of chromosomes in the leukaemic blast can range from near haploid to over 65 chromosomes and is an independent prognostic indicator (63, 64). Hyperdiploidy is associated with an improved survival (65), while survival diminishes with the decreasing number of chromosomes, with the poorest outcome seen in near haploid leukaemias (66, 67).

1.3.3.1 Hyperdiploidy

The most commonly associated findings with hyperdiploid ALL are trisomies, especially chromosome 21 and the X chromosome (68). A number of structural rearrangements are also associated with hyperploidy, including translocations (5 – 10%), duplication of 1q and isochromosome 17q (68-70).

1.3.3.2 Hypodiploidy

In leukaemias with a clonal loss of DNA, survival decreases once the total chromosome complement is less than 46 (71, 72). Particularly poor survival rates are present in patients with near haploid status (33). This abnormality is almost exclusive to children and may not be detected on standard cytogenetic testing. Near haploid leukaemias demonstrate a high frequency of RAS signalling pathway activating mutations (73).

1.4 Response to treatment

The most potent determinant of individual survival is the response to therapy (74). Refinement of assessment has progressed from simple morphological assessment by light microscopy to the detection of sub-microscopic minimal residual disease (MRD) by molecular and flow cytometric techniques.

1.4.1 Assessment of early morphological response

The early morphological response of leukaemia to therapy has historically been identified as a predictor of survival. The method of assessment and definition of response depends on the international co – operative. The cooperatives in the United States started to evaluate

day 7 or 14 bone marrow response to multi – agent therapy in 1970s, while the German BFM study group based response on the reduction of peripheral blasts after 7 days prednisone monotherapy (75). Early reductions in blast counts in both study groups positively correlated with improved outcomes (25, 76, 77).

The benefit of treatment intensification based on the early assessment of *in vivo* response was demonstrated by Nachman *et al.* in the non – randomised CCG1882 trial (78, 79). High risk patients ($WCC > 50 \times 10^9/l$ and age $> 10yr$) with greater than 25% blasts at the day 7 marrow assessment were treated with augmented therapy and achieved event free survival (EFS) similar to the rapid responders. This seminal work laid the basis for intensification of treatment based on *in vivo* response.

1.4.2 Assessment of sub – microscopic disease

Despite the incorporation of morphological assessment into treatment strategies, significant limitations existed, with a high degree of intra – and inter – observer variation and sensitivity limited to the detection of 2 – 3 blasts per 100 normal bone marrow cells. The sub-microscopic persistence of leukaemia in ‘remission’ marrow samples was recognised using a double marker immunofluorescence assay directed at antigens on leukaemic blasts (80, 81), and led to the development of two commonly used techniques to evaluate the presence of sub – microscopic minimal residual disease (MRD).

1.4.3 Assessment of antigen – receptor gene rearrangements

The rearrangement of gene segments encoding the immunoglobulin (Ig) or T – cell receptors (TCR) in normal B – and T – lymphocyte development generate unique combinations. Immunoglobulins are composed of heavy and light chains, both of which contain constant (C) and variable (V) regions. Random combination of genes encoding for the variable (V), diversity (D) and joining (J) segments of the V region allows for the wide scope of antigen recognition. Clonal rearrangements of VDJ segments are detectable in ALL as the oncogenic transformation arises from a single lymphoid progenitor. Using primers

directed at the VDJ junctions, the leukaemia – specific diagnostic clone is identified and sequenced by polymerase chain reaction (PCR). Rearrangements are identifiable in approximately 90% of patients to achieve sensitivity of 0.01% (82, 83). The presence of blast cells at greater than 0.01% at the end of induction therapy correlates with a higher rate of relapse (74, 84-87). A recent study from St Jude's Children's Research Hospital demonstrated the ability of molecular PCR to detect blasts at 0.001% normal marrow population (83). Recent studies have demonstrated that the presence of leukaemia blasts greater than 0.01% with current molecular techniques is the most important indicator of prognosis (74, 88).

1.4.4 Flow cytometry assessment of MRD

Leukaemia cells express aberrant phenotypic markers in comparison to their normal maturing counterparts (89). Normal haematopoietic B – cell precursors follow a regimented and predictable pattern of maturation and antigen expression. ALL blasts demonstrate alterations in antigen expression related to differing stages of maturation, with under – or overexpression of normal antigens and the co – expression of aberrant myeloid antigens.

The leukaemia – associated immunophenotypes (LAIPs) are identified in more than 95% of cases (90) and can reliably be used to distinguish blast cells from normal haematopoietic tissue. The use of selected panels of fluorochrome – labelled antibodies has demonstrated sufficient robustness to detect low levels of LAIP during treatment and discriminate malignant from normal or regenerating haematopoietic tissue.

Flow cytometric evaluation of leukaemia burden is generally reported one log degree less sensitive than the PCR – based technique. Recent studies have detected leukaemia cells at a sensitivity of 0.01% by flow cytometric assessment and for patients treated on BFM – chemotherapy strategies low MRD levels correlate well with survival (74, 91). Borowitz *et al.* reported a 90% EFS in patients with MRD less than 0.01% assayed by flow cytometry on day 8 peripheral blood. In this study, as the level of detectable leukaemia rose the survival of patients reduced (74). Basso *et al.* demonstrated a direct correlation between the presence

of detectable leukaemia and relapse (87). Bone marrow samples assessed on day 15 of induction in which leukaemia was not detected at less than 0.1%, correlated to a low relapse risk, 8% B – precursor ALL and 3% T – ALL (87).

False negatives may arise in either technique as alterations in immunophenotype and Ig/TCR rearrangement profiles may occur during therapy (82, 88, 92, 93). For this reason 2 rearrangements are followed with PCR (94) and at least 2 LAIPs are utilised for flow cytometry (14). Concordance at sensitivity 0.01% is high between the 2 techniques at the end of induction and increases further into therapy (95, 96)

1.5 Current treatment strategies

The outlook for children with ALL has dramatically changed since Farber's first monotherapy experiments with aminopterin in the 1940s (97). With modern strategies, 5 year survival rate of over 80% are achieved in a previously universally fatal disease. The reasons for improved survival include the development of intensive multi – agent chemotherapy regimens, improved supportive care and more refined stratification of therapy.

The basic structure of chemotherapy regimens worldwide is similar, evolving from the St Jude's "Total Therapy" trials (98), consisting of 4 phases: remission induction, consolidation, intensification with CNS directed treatment and continuation therapy.

The goal of induction is a haematological remission, i.e. bone marrow blast count of less than 5% with no evidence of abnormal haematopoiesis. Since the 1970s, the ability of a three-drug induction regimen (vincristine, steroid and asparaginase) has been recognised to induce remission in up to 95% of patients. Recently, with more intensive use of these drugs, remission is achieved in nearly 99% of ALL patients (99). The rate of tumour clearance appears to influence outcome, with rapid resolution associated with an improved relapse – free incidence (74, 85, 87, 100).

Once morphological clearance has been achieved, the need for an intensified phase to consolidate the depth of remission has long been recognised (98, 101). Assessment of leukaemia clearance is now governed predominantly by MRD status after induction, which alters the intensity of the subsequent treatment. Numerous studies have shown that a significant number of patients require a consolidation/intensification block (102, 103), most of which are based on the BFM consolidation template, including cyclophosphamide, cytarabine and mercaptopurine. This combination does not induce a significant amount of myelosuppression and thus almost continuous treatment can occur.

CNS relapse plagued early trials, with approximately 50% of relapses occurring in the neural axis (104, 105). Early trials used craniospinal irradiation as CNS – directed treatment and were associated with significant neuropsychological sequelae (106-109), problems with growth and puberty (109, 110) and secondary malignancies (111, 112). The safe replacement of irradiation with intrathecal (IT) and intensive systemic chemotherapy was initially reported by CCG (113) and later confirmed by UKALL XI (114) .

A common chemotherapy backbone of the final phase of treatment, continuation therapy, consists of oral mercaptopurine and methotrexate. The duration of total therapy in UK trials is arbitrarily assigned as 2 years for girls and 3 years for boys (115). In BFM cooperative trials children of both sexes receive a total of 2 years therapy (116). The precise mechanism of action of this phase is unknown. It has been proposed that the low dose chemotherapy modulates the immune system to suppress residual blasts.

| Cooperative Trial | Dates | Cohort | 5yr Survival | Reference |
|-------------------|-------------|--------|-----------------------------|-----------|
| DCFI – 95 – 01 | 1996 – 2000 | 491 | 5yr EFS 82% 5yr OS 90% | (117) |
| AIEOP – BFM 2000 | 2000 – 2006 | 4016 | EFS 80.4% (7yr) OS 91.8% | (88) |
| NOPHO ALL – 2000 | 2000 – 2007 | 1023 | 5yr EFS 79% 5yr OS 89% | (118) |
| COALL-97 | 1992 – 1997 | 667 | 5yr EFS 76 5yr OS 85 | (119) |
| CCG-1800 | 1989 – 1995 | 5121 | 5yr EFS 75% 5yr OS 73% | (120) |
| EORTC-58881 | 1989 – 1998 | 2065 | 5yr EFS 70.9% 5yr OS 82% | (121) |
| AIEOP-91 | 1991 – 1995 | 1194 | 5yr EFS 71% 5yr OS 80.3% | (122) |
| UKALL97/99 | 1997 – 2003 | 1725 | EFS 78% OS 87% | (33) |
| SJCH Total XV | 2000 – 2007 | 498 | EFS 85.6% OS 92.6% | (91) |

Table 1.3 Summary of results from Co-operative Groups trials of ALL. Since the early 1990's overall survival rates have generally been in excess of 80%.

1.6 Relapsed/Refractory ALL

Up to 20% of patients will relapse and treatment strategies depend on the duration of first remission, the site of relapse and immunophenotype of the leukaemia (123-125). Survival rates range from 0 – 60% (126-128) with catastrophic results for early (<18 months from diagnosis) bone marrow relapses.

The emergence of resistant/relapsed leukaemia may arise from clones which have acquired a chemoresistant phenotype secondary to therapy or from the selection of an intrinsically resistant sub – clone which persists from diagnosis or the formation of a new sub – clone which arises from additional mutations. While alteration of clonal markers and immunophenotype at diagnosis and relapse are described, the relapsed clone or an ancestral clone has been demonstrated in the diagnostic sample (129, 130). A high quantitative level of this subpopulation at diagnosis has been correlated with early relapse (130, 131) and this subpopulation has been demonstrated to be chemoresistant (130, 132).

1.7 Signal transduction pathways associated with chemoresistance:

1.7.1 PI3K/Akt/mTOR Pathway

The phosphatidyl – inositol 3 kinase (PI3K)/Akt-protein B/ mammalian target of rapamycin (mTOR) pathway is involved in cell survival, glucose metabolism, protein synthesis, motility and proliferation. PI3K is a membrane – bound serine/threonine kinase, activated by receptor tyrosine kinases (RTKs), cytokine receptors, integrins and B – cell receptors. Activation of PI3K induces phosphorylation of its target phosphatidylinositol (3,4,5)-trisphosphate (PIP3), which via phosphoinositide-dependent kinase-1 (PDK1) activates Akt. Downstream targets of Akt include inhibition of pro – apoptotic proteins (Bim, Bax, Bad and FoxO1), cell cycle progression (inhibition of p27Kip1, p21Waf1/cip1 and Wee1) and induction of protein synthesis by inhibition of tumour suppressors, TSC 1/2, and induction of mTOR. mTOR is vital for normal homeostasis, acting as a sensor to ensure adequate energy supply to the cell. Activation is required for protein translation, protein synthesis, cell cycle progression and survival (133). Negative regulators of the PI3K/Akt pathway include the phosphatase PTEN, which dephosphorylates PIP3 to PIP2 preventing activation of Akt, and phosphatases which directly dephosphorylate Akt, including PP2A.

Constitutive activation of the PI3K/Akt pathway occurs frequently in childhood T – ALL and can be mediated by overexpression of RTK, loss of PTEN phosphatase regulation, mutations of PI3K or gain – of – function mutations of mTOR itself or associated pathways (134, 135). Constitutive activation of Akt has recently been associated with poor response to induction therapy and shorter OS and EFS in pre – B ALL (136) and reduced *in vitro* sensitivity to induction agents, dexamethasone, doxorubicin and vincristine. mTOR inhibitors have demonstrated anti – leukaemic activity in transgenic and xenograft murine models of pre – B ALL (137, 138) and sensitise ionising radiation – resistant cell lines to chemotherapy (134, 138-141). Upregulation of PI3K in response to chemotherapy may also contribute to chemoresistance (142).

1.7.2 Ras/Raf/MAPK Pathway

The Mitogen – activated protein kinase (MAPK) pathway transmits growth signals from membrane – bound receptors to the nucleus of the cell. The canonical pathway relies on phosphorylation of the cytoplasmic domain of a RTK activating the docking protein GRB2 and guanine nucleotide exchange factor, Son – of – Sevenless (SOS). The receptor signal is transmitted via activated GRB2 and SOS, thus activating the GTPase protein, Ras. The signal is cascaded via Ras, Raf kinase, Mitogen – activating protein kinase kinase (MAPKK) and the MAPK, Extracellular signal – regulated kinases (ERK1/2). Phosphorylated ERK is transported across the nuclear membrane and activated a significant number of transcription factors, including c-Fos, PAX5, ELK1 and Ets.

Activation of the MAPK pathway has been demonstrated in T – cell and adult lymphoblastic leukaemias, with up to 30% of leukaemias possessing constitutively phosphorylated ERK (143, 144). In adult series, pathway activation has been associated with higher WCC and failure to achieve remission (143). Recently, upregulation of MAPK and PI3K pathways in response to chemotherapy in T – cell ALL was demonstrated, leading to increased expression of the anti – apoptotic proteins, survivin and Bcl-2, and chemoresistance (142). In pre – B ALL, the relationship between mutations and chemoresistance is less well defined. Ras mutations are identified in 10 - 20% unselected ALL population (145-147), with an increased incidence in hyperdiploid (30%) (145, 148) and half the cases of *MLL* – rearranged ALL (149). Activation of the MAPK pathway can arise from mutations in other genes, including RTKs, *BRAF*, the E3 – ligase *CBL* and the phosphatase *PTPN11* (150-152). Lübbert *et al.* demonstrated a direct correlation between *RAS* mutations and higher rate of relapse and a non – significant lower rate of remission(153). These findings have not been able to be repeated (145, 146, 154). Increased activation of the MAPK pathway is demonstrated in relapsed leukaemias and blasts with characteristic p-ERK activating *RAS* mutations at relapse have been cloned in the diagnostic sample (155). This finding may support the idea that sub-clone populations bearing *RAS* – mutations may contribute to chemoresistance and relapse (145). Pharmacological MAPK

pathway inhibitors are able to sensitise leukaemias resistant to conventional chemotherapy (156, 157).

The Stankovic group (158) described microarray analysis of a cohort of primary ALL samples demonstrated to be resistant and sensitive to ionising radiation (IR) – induced apoptosis, as a proxy of response to chemotherapy. No single gene was found to discriminate between the two phenotypes at baseline or after exposure to IR. Microarray analysis of leukaemias which were resistant to IR – induced apoptosis identified 13 gene sets with pro – survival function on gene set enrichment analysis. The pro – survival pathways included the intracellular kinase signalling modules, PI3K and MAPK, and upregulation of gene sets of the receptor tyrosine kinase (RTK) pathways, Epidermal growth factor (EGF), Platelet derived growth factor (PDGF) and Insulin growth factor 1 (IGF – 1).

1.8 Role of Receptor Tyrosine Kinases (RTK) in malignancies

A total of 518 protein kinases have been identified by the Human Genome Project, of which 90 are classified as tyrosine kinases (TK) (159). TKs play key roles in proliferation, migration, adhesion, metabolism, glucose utilisation, differentiation, cell survival, inter- and intracellular signalling (160).

1.8.1 Classification and structure of Tyrosine Kinases

TK are characterised by their relationship with the cell membrane, which defines their role. RTKs are single pass proteins which span the membrane, composed of an extracellular domain, transmembranous region and cytoplasmic component. RTKs transduce extracellular growth factor signals to the cytoplasm, as they contain both the ligand – binding ectodomain and the cytoplasmic kinase domain. RTKs have been grouped into 20 classes, classified by the composition of the N – terminal external domain (161). The intracellular C – terminal displays the highest degree of conservation between the receptor classes. The intracellular component of RTKs consists of docking sites for intracellular proteins and the catalytic domain, which is responsible for the receptor's kinase activity.

The catalytic domain induces autophosphorylation and phosphorylation of receptor substrates.

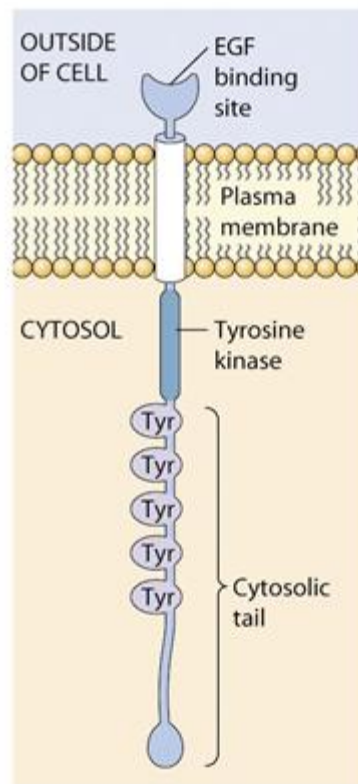


Figure 1.2 Schematic representation of Epidermal Growth Factor Receptor, the prototypical RTK (Reproduced from Pearson Education). The EGFR RTK was the first RTK characterised. The canonical RTK is composed of an extracellular ectodomain, transmembranous region and the cytoplasmic tail, which contains the kinase domain, carboxy –tail and the juxtamembranous region.

Non-RTKs are cytoplasmic proteins which do not possess an extracellular or membrane – spanning domain. These TK depend on receptors from other families to transduce signals, e.g. JAK proteins are phosphorylated by interleukin receptors (162). TKs are predominantly involved in intracellular signalling.

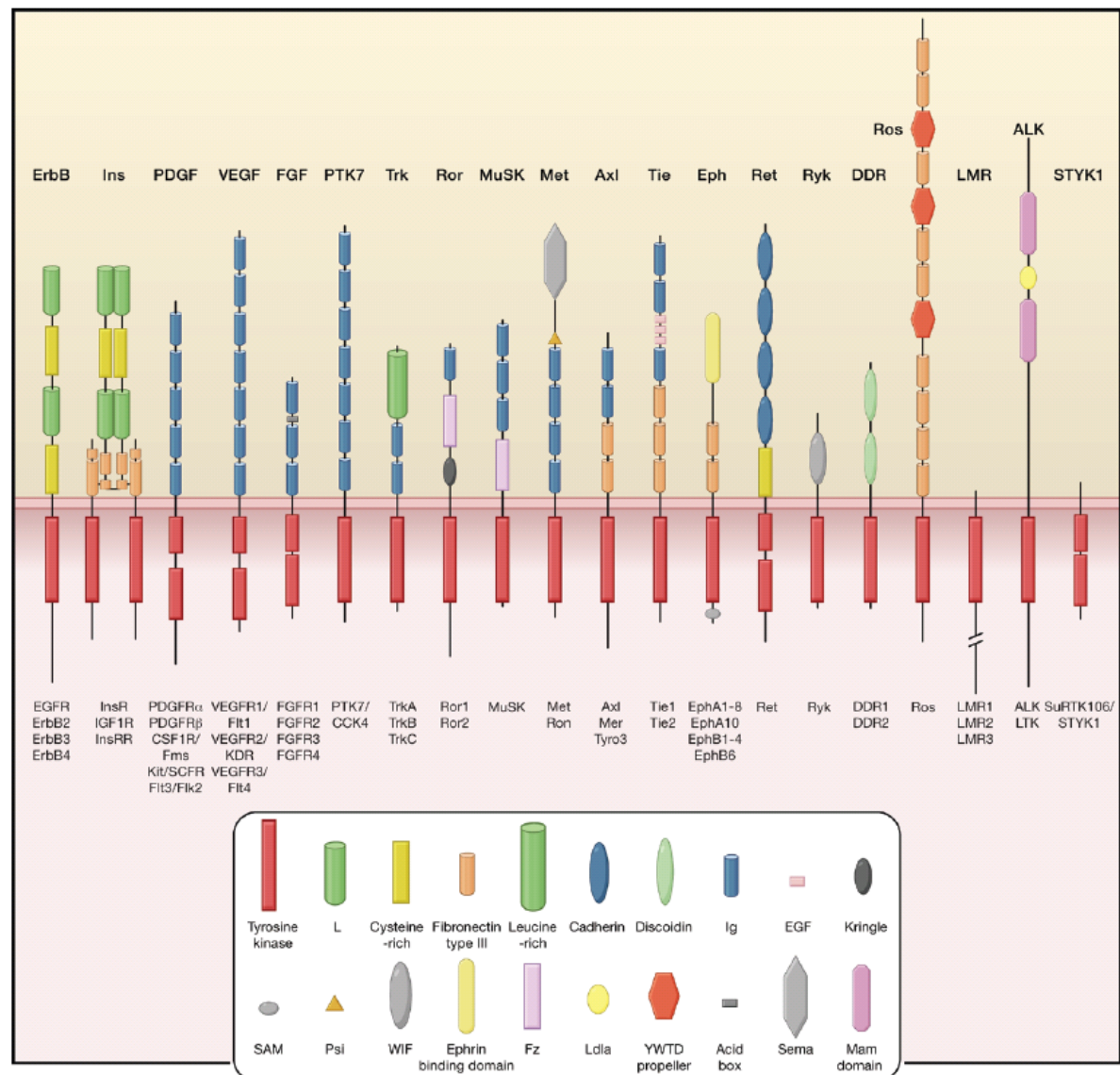


Figure 1.3 Schematic representation of structure of extracellular domains used to classify the 20 families of RTK (Reproduced from Lemmon and Schlessinger (163). RTKs are classified predominantly by the extracellular ectodomain. The intracellular cytoplasmic region is usually conserved.

1.8.2 Activation of RTK

Phosphorylation is the most common post-translational modification and is utilised to modulate specific functions of the affected protein. Kinases catalyse the phosphorylation of proteins by transferring a terminal gamma phosphate from adenine tri-phosphate (ATP) to the free hydroxyl group of an amino acid residue. The original model of RTK activation described the binding of 2 inactive RTK monomers to a bivalent cognate ligand, which

induced receptor dimerization, autophosphorylation of the kinase domain and subsequent phosphorylation of the c – terminal tyrosine residues. This model has proven too crude as the inactive state and binding partners of RTKs exhibit a high degree of complexity. Some RTKs, for example insulin and IGF – 1R (164), can exist as oligomers in their inactive state and ligand – induced oligomerisation occurs at a higher order of interaction.

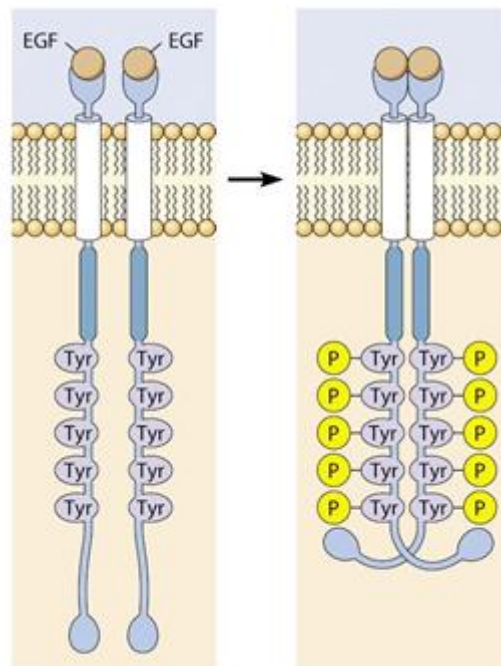


Figure 1.4 Representation of activation of EGFR monomers by binding of EGF – ligand to extracellular domain. The cognate ligand induces dimerisation of the individual receptors. Alteration in the structure induces kinase domain activity leading to autophosphorylation of the cytoplasmic domain tyrosine substrates. (Reproduced from Pearson Education).

While physiological activation of a RTK is a ligand – mediated event, RTKs display significant promiscuity with respect to binding partner. RTKs may bind to the same type of receptor, e.g. VEGFR1/VEGFR1 (homodimerisation) (165), partners within the same class, e.g. EGFR/HER2 (heterodimerisation) (166) or dimerise across classes, e.g. EGFR/Met (cross-talk/heterotypic dimerization) (167).

Different mechanisms of activation have been described (163), based on the type of interaction between ligand and extracellular domain of the RTK.

The first mode of binding involves a dimeric ligand binding to the extracellular domains of 2 RTKs, with no contact between the extracellular components of the 2 RTKs molecules themselves, as exhibited by the Axl (168) and VEGF receptors (165).

A second mechanism has been described in the Kit receptor, where the cognate bivalent ligand, Stem Cell Factor (SCF), mediates cross – linking of the ligand – binding site and brings the extracellular domains of the RTK into intimate contact. The ligand – receptor complex induces an allosteric change proximal to the ligand – binding site, which orientates the Kit molecules for activation (169).

The third mechanism of activation is utilised by the fibroblast growth factor receptor (FGFR) family, where a dimeric ligand induces direct contact between the extracellular components of 2 receptors, but requires an accessory molecule to establish the active conformation. FGFR requires the binding of heparin to stabilise the ligand and receptors for activation (170).

The fourth mechanism of activation, is “receptor – mediated” and employed by EGFR, where the dimerization interface is composed only the receptors. The ligand does not cross – link the 2 receptors, but 2 separate domains of the extracellular component within the same receptor binds to alter the structure and reveal the dimerisation site (171).

In general, dimerisation of the receptors induces trans – phosphorylation of the kinase domain, exposing the catalytic active site allowing for transfer of a phosphate group from ATP to the amino acid residue. The catalytic region is composed of the amino – terminal (N –) lobe, the carboxy – terminal (C –) lobe and an activating – loop. The 2 lobes form a cleft, which acts as the ATP – binding site while the C – lobes form the substrate binding site which accepts the peptide with the tyrosine residue (172). The unstimulated receptor is kept quiescent by auto-inhibitory mechanisms which may be mediated by the activation loop, juxtamembranous region or c – terminal.

The first mechanism of cis – inhibition is mediated by the activation – loop. In the unphosphorylated ‘inactive’ form the activation – loop blocks the ATP – and substrate – binding sites, preventing access and inhibiting the catalytic ability of the RTK. Dimerisation induces trans – phosphorylation of key tyrosine residues on the activation loop, altering its conformation into an ‘active’ position, allowing access to the ATP/binding site and exponentially increasing the catalytic ability of the domain. The insulin activation loop occludes the ATP binding site (173), while FGFR1 prevents access to the substrate site (174).

The second mechanism of autoregulation involves juxtamembranous inhibition of the catalytic domain of RTKs, which is seen in the FLT3 and Kit receptors. The intracytoplasmic region projects into the catalytic domain preventing it from adopting an active form and blocking access to the active site. An example of this is the FLT3 RTK which possesses the key juxtamembranous tyrosine residues, Tyr⁵⁸⁹ and Tyr⁵⁹¹. When these residues are transphosphorylated they alter the inhibitory structure of the region, allowing access to the catalytic domain (175).

A third mechanism of occluding the catalytic domain in the inactive form is present in the Tie -2 RTK. The activation loop of this receptor is positioned in an active conformation even when not phosphorylated (176), however residues in the c – terminal protrude into the catalytic domain and prevent access. Phosphorylation of c – terminal tyrosine residues alters its conformation and allows access to the active site (177).

Once the auto – inhibition is released the efficacy of the catalytic domain is exponentially increased, allowing for further phosphorylation of tyrosine residues in the cytoplasmic region of the receptor. The c – terminal phosphorylated sites recruit a variety of molecules important in intracellular signal transduction. These phosphorylated residues act as binding sites for proteins which contain phosphotyrosine binding (PTB) or Src homology – 2 (SH2) domains. PTB – and SH2 – containing proteins, such as Grb2 or IRS1, bind to the

RTK platform, and mediate interactions with downstream signalling pathways, such as the recruitment of the guanine nucleotide releasing factor Sos which in turn activates the Ras/MAPK pathway (178) or IRS – 1 recruits and activates the catalytic component of PI3K (179).

1.9 Negative regulation of the RTK

The proliferative and pro – survival functions of RTKs need to be tightly controlled and the attenuation of RTK signalling is regulated by receptor dephosphorylation and ubiquitination.

1.9.1 Protein tyrosine Phosphatases

RTK dephosphorylation, and thus inactivation, is mediated via the “classical” protein-tyrosine phosphatases (PTP). These enzymes dephosphorylate tyrosine substrates through a conserved active catalytic domain, which contains an oxidation – sensitive active – site cysteine residue, thus attenuating RTK signalling (180, 181). For example, the PTP DEP – 1 has revealed an important antagonistic role in PDGFR (182), VEGFR (183) and Met (184) signalling via a direct dephosphorylation of RTKs. DEP – 1 deletion induced hyperphosphorylation of FLT3 in AML cell lines with associated ERK pathway signalling and cellular proliferation; whereas activated FLT3 signalling was attenuated by DEPI overexpression (185), thus PTP loss of function mutations have been implicated in more aggressive tumours.

1.9.2 Ubiquitination

Negative regulation of the RTK is also mediated by the multidomain E3 ubiquitin ligase, Casitas B – lineage Lymphoma (Cbl), which plays an important role in modulating the EGFR (186), CSF – 1R (187), PDGFR (188), VEGFR (189), Met (190) pathways. Cbl is recruited to specific phosphorylated tyrosine residues on activated receptors and binds by a highly conserved N – terminal phosphotyrosine binding domain. Cbl conjugates ubiquitin to the receptor’s cytoplasmic domains, targeting it for degradation. Signal attenuation is

also induced by ubiquitination of adaptor molecules, for example Gab1 in Met pathway (191). Dysfunction of Cbl results in aberrant RTK signalling (152) and malignant transformation of fibroblasts has been reported as a result of RTKs unable to recruit and bind Cbl (192).

1.10 Role of TK in B – cell physiology

1.10.1 Tyrosine kinases in normal B – cell development

The non – receptor TKs, Btk, Syk and the Src family, are involved in pre – B and B – cell receptor signalling and in the development of normal B – cells.

Murine knockout models of these TKs have demonstrated their importance in the development and maturation of normal B – lymphocytes. Homozygous *Syk*^{-/-} are embryonically lethal (193), while individual knockdowns of Lyn and Btk demonstrate arrest after the pre – B stage of differentiation. In these models, normal development is present in the bone marrow of cells up to the pre – B stage but then a reduction of peripheral mature lymphocytes (194-197). Triple knockdowns of the Src family kinases, Blk/Fyn/Lyn induced severe lymphopaenia with an arrest at pro – to pre – B development (198). Lyn^{up/up} also lead to a reduction of peripheral B – cells, most likely related to the development of autoantibodies (199).

1.10.2 RTKs in B – cell development

The role of RTKs in normal lymphocyte development is less certain. While a significant number of RTKs are expressed in normal haematopoietic tissue, limited functional assessment has been performed. The protein expression of PDGFR (200), VEGFR 1 – 3 (201), Trk family (202, 203) and Tie – 1 and Tie – 2 (201) have all been reported in CD34+ cells and myeloid precursors. The expression and function of Kit and FLT3 in normal lymphoid progenitors is better defined. Despite the expression of RTKs on haematopoietic cells, normal haematopoiesis does not depend on ALK, FGFR or PDGFR (204-206) .

FLT3 is preferentially expressed in CD34+, pro – B cells and CD4-CD8- thymocytes. *FLT3*^{-/-} knockdown mice demonstrate a reduction in the precursor - B cell in the bone marrow, however apart from a reduction in peripheral dendritic cells the composition of the peripheral blood is indistinguishable from *FLT3*^{wt} mice (207, 208). Kit is expressed on early haematopoietic stem cells and extensively on myeloid, dendritic and B- and T – lymphoid progenitors (209). While no haematological abnormalities are present in single *Kit*^{-/-} the complimentary nature of these 2 RTKs in signalling was confirmed when double *Kit/FLT3* knockdowns demonstrated a more severe phenotype (207). These findings suggest that neither RTK is individually central to the development of lymphocytes.

1.11 RTK deregulation in cancer

RTKs are intimately involved in the proliferation and survival of normal cells and deregulation has been implicated in a wide variety of tumours. The mechanisms of deregulation as summarised in table 1.5.

| Mechanism of Dysregulation | Wild type receptor | Receptor Gene alterations |
|----------------------------|---|---|
| Ligand – dependent | <ol style="list-style-type: none"> 1. Autocrine 2. Paracrine | |
| Ligand – independent | <ol style="list-style-type: none"> 1. Overexpression 2. Abnormal receptor processing 3. Defects in negative regulation | <ol style="list-style-type: none"> 1. Overexpression due to gene amplification 2. Gene rearrangement 3. Mutations 4. Truncation |

Table 1.4 Mechanisms of RTK dysregulation in malignancies. Aberrant RTK signalling can be classified on the presence of ligand binding to the receptor domain, or the kinase activating itself alone.

1.11.1 Epidermal Growth Factor (EGFR)

The constitutive activation of EGFR is described in a wide range of adult tumours, including breast, gastric, colon and lung cancer. Dysregulation occurs by receptor overexpression or mutation. Overexpression promotes spontaneous dimerisation and ligand – independent activation and is present in higher stage non – small cell lung cancer

and correlates with poor prognosis (210). Mutations, such as the truncated EGFRvIII, resist endosomal degradation and signal downregulation, are detected in up to 42% head and neck squamous cell carcinoma (211) and may contribute to EGFR – monoclonal and tyrosine kinase inhibitor (TKI) resistance.

1.11.2 Insulin Growth Factor – 1 receptor (IGF-1R)

Increased IGF – 1R activity has been reported in paediatric tumours, including rhabdomyosarcoma (RMS), Ewing's sarcoma, osteosarcoma, Wilms tumour and neuroblastoma. Mutations of the RTK are not described in malignancies, thus increased activity is due to ligand – dependent activation, receptor overexpression or aberrant regulation of the gene promoter. Increased autocrine secretion of IGF – II has been reported in primary RMS tumours, as a result of maternal loss of imprinting or biallelic expression of the IGF – II. The IGF-1R gene is regulated by the tumour suppressor Wilms tumour gene 1 (*WT1*), the product represses the promoter of *IGF – 1R* (212). The loss of *WT1* results in derepression of IGF – 1R and increased activity in Wilms and aggressive solid tumours (213, 214).

1.11.3 Anaplastic lymphoma kinase (ALK)

Gain – of – function mutations of the ALK receptor are associated with several tumours, including anaplastic thyroid carcinoma, lung carcinoma and neuroblastoma (215). The predominant mutations cluster around the kinase domain and result in increased PI3K/AKT (216) and MAPK signalling (217). Constitutively active chimeric oncoproteins are found in anaplastic large cell lymphoma (NPM – ALK) (218) and lung cancer (EML4 – ALK) (219).

1.12 Review of involvement of Tyrosine Kinases in ALL

A limited number of RTKs have been demonstrated in childhood ALL. Global gene expression analysis has identified the overexpression of *MER* in t(1;19) (220) and *FLT3* in *MLL* – rearranged leukaemias (221). Recent gene expression array studies have implicated

the non – RTK *JAK* family in chemoresistant ALL(222). Gene expression profiling of adult ALL confirmed similar gene expression profiles to childhood ALL, including similar profiles for *MLL* – rearranged, *Bcr/Abl* and *t(1;19)* leukaemias (223). The study identified overexpression of the RTKs *FLT3*, *NTRK3*, *AXL*, *MER* and *DDR1*. Unlike childhood ALL, the increased expression of *FLT3* was not limited to *MLL* – rearranged profiles.

1.12.1 Philadelphia positive ALL

In Ph⁺ ALL the resultant oncoprotein encodes a constitutively activated tyrosine kinase which is proliferative in cellular models, however requires additional genetic mutations to achieve full malignant transformation. Murine models of transplantation of cells transfected with *Bcr/Abl* demonstrate the p190^{Bcr-abl} isoform is more potently leukaemogenic and aggressive in comparison to the p210^{Bcr-abl} (224-226). Transgenic models have demonstrated a wide variety of phenotype but p190^{Bcr-abl} mice with metallothionein promoter exclusively develop B – ALL (227).

Chemoresistance in Ph⁺ ALL is mediated by aberrant activation of intracellular pathways, including JAK/STAT, Ras/Raf/MEK, PI3K/Akt (228-230), as well as resistance to DNA – damage dependent apoptosis by modulating DNA repair checkpoints (231). Constitutively activated STAT signalling is reported to increase expression of anti – apoptotic Bcl - X_L (232).

1.12.2 CRLF2/JAK in Down Syndrome and High Risk ALL

The non – receptor tyrosine kinase JAK family (JAK1 – 3, Tyk2) is implicated in the aetiology of haematological malignancies, predominantly myelodysplastic disorders and AML (233). The most common mutation, V617F valine – to – phenylalanine substitution in *JAK2*, results in constitutive activation as the auto-inhibitory JH2 pseudokinase region is defective. This mutation has not been found in childhood ALL (234). Constitutively activated JAK was initially described in relapsed ALL (235) , but more recently activating mutations in the JAK pathway have been associated with overexpression of the cytokine

receptor – like factor 2 (*CRLF2*) in Down Syndrome – associated ALL (236-239) and high risk leukaemias with a Bcr/Abl – like gene expression profile (222, 240, 241). These high risk leukaemias demonstrated a strong association between *CRLF2* overexpression, *JAK2* mutations and deletions of *PAX5*, *IKZF* and *CDKN2A* (222). *JAK* mutations are reported in up to 20% of DS – ALL (236, 239, 242), 10% high risk and 3% in the unselected ALL population (222). Murine modelling demonstrated co – expression of both *JAK* mutation and *CRLF2* overexpression is required for constitutive STAT5 signalling and cytokine independence (237, 238, 243). Mutations of *JAK1* are uncommon in childhood B – cell ALL (222), but have been reported in 3% childhood T – ALL and up to 18% in adult T – ALL (244-246).

1.12.3 Fms – like tyrosine kinase 3 (FLT3) in childhood ALL

The FLT3 receptor is encoded by a gene on chromosome 13q12 and is structurally related to the Kit, Platelet Derived Growth Factor (PDGFR), and Colony stimulating factor – 1 (CSF-1R) receptors, all of which possess two split catalytic kinase domains. Physiological expression is relatively restricted to primitive lymphoid and myeloid precursors, natural killer and dendritic cells, in addition to placenta, brain and gonads. FLT3 – ligand (FLT3L) is the cognate ligand (encoded by 19q1.3) and expressed on the membranes of most tissue and stimulates FLT3 in a paracrine manner. Dimerisation of FLT3 releases the juxtamembranous *cis* – inhibition and exposes the kinase domain, which allows for initiation of intracellular signalling via PI3K, Ras/MAPK, PLC γ and NF κ B (247-249)

In the unselected paediatric ALL population the frequency of *FLT3* mutations is low (3 – 5%), however aberrant activation is more common in *MLL* – rearranged and hyperdiploid leukaemias (250). Mutations of the JM regions, *FLT3* – internal tandem duplication (*FLT3* – *ITD*) are the most common mutation in AML however these are rare in paediatric ALL (250). *FLT3* – *ITD* results from segmental duplication of the autoinhibitory JM domain, encoded by exons 14 and 15 (251). This allosteric alteration abolishes the structural

autoinhibition of the inactive RTK, inducing autophosphorylation and ligand – independent signalling.

The more common gain – of – function mutations in childhood ALL are missense point mutations, deletions or insertions in the activating loop of the second kinase domain, including D835Y (215). Constitutive activation of FLT3 has been reported in *MLL* – rearranged infant ALL via overexpression of wild type receptor (221, 252)

1.12.4 Mer in childhood ALL

Mer, encoded by a gene located at chromosome 2q14.1 (253), was initially cloned from a B – cell lymphoblastoid library (254) and is part of the TAM receptor family, which includes Axl and Dtk/Tyro – 3. Mer is not required for normal B/T-lymphocyte development (255, 256). The common ligand for all 3 TAM receptors is growth arrest specific gene (Gas) 6, while protein S is a second ligand for Mer and Dtk. Ligand – binding mediates downstream signalling via PLC γ , PI3K/Akt, MAPK and vav1 (257, 258).

No mutations of the Mer receptor have been described, but several human cancers demonstrate overexpression, including rhabdomyosarcoma (259) and gastric cancer (260). Ectopic expression of Mer at mRNA and protein level has been demonstrated in both T-cell (255, 256) and t(1;19) pre – B ALL (261) cell lines and primary samples. Keating *et al.* confirmed Mer's leukaemogenic potential in transgenic mice, (Mer_{tg}) which displayed circulating lymphoblasts consistent with T – cell lymphoma/leukaemia (262). The blasts exhibited increased Akt and ERK1/2 signalling and relative resistance to dexamethasone when compared to wild type lymphocytes.

Ectopic overexpression of Mer is observed in the gene expression profile of t(1;19) pre – B leukaemias (220) and differentially increased expression of transcript and protein has been confirmed in this cytogenetic subtype (261). While Mer is often expressed in pre – B ALL cell lines irrespective of translocation status, Linger *et al.* demonstrated protein expression was weighted towards primary t(1;19) leukaemias (261). The same group proposed a pro –

survival function for Mer as knockdown models demonstrated increased apoptosis to serum starvation and potentiated the apoptotic response when combined with cytotoxic agents. This has been supported by siRNA screens performed by Tyner *et al.* (263).

1.12.5 Tropomyosin – receptor kinase (Trk) in ALL

The high affinity neurotrophic tyrosine kinase receptor family which include Trk A (1q21 – 22), B (9q22.1) and C (15q25), were first identified as a colon – derived oncogene (264). These receptors are important in normal neurological development, as knockout mice have demonstrated neurodevelopmental abnormalities specific to the ablated receptor (265).

Five different neurotrophins are the cognate ligands, all of which display preferential binding for specific receptors. Nerve growth factor (NGF) preferentially binds Trk A, while Trk B binds brain – derived neurotrophic factor, neurotrophin – 4 and – 5 (NT – 4/5) and Trk C binds NT – 3. All receptors are expressed predominantly on neuronal tissue, but Trk A and B are detected in normal B – lymphocytes.

Meyer *et al.* described the induction of lymphoblastic leukaemogenesis in mice serially transplanted with cells with the oncogenic truncated Trk A (Δ TrkA) receptor (266). The blasts demonstrated constitutively active PI3K signalling and demonstrated sensitivity to mTOR inhibition (267). The same group investigated the expression of Trk in adult primary leukaemias and observed myeloid (52%) and lymphoblastic leukaemias (73%) expressed at least 1 Trk receptor (268). Co – expression of Trk A/B/C was present on myeloid blasts, whereas lymphoblastic leukaemias were restricted to TrkB. A strong correlation existed between the myeloid cytogenetic subgroup and the expression of specific Trk, however the molecular findings of the ALL samples was not reported. Furthermore, activation of Trk A and B in transfected murine myeloid cells reduced radiation – induced apoptosis and co – expression of the Trk A/B receptor and ligand induced myeloid leukaemia (268).

1.12.6 c – Met/Hepatocyte Growth Factor Receptor in leukaemia

The Met receptor, encoded by the gene located at chromosome 7q31, was first isolated from a chemically induced human osteosarcoma cell line (HOS) (269) and is part of the Met family of receptors. The cognate ligand is hepatocyte growth factor (HGF), and receptor and ligand are widely expressed. Both Met and HGF are required for normal embryogenesis, and dysregulation of either gene results in lethality (270-272). Physiological activity of the Met receptor includes angiogenesis, tissue repair and wound healing. Subversion of these properties explains the increased invasion, metastasis and anti – apoptotic properties in cells with deregulated Met (273, 274). Dysregulation of the Met pathway can occur by overexpression of Met/HGF, *MET* amplification and germline or somatic Met mutations. While functional Met is expressed in Adult T – cell Leukaemia (ATL) and pre – B ALL, the biological effect of activation appears different. In ATL, a Met autocrine loop was shown to drive proliferation (275) while paradoxically activation of Met in the t(12;21) leukaemia sensitised cells to doxorubicin (276). The role of Met in leukaemogenesis and chemoresistance is uncertain.

1.12.7 Novel chimeric tyrosine kinase – containing oncogenes

Approximately half of leukaemias with Bcr/Abl – like gene expression profiles do not possess *CRLF2* or *JAK* lesions. More detailed sequencing of this group has identified a subset of leukaemias with diverse kinase rearrangements, including *NUP214 – ABL1*, previously described in T – cell ALL, *BCR – JAK2*, *STRN3 – JAK2* and *EBF1 – PDGFRB* (277, 278) (279). Each of these lesions is thought to result in aberrant activation of the chimeric tyrosine kinase domain and constitutive signalling. A small study has demonstrated that the leukaemias with *ABL* and *PDGFRB* mutations were inhibited by TKIs, which resulted in reduced tyrosine phosphorylation (280).

1.13 Discovery of targets and novel agents for the treatment in cancer

1.13.1 Rationale for molecular targeted therapy

Although cancer is the culmination of numerous complex events (281) the rationale for molecularly targeted therapy relies on the restricted repertoire of pathways required by malignant cells for proliferation and survival. Weinstein *et al.* coined the term “oncogene addiction” to describe the absolute dependence of tumour survival on the activity of a single pathway (282, 283).

Moody *et al.* demonstrated the conditional activation of *HER2* in a transgenic mouse model of inducible invasive mammary tumours (284). Regression of both the primary and metastatic tumours was seen when the *HER2* gene was deactivated. The clinical application of this concept was demonstrated with the successful use of the monoclonal antibody, trastuzumab, in *HER2* – expressing tumours (285). In the murine model, the tumours recurred as they developed *HER2* – independent survival pathways (286) and this development is mirrored in clinical practice.

1.13.2 Small molecule tyrosine kinase inhibitors

RTKs are important targets for cancer not only because they are deregulated in many malignancies, but the catalytic domain clefts possessed by tyrosine kinases make them a particularly ‘druggable’ target. Small molecules can bind in the active sites of the kinase domain interfering with the transfer of the phosphate group to substrate, thus disrupting signal transduction.

Three classes of TKI are described on the basis of interaction between the inhibitor and the kinase and on the mechanism of interference (287):

- Type I inhibitors, e.g. sunitinib, bind the active form of the kinase in the ATP – binding site and are direct ATP competitors (288).

- Type II inhibitors, for example imatinib, sorafenib and nilotinib, bind to the inactive form of the kinase and indirectly compete with ATP by occupying the hydrophobic pocket, preventing the catalytic transfer of phosphate (289).
- Type III inhibitors, e.g. the aniline – quinazoline family of inhibitors, block the ATP – binding site by forming irreversible covalent bond with the cysteine residues in the catalytic domain, preventing the binding of ATP for phosphotransfer (290) .

The first 2 classes of TKIs are ATP competitors, which block the ATP – or substrate – binding site of the receptor and prevent the transfer of the phosphate. These inhibitors are relatively non – specific as these kinase regions are conserved throughout the tyrosine kinase family.

The biological effect of a tyrosine kinase inhibitor depends not only on the presence of a target, but also the binding affinity of the molecule for the kinase, the expression or activation status of targets and the presence of resistance mechanisms, including efflux pumps, kinase mutations or the co – opting of redundant/alternative pro – survival pathways. Resistance to imatinib was quickly identified (291), mutations in the activation loop altering the accessibility of the compound to hydrophobic pocket adjacent to ATP – binding pocket, with little or no change in kinase activity. The most potent Bcr/Abl mutation, T315I, completely abrogates the ability of imatinib to bind to the receptor (292).

The accrual of further mutations in other signalling pathways can circumvent the targeting of an oncogene addiction, by leading to the activation of intracellular pathways despite inhibition of the original oncogenic mutation. For example, mutation of the downstream *K – RAS* oncogene negates the activity of the EGFR monoclonal antibody cetuximab, in EGFR – expressing colorectal and lung tumours (293). The activating mutation bypasses the inhibitory effect of the antibody as the tumour persistently signals via the MAPK pathway, independent of the RTK. Resistance to TKI and monoclonal antibodies can also occur with the co – operative activation of numerous RTK in tumours (294, 295). Simultaneous

activation of two or more RTKs allows for robust and continuous intracellular signalling if one the RTKs were to be inhibited. This phenomenon of “coactivation” was first demonstrated by Stommel *et al.* in glioblastoma multiforme, where activation of the PI3K pathway is induced by both EGFR and Met (294). Individual inhibition of either of these pathways did not alter cell survival, and the phenotype was only altered when multi-targeted therapy directed against PDGFR, EGFR and Met occurred. Co – activation and cross talk of RTK networks in breast and lung cancers has driven the rational design of dual RTK inhibitors (296, 297).

1.14 Role of TKI in paediatric ALL

At present the role of TKI in paediatric ALL is limited to clinical trials for the treatment of Ph+ ALL, FLT3 inhibitors for myeloid and infant ALL and more recently the development of early phase trials for JAK inhibition in leukaemia. The most robust evidence for the successful use of TKI was recently demonstrated when the 3yr EFS for Ph+ ALL was dramatically increased to 80%, for patients treated with imatinib and intensive chemotherapy in comparison with historical controls (35%±4) (298). A recent European study, utilising imatinib in combination with an intensive chemotherapy backbone has corroborated the increased EFS (299).

1.15 Aims of study

There has been limited exploration into the use of TKIs outside of Ph+ ALL and the literature reviewed above. This area warrants further investigation if a targeted therapy approach has a wider application for childhood ALL. For this reason the research in this thesis was undertaken.

The specific aims of this thesis are to:

1. Undertake an assessment of baseline RTK activation in primary ALL samples to determine whether a distinct kinase signature may account for increased chemoresistance
2. The identification of “kinase – associated signatures” and the elucidation of the induction of RTK pathways in high risk ALL
3. To screen a kinase inhibitor library, identify candidate compounds and by inference the putative kinases central to cell viability
4. Evaluate the candidate inhibitors in *in vitro* and *in vivo* models of childhood ALL

2 Materials and Methods

2.1. Cell culture

2.1.1. ALL primary samples

Primary leukaemia cells were collected from patients enrolled on the UKALL2003/R3 trial with precursor – B ALL at initial diagnosis or relapse at Birmingham Children's Hospital. Samples were collected after written informed consent, in accordance with the Declaration of Helsinki and stored in compliance with the Human Tissue Act. Samples are provided in an anonymised manner but linked to clinical data. Local Research Ethics Committee approval was granted for all experiments (LREC 09/H1202/101).

2.1.2. Separation of mononuclear cells from bone marrow

Mononuclear cells were isolated from bone marrow on a Ficoll – Paque gradient. Bone marrow samples were diluted to 15ml RPMI (Gibco®, Invitrogen) supplemented with heat inactivated foetal calf serum (FCS) 10%v/v (PAA, The Cell Culture Company) and penicillin/streptomycin 1% v/v (Gibco®, Invitrogen) and layered on 35ml Lymphoprep (Axis Shield). The cells were centrifuged for 30 minutes at 1600rpm with no brake. The mononuclear layer was harvested into a universal container (Sterilin, UK) and washed in 10ml media. The cells were re – centrifuged at 1600rpm and the pellets resuspended in 10ml media. Cells were counted and cryopreserved in aliquots of 1×10^7 cells in 1ml freezing media, 10% dimethyl sulfoxamide (DMSO) (Sigma) and 90% FCS, in cryovials (Nunc, Denmark). Cells were gradually frozen overnight in -80°C freezer in a freezing box. The next day, samples were transferred to liquid nitrogen for long term preservation.

2.1.3. Maintenance of cell lines

Suspension leukaemia cell lines (table 2.1) were maintained in RPMI, FCS 10%v/v, penicillin/streptomycin 1%v/v, in 25cm² flasks (Iwaki, UK) incubated at 37°C in 5% CO₂ and 95% air (incubator make). Cells were grown at a density of 2×10^6 /ml and divided 1:3 twice weekly.

| Cell line | Growth Characteristics | Cytogenetic/Molecular features | Response to IR - induced apoptosis | Reference: |
|-----------|------------------------|--|------------------------------------|------------|
| Nalm 6 | Suspension | Pre – B ALL translocation (5;12) | Intermediate | (300) |
| Nalm 17 | Suspension | Pre – B ALL normal karyotype | Proficient | (301) |
| REH | Suspension | Pre – B ALL t(12;21) | Defective | (302) |
| SD – 1 | Suspension | Pre – B lymphoblastoid t(9;22) | Defective | (303) |
| SupB15 | Suspension | Pre- B ALL t(9;22) | Proficient | (304) |
| TOM -1 | Suspension | Pre – B ALL t(9;22) | Defective | (305) |
| CEMC-1 | Suspension | T – cell ALL | Not assessed | (306) |
| Kasumi -1 | Suspension | AML t(8;21) Kit mutant | Not assessed | (307) |
| HL60 | Suspension | AML | Not assessed | (308) |
| K562 | Suspension | CML t(9;22) | Not assessed | (309) |
| KM-H2 | Suspension | Hodgkin Lymphoma | Not assessed | (310) |
| L428 | Suspension | Hodgkin Lymphoma | Not assessed | (311) |
| MCF-7 | Adherent | Breast adenocarcinoma | Not assessed | (312) |
| HB2 | Adherent | Human mammary luminal epithelial cell line | Not assessed | (313) |
| SY – 5Y | Adherent | Neuroblastoma ALK positive | Not assessed | (314) |

Table 2.1 Summary of cell lines used in experiments

The adherent cell lines, HB2, MCF7 and SY-5Y, were cultured in Dulbecco's Modified Eagle Medium (DMEM) (Sigma), supplemented with FCS 8%v/v and penicillin/streptomycin 1% v/v, in 10mm plastic dishes (Corning, USA). Cells were passaged when the dishes were 80% confluent. Cells were washed with 10ml warm phosphate – buffered saline (PBS) and incubated with 1ml trypsin substitute (TrypLE™ Express, Gibco®, Invitrogen) for 5 minutes at 37°C in an incubator. The detached cells were resuspended in 10ml FCS – containing media to inactivate the trypsin substitute, centrifuged at 1600rpm for 5 minutes and resuspended in DMEM and plated at 1:10 dilution. For all cell lines, fresh cultures were replenished from cryopreserved stock every 2 months.

2.1.4. Recovery of cryopreserved cells

Vials of frozen cells were rapidly defrosted in 37°C water bath to reduce DMSO contact. 10ml media was applied in drop – wise manner to acclimatise cells and to dilute the DMSO. Cells were centrifuged 1600 rpm for 5 minutes, the supernatant discarded and pellets re-suspended in 10ml media. The cells were counted and utilised for experiments or to re – establish fresh cultures in the case of cell lines.

2.1.5. Cell counting

Cells were suspended in 10ml media and counted using a haemocytometer, Glasstic® slide (Hycor Biomedical Ltd, Edinburgh). 10µl of cell suspension was added to an equal volume of 0.2% trypan blue (Sigma, UK) and loaded onto the counting chamber. A light microscope was used to visualise all viable bright, non – stained cells and 9 squares were counted. The cell concentration was determined by multiplying the counted cells by 2×10^4 to equate to number of cells per ml. For all primary leukaemia experiments 80% viability was the minimum accepted.

2.1.6. Characteristics of primary ALL samples

Biological and clinical characteristics of the primary ALL samples used in this study are displayed in tables 2.2 and 2.3. The minimal residual disease (MRD) status of leukaemias was determined by the Regional National Health Service molecular genetics laboratory in the case of molecular MRD status and by the Birmingham Children's Hospital Haematology Department in the case of flow cytometric MRD status.

| Sample code | Age (yrs) | Sex | WCC (x10 ⁹ /L) | Outcome | Cytogenetics | Response at D8/15 | Flow MRD | Molecular MRD | Apoptosis phenotype |
|-------------|-----------|-----|---------------------------|---------|--|-------------------|----------|---------------|---------------------|
| ALL-1 | 1 | M | 62 | CR | Hyperdiploid (52) | GER | HR | HR | Defective |
| ALL-2 | 2 | M | 391 | CR | 45XY, dic(9;20)+8, -13 | GER | SR | HR | Defective |
| ALL-3 | 15 | M | 117 | CR | Hyperdiploid | PER | SR | HR | Defective |
| ALL-4 | 4 | M | 2.4 | CR | Normal | GER | HR | NK | Defective |
| ALL-5 | 14 | M | 11 | CR | 46XY, add 7q, add 12p | GER | HR | HR | Defective |
| ALL-6 | 8 | M | 22 | CR | t(12;21) | GER | SR | NK | Defective |
| ALL-7 | 4.1 | M | 51 | CR | t(12;21) | N/K | HR | SR | Defective |
| ALL-8 | 10.1 | F | 1.1 | D | Normal | PER | HR | HR | Defective |
| ALL-9 | 14 | M | 150 | D | Normal | PER | HR | HR | Defective |
| ALL-10 | 7.1 | M | 82 | CR | None | GER | SR | SR | Proficient |
| ALL-11 | 2.2 | F | 88 | CR | t(3;22) | PER | HR | HR | Proficient |
| ALL-12 | 3 | F | 5 | CR | t(12;21) | GER | SR | SR | Proficient |
| ALL-13 | 2.75 | F | 5.2 | CR | t(12;21) | GER | SR | SR | Proficient |
| ALL-14 | 8.9 | F | 74 | CR | t(12;21) | GER | SR | SR | Proficient |
| ALL-15 | 11.1 | M | 10 | CR | t(12;21) | PER | SR | SR | Proficient |
| ALL-16 | 3.5 | M | 3.4 | CR | t(12;21) | GER | HR | HR | Proficient |
| ALL-17 | 2.1 | M | 26 | CR | Normal | GER | NK | SR | Proficient |
| ALL-18 | 7.8 | M | 9 | CR | 53XY | GER | NK | SR | Proficient |
| ALL-19 | 5 | M | 10 | CR | t(12;21) | GER | SR | SR | Proficient |
| ALL-20 | 12 | F | 109 | CR | 46XX, t(3;10) t(9;16) +8 biallelic del p16 | GER | Ind | SR | Proficient |

Key:

| | |
|------|--|
| CR: | Complete Remission |
| D: | Died of disease |
| GER: | Good early response (Blasts < 25% on day 8/15) |
| PER: | Poor early response (Blasts ≥ 25% on day 8/15) |
| MRD: | Minimal residual disease |
| HR: | High Risk leukaemia cells detectable >0.01% |
| SR: | Standard Risk leukaemia cell not detectable <0.01% |
| NK | Not known |
| Ind | Indeterminate |

Highlight grey: Leukaemia samples with defective phenotype in response to IR – induced apoptosis

Table 2.2 Clinical features of primary paediatric B – precursor ALL used in the phospho – RTK array experiments. Eighteen of the 20 samples were interrogated with the R&D array and 6 samples interrogated with the Raybiotech array. The samples highlighted in grey were demonstrated to have defective apoptotic phenotypes in response to IR – induced apoptosis.

| Sample code | Age (yrs) | Sex | WCC (x10 ⁹ /L) | Outcome | Cytogenetics | Response at day 8/15 | Flow MRD | Molecular MRD |
|-------------|-----------|-----|---------------------------|---------------------|---|----------------------|----------|---------------|
| ALL-16 | 3.5 | M | 3.4 | CR | t(12;21) | GER | HR | HR |
| ALL-20 | 12 | F | 109 | CR | 46XX, t(3;10) t(9;16) +8 biallelic del p16 | GER | Ind | SR |
| ALL-21 | 12 | F | 8 | CR | t(12;21) | GER | SR | NK |
| ALL-22 | 2 | F | 20 | CR | Normal | GER | SR | SR |
| ALL-23 | 9.5 | M | 24 | CR | 45XY, der19, t(1;19) | GER | HR | SR |
| ALL-24 | 10.92 | M | 59.7 | CR | 46XY, del9p21p21, monoallelic CDKN2A loss, 13q14 loss | PER | HR | HR |
| ALL-25 | 3 | M | 12.7 | CR | No report | GER | HR | HR |
| ALL-26 | 0.5 | M | 109.9 | CR | t(9;11) | GPR | NK | SR |
| ALL-27 | 9.5 | M | 26 | CR | 46XY | GER | HR | HR |
| ALL-28 | 8.5 | M | 4 | CR | Hyperdiploid | GER | HR | SR |
| ALL-29 | 3 | F | 5 | CR | t(12;21) | GER | SR | SR |
| ALL-30 | 10.5 | F | 83 | CR | 47XX, t(12;21) | GER | SR | SR |
| ALL-31 | 11 | F | 73 | CR | 46XX, der 19, t(1;19) | GER | SR | SR |
| ALL-32 | 0.5 | F | 44.7 | CR | t(4;11) | GPR | NK | SR |
| ALL-33 | 3 | M | 43 | CR | Hyperdiploid | GER | SR | SR |
| ALL-34 | 9.92 | M | 15.8 | awaiting transplant | t(12;21) | GER | HR | NK |
| ALL-35 | 2 | F | 41 | CR | Hyperdiploid | GER | HR | HR |
| ALL-36 | 16 | F | 60 | Died | 46XX, t(2;12), p1p13(8) | GER | HR | HR |
| ALL-37 | 2 | F | 45 | CR | Hyperdiploid | GER | HR | HR |
| ALL-38 | 5 | F | 15 | CR | Normal | GER | HR | SR |
| AML- 2 | 15 | M | 63 | Died | FLT3 – ITD | n/a | n/a | n/a |

Key:**CR:** Complete Remission**D:** Died**GER:** Good early response (Blasts < 25% on day 8/15 bone marrow)**GPR:** Good Prednisolone response (Peripheral Blasts <1x10⁹/L after 7 days prednisolone monotherapy)**PER:** Poor early response (Blasts ≥ 25% on day 8/15 bone marrow)**MRD:** Minimal residual disease**HR:** High Risk, leukaemia cells detectable >0.01%**SR:** Standard Risk, leukaemia cells not detectable < 0.01%**NK** Not known**n/a:** not applicable

Table 2.3 Clinical and biological features of the primary Acute Leukaemia samples used in the tyrosine kinase inhibitor screening experiments of this study. The myeloid primary leukaemia sample, AML – 2, was demonstrated to the FLT3 – internal tandem duplication (FLT3 – ITD) when sequenced by the regional National Health Service molecular genetics laboratory.

2.2. Cell lysis and protein extraction

Cells in suspension were transferred to a universal container and harvested by centrifuging at 1600rpm for 5 minutes at 4°C. The supernatant was aspirated and the pellet was washed in 10ml ice cold PBS to remove media and serum. The centrifuge was repeated and the PBS aspirated. The cells were kept on ice until lysed. Adherent cells were harvested when 80%

confluent. After aspiration of the media the cells were washed twice in 10ml ice cold PBS and kept on ice. For immunoblotting, cells were lysed in ice cold Radio – Immuno – Precipitation Assay (RIPA) lysis buffer, unless otherwise stated. 50 ml of stock solution was made of Tris – HCl pH8 (Calbiochem, USA), 1% Triton X – 100 (Sigma), 0.1% SDS (Sigma), 0.1% Sodium deoxycholate (Sigma) and 150mM NaCl (Severn Biotech, UK) and kept for a week. For each experiment 10ml of stock was utilised, to which 1 Protease inhibitor tablet (Roche) and 100µl 10x PhosSTOP (Roche) solution was added.

For suspension cells, 40 - 80µl of chilled RIPA buffer was added to $1 - 5 \times 10^6$ cells, mixed and sonicated. For adherent cells 500µl of cold buffer was added directly to plate, the cells harvested with scraper, thoroughly mixed and transferred to 1.5 ml tube for sonication. Cells were sonicated for 7 sec at level 4. Post – sonication, cells were lysed on ice for 30 minutes. Thereafter the cells were transferred to 1.5ml tubes, centrifuged at 13000rpm at 4°C to clear cellular and nuclear debris. The supernatant was aspirated and transferred to clean 1.5ml tubes and kept on ice or snap frozen and transferred to -80°C freezer.

2.3. Protein quantification

Bovine serum albumin (BSA) (Sigma, USA) 1mg/ml stock was diluted to 0.1µg/ml, 0.2µg/ml, 0.3µg/ml, 0.4µg/ml and 0.5µg/ml for protein standards and 10µl pipetted in triplicate into 96-well plate (Iwaki). For each sample, whole cell lysate was diluted 1:10 in distilled water and 10µl of diluted sample pipetted into a 96 well plate (Iwaki) in triplicate. 200µl of 1x Bradford Protein Assay (Bio-Rad Laboratories) was added to protein standards and samples then absorbance analysed on Bio-Rad 680 microplate reader at 595nm. The absorbance readings of the BSA standards were utilised to generate a standard curve to determine the protein concentrations of each sample.

2.4. Sodium dodecyl sulphate polyacrylamide gel electrophoresis (SDS – PAGE)

Proteins were resolved on single phase SDS – PAGE gels, with the final acrylamide concentration determined by the size of the proteins of interest, 6 – 12%. Resolving gels consisted of 30% Acrylamide (Severn Biotech, UK), 0.1% SDS, 390mM Tris-HCL pH8, 0.06% N,N,N,N – tetramethylethylenediamine (Temed, Sigma) and 0.1% Ammonium Persulphate (Sigma) prepared with each gel. The apparatus plates were cleaned with distilled water and 70% ethanol prior to mixing the gel. The gel was mixed and poured into the gel apparatus, a comb was inserted and the gel was left to polymerise. Once set, the comb was removed and the wells washed with distilled water and running buffer, 0.1M Tris/Bicine, 0.1% SDS made to 1000ml distilled water .

30 - 50µg of protein was transferred to 1.5ml tube and diluted 1:1 with 2x Laemmli buffer, consisting of 10% β – mercaptoethanol (Sigma), 125mM Tris – HCl (pH 6.8), 0.004% bromophenol blue (Sigma), 20% glycerol (Sigma) and 4% SDS. The protein was denatured by boiling at 95°C for 5 minutes and then returned to ice. The first lane of the gel was loaded with 10µl of Laemmli buffer and the second lane was loaded with full range protein marker (Rainbow Marker GE Healthcare or Spectra™ Multicolour Broad Range Ladder, Fermentas). The samples were centrifuged at 13 000 rpm for 10 seconds and transferred with a Hamilton syringe to the wells. Gels were run at 30mA for 5 – 8 hours to resolve proteins.

2.5. Protein transfer

Transfer buffer, 40.6 g Tris (Calbiochem), 203g Glycine (Fisher Scientific), 1400ml methanol (Sigma) and distilled water to a total volume of 7000ml, was prepared and added to the transfer tank (Geneflow, EBM 20) and a plastic tray to soak the nitrocellulose membrane (Biotrace NT, Pall Life Sciences), Whatman® paper (Sigma - Aldrich) and sponges required for transfer. SDS-PAGE gels were layered onto nitrocellulose membranes and placed between two layers of blotting paper and encased in sponge in cassettes and placed into the transfer tank for overnight transfer at 200mA at 4°C.

2.6. Western Blotting with antibodies

The protein loading was assessed with Poncaeau Red (Sigma) then washed with Tris – buffered saline – Tween (TBST), consisting of 1.21g Tris and 8.77g NaCl (Sigma) in 1 litre ionised water with 0.5ml Tween20 (Fisher Scientific), titrated to pH7.6 with HCl (Sigma). Non – specific protein binding was blocked by incubating nitrocellulose blots for 2 hours in 5% non – fat milk/TBST when blotting for total protein and in 5% BSA/TBST when blotting for phospho – proteins. Membranes were incubated with primary antibodies (table 2.4) overnight at 4°C in 5% milk or 5%BSA/TBST. The membranes were washed 3 times for 10 minutes in TBST, incubated with the corresponding secondary antibody (table 2.4) for 2 hours at room temperature and rinsed three times in TBST.

The presence of protein – bound antibody was detected with Immobilon Western Chemiluminescence kit (Millipore). A 1:1 dilution of luminol and peroxide was mixed for 1 minute and the membrane was incubated for a further minute. Excess solution was removed, the membrane inverted onto Saran wrap and transferred to an autoradiography cassette. In a dark room, radiographic film (Kodak, UK) was exposed to the membrane for between 5sec and 10min. The film was developed in a Kodak X – OMAT 1000 processor.

| Primary antibodies | | | |
|---|---------|-----------------|-----------------------|
| Antibody | Species | Dilution | Company |
| PARP – 1 | Rabbit | 1:400 | Cell signaling |
| Caspase – 7 | Mouse | 1:1000 | Cell signaling |
| p53 | Mouse | 1:20 | Dr R Grand (serum) |
| p21 ^{Waf1/Cip1} | Mouse | 1:1000 | Cell signaling |
| β -Actin | Mouse | 1:10 000 | Sigma |
| Tubulin – α | Rabbit | 1:1000 | Cell signaling |
| Cyclin B1 | Mouse | 1:1000 | Santa Cruz |
| Total IGF – 1R | Rabbit | 1:1000 | Cell signaling |
| Phospho – IGF – 1R (Y1131) | Rabbit | 1:1000 | Cell signaling |
| ERK | Rabbit | 1:1000 | Cell signalling |
| Phospho– p44/42 MAPK (ERK1/2) | Rabbit | 1:1000 | Cell signaling #9106 |
| AKT | Rabbit | 1:1000 | Cell signaling |
| Phospho-AKT (ser473) | Mouse | 1:1000 | Cell signalling #4051 |
| EGFR | Mouse | 1:100 | Thermo – Scientific |
| Phospho – EGFR (Y992) | Rabbit | 1:100 | Cell signaling |
| Pan – phosphotyrosine (pTyr – 100) | Mouse | 1:1000 – 1:2000 | Cell signaling #9411S |
| Phospho - γ H2AX | Mouse | 1:500 | Upstate |
| Secondary antibodies | | | |
| Antibody | Species | Dilution | Company |
| Polyclonal anti – Rabbit (Horse radish peroxidase conjugated) | Swine | 1:3000 | Dako, Denmark |
| Polyclonal anti – Mouse (Horse radish peroxidase conjugated) | Goat | 1:2000 | Dako, Denmark |
| Polyclonal anti – Mouse Alexa Flour 594 (Fluorochrome conjugated) | Rabbit | 1:1000 | Invitrogen |

Table 2.4 List of antibodies used for immunoblotting and immunofluorescence

2.7. Model for assessing apoptosis response to IR – induced damage

Weston *et al.* (315) reported the stratification of ALL in response to ionising radiation. Leukaemia cells with a proficient intrinsic apoptosis pathway demonstrated p53 accumulation in response to 5Gy ionising irradiation, with cleavage of PARP – 1 and procaspase 7; beginning by 4 – 8 hours and completed by 24 hours. Normal accumulation of p53 was present in cells which were apoptosis defective, however no cleavage of PARP – 1 and procaspase 7 was evident.

Primary cells and cell lines were defrosted, harvested, counted and suspended in media. For cell lines 5×10^6 cells per time point were and for primary cells 2×10^6 cells per time point. Cells were subjected to 5Gy ionising radiation from a Cobalt60 source, transferred to an incubator and harvested onto ice at 4, 8, 24 hours and protein prepared as described. 30µg of protein was loaded onto 8% SDS – PAGE gel and blotted for actin, cleavage of PARP – 1 and procaspases 7 and p53 accumulation to assess apoptosis phenotype.

2.8. Assessment of phospho – tyrosine kinase status by array systems

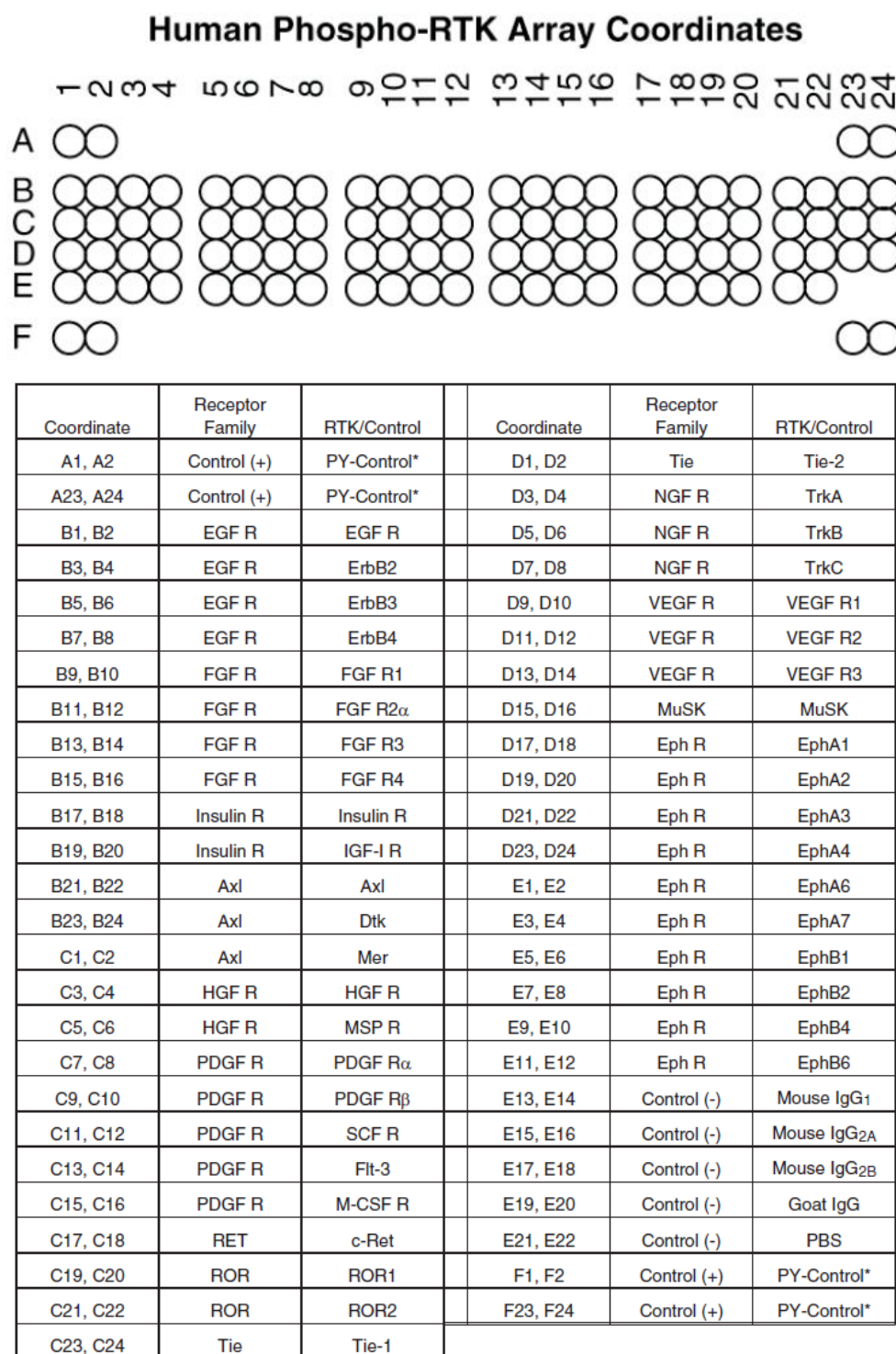
2.8.1. Principle of phospho – tyrosine kinase array kits

The simultaneous assessment of phosphorylated tyrosine kinases was assessed using 2 array systems, the Raybio® Human RTK Phosphorylation Antibody Array 1 (Raybiotech, Inc. Norcross, USA) and the R&D Proteome Profiler™ Array Human Phospho-RTK Array kit (R&D, Minneapolis). Each array system has antibodies directed against the total tyrosine kinase spotted in duplicate on a nitrocellulose membrane. Positive and negative internal controls are also spotted on the membranes.

RayBio® Human RTK Phosphorylation Antibody Array 1 Map

| | A | B | C | D | E | F | G | H | I | J | K | L |
|----|-----------|-----------|---------|---------|--------|--------|--------|--------|-------|-------|----------------------|----------------------|
| 1 | POS 1 | POS 1 | POS 2 | POS 2 | POS3 | POS3 | ABL1 | ABL1 | ACK1 | ACK1 | ALK | ALK |
| 2 | NEG | NEG | NEG | NEG | Axl | Axl | Blk | Blk | BMX | BMX | Btk | Btk |
| 3 | Csk | Csk | Dtk | Dtk | EGFR | EGFR | EphA1 | EphA1 | EphA2 | EphA2 | EphA3 | EphA3 |
| 4 | EphA4 | EphA4 | EphA5 | EphA5 | EphA6 | EphA6 | EphA7 | EphA7 | EphA8 | EphA8 | EphB1 | EphB1 |
| 5 | EphB2 | EphB2 | EphB3 | EphB3 | EphB4 | EphB4 | EphB6 | EphB6 | ErbB2 | ErbB2 | ErbB3 | ErbB3 |
| 6 | ErbB4 | ErbB4 | FAK | FAK | FER | FER | FGFR1 | FGFR1 | FGFR2 | FGFR2 | FGFR2 (α isoform) | FGFR2 (α isoform) |
| 7 | Fgr | Fgr | FRK | FRK | Fyn | Fyn | Hck | Hck | HGFR | HGFR | IGF-1 R | IGF-1 R |
| 8 | Insulin R | Insulin R | Itk | Itk | JAK1 | JAK1 | JAK2 | JAK2 | JAK3 | JAK3 | LCK | LCK |
| 9 | LTK | LTK | Lyn | Lyn | MATK | MATK | M-CSFR | M-CSFR | MUSK | MUSK | NGFR | NGFR |
| 10 | PDGFR-α | PDGFR-α | PDGFR-β | PDGFR-β | PYK2 | PYK2 | RET | RET | ROR1 | ROR1 | ROR2 | ROR2 |
| 11 | ROS | ROS | RYK | RYK | SCFR | SCFR | SRMS | SRMS | SYK | SYK | Tec | Tec |
| 12 | Tie-1 | Tie-1 | Tie-2 | Tie-2 | TNK1 | TNK1 | TRKB | TRKB | TXK | TXK | NEG | NEG |
| 13 | Tyk2 | Tyk2 | TYRO10 | TYRO10 | VEGFR2 | VEGFR2 | VEGFR3 | VEGFR3 | ZAP70 | ZAP70 | POS2 | POS2 |

Figure 2.1 Map of outlay of phospho – tyrosine kinase antibodies embedded on the RayBio® Human RTK Phosphorylation Antibody Array. The Raybiotech array system can identify up to 71 tyrosine kinases. Each point represents an embedded antibody (in duplicate) directed against a specific phosphorylated tyrosine kinase.



*Phospho-Tyrosine Positive Control

Figure 2.2 Map of outlay of antibodies directed against phosphorylated RTKs on the R&D Human Phospho – RTK array. The R&D array can simultaneously assess the phosphorylation status of 42 RTKs. Each circle represents an embedded antibody (in duplicate) directed against a specific phosphorylated tyrosine kinase.

| Similarities | Differences |
|---|---|
| Both arrays used an embedded antibody to capture the tyrosine kinase | Difference in the RTKs investigated in each array system: <ul style="list-style-type: none"> - Raybiotech array included antibodies for non – receptor tyrosine kinases - No FLT3 on Raybio® Human RTK Phosphorylation Antibody Array |
| Arrays utilised a pan – phosphotyrosine secondary antibody to detect activated tyrosine kinases | The R&D anti – phosphotyrosine antibody is conjugated HRP |

Table 2.5 Summary of similarities and differences noted between the 2 array systems.

2.8.2. Protocol for preparation of phospho – array membranes

All primary cells were retrieved from cryopreservation and suspended in media. Cell lines were maintained as per section 2.1.3. For the Raybiotech array the cell lysis buffer, protease inhibitor and phosphatase inhibitor cocktails are provided with the kit with no details about the constituent components. Cells were prepared and hybridised to the arrays according to manufacturer's protocol, with all buffers were kept on ice. For the R&D Array system, cells were lysed according to manufacturer's suggested buffer: 1% NP – 40 (Sigma), 20mM Tris – HCl (pH8), 137mM NaCl, 10% glycerol, 2mM EDTA (Sigma), PhosSTOP Phosphatase inhibitor 10%v/v, cOmplete ULTRA Protease Inhibitor Tablet 1 per 10ml buffer.

For both array systems, protein determination was performed and 50µg of whole cell lysate incubated with each array overnight at 4°C, hybridising to the arrays via the membrane – bound antibody. The membranes were washed 6 times in TBST for 5 minutes each wash to remove excess lysate. A secondary pan – phosphotyrosine antibody was applied for 4 hours which bound to the phosphorylated tyrosine residues. The membranes were washed 6 times in TBST for 5 minutes each wash to remove antibody.

Signals were detected by chemiluminescence provided by each kit and developed on radiograph film (Kodak). The pixel density of each array spot was measured and expressed as optical density (OD)/mm². To account for variation in exposure, 6 blank readings and readings over the negative control markers were performed. All signal readings were exported to Microsoft Excel. The mean signal for the pair of duplicate spots representing each TK was determined and the median blank and negative reading was subtracted to give the final reading.

2.9. Treatment of cells with Tyrosine Kinase Inhibitors (TKIs) and cytotoxics

A library of 33 tyrosine kinase inhibitors (table 2.6) was purchased from Selleck® Chemicals, USA. CEP – 701 (lestaurtinib) and dovitinib were purchased from LC Laboratories (Woburn, MA, USA) and AMG – Tie – 2 – 1 inhibitor from SYN|thesis med chem Ltd. Vatalinib and PF – 04217903 were dissolved in distilled sterile water, while the remaining 31 inhibitors were dissolved in DMSO, to produce 10mM stock aliquots, stored at -20°C.

The chemotherapeutic agents, cytarabine, dexamethasone, doxorubicin, fludarabine, methotrexate, mitoxantrone and vincristine were kindly provided by the Birmingham Children's Hospital Pharmacy department. All cytotoxics were provided in normal saline and 2x serial dilutions in media were prepared, 0.02 - 20µM.

For initial screening of cell lines and primary cells, 10mM stock solution was serially diluted to prepare 2x concentration, 2µM and 20µM. For more detailed investigation aliquots were serially diluted to desired concentrations. For cell lines, the TKI was diluted in RPMI/10%FCS/PS and for primary leukaemia cells RPMI/10%FCS/1%PS with additional 100µM β – mercaptoethanol (2x dilution).

The 2x dilution of TKI/drug was to ensure a final concentration between 0.001 - 10µM after the addition of an equal volume of media containing cells.

| TKI | Putative primary targets | References |
|--|---|------------|
| JAK inhibitors | | |
| AG490 | JAK 2 – 3, EGFR | (316) |
| CP690550 | JAK 1 – 3 | (317) |
| IGF-1R/Insulin inhibitors | | |
| GSK1904529A | IGF – 1R/Insulin | (318) |
| NVPAEW541 | IGF – 1R/Insulin | (319) |
| Irreversible EGFR/HER2 | | |
| BIBW-2992 | EGFR/HER2 | (320) |
| CI – 1033 | EGFR/HER2/HER4 | (321) |
| Restricted spectrum inhibitors | | |
| AZD0530 | Abl/Src/EGFR | (322) |
| Bosutinib | Abl/Src/Axl/EGFR/Trk | (323) |
| Dasatinib | Abl/Src/CSF-1R/Kit/PDGFR α / β | (324) |
| Imatinib | Abl/CSF-1R/Kit/PDGFR α / β | (325) |
| Masitinib | Kit/PDGFR α / β | (326) |
| Nilotinib | Abl/Kit/PDGFR α / β | (325) |
| PF-04217903 | Met | (327). |
| PF-2341066 | Met/ALK | (328) |
| PHA739358 | Aurora kinase A – C/Abl/Src/RET | (329) |
| AMG – TIE-2 – 1 | Tie – 2 | (330) |
| Multikinase inhibitors (VEGFR/PDGFR) | | |
| Axitinib | VEGFR 1 – 3/PDGFR α / β /CSF – 1R/Kit/FGFR 1 | (331) |
| Brivanib | VEGFR 1 -3/FGFR 1 – 3 | (332) |
| Cediranib | VEGFR 1 – 3/PDGFR α / β /CSF – 1R/Kit/FGFR 1 | (333) |
| Motesanib | VEGFR 1 – 3/PDGFR α /Kit/RET | (334) |
| Pazopanib | VEGFR 1 – 3/PDGFR α / β /CSF – 1R/Kit/FGFR 1, 3 and 4 | (335) |
| Vandetanib | VEGFR 1 -3/EGFR/RET | (336) |
| Vatalinib | VEGFR 1 – 3/PDGFR β /Kit | (337) |
| Multikinase inhibitors with FLT3 activity | | |
| ABT-869 | FLT3/VEGFR 1 – 3/PDGFR β /CSF – 1R/Kit | (338) |
| BIBF1120 | FLT3/VEGFR 1 – 3/PDGFR α / β /FGFR 1 – 4/Src | (339) |
| CEP-701 | FLT3/VEGFR 1 – 2/PDGFR β /RET/TrkA | (340, 341) |
| Dovitinib | FLT3/VEGFR 1 – 3/PDGFR α / β /CSF – 1R/Kit/FGFR 1 and 3 | (342) |
| Foretinib | FLT3/Axl/ CSF –1R/ FGFR1/ PDGFR α / β / Kit/ Ron/ Tie-2 /VEGFR1–3 | (297) |
| NVPTAE684 | FLT3/Met/ALK | (343) |
| Sorafenib | FLT3/VEGFR 2 -3/PDGFR β /Kit/B – raf | (344) |
| Sunitinib | FLT3/VEGFR 1 – 3/PDGFR α / β /CSF – 1R/Kit/RET/FGFR1 | (345) |
| Tandutinib | FLT3/PDGFR α / β /Kit | (346) |
| VX-680 | FLT3/Aurora kinase A – C/Abl | (347) |

Table 2.6 List of tyrosine kinase inhibitors with primary putative targets (348). TKIs were chosen to cover the kinome. The inhibitors have been grouped together by principle activity: (i) Jak inhibitors, (ii) IR/IGF – 1R, (iii) EGFR/HER2 inhibitors, (iv) restricted inhibitors with no FLT3 activity, (v) multikinase inhibitors with no FLT3 activity and (vi) multikinase inhibitors with FLT3 activity.

2.10. Cell viability assays

2.10.1. Promega CellTiter-Glo[®] luminescence ATP – based cell viability assay

Cell viability was assessed with the Promega CellTiter – Glo[®] Luminescent Cell Viability Assay (Promega, UK) which is a luciferase – based assay measuring intracellular ATP, as a proxy of cell viability and proliferation. The reagent lyses the cells and complexes thermostable luciferase with ATP to generate a luminescent signal. CellTiter – Glo[®] demonstrates excellent signal to noise and background ratios (349). In addition, there have been recent concerns about the reliability of alternative cell viability assays using tetrazolium (MTT) salt – based assays for TKI assessment, as doses above 1 μ M can interfere with the reduction of MTT to formazan (350). However, the Promega assay which measures intracellular ATP by luminescence is not dependent on compound reduction and so provides a more robust method for cell viability following TKI treatment.

2.10.2. Assessment of activity of TKIs, cytotoxics and combination therapy

Fifty microlitres of 2x serial dilutions of inhibitor/cytotoxic were pipetted, in triplicate, into the wells of opaque – walled 96 well plates (Corning Costar[®]). For screening, each experiment investigated 33 TKIs and a DMSO/distilled water control to account for the effect of the vehicle on cell growth. To account for background luminescent wells containing 100 μ l media but no cells/inhibitor, were assayed. For detailed dose response curves, 50 μ l of serial log concentration dilutions (0.001 μ M – 10 μ M) of 2x concentrations were plated in triplicate.

Cell lines were harvested, counted and suspended in media at 2x10⁵/ml and 50 μ l added to each well. Primary cells were defrosted, counted and viability assessed. Only primary samples with viability >80% were used, suspended in media and seeded at 2000 – 22 000 cells per well. The plates were incubated with TKI at 37°C, 5% CO₂ for 72 hours for cell lines and 48 hours for primary cells. One hour prior to assessing the luminescence of the cells, the plates were removed from the incubator and allowed to equilibrate to room temperature. One hundred microlitres of CellTiter-Glo[®] reagent was added to the wells and the plates were placed on a rotary shaker for 2 minutes, to lyse the cells and aid mixing. The

plates were left for at least 10 minutes to ensure mixing and luminescence assessed with Wallac Victor² 1420 Multilabel Counter (Perkin – Elmer, Boston, USA). The change in cell viability was calculated by reflecting the mean luminescence reading of the treated cells as a percentage of the mean untreated cell wells. The untreated cells were designated 100%. The readings were normalised to the control luminescence readings of DMSO/water to account for their effect on cell growth. Dose response curves were analysed by Graphpad Prism® *vers5.01* for Windows (GraphPad Software Inc., La Jolla, CA, USA) and IC₅₀ generated.

2.10.3. Interaction of TKI and conventional cytotoxic combination therapy

To assess the interaction of specified TKIs with conventional cytotoxics, dose response curves were initially generated for the TKI and chemotherapy in cell lines. To assess drug interactions cell lines were incubated with serial dilutions of TKI and chemotherapy, log concentration dose ranges 0.0001 – 10 μ M, and in combination with a fixed sub – IC₅₀ dose of TKI with serial dilutions of chemotherapy, log concentration dose ranges 0.0001 μ M – 10 μ M. Cell lines and primary cells were prepared as above and 50 μ l added to untreated well in triplicate with a multichannel pipette. 2x dilution of TKI was added to the cells just prior to plating into chemotherapies in triplicate.

Calculusyn (Biosoft, Cambridge UK) was used to analyse the effect of drug – combination studies, using the Cho – Talalay median effect method. Interactions were expressed as combination indices (CI), synergy expressed by CI<1, antagonism CI>1 and an additive effect CI=1 (351, 352) (table 2.7).

| Range of CI | Symbol | Description |
|-------------|--------|------------------------|
| <0.1 | +++++ | Very strong synergism |
| 0.1 – 0.3 | ++++ | Strong synergism |
| 0.3 – 0.7 | +++ | Synergism |
| 0.7 – 0.85 | ++ | Moderate synergism |
| 0.85 – 0.90 | + | Slight Synergism |
| 0.90 – 1.10 | ± | Nearly additive |
| 1.10 – 1.20 | - | Slight antagonism |
| 1.20 – 1.45 | -- | Moderate Antagonism |
| 1.45 – 3.3 | --- | Antagonism |
| 3.3 – 10 | ---- | Strong antagonism |
| >10 | ----- | Very strong antagonism |

Table 2.7 Recommended symbols for describing synergism or antagonism in drug Combination Studies analysed with the Combination Index (CI) Method.

2.11. Cell cycle profiling with Propidium Iodide (PI)

Cell lines were harvested, counted and resuspended in media at concentration of 5×10^5 cells/ml. 2ml was added to 24 well plates (Iwaki) and 1x dilution of the TKI added to prepare 0.15, 0.5 or 1 μ M concentration. Controls were treated with 0.1% DMSO. Cells were harvested at 24, 48 and 72 hours and washed in ice cold PBS, centrifuged at 1600rpm for 5 minutes and permeabilised in 1ml 80% ice cold ethanol for at least 1 hour. Samples which were not analysed on the same day were stored at -20°C , up to 1 week. Post – permeabilisation, cells were washed twice in ice cold PBS, resuspended in 0.25mg/ml Propidium Iodide (Fluka), 0.02mg/ml Concert TM RNase A (Invitrogen) and incubated in the dark for 30 minutes. 500 μ l of PBS was added and samples analysis performed on a Coulter EPICS[®] XL-MCL flow cytometer. Cell cycle profiles were analysed with WinMDI2.9 freeware (Phoenix, USA).

2.12. Assessment of apoptosis

2.12.1. Assessment of Apoptosis by DNA fragmentation

To assess the mechanism of cell death, assessment of apoptosis by DNA fragmentation was performed (353, 354). The cell lines were harvested, counted and resuspended at 1×10^6 cells/ml in 5ml media in 6 well plates (Iwaki). For TKI treated cells 0.5 μ l of 10mM stock was added to prepare final concentration of 1 μ M, DMSO controls had 0.5 μ l added. Control and

treated cells were harvested at 24, 48 and 72 hours. The cells were harvested and centrifuged at 2000rpm for 5 minutes and the supernatant was discarded. The pellet was rinsed to remove the cytoplasmic fraction in 1ml 10mM Tris-HCL pH 8.7, 3mM MgCl₂ (Sigma) and transferred to 1.5ml Eppendorf. The samples were centrifuged at 13 000rpm for 5 minutes and the supernatant discarded. The pellets were dissolved in 100µl 10mM EDTA, 50mM Tris – HCl pH 7.8, 0.5% SDS and RNase A and incubated at 50°C for 15 minutes. Proteinase K (ThermoScientific) was added at a concentration of 1mg/ml and lysates were incubated for a further 30 minutes at 50°C. The samples were diluted 1:1 with 1x Tris, Borate, EDTA (TBE) buffer (Sigma Aldrich), 20% glycerol, and 0.01% v/v bromophenol blue and 20 µl loaded onto a 1.8% agarose gel in 1x TBE. Samples were run alongside 5µl 100bp DNA ladder (Invitrogen) at 100V for 2 hours and incubated in SYBR® Safe (Invitrogen) for visualisation. Images were taken using UV GeneFlash imager (Syngene Bio Imaging, UK).

2.12.2. Assessment of Annexin V – PI staining by flow cytometry

Cell membrane changes occur early in apoptosis with externalisation of the phospholipid, phosphatidylserine (PS), from the inner membrane to the outer leaflet. The calcium – dependent phospholipid – binding protein Annexin V binds strongly to PS on the external membrane. Detection of fluorochrome – labelled Annexin V by flow cytometry has been exploited as a marker of early apoptosis (355). This assay was used assess the mechanism of cell death and to quantify the induction of apoptosis in cells treated with TKI alone, chemotherapy alone or a combination of TKI and chemotherapy.

5x10⁶ cells were harvested, washed, resuspended in 5ml media and seeded in 6 – well plates. The cells were treated with DMSO, TKI, dexamethasone or combination of TKI and dexamethasone and harvested at 24h intervals. Cells were harvested, washed twice in cold PBS, centrifuged at 4°C 1600rpm and resuspended in 100µl 1X Binding Buffer (Invitrogen). Each sample had 2µl FITC – labelled Annexin V (Invitrogen) and 4µl PI (Invitrogen) added and was incubated in the dark for 15 minutes at room temperature. 400µl of binding buffer

was added to each sample, which were analysed by Coulter XL – MCL flow cytometer. Control samples for compensation were made of untreated, Annexin – and PI – only stained cells.

2.13. Immunofluorescence staining

To assess whether the TKIs induced DNA damage, γ H2AX foci were assessed as a proxy of DNA DSB. Nalm17 cell line was exposed to 2Gy ionising radiation to induce DSB as a positive control.

The day prior to the experiment, slides were washed with 70% ethanol/1% HCl on a rotary – shaker for 1 hour and rinsed 4 times in distilled water for 20 minutes. The slides were dried in 37°C incubator overnight. On the day of the experiment poly – L – lysine (Sigma) was placed on each well and left for 20 minutes at room temperature. Excess poly – L – lysine was aspirated and distilled water placed on each well and aspirated off. The slides were placed in 37°C incubator for at least 30 minutes to dry. Cells were harvested, counted and resuspended at concentration 5×10^5 cells/ml in 5ml media. The cells were incubated under 3 conditions: (i) untreated, (ii) 2Gy IR or (iii) inhibitor 1 μ M. The irradiated cells were harvested at 2 hours and cells treated with inhibitor at 24 hours. Cells were centrifuged at 1200rpm for 3 minutes and the supernatant removed. The pellet was resuspended in the remaining media and placed on a well in triplicate and left to adhere for at least 30 minutes. The slides were fixed by being placed upright in a coplin jar in ice cold methanol (Sigma) for 15 minutes. The slides were washed in PBS for 5 minutes, 3 times, at room temperature. Once fixed, the cells were blocked with 10% FCS in PBS and left overnight in a moist box at 4°C. After blocking, the slides were washed for 5 minutes in PBS, 3 times. The excess PBS was wiped off with a cotton bud and 30 μ l of 1:500 mouse phospho - γ H2AX (Upstate) 1%FCS/PBS antibody added to each well. The primary antibody was incubated in moist dark box for 1 hour. Thereafter the slides were washed for 5 minutes in PBS for 3 times. The slides were dried with a cotton bud and 10 μ l of 1:1000 dilution of Alexa Fluor 594 (Invitrogen) secondary antibody was applied to each well and incubated in a moist box at

room temperature for 1 hour. The slides were washed 3 times for 5 minutes in PBS in a foil – covered coplin jar. Excess PBS was dried in between wells and DAPI (Vector Laboratories) placed between each well with a cut 20µl pipette tip. Ethanol – cleaned cover slips were placed over the well and all bubbles removed. Cells were visualised with high – power oil immersion Nikon microscope at 100X and the number of γ H2AX foci in 100 cells counted. DNA damage was present in the irradiated cell line, Nalm 17, with increase in the number of γ H2AX foci. Ten foci per nucleus appeared discriminatory between normal cell cycling and DNA damage. Cells with greater than 10 foci per nucleus were considered to have DNA damage.

2.14. Confirmation of polypoidy by DAPI staining

To assess the nuclear changes induced by TKIs, cell lines were harvested, counted and resuspended at 5×10^5 cells/ml and treated with 1µM TKI. Cells were harvested and centrifuged at 1500rpm for 5 minutes and the supernatant discarded. The cells were rinsed in PBS, recentrifuged at 1500rpm for 5 minutes and the supernatant was discarded. The cells were resuspended in the remaining PBS and pipette onto slide wells in triplicate. 10µL of VECTASHIELD (Vector Laboratories) was pipetted onto each well and mounted with an ethanol cleaned coverslip. The nuclei were visualised with high – power oil immersion Nikon microscope at 100X. Size and shape of nuclei were assessed to demonstrate polyploidy.

2.15. Nucleic acid work

2.15.1. Primer design for Real Time Quantitative Polymerase Chain Reaction

Polymerase chain reaction (PCR) primers were designed on Invitrogen® website (www.invitrogen.com) and synthesised by Invitrogen. Desirable characteristics of the primer sequence were an annealing temperature approximately 70°C with product length of approximately 100bp. The specificity of the primers was assessed with the basic local alignment search tool (BLAST) (www.ncbi.nlm.nih.gov/BLAST). Primers were

reconstituted in sterile RNA free water (Sigma) to a concentration of 200 μ M and stored at -20°C.

2.15.2. Purification of RNA

RNA was typically purified from 5x10⁶ cells with the RNeasy Miniprep kit (Qiagen) according to manufacturer's protocol. RNA was eluted with 40 μ l RNA – free sterile water (Qiagen) and DNA degraded with addition of 1 μ l DNase (Qiagen), incubated for 20 minutes at 37°C and the DNase degraded thereafter for 10minutes at 80°C. RNA content was quantified with a nanodrop spectrophotometer.

2.15.3. Synthesis of complementary DNA (cDNA)

cDNA was synthesised in a 2 stage process. Initially a mastermix consisting of 1 μ g RNA, sterile water, 10mM mixed dNTPs (Promega) and 1 μ l random hexamers (Promega) to a total volume of 12 μ l was denatured for 5 minutes at 65°C then placed on ice for 2minutes. To each sample 4 μ l first strand (FS) buffer, 2 μ l 100mM dithiothreitol (DTT) and 1 μ l Superscript™ II Reverse Transcriptase (Invitrogen) was added for 5 minutes at room temperature. Each sample was incubated at 42°C for 50minutes in an Eppendorf Thermal Cycler, followed by inactivation at 80°C 15minutes. cDNA was used for amplification or stored at -20°C.

2.15.4. FAST SYBR® Green Real time quantitative PCR of cDNA

For each gene, a mastermix was prepared in a sterile 1.5ml tube for each of the genes of interest. For each gene of interest 16 μ l of the mastermix, consisting of 0.25 μ l of 20 μ M forward and reverse primers (table 2.8), 10 μ l FAST SYBR® Green 2x and 5.5 μ l of sterile RNA – free water, and 4 μ l cDNA was added to each well in triplicate on the PCR plate. For each reaction β -actin was utilised as an endogenous control. PCR amplification was performed with Applied Biosystems 7500 Fast Real-Time PCR System for 35 cycles, commencing with denaturing for 3sec at 95°C, annealing/extension step for 30sec at 60°C.

2.15.5. Agarose gel electrophoresis

10x TBE was diluted to 500ml (1x) and 100ml transferred into a 250ml glass container. 1.8g agarose (ThermoScientific) was added to 100ml TBE1x, boiled in a microwave and allowed to cool. 4µl SYBR® Safe DNA gel stain (Life Technologies, UK) was added, the gel poured and combs inserted. 5µl of 100bp DNA ladder (Invitrogen) was pipette into the first lane of the submerged gel and samples, 20µl DNA or RNA transcript, added to the subsequent lanes. The gel was run at 100V for up to 2 hours. Images were taken using UV GeneFlash imager (Syngene Bio Imaging, UK).

2.15.6. Gel extraction and purification

PCR products were visualised with a UV light and individual bands excised with a scalpel blade. The gel was transferred to a clean eppendorf and extraction of product was performed according to the manufacturer's guidelines of the Qiagen QIAquick® Gel extraction kit.

| Primer | Sequence | T _m (°C) | Length (bp) | Control |
|----------------|-------------------------------------|---------------------|-------------|---------|
| Beta actin | Forward CACCATTGGCAATGAGCGGTTTC | 68 | 22 | REH |
| | Reverse AGGTCTTTGCGGATGTCCACGT | 72 | 22 | |
| ALK | Forward TTGTTGGTGATTCCAAGGAG | 67 | 21 | SY-5Y |
| | Reverse GCAGAGAGGGAAGGCTGTC | 72 | 19 | |
| AXL | Forward TGGCTGTGAAGACGATGAAG | 68 | 20 | MCF7 |
| | Reverse TCGTTCAGAACCCTGGAAAC | 68 | 20 | |
| CSF -1R | Forward GTGGCTGTGAAGATGCTGAA | 70 | 20 | HL60 |
| | Reverse CCCAGAAGGTTGACGATGTT | 68 | 20 | |
| EGFR | Forward AACTGTGAGGTGGTCTTGG | 70 | 20 | MCF7 |
| | Reverse GTTGAGGGCAATGAGGACAT | 68 | 20 | |
| HER2 | Forward ACCAAGCTCTGCTCCACACT | 70 | 20 | MCF7 |
| | Reverse ACTGGCTGCAGTTGACACAC | 70 | 20 | |
| HER3 | Forward CAGGGGTGTAAAGGACCAGA | 70 | 20 | MCF7 |
| | Reverse CCCACGCCAGTAGAGAAAAAG | 70 | 20 | |
| HER4 | Forward ACCCCAGTGTGAGAAGATG | 70 | 20 | MCF7 |
| | Reverse GAAACTGTTGCCCTCTGTA | 68 | 20 | |
| FGFR1 | Forward ATGCTAGCAGGGGTCTCTGA | 70 | 20 | HL60 |
| | Reverse ATAGCCTCTGCCAACACCAC | 70 | 20 | |
| FGFR2 | Forward CGCAGCCACGTACACTTCT | 70 | 19 | MCF7 |
| | Reverse CGGCCCTCCTCAGTTTAGT | 70 | 20 | |
| FGFR3 | Forward GACGTGCACAACCTCGACTA | 70 | 20 | REH |
| | Reverse CCAAAGGACCAGACGTCAC | 70 | 20 | |
| FGFR4 | Forward GTGCTGGTGACTGAGGACAA | 70 | 20 | MCF7 |
| | Reverse GTACACCCGGTCAAACAAGG | 70 | 20 | |
| FLT3 | Forward GGACGGACATAAGGTGCTGT | 70 | 20 | SupB15 |
| | Reverse GGCAATGTGGTCTGAGGAGT | 70 | 20 | |
| Kit | Forward TGACTTACGACAGGCTCGTG | 70 | 20 | Kasumi |
| | Reverse CCACTGGCAGTACAGAAGCA | 70 | 20 | |
| Met | Forward TTGGACAATGATGGCAAGAA | 64 | 20 | L428 |
| | Reverse GATGATTCCCTCGGTCAGAA | 68 | 20 | |
| PDGFR α | Forward GCTCAGCCCTGTGAGAAGAC | 72 | 20 | KMH2 |
| | Reverse ATTGCGGAATAACATCGGAG | 66 | 20 | |
| PDGFR β | Forward GACAGGGAGGTGGATTCTGA | 70 | 20 | Nalm 17 |
| | Reverse AGGTGTAGGTCCCCGAGTCT | 72 | 20 | |
| Ron | Forward GTGACTTGATGGCACATTGG | 68 | 20 | KMH2 |
| | Reverse GTCACCCACAGTGACCGAGT | 72 | 20 | |
| RET | Forward ACAGGGGATGCAGTATCTGG | 70 | 20 | HL60 |
| | Reverse AAGCCGAAATCCGAAATCTT | 64 | 20 | |
| Tie - 2 | Forward AGGCAATGCAGGTGAGAGAT | 68 | 20 | MCF7 |
| | Reverse GGAGTCAGCTTGCTCCTTTC | 70 | 20 | |
| Trk A | Forward GTGAGGTTTCTCAGCTCCCC | 72 | 20 | SY - 5Y |
| | Reverse GCGCAGAGAACCTGACTGA | 70 | 19 | |
| VEGFR1 | Forward TCC CTT CCT TCA GTC ATG TGT | 69 | 21 | MCF7 |
| | Reverse AAGAAGGAAACAGAATCTGCAA | 66 | 22 | |
| VEGFR2 | Forward TGATCGGAAATGACACTGGA | 66 | 20 | MCF7 |
| | Reverse CACGACTCCATGTTGGTCAC | 70 | 20 | |
| VEGFR3 | Forward TCGGAGCTCAAGATCCTCAT | 68 | 20 | MCF7 |
| | Reverse CTTGCAGAACTCCACGATCA | 68 | 20 | |
| VDJ Primers | | | | |
| Fr3A | 3'- ACACGGCYSTGTATTACTGT-5' | 57 | 100 | |
| J1H | 3'-ACCTGAGGAGACGGTGACCAGGGT-5' | 57 | 100 | |

Table 2.8 Primers for sequencing nucleic acid work in this study. Transcript for putative RTK targets were assessed with FAST SYBR® Green Reverse Transcriptase quantitative polymerase chain reactions (RT qPCR).

2.15.7. Sequencing of primer products to confirm target

DNA was sequenced using the Big Dye® sequencing kit (Applied Biosystems, UK). For each extracted DNA sample, a final volume of 20µl was added to a 0.2ml PCR tube, which included 4µl 5x buffer, 1µl Big Dye®, 1µl forward/reverse primer and 14µl of DNA. Applied Biosystems 7500 Fast Real-Time PCR System, was used to initially denature the sample for 10 seconds followed by 25 cycles of denaturing for 10 seconds at 95 °C, annealing at 50°C for 5 seconds and 60 °C extension for 4 minutes. The final extension was at 60°C for 10 seconds, followed by 25°C indefinitely. After amplification, each sample was resuspended in 2µl sodium acetate and 50µl ethanol and transferred to 1.5ml tube, vortexed and left at room temperature for 20 minutes to precipitate. Each sample was centrifuged at 13000rpm and the supernatant aspirated. Samples were washed in 250µl 100% ethanol, vortexed, centrifuged at 13000rpm and aspirated dry. After 20 minutes at room temperature, 12µl of Hi – Di™ Formamide (Invitrogen) was added and boiled at 95°C for 5 minutes. Samples were sequenced on 3100 DNA Sequencer 3130xl Genetic Analyzer, Applied Biosystems, Hitachi.

2.16. Xenograft model methods

All murine experiments were conducted according to Home Office Guidelines (Licence 30/2904). Non – obese diabetic/severe combined immunodeficient (NOD/Scid) or Non – obese/severe combined immunodeficient/IL-2 receptor gamma chain deficiency (NOG) mice were used for experiments (Jackson lab, Maine, USA). Both strains of mice lack mature functional B - and T – lymphocytes which enable efficient engraftment of human cells, NOG mice demonstrate additional Natural Killer cell deficiency.

2.16.1. Analysis of engraftment patterns of leukaemic populations

B – cells follow a reproducible pattern of maturity from stem cells to mature plasma B – cells. ALL mirrors the development of normal B – cells, with maturational arrest leading to clonal expansion of B – cell progenitor (pro – B), B – cell precursor (pre – B) or common components. Expression of the surface antigens can be used to identify human leukaemias

(CD45) in murine xenografts and define the subtype of B – cell precursor ALL. To quantify the degree of leukaemia engraftment and the TKI activity on the engrafted leukaemic cells, flow cytometric assessment of human leukaemia cells was performed using fluorochrome – conjugated antibodies (table 2.9).

2.16.2. Primagraft model

Primary leukaemia cells were rapidly thawed, centrifuged, resuspended in media and viability assessed as previously described. Cells were centrifuged and resuspended 1×10^6 cells/ 100 μ l ice – cold PBS and stored on ice until injected. For the initial engraftment kinetic experiments 1×10^6 cells were injected into 8 NOG mice via the lateral tail vein. For TKI experiments, 1×10^6 cells were injected into NOD/Scid mice.

Mice were examined daily for well – being and a maximum of 80 μ l peripheral murine blood was sampled in a week. Red cells were lysed with 1ml 1x red cell lysis concentrate (BD Pharm) for 5 minutes at room temperature, centrifuged at 1600rpm for 5 minutes and the supernatant aspirated. The cells were resuspended in 2ml PBS, transferred to 2 clean 5ml Falcon tubes (one for isotype control and the other for antibody stained cells), centrifuged at 1600rpm, the supernatant aspirated and 14.5 μ l of antibody mastermix (table 2.9) was added to each sample tube and incubated in the fridge for 30 minutes. Cells were washed in ice cold PBS, centrifuged at 1600rpm and the supernatant aspirated. The cells were resuspended in 500 μ l 1% formaldehyde/PBS and assessed with BD™ LSRII Flow Cytometer (BD Biosciences, San Jose, USA). Cell viability was assessed by plotting forward vs. side scatter and the live cells gated for further analysis. Engraftment was established when the human CD45 (hCD45) >1% of total viable cells in murine peripheral blood.

At the end of experiments, mice were killed by cervical dislocation (schedule 1) and the liver, spleen and BM harvested. Single cell suspensions were made by macerating the liver, spleen through a tea-strainer and passed through a 40 μ m cell – strainer (BD Biosciences) into 50ml Falcon tube. Blasts were harvested from femoral bone marrow by flushing femurs with RPMI.

Cells harvested from the liver and spleen were resuspended in 15ml media, layered on 35ml lymphoprep and centrifuged 1600rpm for 30minutes with the brake off. The mononuclear cells were aspirated and washed twice in 10ml media. An aliquot of cells was transferred for analysis and the remaining cells counted and aliquots frozen in 10% DMSO/FCS for storage at -80°C.

Bone marrow cells were washed twice in media and transferred to FACS Falcon tube for staining. Cells were stained with the antibody mastermix (table 2.9) and analysed on BD™ LSRII Flow Cytometer (BD Biosciences, San Jose, USA).

| Antibody | Fluorochrome | Volume per sample (µl) | Company |
|---------------------------|-----------------|------------------------|-------------|
| CD10 | APC | 5 | eBioscience |
| CD19 | PerCP cy 5.5 | 2 | eBioscience |
| CD34 | PE Cy7 | 3 | eBioscience |
| Human CD45 (hCD45) | Pacific Blue | 4 | eBioscience |
| Murine CD45 (mCD45) | Alexa Fluor 700 | 0.5 | eBioscience |
| Total volume of mastermix | | 14.5 | |

Table 2.9 List of fluorochrome – conjugated antibodies for xenograft experiments

2.16.3. Preparation and treatment protocols of TKIs for primagraft experiments

Dovitinib and foretinib were prepared in sterile conditions, dissolved in DMSO and aliquots transferred into sterile tubes. Doses which were not used on the first day were kept at -20°C until required. Drugs were administered via oral gavage.

Mice were randomised to receive treatment or an equal volume of DMSO. For the foretinib experiment, 5 mice were treated with foretinib 30mg/kg/day 5 days on and 9 days off for 2 cycles. Five mice received an equal volume of DMSO as the control cohort. Six mice were treated with dovitinib 65mg/kg/day for 5 days on, 2 days off for 3 cycles, while the control cohort consisted of 5 mice treated with equal volumes of DMSO.

2.16.4. Taqman Molecular analysis of VDJ rearrangement Taq polymerase

To confirm the clonal stability of the murine xenograft model, VDJ rearrangements of transplanted lymphoblasts were assessed by Taq polymerase PCR. 5×10^6 cells of the ALL – 20 pre – injected primary sample and bone marrow, liver and spleen harvested from mice after engraftment were counted, suspended in 10ml media and centrifuged at 1600rpm for 5 minutes at 4°C to pellet the cells. The supernatant was aspirated, the cells washed in chilled PBS and transferred to 1.5ml tubes and kept on ice. Genomic DNA was extracted with Qiagen DNA QIAamp mini-kit according to the manufacturer's protocol. Each reaction was set up to total volume 50µl, consisting of 100 – 500ng DNA, 250ng each primer (table 2.7), 5µl 5x buffer, 20mM each dNTP, DNA/RNA free sterile water (Sigma), a drop of mineral oil and 2Units Taq polymerase. Using an Eppendorf Thermal cycler, hot start amplification was commenced initially denaturing for 94°C for 3 minutes, after which the Taq polymerase was added, then elongation at 80°C for 2 minutes. The reaction was halted and 2 Units Taq polymerase added. The samples were subjected to 38 cycles of denaturing at 94°C for 30 seconds, annealing at 57 °C for 30 seconds and extension at 68 °C for 30 seconds. A final extension of 5 minutes at 80°C. DNA was run on a TBE/agarose gel and sequenced as described 2.15.7.

2.17. Statistical analysis

2.17.1. Analysis of groups

Graphpad Prism® version 5.01 for Windows (GraphPad Software Inc., La Jolla, CA, USA) was used for statistical analysis. Student's t – test as used to measure statistical significance between 2 groups and multiple comparisons were performed with one – way ANOVA. Comparison of 2x2 contingency tables was performed with Chi square or Fisher's exact test. Differences were considered statistically significant when $p < 0.05$ (two – tailed).

2.17.2. Survival comparison

For *in vivo* studies, Kaplan – Meier survival curves were generated by Graphpad Prism vers5 and comparison of vehicle and treatment groups performed by log rank test.

3 Baseline phosphorylation tyrosine kinase profiles of childhood ALL

3.1 Introduction

Recent work by the Stankovic group identified a group of high risk leukaemias which fail to undergo apoptosis by using a robust *in vitro* model for evaluating the mechanisms of resistance to DNA damage induced by ionising radiation (158, 315). Failure to undergo apoptosis after IR – induced DNA damage correlated with poor clinical responses to induction therapy (158). In response to IR, these high risk leukaemias revealed aberrant activation of NF- κ B (315) as well as heterogeneous enrichment of gene sets with anti – apoptotic and proliferative functions which included overrepresentation of gene sets involved in EGF, IGF and PDGF signalling (158). Gene expression array analysis did not reveal significant differences in basal gene expression between apoptotic sensitive and apoptotic resistant tumours, however aberrant activation of (R)TKs by phosphorylation may account for these responses to DNA damage and could provide useful novel biomarkers as well as therapeutic targets.

To address the possible role of aberrant constitutive phosphorylation of RTKs in primary ALL with impaired apoptotic responses to DNA damage, 2 commercially available phospho – RTK array systems were used to detect the phosphorylation status of up to 71 tyrosine kinases in 20 primary ALLs and their relationship with biological and clinical features was investigated. The first tyrosine kinase phosphorylation array is produced by RaybioInc. (Norcross, GA, USA) and enables simultaneous detection of 71 receptor and non – receptor tyrosine kinases. The second array from R&D Systems (Minneapolis, MN, USA) assesses the activation status of 42 RTKs in parallel. Both array systems capture non – phosphorylated and phosphorylated proteins on the membrane – embedded antibodies. Antibodies to the specific (R)TK were spotted in duplicate on the membrane. Only the phosphorylated form is visualised with the binding of a secondary pan – tyrosine antibody.

The main difference between the array systems is the Raybiotech array possesses antibodies for 26 cytoplasmic TKs, while the R&D array only binds RTKs. Table 3.1 demonstrates the

spectrum of RTKs bound by each array with differences between the 2 systems highlighted. Of particular note, the Raybiotech array does not bind FLT3, Mer, Ron or VEGFR – 1 while R&D does not bind ALK, DDR2, EphA5, EphB3, LTK, ROS and RYK. The full spectrum of each array is presented in section 2.8. Neither company has published information about the primary antibodies which are impregnated on the membranes.

The objectives of the work presented in this chapter were to establish baseline phosphorylation profiles of leukaemias stratified by previously identified patterns of apoptotic response to IR – induced DNA damage. Subsequently, current ALL risk criteria were correlated with phosphorylation signals of individual RTK to identify any associations.

| Tyrosine kinase | Raybio® Human RTK array | R&D Systems® Proteome Profiler™ Human Phospho-RTK array |
|-----------------|-------------------------|---|
| ALK | + | - |
| Axl | + | + |
| Dtk | + | + |
| EGFR | + | + |
| ERBB2/HER2 | + | + |
| ERBB3/HER3 | + | + |
| ERBB4/HER4 | + | + |
| EphA1 | + | + |
| EphA2 | + | + |
| EphA3 | + | + |
| EphA4 | + | + |
| EphA5 | + | - |
| EphA6 | + | + |
| EphA7 | + | + |
| EphA8 | + | + |
| EphB1 | + | + |
| EphB2 | + | + |
| EphB3 | + | - |
| EphB4 | + | + |
| EphB6 | + | + |
| FGFR1 | + | + |
| FGFR2 | + | + |
| FGFR3 | + | + |
| FGFR4 | + | + |
| FLT3 | - | + |
| IGF1 – R | + | + |
| Insulin | + | + |
| Kit | + | + |
| LTK | + | - |
| CSF-1R/MCSFR | + | + |
| Mer | - | + |
| Met/HGFR | + | + |
| MuSK | + | + |
| NGFR/TrkA | + | + |
| PDGFR α | + | + |
| PDGFR β | + | + |
| RET | + | + |
| Ron | - | + |
| ROR1 | + | + |
| ROR2 | + | + |
| ROS | + | - |
| RYK | + | - |
| Tie – 1 | + | + |
| Tie – 2 | + | + |
| TrkB | + | + |
| Tyro10/DDR2 | + | - |
| VEGFR1 | - | + |
| VEGFR2 | + | + |
| VEGFR3 | + | + |

Table3.1. Summary of RTK antibodies imprinted on the membrane arrays for each system. Kinases highlighted in grey were imprinted on only 1 of the 2 arrays systems.

3.2 Stratification of primary ALL samples by clinical, genetic features and response to apoptotic induction by IR – induced apoptosis

The 20 childhood B – precursor ALL samples evaluated for RTK phosphorylation profiling were characterised for treatment response based on the biological evaluation of early bone marrow morphology, for the presence or absence of blasts, and the MRD status on day 29 of induction therapy. MRD assessment was performed by identification of a persistent aberrant immunophenotype by flow cytometry (flow MRD) or distinguishing immunoglobulin or T – cell receptor gene rearrangements by polymerase chain reaction techniques (molecular MRD). The patterns of apoptotic response following IR – induced DNA damage were established as a predictive marker for treatment response, according to the methodology previously described (315).

Following the induction of DNA double stranded breaks (DSBs) by 5Gy IR, cells were harvested at 4, 8 and 24 hours. Proficiency of apoptosis was assessed by detecting cleaved products of procaspase 3 and 7 and PARP – 1 proteins at these time points. Normal accumulation of the tumour suppressor p53 protein was also assessed to exclude potential involvement in apoptosis resistance.

Eleven of the 20 ALLs (samples ALL 10 – 20) displayed a proficient apoptotic response after IR – damage with accumulation of p53, cleavage of PARP – 1 and procaspase 3 and 7 by 24 hours (fig 3.1a). The remaining 9 ALLs (samples ALL 1 – 9) displayed an apoptosis defective phenotype, normal accumulation of p53 with no concomitant cleavage of PARP-1 or the procaspases (fig 3.1b). Table 3.2 shows the clinical features, genetic characterisation and apoptotic responses of leukaemias analysed using the R& D and Raybiotech phospho – RTK arrays.

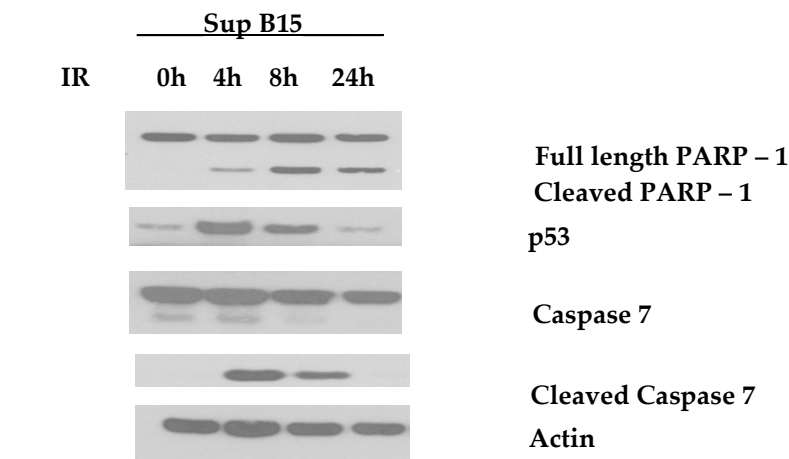


Figure 3.1a

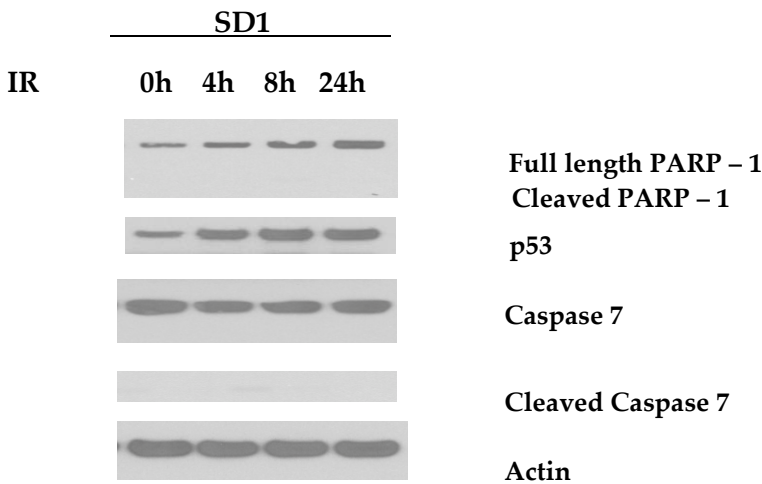


Figure 3.1b

Figure 3.1 Western Blots of representative responses in cell lines to IR – induced apoptosis by 5Gy IR. (a) Ionising radiation induced apoptosis the apoptosis proficient cell line (SupB15). Exposure to 5Gy ionising radiation induces the activation of p53 and leads to apoptosis, demonstrated by the cleavage of PARP – 1 and procaspase 7 (b) Ionising radiation did not induce PARP – 1 cleavage in the apoptosis defective cell line (SD – 1). Exposure to 5Gy IR induces the accumulation of p53 but does not lead to apoptosis.

| Sample code | Age | Sex | WCC | Cytogenetics | Response | Flow MRD | Mol MRD | Apoptosis Phenotype | R&D | Raybiotech |
|-------------|------|-----|-----|--------------------|----------|----------|---------|---------------------|-----|------------|
| ALL-1 | 1 | M | 62 | Hyperdiploid | GER | HR | HR | Defective | + | + |
| ALL-2 | 2 | M | 391 | Non – contributory | GER | SR | HR | Defective | + | + |
| ALL-3 | 15 | M | 117 | Hyperdiploid | PER | SR | HR | Defective | + | + |
| ALL-4 | 4 | M | 2.4 | Non – contributory | GER | HR | NK | Defective | + | + |
| ALL-5 | 14 | M | 11 | Non – contributory | GER | HR | HR | Defective | + | - |
| ALL-6 | 8 | M | 22 | t(12;21) | GER | SR | NK | Defective | + | - |
| ALL-7 | 4.1 | M | 51 | t(12;21) | N/K | HR | SR | Defective | + | - |
| ALL-8 | 10.1 | F | 1.1 | Non – contributory | PER | HR | HR | Defective | + | - |
| ALL-9 | 14 | M | 150 | Non – contributory | PER | HR | HR | Defective | + | - |
| ALL-10 | 7.1 | M | 82 | Non – contributory | GER | SR | SR | Proficient | + | - |
| ALL-11 | 2.2 | F | 88 | Non – contributory | PER | HR | HR | Proficient | + | - |
| ALL-12 | 3 | F | 5 | t(12;21) | GER | SR | SR | Proficient | + | - |
| ALL-13 | 2.75 | F | 5.2 | t(12;21) | GER | SR | SR | Proficient | + | - |
| ALL-14 | 8.9 | F | 74 | t(12;21) | GER | SR | SR | Proficient | + | - |
| ALL-15 | 11.1 | M | 10 | t(12;21) | PER | SR | SR | Proficient | + | - |
| ALL-16 | 3.5 | M | 3.4 | t(12;21) | GER | HR | HR | Proficient | + | - |
| ALL-17 | 2.1 | M | 26 | Non – contributory | GER | NK | SR | Proficient | + | + |
| ALL-18 | 7.8 | M | 9 | Hyperdiploid | GER | NK | SR | Proficient | + | + |
| ALL-19 | 5 | M | 10 | t(12;21) | GER | SR | SR | Proficient | - | + |
| ALL-20 | 12 | F | 109 | Non – contributory | GER | Ind | SR | Proficient | - | + |

Key:

| | |
|------------------|---|
| CR: | Complete Remission |
| D: | Died of disease |
| GER: | Good early response (Blasts < 25% on day 8/15) |
| PER: | Poor early response (Blasts ≥ 25% on day 8/15) |
| MRD: | Minimal residual disease |
| Mol MRD: | Molecular MRD |
| Flow MRD: | Flow cytometric MRD |
| HR: | High Risk leukaemia cells detectable > 0.01% |
| SR: | Standard Risk leukaemia cell not detectable < 0.01% |
| NK | Not known |
| Ind | Indeterminate |

Table 3.2 Clinical features of primary paediatric B – precursor ALL used in this study. Eighteen of the 20 samples were interrogated with the R&D array and 6 samples interrogated with the Raybiotech array.

3.3 Evaluation of Phospho – RTK arrays with human cell lines

Prior to screening the primary leukaemias, the two array systems were evaluated using haematological and non – haematological human cell lines.

3.3.1 Evaluation of Raybio® Human RTK array

The pre – B ALL cell lines Nalm 17 and REH were used for evaluation of the Raybio® Human RTK array. These cells display model patterns of response as described by the *in vitro* model of IR – induced apoptosis (158, 315); Nalm 17 was apoptosis proficient and REH apoptosis defective. Whole cell lysates were prepared from the cell lines and hybridised to the arrays at 4°C overnight. Signal intensities of the RTKs were quantified by optical densitometry, expressed as pixel density and compared (fig 3.2a - c). A clear differential in the phosphorylation of kinases was evident in the 2 cell lines tested (fig 3.2a and b). Nalm 17 demonstrated phosphorylation of specific members of the Eph family (EphA3, EphA5, EphA6, EphA8, EphB1-2), platelet – derived growth factor receptor β (PDGFR β) and vascular endothelial growth factor receptor – 2 (VEGFR2), while REH expressed signal from the non – receptor kinases JAK3, Lck and ZAP-70. Of the RTK signals common to both cell lines IGF-1R demonstrated a marked reduction in intensity in the Nalm17 cell line compared with REH. IGF – 1R was selected as the candidate protein for validation using Western Blotting as an independent technique for comparing RTK phosphorylation.

Subsequently, immunoblotting revealed the presence of IGF-1R beta subunit at 95kDa in both Nalm17 and REH lysates, while phosphorylation of IGF-1R Tyr¹¹³¹ was detectable only in the REH and not Nalm 17 lysates (fig 3.3). The tyrosine residue Tyr¹¹³¹ is located in the intrinsic kinase domain. These data independently validate the array data indicating that the arrays can be used to differentiate between phospho – RTK profiles in haematological cells.

Baseline phosphorylation profiles

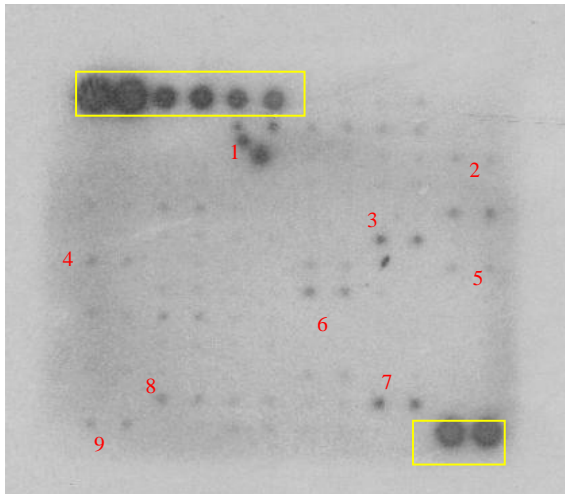


Figure 3.2a

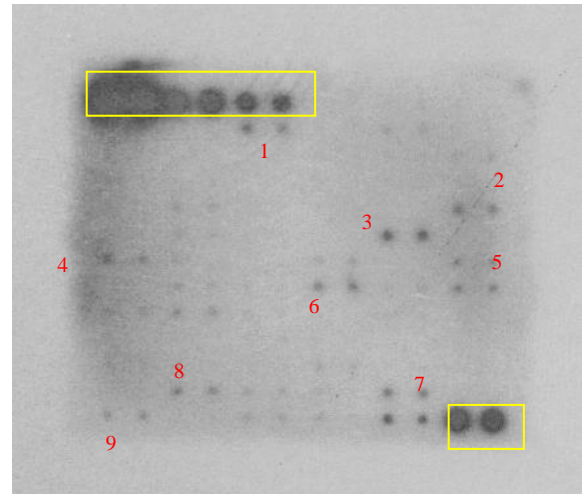


Figure 3.2b

Key: (R) TKs phosphorylated in both cell lines: Positive controls are boxed in yellow

- | | |
|------------|------------|
| 1. Axl | 6. JAK2 |
| 2. ErbB3 | 7. TXK |
| 3. FGFR2 | 8. Tie – 2 |
| 4. Fgr | 9. Tyk2 |
| 5. IGF -1R | |

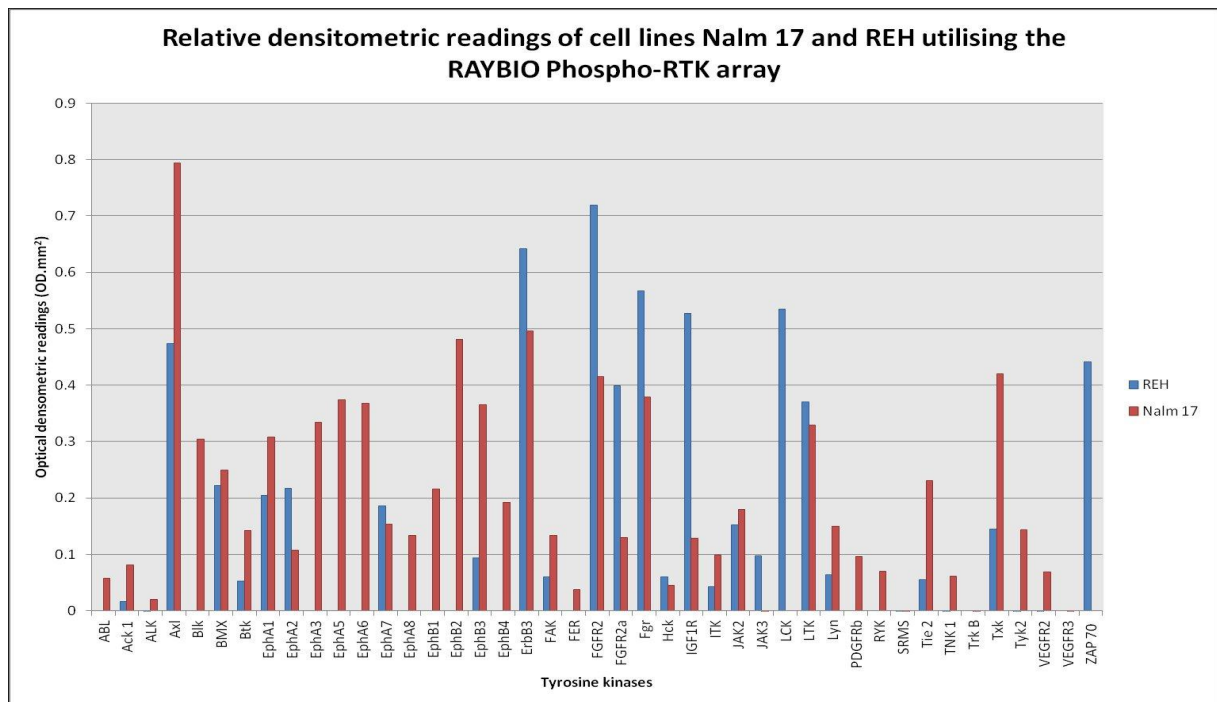


Figure 3.2c

Figure 3.2 Phosphorylation signal of (R)TKs in pre – B ALL cell lines (Nalm 17 and REH) using Raybiotech arrays. Both cell lines demonstrated phosphorylation of Axl, EphA1, EphA7, EphB3, FGFR2, FGFR2α, IGF – 1R, LTK and Tie – 2. Differential phosphorylation of numerous (R) TKs was identified using the Raybiotech array in: (a) Nalm 17 and (b) REH cell lines. Phosphorylated tyrosine kinases common to both cell lines are numbered in the key. The positive controls are contained in the yellow boxes. (c) Optical densitometry was performed on the duplicate signals and phosphorylation profiles established for each ALL cell line.

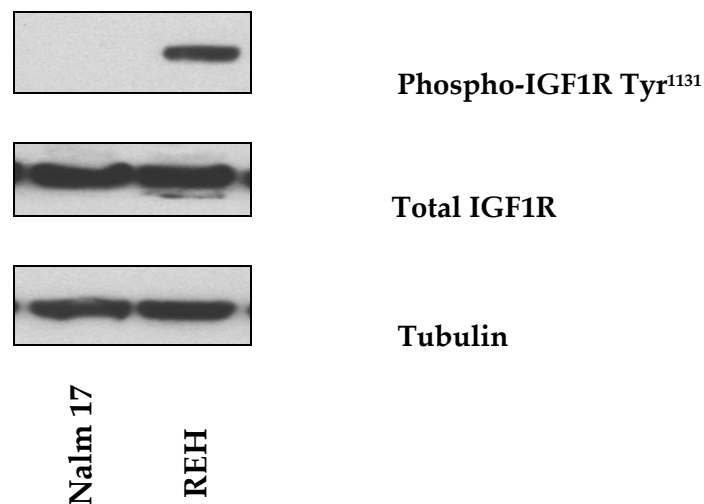


Figure 3.3 Western Blot analysis demonstrates differential phosphorylation signal of IGF – 1R in REH and Nalm 17 B – cell precursor ALL cell lines. The difference in phosphorylation intensity observed on the Raybio® Human Proteome RTK Arrays was confirmed on Western Blot. Total expression of IGF – 1R was equal in both cell lines.

3.3.2 R&D Systems® Proteome Profiler™ Human Phospho-RTK array

To evaluate the sensitivity of the second phospho – RTK array (R&D), the HB2 human mammary luminal epithelial cell line was used, which overexpresses EGFR (356). To assess the sensitivity and specificity of the arrays HB2 cells were subjected to three pre-treatment conditions in DMEM media with 10% FCS; (i) no pretreatment, (ii) 20 ng/ml EGF for 10 minutes and (iii) 0.5 μ M gefitinib (EGFR/HER2 inhibitor) for 5 hours followed by 20ng/ml EGF for 10 minutes. Whole cell lysates were hybridised to the arrays and visualised by chemiluminescence. Fig 3.4a (i-iii) shows the arrays hybridised with HB2 lysates from each of the corresponding conditions described. As expected, the EGFR phosphorylation signal increased following the addition of EGF and with concomitant activation of receptors, Mer and Tie-2 and pre – incubation with an EGFR inhibitor reduced EGFR phosphorylation corresponding to a decrease in signal intensity. Quantification by optical densitometry of pixel density (OD/mm²) confirmed more than a four-fold increase in EGFR phosphorylation by EGF treatment which reduced to below the basal level following gefitinib treatment (fig 3.4b).



Fig 3.4a (i)

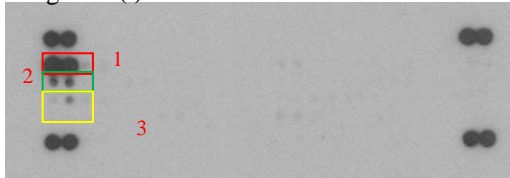


Fig 3.4a (ii)

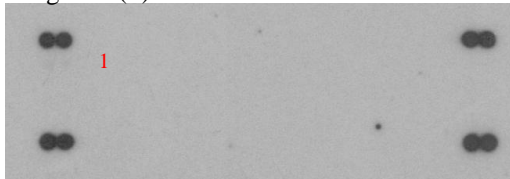


Fig 3.4a (iii)

Figure 3.4a

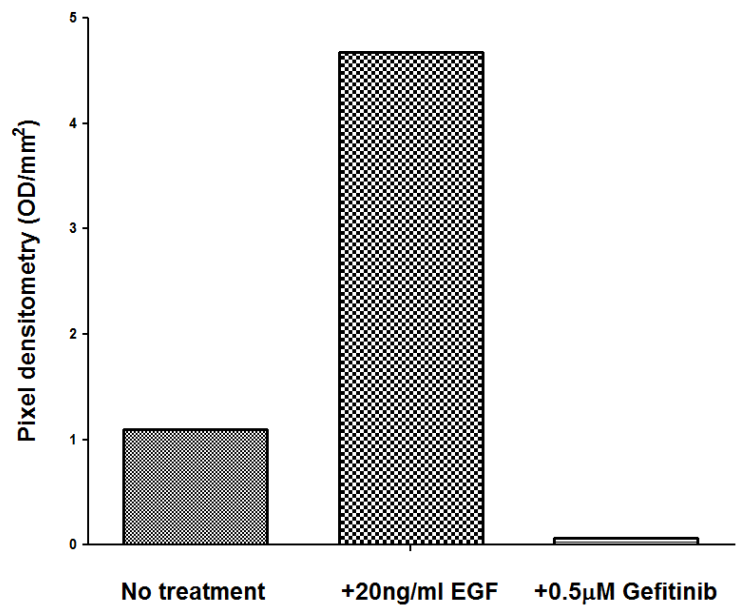


Figure 3.4 R&D phospho – RTK arrays hybridised with lysates from HB2 mammary epithelial cells. (a) Arrays reveal EGFR expression (red box) in untreated cells (i) which increases following EGF pre-treatment concomitantly with Mer (green box) and Tie 2 (yellow box) (ii), and which are inhibited following gefitinib treatment (iii). Blue boxes show duplicate positive controls in all conditions, (B) Graph of densitometry value of phosphorylated EGFR from arrays from each condition.

Western Blot analysis was used to validate these array data (fig 3.5). EGFR protein levels were consistent between the three conditions whereas phosphorylated EGFR Tyr⁹⁹² increased following EGF treatment and reduced profoundly following gefitinib – mediated inhibition. These data show that the R&D phospho – arrays can provide quantifiable and reproducible data regarding phosphorylation status of RTKs.

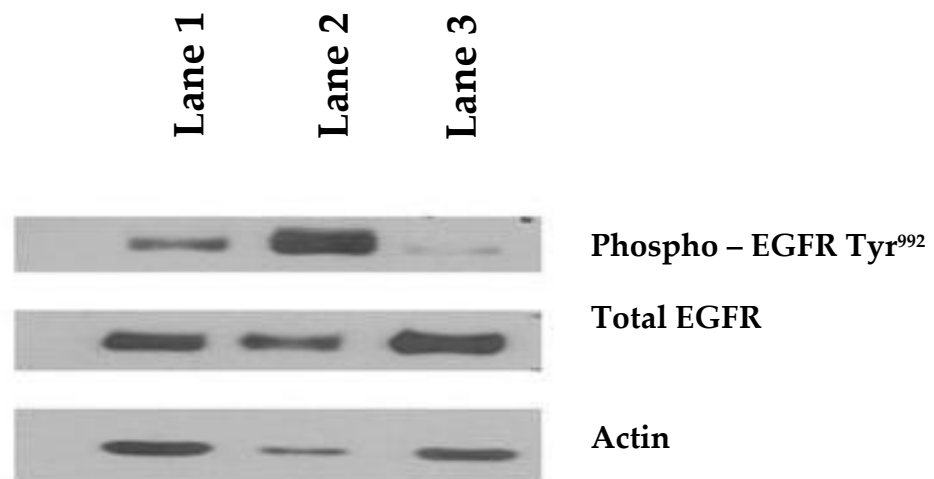


Figure 3.5 Western Blot showing stimulation and inhibition of EGFR phosphorylation in HB2 cell line, validating the phospho – RTK array findings. The phosphorylation site Tyr⁹⁹² was blotted for following addition of 20ng/ml EGF (lane 2) and incubation with 0.5μM gefitinib (lane 3) treatment compared with no treatment (lane 1) confirming previous array data. Total EGFR and Actin serve as loading controls

3.4 Screening of primary ALL cells for baseline phosphorylation profiles with Phospho – RTK arrays

Subsequent to the successful evaluation of the arrays, screening for baseline RTK phosphorylation profiles in 20 primary ALL was initiated. Of the 20 samples, 18 leukaemias were profiled with the R&D array system, while 8 were hybridised to the Raybiotech array and 6 samples were investigated with both arrays (table 3.2). Cells were thawed in RPMI media with 10% serum and then washed twice in warm PBS and prepared for the arrays according to the manufacturer's instructions. Multiple RTK signals were detected on both arrays in all primary cells tested by both arrays, over a range of intensities. Optical densitometric readings were performed on all visible phosphorylation signals to develop a profile of parallel kinase activation for each ALL.

3.4.1 Baseline phosphorylation profiles of 8 leukaemias with Raybiotech array

In the 8 leukaemia samples investigated with the Raybiotech array, a restricted and relatively homogeneous population of phosphorylated kinases was detected. Signals were present for only 4 tyrosine kinases in total (fig 3.6). Two non – receptor tyrosine kinases Txk and JAK2 were detected, with Txk present in all 8 samples and JAK2 in 7/8. The RTKs, Axl and FGFR2, were present in 4 and 7 of the 8 samples respectively. Signal intensity ranged from 0.0078 – 0.1462 OD/mm².

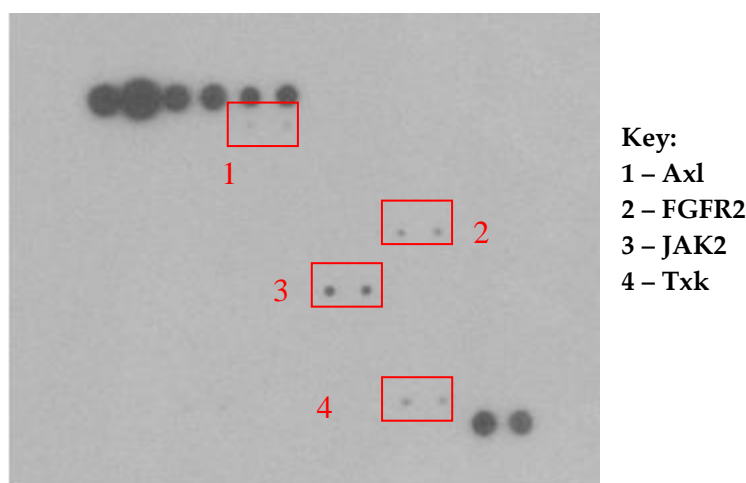


Figure 3.6a

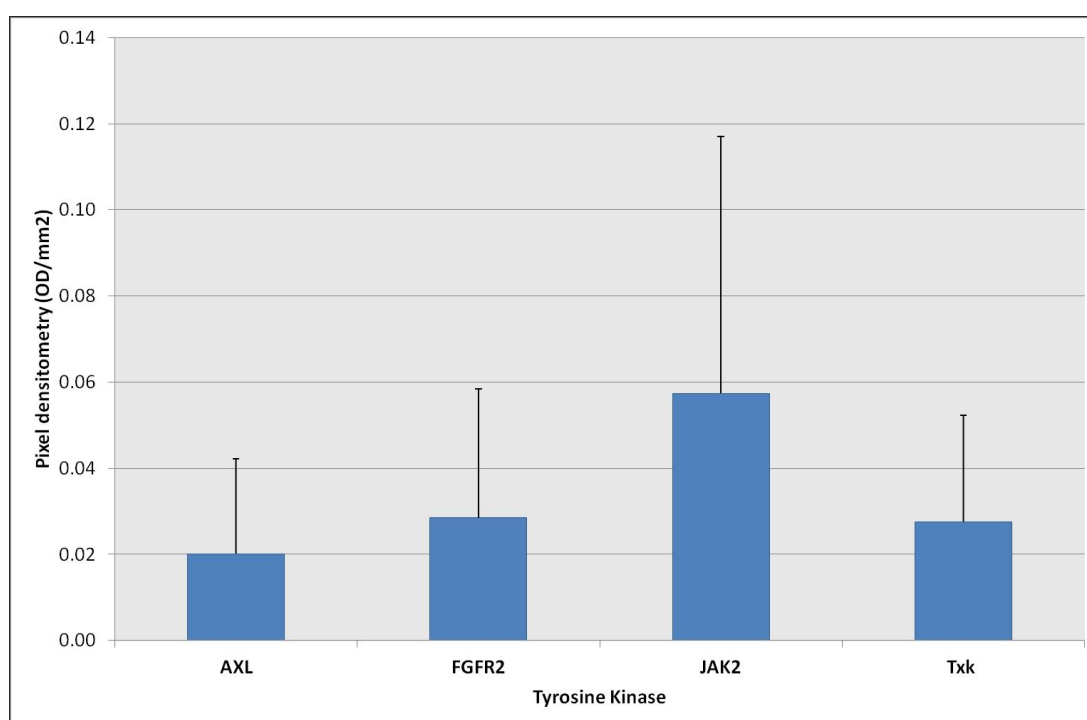


Figure 3.6b

Figure 3.6 The Raybiotech array system identified a restricted repertoire of (R) TKs in the 8 primary leukaemia samples investigated (a) The presented array is representative of the 8 ALL samples as it reveals the 4 phosphorylated tyrosine kinases, namely 2 non – receptor tyrosine kinases (JAK and Txk) and 2 RTKs (Axl, FGFR2). (b) The bar graph demonstrates the mean phosphorylation signals measured by pixel densitometry (optical density per millimetre squared) of each of the (R)TKs reported of the 8 primary ALL samples; error bars are expression of standard deviation. The most intense mean phosphorylation signal was JAK2.

3.4.2 Baseline phosphorylation profiles of 18 leukaemias with R&D array

Subsequently the baseline phosphorylation profiles of 18 samples were assessed with the R&D arrays (representative blot displayed in fig 3.7a). Unlike the Raybiotech array, marked heterogeneity was observed in the leukaemia phosphorylation patterns assessed by the R&D array. Signals were derived from an average of 33 RTKs per sample, with a wide variation in intensity after accounting for background, from 0.0007 to 3.71 OD/mm².

Fig 3.7b shows the mean phosphorylation of each individual RTK for the 18 leukaemias. Dtk, which exhibited the most activation, was followed in order by EGFR, EphB2, Ron, Tie – 2, Tie – 1, Mer, ErbB2/HER2, ErbB4/HER4 and FGFR3.

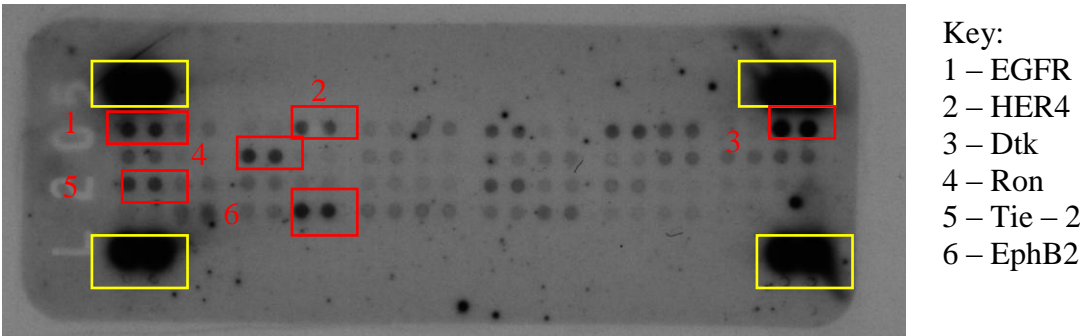


Figure 3.7a

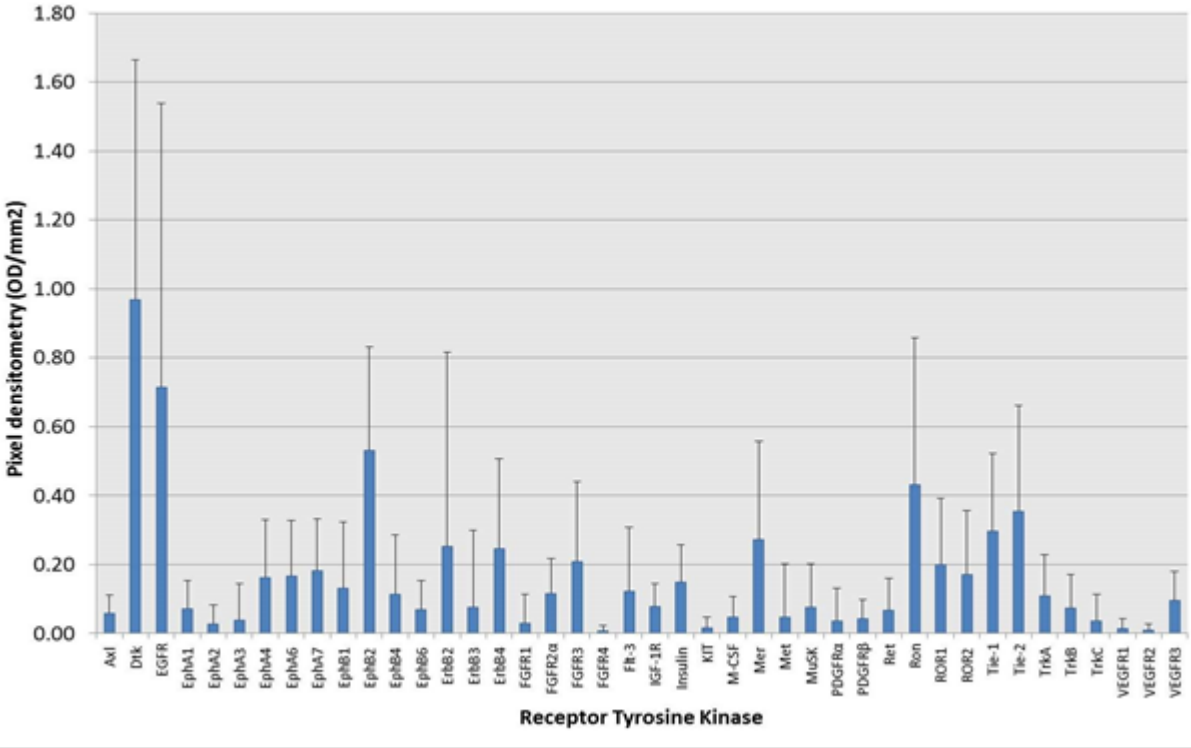


Figure 3.7b

Figure 3.7 An heterogeneous repertoire of RTKs was identified with the R&D array system in 18 primary leukaemia samples. (a) Representative array of a primary ALL sample using the R&D array system. Positive controls are boxed in yellow. Signals from 7 of the 10 most intense signals are demonstrated, namely EGFR, HER4, Dtk, Ron, TIE – 2 and EphB2, (b) Mean phosphorylation signals for the individual RTKs of the 18 primary leukaemia samples assessed with the R&D array. Error bars are standard deviations.

3.4.3 Baseline phosphorylation of 6 samples analysed on both arrays

Six samples were analysed using both arrays, ALL 1 – 4, ALL 17 and ALL – 18. Axl and FGFR2 were the only 2 RTKs detected on both arrays. Phosphorylation of Axl was detectable in 2/6 samples assessed with the Raybiotech array and 4/6 leukaemias on the R&D array system (fig 3.8a and b). Phosphorylation of FGFR2 was present in all 6 samples analysed with both arrays, but there was no direct correlation between the signal intensity derived from each array.

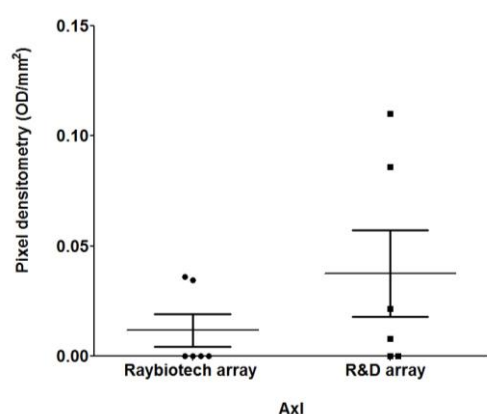


Figure 3.8a

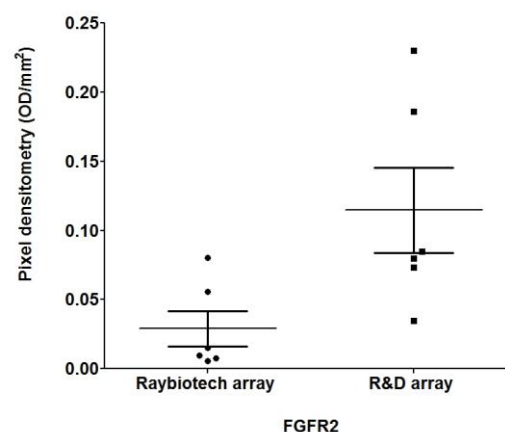


Figure 3.8b

Figure 3.8 Dot plots comparing the Axl and FGFR2 signals derived from the 2 array systems. Mean intensity of phosphorylation signals of the RTKS (a) Axl and (b) FGFR2 were higher in R&D arrays. No obvious relationship was observed between the signal intensities investigated by the 2 arrays.

Table 3.3 shows the level of phosphorylation observed on the Raybiotech did not correlate with signals derived from the R&D array. The lack of concordance may be due to the avidity of antibodies used in the different array systems.

| Leukaemia Sample | Raybio Axl | R&D Axl | Raybio FGFR2 | R&D FGFR2 |
|------------------|------------|---------|--------------|-----------|
| ALL – 1 | 0 | 0.008 | 0.01 | 0.23 |
| ALL – 2 | 0 | 0.11 | 0.0056 | 0.085 |
| ALL – 3 | 0 | 0 | 0.015 | 0.186 |
| ALL – 4 | 0 | 0.086 | 0.008 | 0.079 |
| ALL – 17 | 0.034 | 0 | 0.056 | 0.074 |
| ALL – 18 | 0.036 | 0.022 | 0.08 | 0.035 |

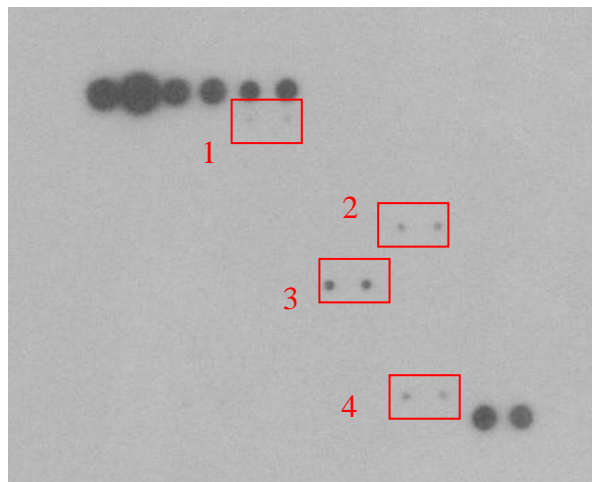
Table 3.3 Comparison of the phosphorylation signals for Axl and FGFR2 derived from the 2 array systems. No direct relationship was present between the phosphorylation signals in the 2 systems used to investigate the 6 primary ALL samples. Data presented is the mean optical densitometry reading for each (R)TK derived for the primary ALLs.

3.5 Association of apoptotic phenotype with baseline phosphorylation signal

RTK phosphorylation profiles were investigated for an association with apoptotic phenotypes, clinical, biological or genetic features. Eight samples (n=4 apoptosis proficient and n=4 apoptosis deficient) were investigated with the Raybiotech array, while 18 leukaemias were assayed for the R&D experiments (9 samples in each apoptotic phenotype).

The RTK phosphorylation profile from the 8 ALLs analysed using the Raybiotech array showed an association with apoptotic phenotype (fig 3.9a and b). JAK2, Txk, Axl and FGFR2 were all phosphorylated in the apoptosis proficient leukaemias, whereas the JAK2, FGFR2 and Txk signal intensities were reduced and Axl virtually absent in the apoptosis defective samples.

The tyrosine kinase with the most intense mean phosphorylation signal was JAK2, with mean intensity of 0.09 (SD±0.06) OD/mm² in the apoptotic sensitive leukaemias, compared with 0.02 (SD±0.01) OD/mm² in the apoptotic defective samples (fig 3.10). Comparison of signal intensities by t – test, identified a significant difference in level of phosphorylation between the 2 groups (apoptotic proficient and apoptotic defective) for the (R)TKs Axl (p<0.0001) and Txk (p<0.005). Comparison of FGFR2 and JAK2 signals exhibited a statistically non – significant difference (p=0.07), with a higher phosphorylation signals present in the apoptotic proficient leukaemias.



Key for both figures:

- 1 – Axl
- 2 – FGFR2
- 3 – JAK2
- 4 – Txk

Figure 3.9a

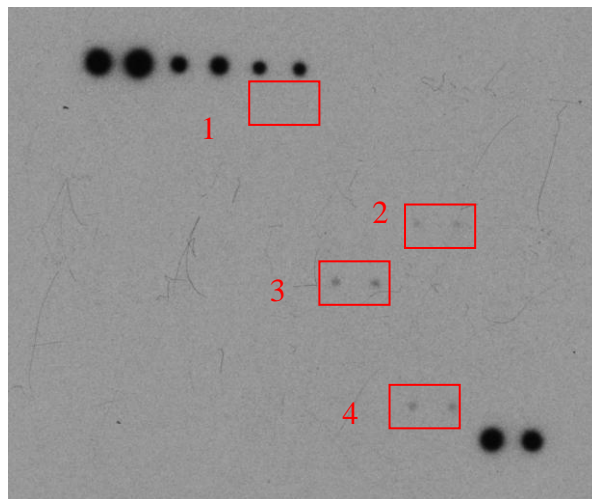


Figure 3.9b

Figure 3.9 Representative Raybiotech arrays of samples stratified by apoptotic phenotype. Phosphorylation signals were present for Txk in all 8 samples. The tyrosine kinases JAK2 and FGFR2 were expressed in (a) 3/4 apoptosis proficient leukaemias and (b) all the apoptosis defective samples. 4/4 apoptotic sensitive samples demonstrated an additional low level signal at Axl. The mean intensity of all signals were greater in cells with proficient apoptotic response. The TKs are numbered 1 – 4.

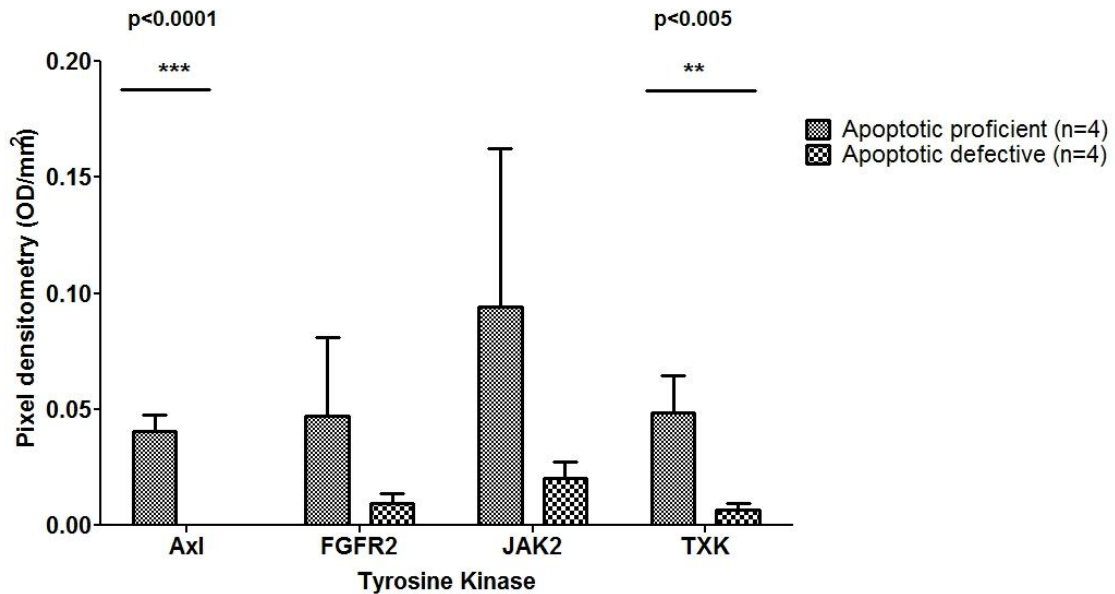


Figure 3.10 Increased phosphorylation signals of the kinases Axl and Txk correlate with the apoptosis proficient leukaemias. The mean intensity of phosphorylation signals for all kinases identified in the 8 primary ALL samples investigated with Raybiotech arrays was higher in the apoptotic proficient samples. Significantly more intense signals were identified in the Axl ($p<0.0001$) and Txk ($p<0.005$) kinases of the apoptotic proficient leukaemia samples. Error bars are standard error of mean.

The baseline phosphorylation profiles of 18 samples derived from the R&D arrays were correlated with the defined apoptotic phenotypes, 9 apoptosis proficient and the 9 apoptosis defective.

Fig 3.11 shows the distribution of the most intense signals in the cohort with normal apoptotic responses to IR (shown in blue) included Dtk which exhibited the most activation, followed in order by EphB2, EGFR, Tie-2, RON, FGFR3 and Mer. Similarly, in the cohort with defective apoptotic responses (shown in red), the RTK with the highest mean phosphorylation signal was Dtk, followed in order by EGFR, EphB2, RON, Tie-1, ErbB2/HER2, ErbB4/HER4 and Mer.

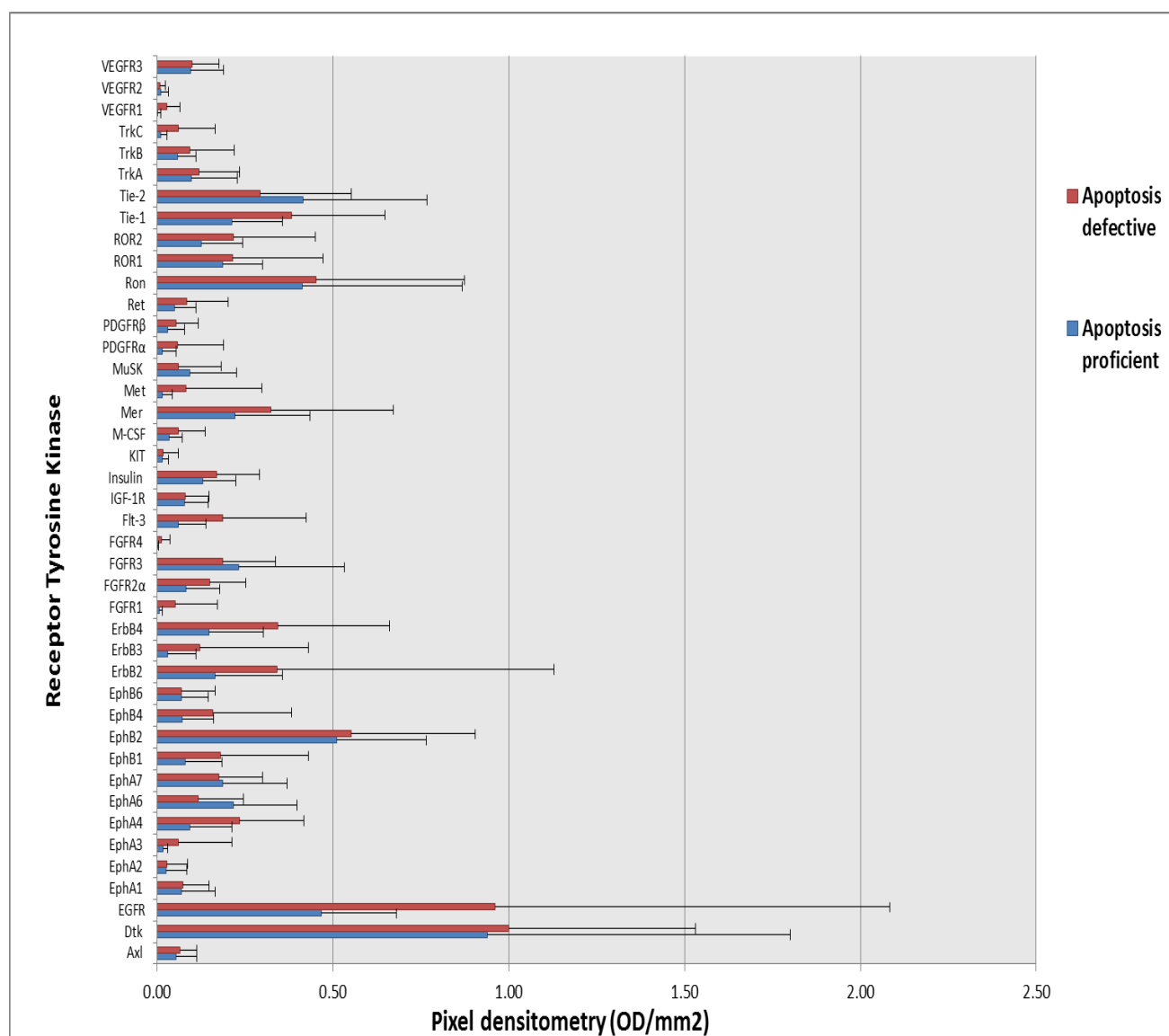


Figure 3.11 Comparison of signal intensity of ALL samples stratified by apoptotic phenotype using R&D array system. The strongest signals were derived from 5 RTK families: TAM, EGFR, Met and Tie. Mean phosphorylation signals were calculated for each cohort (n=9) and plotted, error bars are the standard deviation for each mean RTK signal.

To identify RTKs which were significantly differentially phosphorylated, a direct comparison of signal intensity was performed using the parametric unpaired t-test (table 3.4). No significant difference was identified in mean phosphorylation of any of the RTKs between the 2 groups categorised by apoptotic phenotype.

| | Apoptosis proficient (n=9) | Apoptosis defective (n=9) | | | Apoptosis proficient (n=9) | Apoptosis defective (n=9) | |
|----------------|----------------------------------|---------------------------------|--------------|----------------|----------------------------------|---------------------------------|--------------|
| RTK | Mean (SD) | Mean (SD) | p – value | RTK | Mean (SD) | Mean (SD) | p – value |
| Axl | 0.05 (0.06) | 0.06 (0.05) | 0.64 | IGF-1R | 0.08(0.07) | 0.08(0.07) | 0.99 |
| Dtk | 0.94 (0.86) | 1.00(0.53) | 0.86 | Insulin | 0.13(0.09) | 0.17(0.12) | 0.45 |
| EGFR | 0.47(0.21) | 0.96(1.12) | 0.21 | Kit | 0.02(0.02) | 0.02(0.04) | 0.88 |
| EphA1 | 0.07(0.09) | 0.07(0.07) | 0.93 | M-CSF | 0.03(0.04) | 0.06(0.08) | 0.37 |
| EphA2 | 0.03 (0.06) | 0.03(0.06) | 0.95 | Mer | 0.22(0.21) | 0.32(0.35) | 0.46 |
| EphA3 | 0.02 (0.02) | 0.06(0.15) | 0.39 | Met | 0.01(0.03) | 0.08(0.22) | 0.35 |
| EphA4 | 0.09(0.12) | 0.23(0.18) | 0.07 | Ron | 0.41(0.46) | 0.45(0.42) | 0.86 |
| EphA6 | 0.22(0.18) | 0.12(0.13) | 0.19 | MuSK | 0.09(0.13) | 0.06(0.12) | 0.60 |
| EphA7 | 0.19(0.18) | 0.18(0.12) | 0.89 | PDGFR α | 0.01(0.04) | 0.06(0.13) | 0.35 |
| EphB1 | 0.08(0.10) | 0.18(0.25) | 0.29 | PDGFR β | 0.03(0.05) | 0.05(0.06) | 0.35 |
| EphB2 | 0.51(0.26) | 0.55(0.35) | 0.78 | Ret | 0.05(0.06) | 0.08(0.12) | 0.43 |
| EphB4 | 0.07(0.09) | 0.16(0.23) | 0.30 | ROR1 | 0.19(0.11) | 0.22(0.25) | 0.75 |
| EphB6 | 0.07(0.08) | 0.07(0.10) | 1.00 | ROR2 | 0.12(0.12) | 0.22(0.23) | 0.31 |
| ErbB2/HER2 | 0.16(0.19) | 0.34(0.79) | 0.52 | Tie-1 | 0.21(0.14) | 0.38(0.27) | 0.11 |
| ErbB3/HER3 | 0.03(0.08) | 0.12(0.31) | 0.39 | Tie-2 | 0.41(0.35) | 0.29(0.26) | 0.42 |
| ErbB4/HER4 | 0.15(0.15) | 0.34(0.32) | 0.11 | Trk A | 0.10(0.13) | 0.12(0.12) | 0.73 |
| FGFR1 | 0.01(0.01) | 0.05(0.12) | 0.27 | Trk B | 0.06(0.05) | 0.09(0.13) | 0.44 |
| FGFR2 α | 0.08(0.09) | 0.15(0.10) | 0.16 | Trk C | 0.01(0.02) | 0.06(0.11) | 0.18 |
| FGFR3 | 0.23(0.30) | 0.19(0.15) | 0.68 | VEGFR1 | 0.00(0.01) | 0.03(0.04) | 0.07 |
| FGFR4 | 0.00(0.00) | 0.01(0.02) | 0.22 | VEGFR2 | 0.01(0.02) | 0.01(0.01) | 0.97 |
| FLT3 | 0.06(0.08) | 0.19(0.24) | 0.15 | VEGFR3 | 0.10(0.09) | 0.10(0.08) | 0.94 |

Key

SD

Standard deviation

Statistical analysis

t – test

Table 3.4 Mean RTK phosphorylation signal intensities derived by R&D array in apoptosis proficient and apoptosis defective ALL groups and statistical comparisons. No statistically significant difference in phosphorylation was identified, but differences in EphA4 and VEGFR1 phosphorylation approached significance. Data presented is the mean optical densitometry reading for each RTK derived for the primary ALLs, standard deviation is presented in parentheses.

In summary, significant differential TK signals were identified on the Raybiotech array when the primary leukaemias were stratified by apoptotic phenotype, but not significantly with the R&D array. The phosphorylation signals with the higher intensity were derived from the apoptotic proficient leukaemias on the Raybiotech arrays.

3.6 Association of cytogenetic groups with RTK phosphorylation profiles

To determine whether a relationship could be established between particular cytogenetic abnormalities and RTK phosphorylation profiles, the samples were categorised according to cytogenetic subtype. Of the 20 samples investigated, 8 had t(12;21), 3 were hyperdiploid and the remaining 9 possessed either normal (n=5) or cytogenetic findings which at present are not recognised to influence outcome in current UK treatment protocols and thus do not alter treatment schedules (n=4). The cytogenetic findings for these 4 samples included t(3;22), 46XY +7q+12p, 46XX t(3;10) t(9;16) +8 biallelic del p16 and 45XY dic(9;20)+8-13. For the purpose of this study, the cytogenetic profile for these 9 samples has been designated 'non – contributory' in the text and figures (table 3.2).

The cytogenetic subtypes of the 8 leukaemias used in the Raybiotech experiments, consisted of 1 t(12;21), 3 hyperdiploid and 4 non – contributory samples. There were no differences in the mean phosphorylation signals for JAK2 and Txk across all 3 cytogenetic subtypes (fig 3.12a and b). FGFR2 signals were detected in the hyperdiploid (n=3) and 'non – contributory' (n=4) groups, but not in the t(12;21) sample (fig 3.12c). Phosphorylation of Axl was detected in 1/3 hyperdiploid, 2/4 'non – contributory' samples and the t(12;21) leukaemia (fig 3.12d). The sample size for each cytogenetic group was not sufficient to analyse by column statistics.

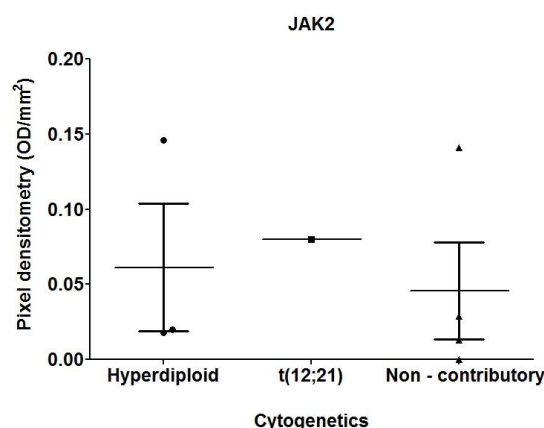


Figure 3.12a

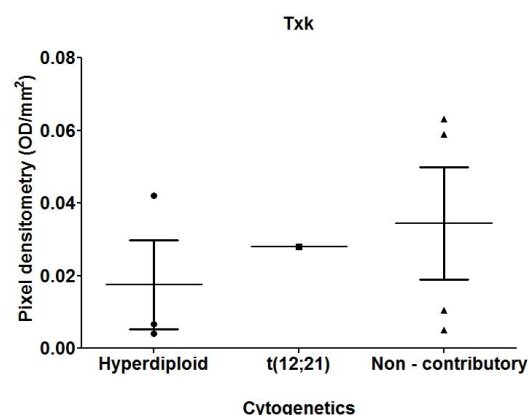


Figure 3.12b

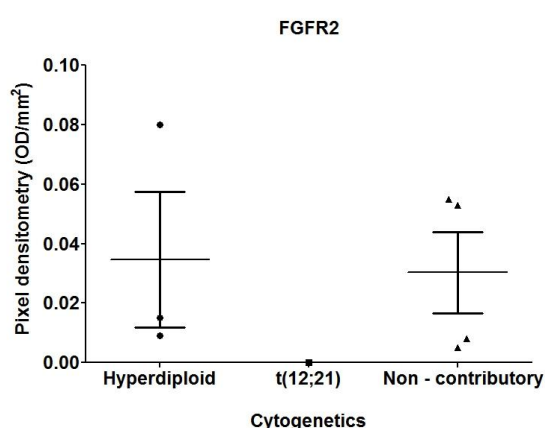


Figure 3.12c

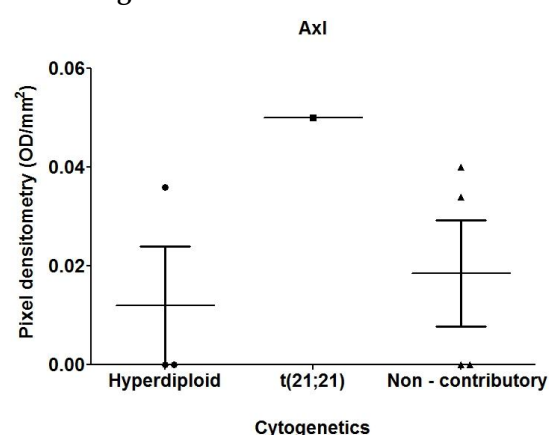


Figure 3.12d

Figure 3.12 a – d Dot plots of phosphorylation signals of primary ALL samples grouped by cytogenetics assayed by Raybiotech arrays. No statistically significant correlations were identified in the cytogenetic subgroups between the phosphorylation signals of (a) JAK2, (b) Txk, (c) FGFR2 and (d) Axl.

The phosphorylation signal intensity observed in the 3 hyperdiploid samples was not significantly different from the other cytogenetic subgroups both when analysed against non – contributory group alone (n=4) or against all other leukaemia samples in the Raybiotech panel (table 3.5).

| | Hyperdiploid (n = 3) | Rest (n = 5) | t-test (p – value) | Non – contributory (n = 4) | Rest (n = 4) | t-test (p – value) |
|-------|-------------------------|-----------------|-----------------------|-------------------------------|-----------------|-----------------------|
| Axl | 0.01(0.02) | 0.03(0.02) | 0.46 | 0.02 (0.02) | 0.02(0.03) | 0.86 |
| FGFR2 | 0.04(0.04) | 0.02 (0.03) | 0.66 | 0.03(0.03) | 0.03 (0.04) | 0.86 |
| JAK2 | 0.06(0.07) | 0.05 (0.06) | 0.89 | 0.05(0.06) | 0.07 (0.06) | 0.64 |
| Txk | 0.02 (0.02) | 0.03(0.03) | 0.44 | 0.03(0.03) | 0.02(0.02) | 0.46 |

Table 3.5 Comparison of cytogenetics groupings in the 8 ALL samples investigated with the Raybiotech array system. No statistically significant differences were identified in the comparison of (a) hyperdiploid samples and (b) non – contributory samples with the remaining samples. Data presented is the mean optical densitometry reading for each RTK derived for the primary ALLs, standard deviation is presented in parentheses.

The cytogenetic profiles of the 18 leukaemias investigated with the R&D array were 3 hyperdiploid, 8 non – contributory and 7 t(12;21) ALLs. Mean RTK phosphorylation signal intensity was determined for each of these subgroups.

In all 3 cytogenetic groups Dtk demonstrated the highest mean signal; however the pattern of highest phosphorylated RTKs were notably different between the cytogenetic groups (fig 3.13). The pattern of phosphorylation was different in the hyperdiploid group, with Mer and FLT3 demonstrating the next highest signals after Dtk. These were followed by Ron, EGFR and EphB2. When the RTK phosphorylation profiles of these three cytogenetic groups were analysed using one way ANOVA (see table 3.6), no statistically significant differences were observed, the phosphorylation signals of 2 RTKs, EphA2 and FLT3, approached significance (p=0.07 and p=0.09, respectively).

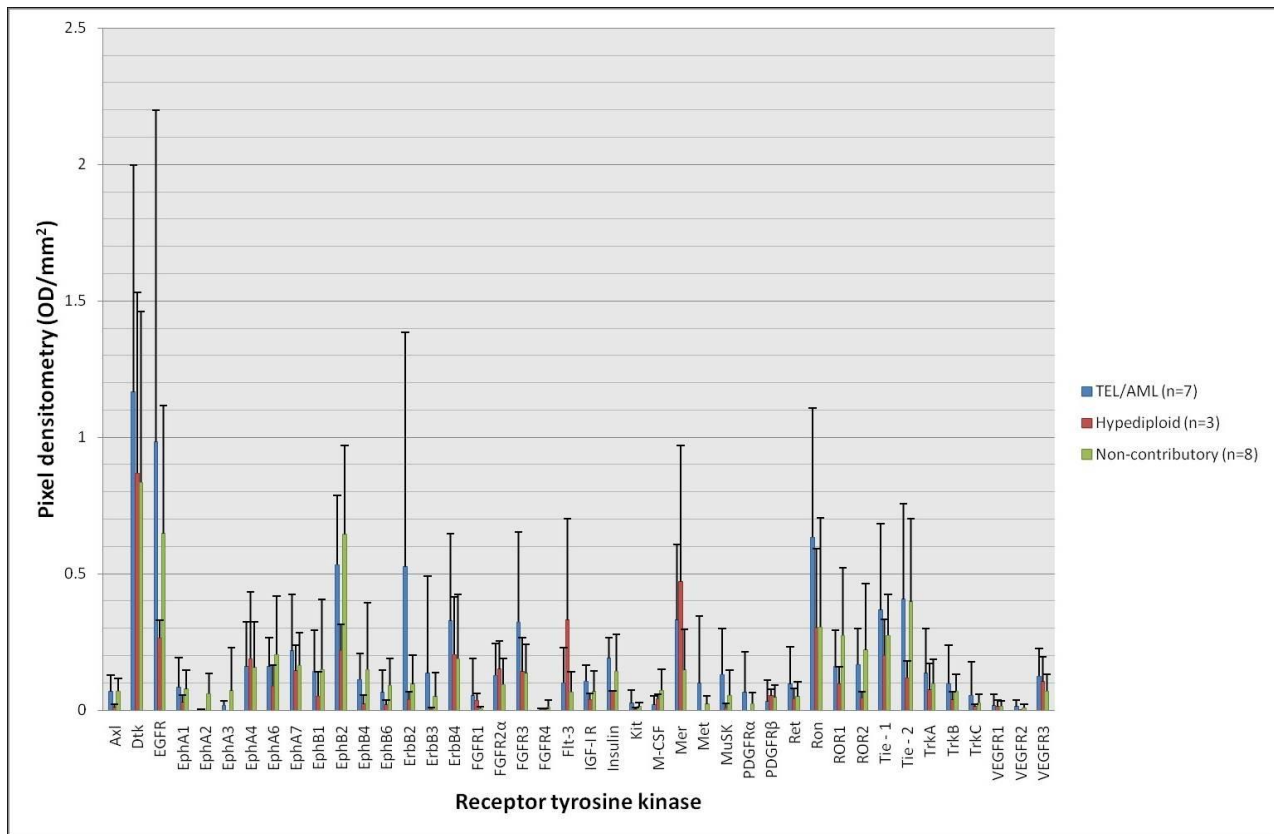


Figure 3.13 Comparison of phosphorylation signals divided into 3 cytogenetic subgroups (TEL/AML hyperdiploid and non – contributory). No significant differences in signal intensity were present between the 3 cytogenetic subgroups of the 18 primary ALLs investigated. The plots are the mean phosphorylation signal for each cytogenetic subgroup, with error bars the standard deviation.

| | t(12;21) (n=8) | Non – contributory (n=9) | Hyperdiploid (n=3) | ANOVA (p value) |
|----------------|-------------------|-----------------------------|-----------------------|--------------------|
| Axl | 0.07 (0.06) | 0.07 (0.04) | 0.01 (0.01) | 0.21 |
| Dtk | 1.17 (0.83) | 0.84 (0.63) | 0.87 (0.66) | 0.66 |
| EGFR | 0.98 (1.21) | 0.65 (0.47) | 0.26 (0.26) | 0.45 |
| EphA1 | 0.08 (0.10) | 0.08 (0.07) | 0.03 (0.02) | 0.63 |
| EphA2 | 0.00 (0.00) | 0.06 (0.07) | 0.00 (0.00) | 0.07 |
| EphA3 | 0.02 (0.01) | 0.07 (0.16) | 0.00 (0.00) | 0.53 |
| EphA4 | 0.16 (0.16) | 0.16 (0.17) | 0.19 (0.24) | 0.96 |
| EphA6 | 0.16 (0.01) | 0.20 (0.22) | 0.09 (0.08) | 0.59 |
| EphA7 | 0.22 (0.21) | 0.16 (0.12) | 0.14 (0.1) | 0.73 |
| EphB1 | 0.14 (0.15) | 0.15 (0.25) | 0.05 (0.09) | 0.76 |
| EphB2 | 0.53 (0.25) | 0.65 (0.32) | 0.22 (0.09) | 0.11 |
| EphB4 | 0.11 (0.09) | 0.15 (0.24) | 0.02 (0.03) | 0.58 |
| EphB6 | 0.06 (0.08) | 0.09 (0.09) | 0.02 (0.02) | 0.46 |
| ErbB2/HER2 | 0.53 (0.86) | 0.09 (0.10) | 0.04 (0.03) | 0.27 |
| ErbB3/HER3 | 0.14 (0.36) | 0.05 (0.09) | 0.01 (0.01) | 0.67 |
| ErbB4/HER4 | 0.33 (0.32) | 0.19 (0.23) | 0.20 (0.20) | 0.59 |
| FGFR1 | 0.05 (0.13) | 0.01 (0.01) | 0.04 (0.03) | 0.58 |
| FGFR2 α | 0.13 (0.11) | 0.09 (1.73) | 0.15 (0.10) | 0.70 |
| FGFR3 | 0.32 (0.33) | 0.14 (0.10) | 0.14 (0.12) | 0.27 |
| FGFR4 | 0.00 (0.00) | 0.01 (0.03) | 0.00 (0.00) | 0.57 |
| FLT3 | 0.10 (0.12) | 0.07 (0.07) | 0.33 (0.37) | 0.09 |
| IGF-1R | 0.11 (0.06) | 0.07 (0.07) | 0.04 (0.02) | 0.29 |
| Insulin | 0.19 (0.08) | 0.14 (0.13) | 0.07 (0.01) | 0.26 |
| KIT | 0.03 (0.05) | 0.01 (0.02) | 0.00 (0.00) | 0.57 |
| M-CSF | 0.02 (0.03) | 0.07 (0.08) | 0.04 (0.02) | 0.24 |
| Mer | 0.33 (0.28) | 0.15 (0.14) | 0.47 (0.49) | 0.20 |
| Met | 0.10 (0.25) | 0.02 (0.03) | 0.00 (0.00) | 0.55 |
| Ron | 0.63 (0.47) | 0.31 (0.40) | 0.30 (0.30) | 0.30 |
| MuSK | 0.13 (0.17) | 0.05 (0.09) | 0.01 (0.01) | 0.31 |
| PDGFR α | 0.06 (0.15) | 0.02 (0.04) | 0.00 (0.00) | 0.59 |
| PDGFR β | 0.03 (0.08) | 0.05 (0.04) | 0.05 (0.02) | 0.85 |
| Ret | 0.10 (0.14) | 0.05 (0.05) | 0.04 (0.03) | 0.59 |
| ROR1 | 0.16 (0.13) | 0.27 (0.25) | 0.10 (0.06) | 0.33 |
| ROR2 | 0.17 (0.13) | 0.22 (0.24) | 0.05 (0.02) | 0.41 |
| Tie-1 | 0.37 (0.32) | 0.27 (0.14) | 0.20 (0.13) | 0.55 |
| Tie-2 | 0.41 (0.35) | 0.40 (0.30) | 0.12 (0.06) | 0.37 |
| Trk A | 0.14 (0.16) | 0.10 (0.09) | 0.07 (0.09) | 0.75 |
| Trk B | 0.10 (0.14) | 0.07 (0.06) | 0.04 (0.03) | 0.68 |
| Trk C | 0.05 (0.12) | 0.03 (0.03) | 0.01 (0.01) | 0.70 |
| VEGFR1 | 0.02 (0.04) | 0.01 (0.02) | 0.01 (0.02) | 0.99 |
| VEGFR2 | 0.01 (0.02) | 0.01 (0.01) | 0.00 (0.00) | 0.60 |
| VEGFR3 | 0.12 (0.01) | 0.07 (0.06) | 0.11 (0.09) | 0.45 |

Table 3.6 Comparison of mean RTK phosphorylation signals in the 3 cytogenetic subgroups by one – way ANOVA (R&D arrays). No statistically significant differences were identified between the 3 cytogenetic subgroups, but EphA2 and FLT3 approached significance (highlighted in grey). Data presented is the mean optical densitometry reading for each RTK derived for the primary ALLs, standard deviation is presented in parentheses.

| | Unpaired t – test (p – value) | | |
|----------------|-------------------------------|-------------------|---------------------------|
| | Hyperdiploid vs. Rest | t(12;21) vs. Rest | Non-Contributory vs. Rest |
| Axl | 0.07 | 0.58 | 0.46 |
| Dtk | 0.79 | 0.35 | 0.48 |
| EGFR | 0.31 | 0.28 | 0.77 |
| EphA1 | 0.33 | 0.64 | 0.79 |
| EphA2 | 0.38 | 0.12 | 0.02 |
| EphA3 | 0.51 | 0.52 | 0.26 |
| EphA4 | 0.78 | 0.95 | 0.89 |
| EphA6 | 0.36 | 0.88 | 0.41 |
| EphA7 | 0.65 | 0.43 | 0.67 |
| EphB1 | 0.45 | 0.83 | 0.73 |
| EphB2 | 0.04 | 0.98 | 0.15 |
| EphB4 | 0.33 | 0.99 | 0.46 |
| EphB6 | 0.27 | 0.87 | 0.32 |
| FGFR1 | 0.88 | 0.35 | 0.30 |
| FGFR2 α | 0.54 | 0.74 | 0.43 |
| FGFR3 | 0.60 | 0.10 | 0.24 |
| FGFR4 | 0.65 | 0.46 | 0.28 |
| FLT3 | 0.03 | 0.68 | 0.25 |
| HER2 | 0.49 | 0.10 | 0.30 |
| HER3 | 0.57 | 0.38 | 0.67 |
| HER4 | 0.77 | 0.30 | 0.43 |
| IGF-I R | 0.27 | 0.15 | 0.57 |
| Insulin | 0.15 | 0.20 | 0.85 |
| Kit | 0.46 | 0.32 | 0.68 |
| M-CSF | 0.88 | 0.13 | 0.11 |
| Mer | 0.19 | 0.51 | 0.10 |
| Met/HGFR | 0.57 | 0.27 | 0.53 |
| RON | 0.58 | 0.11 | 0.27 |
| MuSK | 0.32 | 0.14 | 0.51 |
| PDGFR α | 0.50 | 0.32 | 0.65 |
| PDGFR β | 0.73 | 0.57 | 0.77 |
| Ret | 0.63 | 0.30 | 0.52 |
| ROR1 | 0.32 | 0.51 | 0.16 |
| ROR2 | 0.21 | 0.96 | 0.33 |
| Tie – 1 | 0.43 | 0.31 | 0.70 |
| Tie – 2 | 0.15 | 0.58 | 0.61 |
| Trk A | 0.61 | 0.46 | 0.74 |
| Trk B | 0.48 | 0.45 | 0.83 |
| Trk C | 0.59 | 0.42 | 0.70 |
| VEGFR1 | 0.96 | 0.91 | 0.95 |
| VEGFR2 | 0.35 | 0.46 | 0.97 |
| VEGFR3 | 0.86 | 0.26 | 0.21 |

Table 3.7 Summary of analysis comparing individual cytogenetic groups to the remaining leukaemias (R&D arrays). Statistically significant differences were identified in the phosphorylation signals at EphA2, EphB2 and FLT3. The EphA2 signal for samples with non – contributory cytogenetics was more intense than the other 2 cytogenetic groups. EphB2 phosphorylation was significantly lower in the hyperdiploid leukaemia samples, while FLT3 phosphorylation was significantly more intense in the same hyperdiploid cohort.

Although no significant differences were detected for individual RTK phosphorylation signals, potential patterns of RTK phosphorylation relating to cytogenetics were explored. Each cytogenetic subgroup was compared with the rest of genetically unrelated samples. Table 3.7 displays the summary of the p – values of this comparative approach. Statistically significant differences of phosphorylation signals were identified for the samples with non – contributory cytogenetics vs. rest EphA2 (p=0.02) and hyperdiploid samples vs. rest EphB2 (p=0.04) and FLT3 (p = 0.03). A non – significant difference in signal was identified in hyperdiploid samples for Axl which was approaching statistical significance (p=0.07).

Of the 8 samples with non – contributory cytogenetics, 5/8 had striking higher EphA2 phosphorylation compared to the remaining 3 with non – contributory cytogenetics and with the other cytogenetic groups (fig 3.14b). EphA2 phosphorylation signal appears to correlate with the presenting WCC, a known predictor of clinical outcome. The mean presentation WCC was $133.2 \times 10^9/l$ (SD 154.5) in the 5 strongly EphA2 positive samples compared to $34.3 \times 10^9/l$ (SD 38.8) in the remaining 13 samples (p = 0.04 t – test, table 3.8). In contrast, no relationship was observed between EphA2 phosphorylation and blast clearance (p=0.67), molecular (p=0.16) or flow (p=0.41) MRD status and apoptotic phenotype (p=1).

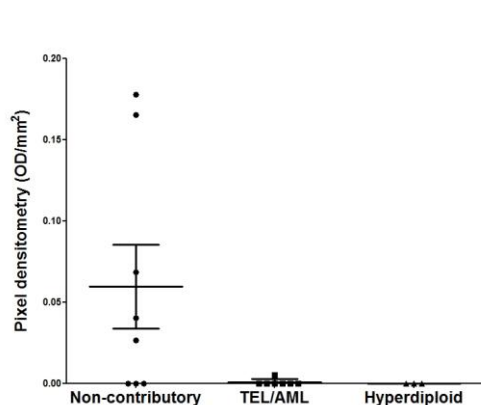
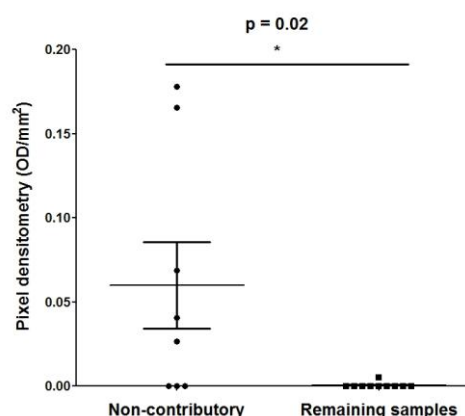
**EphA2****Figure 3.14a****EphA2****Figure 3.14b**

Figure 13.14 Comparison of phosphorylation signals for EphA2 by cytogenetic subgroup. (a) Comparison of mean phosphorylation signals in the 3 cytogenetic subgroups did not reveal a statistically significant difference (One – way ANOVA). (b) Comparison of samples with non – contributory cytogenetics (n = 8) with remaining cytogenetic samples (n = 10) demonstrated a significantly higher phosphorylation signal (p = 0.02).

| | High EphA2 | Low EphA2 | Statistical analysis |
|---------------------|-----------------|-------------|------------------------|
| | (n=5) | (n=13) | |
| Mean WCC (SD) | 133.16 (154.47) | 34.3 (38.8) | p = 0.04 (t – test) |
| Age (SD) | 6.9 (6.6) | 6.66 (4) | p = 0.92 (t – test) |
| Molecular MRD | | | p = 0.16 (Chi square) |
| High Risk | 4 | 4 | |
| Standard Risk | 1 | 7 | |
| Not known | 0 | 2 | |
| Flow MRD | | | p = 0.4 (Chi square) |
| High risk | 3 | 5 | |
| Standard risk | 1 | 7 | |
| Not known | 1 | 1 | |
| Blast clearance | | | p = 0.67 (Chi square) |
| Poor early response | 2 | 3 | |
| Good early response | 3 | 9 | |
| Not known | 0 | 1 | |

SD = standard deviation

Table 3.8 Comparison of the 5 leukaemias with phosphorylated EphA2 with 13 samples with low phosphorylation signals. A positive correlation was identified between the 5 leukaemias with increased EphA2 signal and the adverse NCI/Rome WCC risk factor. The 5 samples with increase EphA2 all had normal cytogenetics.

The other differentially phosphorylated RTKs, EphB2 and FLT3, demonstrated a significant difference in activation between the hyperdiploid and remaining 15 leukaemia samples. The FLT3 phosphorylation status was statistically higher in the 3 hyperdiploid samples (fig 3.15a and b), when compared with the remaining 15 samples ($p = 0.03$ Student's t – test).

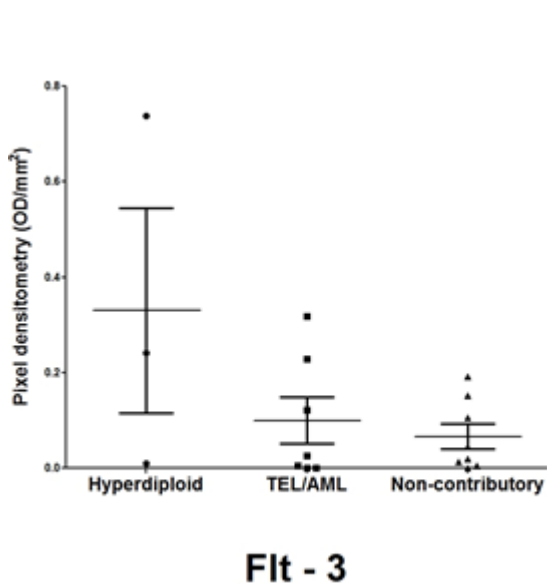


Figure 3.15a

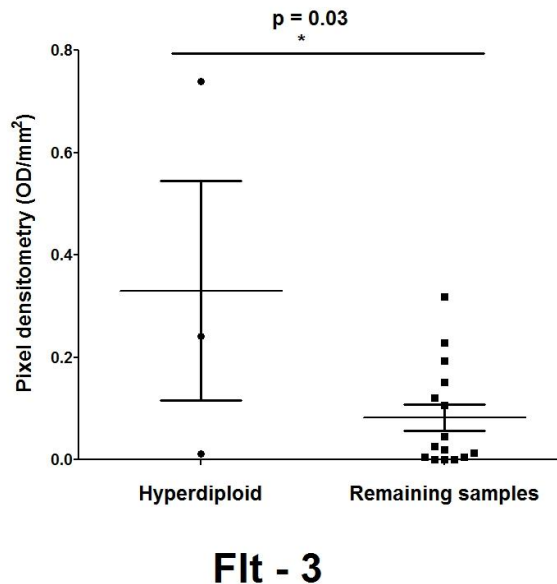
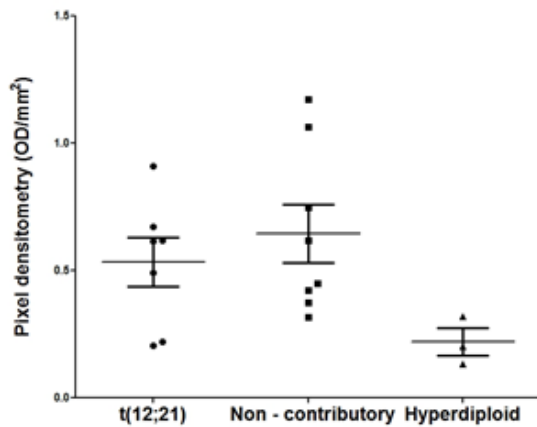


Figure 3.15b

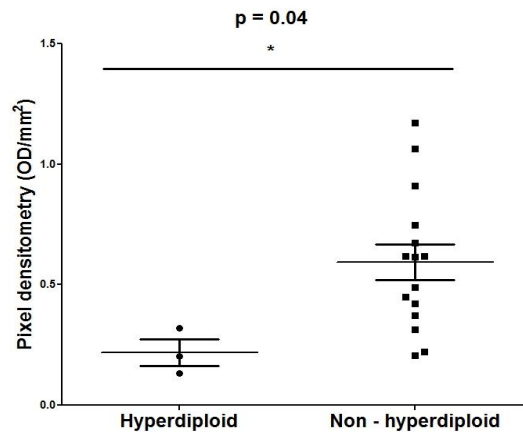
Figure 3.15 Comparison phosphorylation signals for FLT3 in cytogenetic subtypes. (a) Comparison of mean phosphorylation signals in the 3 cytogenetic subgroups did not reveal a statistically significant difference (One – way ANOVA). (b) Comparison of samples with non – contributory cytogenetics ($n = 3$) with remaining cytogenetic samples ($n = 15$) demonstrated a significantly higher phosphorylation signal ($p = 0.03$).

Conversely, EphB2 demonstrated a lower level of expression in the hyperdiploid group ($p = 0.04$, fig 3.16a).



EphB2

Figure 3.16a



EphB2

Figure 3.16b

Figure 3.16 Comparison phosphorylation signals for EphB2 by cytogenetic subgroup. (a) Comparison of mean phosphorylation signals in the 3 cytogenetic subgroups did not reveal a statistically significant difference (One – way ANOVA). (b) Comparison of samples with hyperdiploid cytogenetics (n = 3) with remaining cytogenetic samples (n = 15) demonstrated a significantly higher phosphorylation signal (p = 0.04).

In summary, differential expression between cytogenetic subgroups was observed for 3 RTKs when using the R&D array only. Of the RTKs exhibiting differential activation, EphB2 demonstrated significantly lower phosphorylation in the favourable hyperdiploid cytogenetic group, while Axl revealed a trend to lower expression in this group. In contrast, the hyperdiploid leukaemias demonstrated a significantly higher phosphorylation signature for FLT3. The increased phosphorylation of EphA2 in the leukaemias with non – contributory cytogenetics and high WCC may identify a new risk group.

3.7 Association of NCI/Rome risk criteria with RTK phosphorylation profiles

To address the possibility that clinical features could correlate with particular RTK activation, the relationships with NCI/Rome white cell and age risk classification criteria were explored.

The presentation WCC was compared with the phosphorylation signal of (R)TKs from the Raybiotech array in all 8 samples. While both risk categories were associated with phosphorylation signal detection of 4 TKs Axl, FGFR2, JAK2 and TXK, the mean intensity

of all four kinases was higher in the favourable risk category (fig 3.17). This inverse relationship between phosphorylation and adverse WCC was only statistically significant for JAK2 ($p=0.02$ t - test) (fig 3.17).

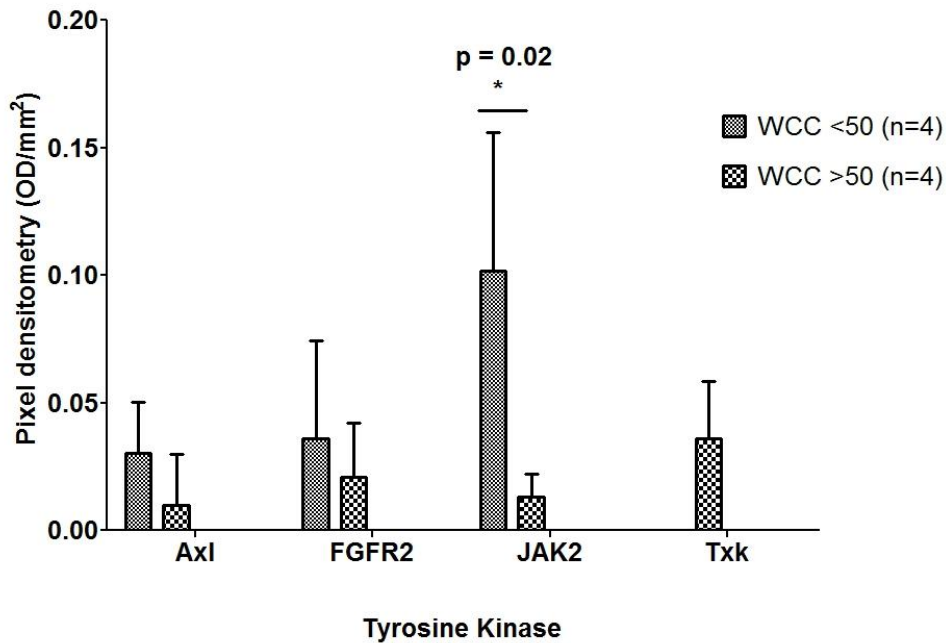


Figure 3.17 Phosphorylation signal of JAK2 detected by the Raybiotech array inversely correlated with the WCC at presentation. The phosphorylation signal for the non – receptor tyrosine kinase JAK2 was statistically significantly higher in the ALL samples with an adverse WCC risk factor (p – value = 0.02).

The association of WCC risk criteria and RTK phosphorylation in 18 leukaemias assessed by the R&D arrays was analysed (fig 3.18). Elevated phosphorylation of FGFR2 α ($p < 0.01$ t – test) and Mer ($p = 0.04$ t – test) positively correlated with an adverse WCC ($>50 \times 10^9/l$) and were statistically significant (figs 3.19a and b). In addition, a trend towards differentially increased phosphorylation of EphB2 ($p = 0.08$) and Trk A ($p = 0.08$) in those tumours with adverse WCC ($>50 \times 10^9/l$) compared with those with standard risk ($<50 \times 10^9/l$) was also observed.

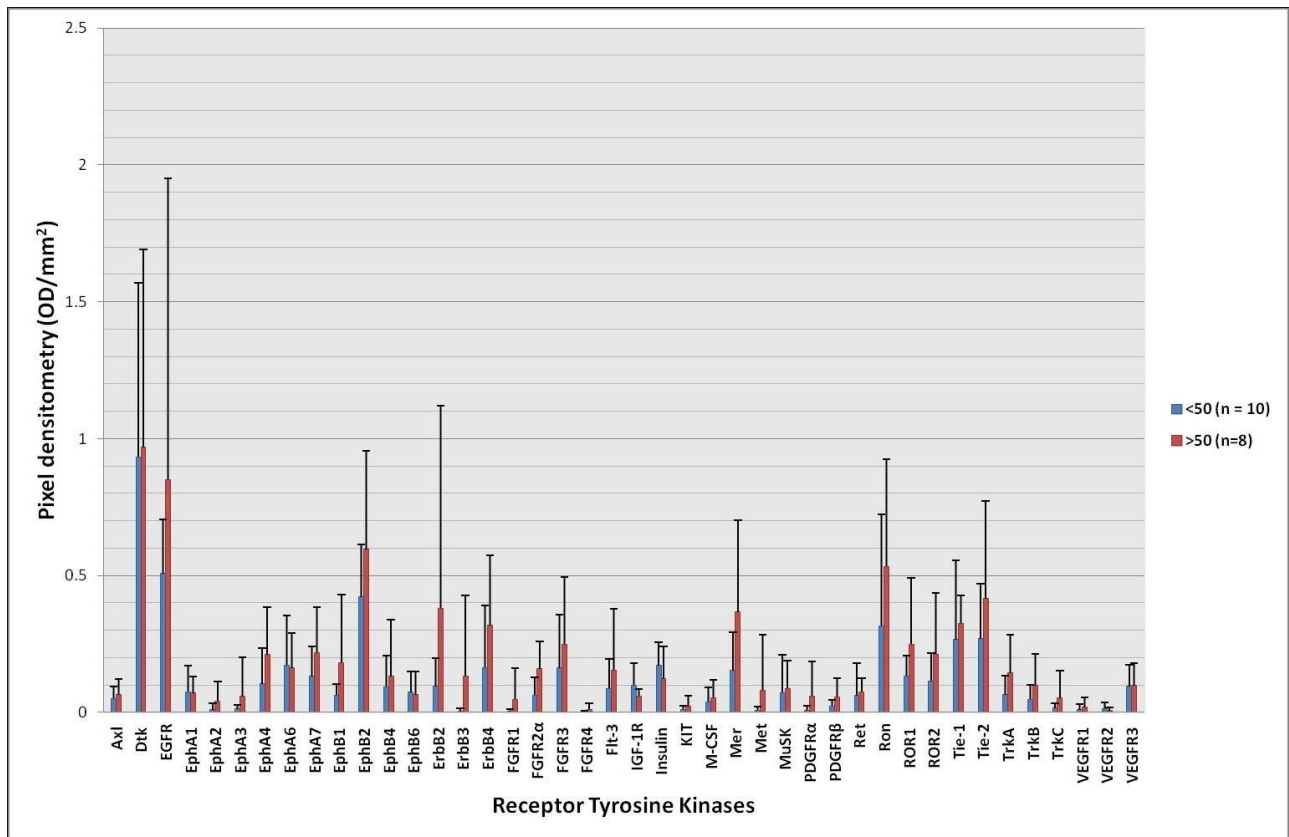


Figure 3.18 Representation of mean phosphorylation signals of individual RTKs in ALL samples grouped by NCI/Rome WCC risk classification. Statistically significant differences were observed in the phosphorylation signals of FGFR2 and Mer between the 2 NCI/Rome risk groups. The plots are the mean phosphorylation signal for each risk category, error bars are standard deviation.

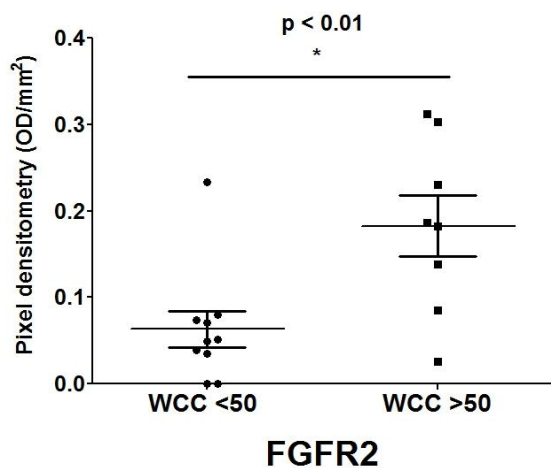


Figure 3.19a

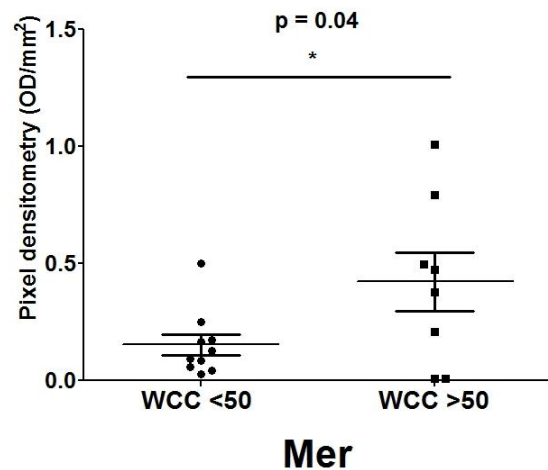


Figure 3.19b

Figure 3.19 Differential RTK phosphorylation expression of FGFR2 and Mer in adverse compared with standard risk WCC. Both (a) FGFR2 and (b) Mer RTKs demonstrated higher phosphorylation signal in ALL samples with adverse NCI/Rome risk criteria. Error bars are standard error of mean (SEM).

Subsequently the age criteria were correlated with the phosphorylation signals derived from both arrays. Due to the limited sample size, it was not possible to assess whether correlations were present between the age and TK signals in the Raybiotech arrays, as only 2 leukaemias were >10years and 6 leukaemias <10years. While signals from all TK were detectable in both groups, the mean JAK2 signal was higher in the favourable age group (0.07 vs. 0.01 OD/mm²).

In the 18 R&D array samples, both age groups (≤ 10 y and >10 y), exhibited the highest mean RTK phosphorylation signal in Dtk, followed by EGFR and EphB2 (fig 3.20). However, statistical analysis failed to reveal any statistically significant differences in individual RTK phosphorylation between the two groups.

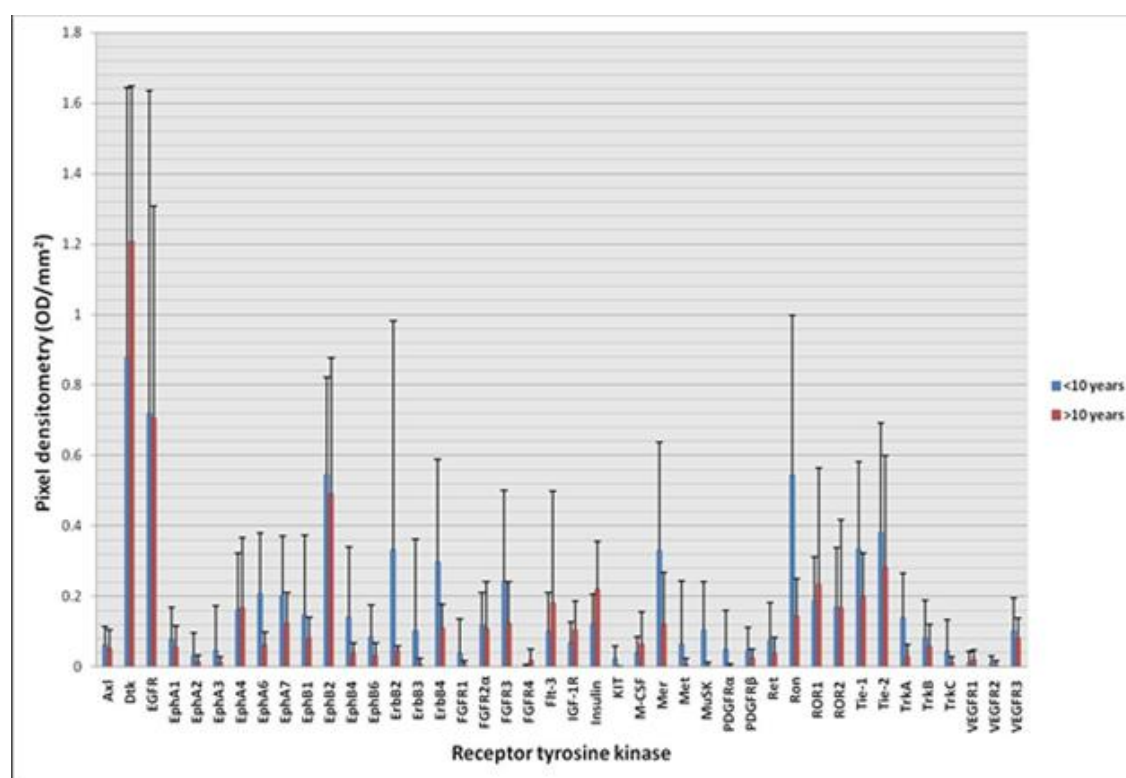


Figure 3.20 Mean phosphorylation signals of RTK in ALLs grouped by age according to NCI/Rome criteria. No statistically significant differences were observed between the risk groups. The plots are the mean phosphorylation signal for each risk category, error bars are standard deviation.

3.8 Association of blast clearance and MRD status with RTK phosphorylation profiles

The question whether RTK phosphorylation patterns could be a predictor of chemosensitivity, as determined by assessment of bone marrow at D8/15 and minimal residual disease at D29 of induction therapy was subsequently addressed.

For the 8 leukaemias investigated using the Raybiotech array, analysis could not be performed for blast clearance and flow MRD, because 7/8 leukaemias demonstrated good early blast clearance and flow MRD data was not available for 3/8 samples. Nevertheless, molecular MRD data was available for 7/8, and analysis of these samples revealed a strong relationship between the molecular MRD negative status and the phosphorylation signal of Axl and Txk, $p = 0.0002$ and $p = 0.006$ respectively (fig.3.21).

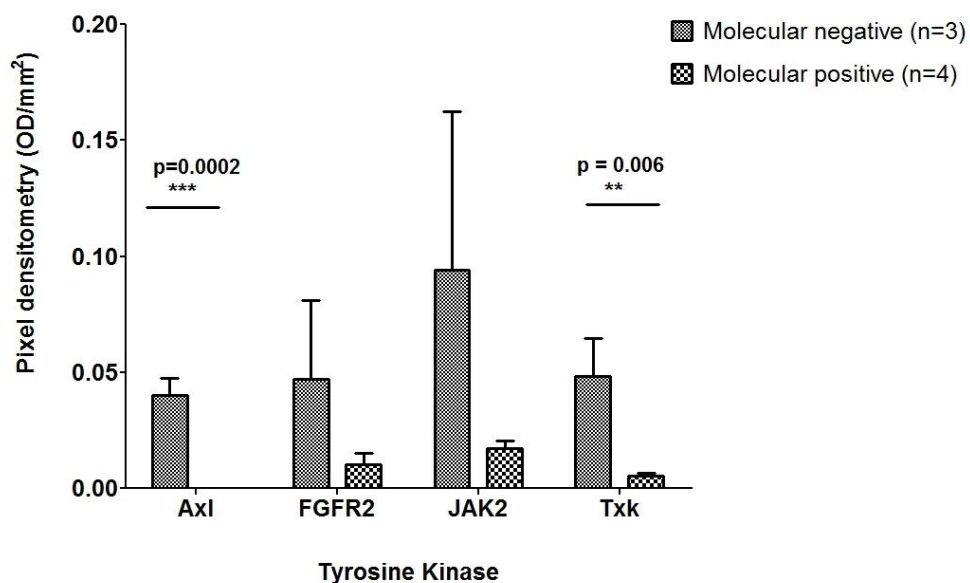


Figure 3.21 Increased Axl and JAK2 phosphorylation signals were evident in the leukaemia samples with detectable molecular MRD assessed by the Raybiotech arrays. Statistically significantly increased signal was evident in the Molecular MRD negative leukaemia samples, Axl ($p=0.002$) and JAK2 ($p = 0.006$). Error bars are SEM.

Data for blast clearance and MRD (PCR and flow) was available for 17/18 and 16/18 of the ALL cohort investigated with R&D array, respectively. When analysed (table 3.9), no association was observed between the individual phosphorylation signals and rate of blast clearance (fig3.22). Furthermore, no association was identified between RTK phosphorylation signals and day 29 molecular MRD status (fig 3.23).

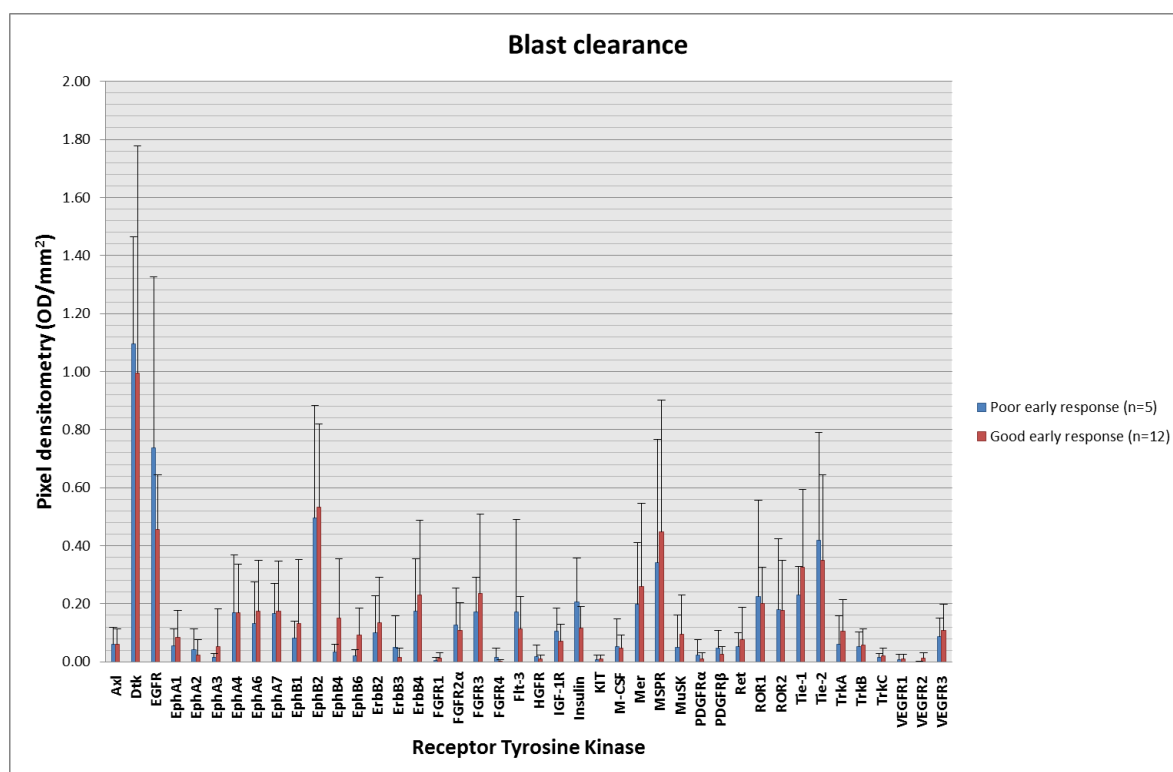


Figure 3.22 Association of blast clearance with individual RTK phosphorylation signals (R&D Array). No statistically significant differences were observed between the risk groups. The plots are the mean phosphorylation signal for each risk category, error bars are standard deviation.

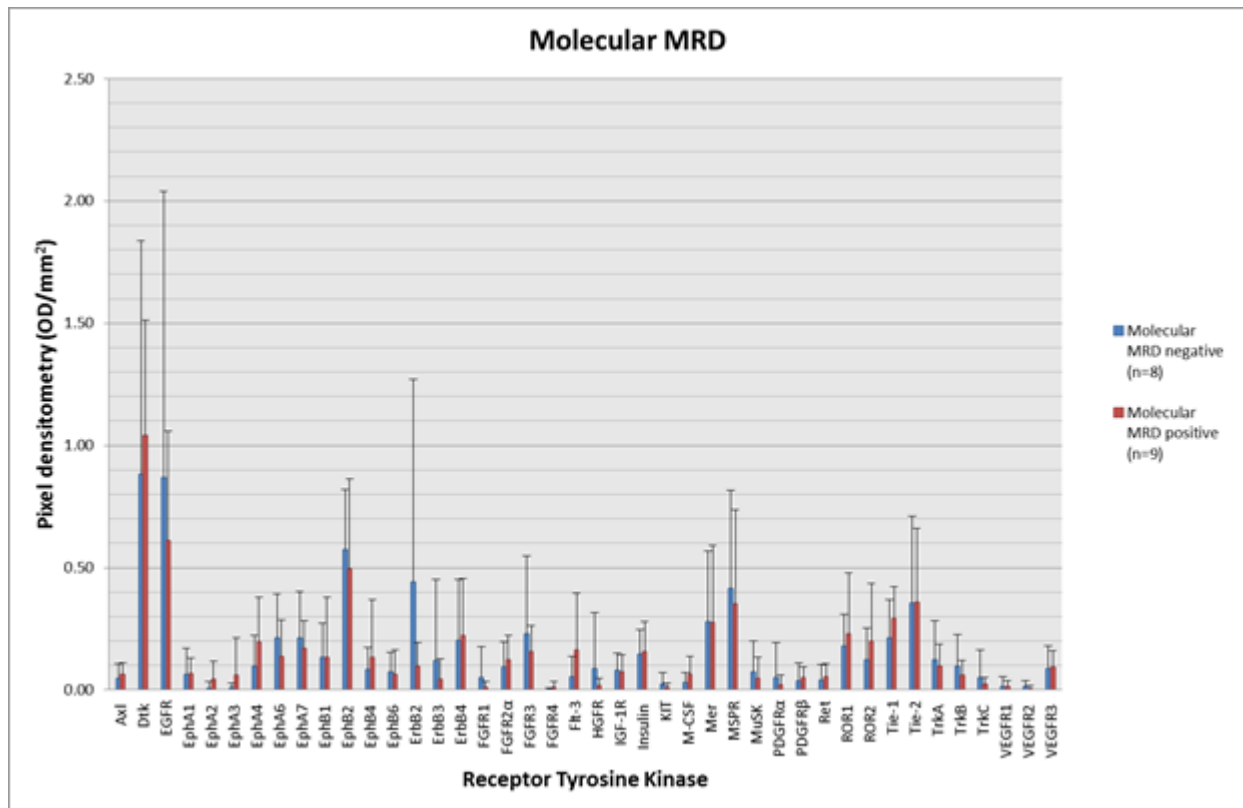


Figure 3.23 Association of molecular MRD status with individual RTK phosphorylation signals identified with R&D array. No statistically significant differences were observed between the risk groups. The plots are the mean phosphorylation signal for each risk category, error bars are standard deviation.

Analysis of 16/18 samples for which flow MRD data was available identified a significantly higher level of phosphorylation of the PDGFR β kinase in cells from patients positive for MRD by flow cytometry at D28 ($p=0.02$ by t-test, table 3.10).

| | Blast clearance | | | | | Molecular MRD status | | | | |
|----------------|-----------------|------------|--------------|------------|--------|----------------------|------------|------------------|------------|--------|
| | GER (n=12) | Std dev | PER (n=5) | Std Dev | t-test | Mol neg (n=8) | Std dev | Mol pos (n=9) | Std Dev | t-test |
| Axl | 0.06 | 0.05 | 0.06 | 0.06 | 0.97 | 0.05 | 0.06 | 0.06 | 0.05 | 0.49 |
| Dtk | 0.99 | 0.78 | 1.09 | 0.37 | 0.79 | 0.88 | 0.95 | 1.04 | 0.47 | 0.66 |
| EGFR | 0.46 | 0.19 | 0.74 | 0.59 | 0.15 | 0.87 | 1.17 | 0.61 | 0.45 | 0.54 |
| EphA1 | 0.09 | 0.09 | 0.05 | 0.06 | 0.50 | 0.07 | 0.10 | 0.07 | 0.06 | 0.95 |
| EphA2 | 0.02 | 0.05 | 0.04 | 0.07 | 0.57 | 0.01 | 0.02 | 0.05 | 0.07 | 0.19 |
| EphA3 | 0.05 | 0.13 | 0.01 | 0.01 | 0.54 | 0.01 | 0.02 | 0.06 | 0.15 | 0.37 |
| EphA4 | 0.17 | 0.17 | 0.17 | 0.20 | 0.99 | 0.10 | 0.13 | 0.20 | 0.18 | 0.21 |
| EphA6 | 0.17 | 0.18 | 0.13 | 0.14 | 0.64 | 0.21 | 0.18 | 0.14 | 0.15 | 0.35 |
| EphA7 | 0.17 | 0.17 | 0.17 | 0.10 | 0.92 | 0.21 | 0.19 | 0.17 | 0.11 | 0.58 |
| EphB1 | 0.13 | 0.22 | 0.08 | 0.06 | 0.63 | 0.13 | 0.14 | 0.13 | 0.25 | 0.99 |
| EphB2 | 0.53 | 0.29 | 0.50 | 0.39 | 0.83 | 0.58 | 0.24 | 0.50 | 0.37 | 0.61 |
| EphB4 | 0.15 | 0.20 | 0.03 | 0.03 | 0.22 | 0.08 | 0.09 | 0.13 | 0.23 | 0.56 |
| EphB6 | 0.09 | 0.09 | 0.02 | 0.02 | 0.11 | 0.08 | 0.08 | 0.07 | 0.10 | 0.83 |
| ErbB2 | 0.14 | 0.16 | 0.10 | 0.13 | 0.66 | 0.44 | 0.83 | 0.10 | 0.10 | 0.23 |
| ErbB3 | 0.01 | 0.03 | 0.05 | 0.11 | 0.32 | 0.12 | 0.33 | 0.04 | 0.08 | 0.52 |
| ErbB4 | 0.23 | 0.26 | 0.18 | 0.18 | 0.67 | 0.20 | 0.25 | 0.22 | 0.23 | 0.86 |
| FGFR1 | 0.01 | 0.02 | 0.00 | 0.01 | 0.46 | 0.05 | 0.13 | 0.01 | 0.02 | 0.37 |
| FGFR2 α | 0.11 | 0.10 | 0.13 | 0.13 | 0.75 | 0.09 | 0.10 | 0.12 | 0.10 | 0.56 |
| FGFR3 | 0.24 | 0.27 | 0.17 | 0.12 | 0.62 | 0.23 | 0.32 | 0.16 | 0.10 | 0.52 |
| FGFR4 | 0.00 | 0.00 | 0.02 | 0.03 | 0.18 | 0.00 | 0.00 | 0.01 | 0.02 | 0.33 |
| Flt-3 | 0.11 | 0.11 | 0.17 | 0.32 | 0.58 | 0.06 | 0.08 | 0.16 | 0.23 | 0.24 |
| IGF-1R | 0.07 | 0.06 | 0.10 | 0.08 | 0.35 | 0.08 | 0.07 | 0.08 | 0.07 | 0.89 |
| Insulin | 0.12 | 0.08 | 0.21 | 0.15 | 0.11 | 0.15 | 0.10 | 0.16 | 0.12 | 0.87 |
| KIT | 0.01 | 0.01 | 0.01 | 0.02 | 0.71 | 0.02 | 0.05 | 0.01 | 0.02 | 0.42 |
| M-CSF | 0.05 | 0.05 | 0.05 | 0.09 | 0.84 | 0.03 | 0.04 | 0.06 | 0.07 | 0.27 |
| Mer | 0.26 | 0.29 | 0.20 | 0.21 | 0.67 | 0.28 | 0.29 | 0.28 | 0.31 | 0.97 |
| Met | 0.01 | 0.01 | 0.02 | 0.04 | 0.58 | 0.09 | 0.23 | 0.02 | 0.03 | 0.39 |
| MuSK | 0.09 | 0.14 | 0.05 | 0.11 | 0.53 | 0.07 | 0.13 | 0.05 | 0.09 | 0.64 |
| PDGFR α | 0.01 | 0.02 | 0.02 | 0.05 | 0.46 | 0.05 | 0.14 | 0.02 | 0.04 | 0.54 |
| PDGFR β | 0.03 | 0.03 | 0.05 | 0.06 | 0.29 | 0.04 | 0.07 | 0.05 | 0.04 | 0.69 |
| Ret | 0.08 | 0.11 | 0.05 | 0.05 | 0.64 | 0.04 | 0.06 | 0.06 | 0.05 | 0.59 |
| Ron | 0.45 | 0.45 | 0.34 | 0.43 | 0.66 | 0.42 | 0.40 | 0.35 | 0.38 | 0.74 |
| ROR1 | 0.20 | 0.12 | 0.22 | 0.33 | 0.84 | 0.18 | 0.13 | 0.23 | 0.25 | 0.62 |
| ROR2 | 0.18 | 0.17 | 0.18 | 0.24 | 0.98 | 0.12 | 0.13 | 0.20 | 0.23 | 0.43 |
| Tie-1 | 0.33 | 0.27 | 0.23 | 0.10 | 0.46 | 0.21 | 0.15 | 0.29 | 0.13 | 0.27 |
| Tie-2 | 0.35 | 0.29 | 0.42 | 0.37 | 0.68 | 0.36 | 0.35 | 0.36 | 0.30 | 0.98 |
| Trk A | 0.11 | 0.11 | 0.06 | 0.10 | 0.42 | 0.13 | 0.16 | 0.10 | 0.09 | 0.65 |
| Trk B | 0.06 | 0.06 | 0.05 | 0.05 | 0.88 | 0.10 | 0.13 | 0.06 | 0.06 | 0.48 |
| Trk C | 0.02 | 0.03 | 0.01 | 0.01 | 0.66 | 0.05 | 0.11 | 0.02 | 0.03 | 0.52 |
| VEGFR1 | 0.01 | 0.02 | 0.01 | 0.02 | 0.90 | 0.02 | 0.04 | 0.01 | 0.02 | 0.92 |
| VEGFR2 | 0.01 | 0.02 | 0.00 | 0.00 | 0.25 | 0.01 | 0.02 | 0.01 | 0.01 | 0.41 |
| VEGFR3 | 0.11 | 0.09 | 0.09 | 0.06 | 0.64 | 0.09 | 0.09 | 0.09 | 0.07 | 0.88 |

Key:**GER:** Good early response (Blasts <25% day8/15)**PER:** Poor early response (Blasts >25% day 8/15)**Mol neg:** Molecular MRD <0.01%**Mol pos:** Molecular MRD >0.01%**Table 3.9 Association of blast clearance and MRD status with individual RTK phosphorylation profiles.**

No difference in phosphorylation signals were identified when phosphorylation intensity was correlated to rate of blast clearance and MRD status. Data presented is the mean optical densitometry reading for each RTK derived for the primary ALLs.

| | Flow MRD positive D29 (n=8) | Std dev | Flow MRD negative D29 (n=8) | Std dev | p-value (t-test) |
|----------------|-----------------------------------|---------|-----------------------------------|---------|------------------|
| Axl | 0.06 | 0.04 | 0.07 | 0.06 | 0.86 |
| Dtk | 0.85 | 0.58 | 1.31 | 0.67 | 0.16 |
| EGFR | 1.06 | 1.16 | 0.47 | 0.21 | 0.17 |
| EphA1 | 0.05 | 0.05 | 0.10 | 0.11 | 0.29 |
| EphA2 | 0.03 | 0.06 | 0.02 | 0.06 | 0.84 |
| EphA3 | 0.01 | 0.01 | 0.07 | 0.16 | 0.33 |
| EphA4 | 0.11 | 0.11 | 0.25 | 0.20 | 0.11 |
| EphA6 | 0.16 | 0.16 | 0.12 | 0.10 | 0.59 |
| EphA7 | 0.17 | 0.12 | 0.21 | 0.19 | 0.58 |
| EphB1 | 0.08 | 0.12 | 0.20 | 0.25 | 0.25 |
| EphB2 | 0.47 | 0.33 | 0.61 | 0.28 | 0.38 |
| EphB4 | 0.07 | 0.13 | 0.18 | 0.21 | 0.21 |
| EphB6 | 0.03 | 0.05 | 0.10 | 0.11 | 0.12 |
| ErbB2 | 0.39 | 0.83 | 0.17 | 0.18 | 0.49 |
| ErbB3 | 0.15 | 0.33 | 0.01 | 0.04 | 0.26 |
| ErbB4 | 0.25 | 0.28 | 0.29 | 0.27 | 0.79 |
| FGFR1 | 0.06 | 0.13 | 0.01 | 0.01 | 0.27 |
| FGFR2 α | 0.13 | 0.11 | 0.12 | 0.11 | 0.90 |
| FGFR3 | 0.15 | 0.12 | 0.31 | 0.31 | 0.20 |
| FGFR4 | 0.01 | 0.02 | 0.00 | 0.00 | 0.14 |
| Flt-3 | 0.09 | 0.10 | 0.18 | 0.25 | 0.35 |
| IGF-1R | 0.08 | 0.07 | 0.09 | 0.06 | 0.68 |
| Insulin | 0.19 | 0.12 | 0.13 | 0.09 | 0.23 |
| KIT | 0.03 | 0.04 | 0.00 | 0.00 | 0.13 |
| M-CSF | 0.07 | 0.08 | 0.02 | 0.03 | 0.09 |
| Mer | 0.34 | 0.38 | 0.26 | 0.19 | 0.61 |
| Met | 0.10 | 0.23 | 0.01 | 0.01 | 0.30 |
| MuSK | 0.04 | 0.09 | 0.13 | 0.15 | 0.15 |
| PDGFR α | 0.07 | 0.14 | 0.01 | 0.02 | 0.31 |
| PDGFR β | 0.07 | 0.07 | 0.01 | 0.02 | 0.03 |
| Ret | 0.03 | 0.04 | 0.11 | 0.12 | 0.12 |
| Ron | 0.35 | 0.40 | 0.61 | 0.45 | 0.24 |
| ROR1 | 0.21 | 0.25 | 0.20 | 0.16 | 0.92 |
| ROR2 | 0.15 | 0.19 | 0.22 | 0.20 | 0.48 |
| Tie-1 | 0.28 | 0.12 | 0.37 | 0.30 | 0.42 |
| Tie-2 | 0.32 | 0.32 | 0.43 | 0.32 | 0.53 |
| Trk A | 0.14 | 0.13 | 0.09 | 0.12 | 0.44 |
| Trk B | 0.10 | 0.13 | 0.06 | 0.05 | 0.40 |
| Trk C | 0.05 | 0.11 | 0.02 | 0.03 | 0.43 |
| VEGFR1 | 0.02 | 0.04 | 0.01 | 0.01 | 0.28 |
| VEGFR2 | 0.01 | 0.01 | 0.01 | 0.02 | 0.81 |
| VEGFR3 | 0.08 | 0.08 | 0.14 | 0.08 | 0.16 |

Table3.10 Association of flow MRD status with individual RTK phosphorylation profiles.

PDGFR β phosphorylation status was significantly more intense in the leukaemia samples which demonstrated positive flow MRD (>0.01%) at the end of induction (p=0.03). Data presented is the mean optical densitometry reading for each RTK derived for the primary ALLs.

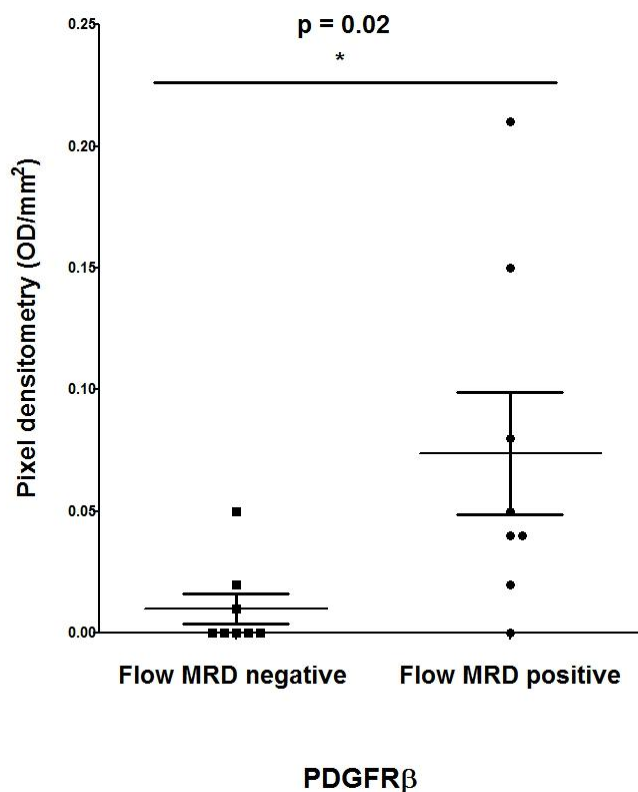


Figure 3.24 Increased PDGFR β signal is associated with presence of MRD detected by flow cytometry. The phosphorylation signal for PDGFR β was significantly more intense for the 8 ALL samples with leukaemia detectable >0.01% when assayed by flow cytometry. Error bars are standard error of the mean (SEM).

Comparison of clinical and biological features of the flow MRD positive and negative groups did not demonstrate a difference in the 2 populations age ($p = 0.82$ t – test), WCC ($p = 0.41$ t – test), cytogenetics ($p = 0.42$ Chi square), molecular MRD status ($p = 0.09$ Chi square) or apoptotic phenotype ($p = 0.31$ Fisher’s exact). The dot plot revealed a split in signal intensity in the 16 samples correlated to flow MRD (fig 3.24), with no signal in 6 leukaemias, while there significant expression in the remaining 10.

In summary, whilst the Raybiotech array suggested molecular MRD negative status correlated with a high phosphorylation signal of Axl and Txk, the R&D array identified PDGFR β expression positively correlated with the persistence of MRD when assessed by flow cytometry and cytogenetic subtype.

3.9 Discussion

The aim of this chapter was to investigate whether aberrant activation of specific receptor tyrosine kinases in childhood ALL could be correlated with clinical features and predictive markers of chemosensitivity, including early response to treatment, MRD and apoptotic patterns to IR – induced DNA damage. To this end, the baseline tyrosine kinase phosphorylation signatures from 20 primary ALLs were investigated using 2 types of antibody – based protein arrays. The hypothesis that differential constitutive phosphorylation of individual RTKs upregulate pro – survival pathways in ALL cells that are resistant to IR – induced apoptosis is not supported by the results from both the array experiments.

Multiple phosphorylated RTKs were detected with the R&D array, with a wide range of intensity. A large number of the kinases demonstrated low levels of phosphorylation when using 50µg of primary leukaemia whole cell lysate for hybridisation. In previous studies, up to 2mg of cell line and primary lysate was used (294). The hybridisation of larger amounts of protein would probably improve the detection rate of RTK activation, but this goal was unachievable in this study because of the limited amount of primary material available. In the initial array validation studies, 50µg of cell lysate from cell lines was sufficient to demonstrate a phosphorylation signal, which could be confirmed by Western Blot. An equal amount of primary tumour protein did not elicit as intense signals. An explanation for this finding may be the more homogenous nature of cell lines and the sub – clonal evolution present in ALL (357, 358). The bone marrow samples used for this study were prepared by gradient density centrifuge and collection of the mononuclear fraction, with no cell sorting. While the total leukaemic yield may still be high an activated RTK may only be expressed in a minor sub – population and thus yield a low level of signal.

Results derived from both the R&D and Raybiotech arrays have been published in peer – reviewed journals, investigating a wide variety of solid tumours, including glioblastoma multiforme, chordoma and mesothelioma (294, 359-361). Phosphorylation profiles derived

from these published studies were reproducible and confirmed by Western Blot. Only 2 published studies have used this technology to investigate acute leukaemias, both of which used the R&D array (158, 362). Ter Elst *et al.* confirmed baseline phosphorylation signals of the EGFR, PDGFR, Ron and Trk A receptors in 3 primary ALL samples (362). The results for these 4 RTKs were reproduced in the current study with EGFR and Ron the second and fourth highest mean expression across all 18 leukaemias investigated with the R&D arrays. The expression of Trk A and PDGFR β in the current study was substantially lower, but this finding may be due to the heterogeneity of ALL. Marston *et al.* (158) utilised the R&D arrays to compare RTK phosphorylation in 6 primary ALL samples after exposure to IR. Baseline phosphorylation of ErbB4 and FLT3 was found in 2 individual samples. Phosphorylation of multiple RTKs occurred after irradiation, including Mer, ErbB4, insulin and IGF-1R. In the analysis reported here Mer and ErbB4 were the seventh and ninth most phosphorylated RTKs detected by the R&D arrays. The RTKs EGFR, Mer, PDGFR β , Ron and Trk A have been identified in both previous and current studies, suggesting that these kinases are possible targets for further targeted therapy in childhood ALL.

Unlike the R&D arrays, the Raybiotech arrays identified a restricted pattern of phosphorylated kinases, namely Axl, FGFR2, JAK2 and Txk. Increased phosphorylation signals for Axl and Txk were observed in the apoptotic proficient leukaemias and leukaemias with negative molecular MRD at less than 0.01%, both of which are markers for chemosensitivity. This different phosphorylation signature for Axl was not mirrored in the R&D array. The presence of constitutively phosphorylated Axl in the apoptotic proficient leukaemias (Raybiotech array) would be contrary to the pro – survival role this kinase exerts in chemoresistant AML (363). Low level phosphorylation of Axl was present in 15/18 samples assayed on the R&D system, but did not correlate with the Axl signals identified in by the Raybiotech arrays. The presence of increased phosphorylation in the chemosensitive apoptotic proficient samples was unexpected.

Similarly, increased JAK2 signal intensity was the dominant signature for 7/8 samples on the Raybiotech array and was associated with presentation WCC $<50 \times 10^9/L$ and samples with an apoptotic proficient phenotype. These results were not consistent with current evidence, since aberrant JAK2 activity appears restricted to Down Syndrome – associated ALL (237, 240) and high risk leukaemias with normal cytogenetics and Bcr/Abl – like transcriptional signatures (222). The samples which expressed phosphorylated JAK2 were not consistent with these populations because recurrent cytogenetic abnormalities were present in 6/8 leukaemias. The remaining 2 leukaemias, which did not demonstrate any cytogenetic abnormalities, were not from patients with DS and only 1 was flow – MRD positive at the end of induction of greater than 0.01%. Interpretation of the Raybiotech data is complicated by the unexpected correlation between markers of chemosensitivity and increased kinase signals and the lack of correlation between the 2 array systems.

While no correlation was observed between the apoptotic phenotype and the phosphorylation signals detected by the R&D array, differential RTK phosphorylation signals were noted when samples were grouped by cytogenetics (EphA2, EphB2, FLT3), diagnostic white cell count (Mer and FGFR2) and MRD status by flow cytometry (PDGFR β), but not molecular MRD.

The lower phosphorylation of EphA2 was demonstrated in the cytogenetically favourable groups, t(12;21) and hyperdiploid, when compared with leukaemias with non-contributory cytogenetics. Consistent with this finding, increased activity of EphA2 is associated with aggressive carcinomas (364, 365). In addition, reduced phosphorylation of EphB2 was also seen in the hyperdiploid group compared to the t(12;21) and non – contributory groups. The role of eph receptors in cancers is complicated because of promiscuous cross – talk (366) with other receptors and they possess the ability for bidirectional signalling (367, 368). Both EphA2 and EphB2 are potentially oncogenic (369, 370) and the increased signals of these 2 kinases in the leukaemias with non – contributory cytogenetics abnormalities

suggest these 2 RTKs may play a role in either the leukaemogenesis or chemoresistance of leukaemias with a non – contributory cytogenetics.

In contrast, the level of FLT3 phosphorylation was significantly higher in the 3 hyperdiploid leukaemias when compared with the remaining 15. Activating FLT3 mutations have previously been described in ALL, with preponderance in hyperdiploid tumours (250, 371) supporting the findings of this study. While the adverse nature of activated FLT3 is well documented in AML (372), its role in ALL is uncertain since the survival rates of patients with hyperdiploid and infant ALL are dramatically different. The presence of activated FLT3 is consistent with published data and thus warrants further investigation for the use of kinase inhibitors in ALL.

In this study, a positive relationship between the intensity phosphorylation signals for the Mer and FGFR2 RTK and high diagnostic WCC was observed in the samples assessed by the R&D Array. Both RTKs are associated with tumorigenesis (162, 262) and chemoresistance in cancers (89, 355). While FGFR2 has not been identified in ALL, Mer contributes to the t(1;19) *E2AX-PBX1* ALL gene expression signature (220, 373). The pro – survival activity of Mer was demonstrated the reduction of cell survival of primary t(1;19) ALL cells (261) caused by small interfering RNA (siRNA) – mediated silencing of Mer. Increased leukaemia survival and chemoresistance associated with increased activity of Mer could contribute to the adverse impact of a high WCC identified in this study. In the future, it would be interesting to compare Mer gene expression with phosphorylation between high WCC and t(1;19) ALL subtypes to address potential different mechanisms of Mer hyperactivation.

A relationship was identified between the level of PDGFR β phosphorylation and leukaemias with positive MRD greater than 0.01% when assessed by flow cytometry at the end of induction. This relationship was not observed when phosphorylation levels were compared in ALLs with positive MRD assessed by molecular techniques. The differences

in correlations by MRD method may be explained partly by the fact that the cohorts examined by flow and PCR did not contain exactly the same samples but also by the incomplete correlation between the 2 techniques. While a high level of concordance between the 2 techniques has been reported (95, 96), this study has limited numbers of samples which might impact on the correlation between these different methods. The presence of PDGFR β has been reported in 2 pre – B ALL cell lines at transcript level (374) and phosphorylation in primary ALL samples (362), suggesting it may be a putative target for therapy in a selected population of childhood ALL.

In summary, there were limitations in this study, partly due to discordance in phosphorylation data between the 2 arrays, which may be attributable to differing affinity of the manufacturers' antibodies but also possible under-detection due to the low protein levels in the size of samples available. In addition, ALL is a very heterogeneous disease in terms of clinical characteristics, cytogenetic profiles and chemosensitivity, which are difficult to fully represent in a small sample size. Nevertheless, within these limitations, it was possible to identify differential phosphorylation signals for specific tyrosine kinases that correlated with clinical and biological features in the 20 ALL samples investigated. The R&D array demonstrated increased mean FLT3 signal in the hyperdiploid leukaemias, which is consistent with published literature. This favourable cytogenetic group also demonstrated a reduction in signal from 2 RTKs, EphA2 and EphB2, both of which are potentially oncogenic. The identification of increased EphA2 signal in leukaemias with normal cytogenetics and an adverse WCC risk may lead to the identification of a new risk category. Further investigation would be justified in a larger cohort with additional validation of mRNA expression of individual RTKs and Western Blotting to confirm levels of total and phosphorylated proteins.

4 Screening of cell line panel and primary ALL cells with library of RTK inhibitors

4.1. Introduction

The introduction of the small molecular TK inhibitor, imatinib, against the leukaemia – specific Bcr/Abl oncoprotein revolutionised the treatment of CML. The International Randomized Study of Interferon and STI571 (IRIS) trial demonstrated significant benefit over best practice of the time, with a dramatic increase in overall survival (375) and indicated the potential of targeted therapeutic approaches in malignancies. The therapeutic potential of targeting tyrosine kinases in malignancies has led to a proliferation of small molecule inhibitors. Such small molecule kinase inhibitors offer investigators useful tools with which to rapidly decipher kinase pathways involved in important pathological processes.

To complement the phospho – RTK array screening undertaken in the previous chapter, a small molecule inhibitor library was constructed, as a tool for identification of candidate kinases and the associated pathways that might be important for the survival and proliferation of ALL blasts. Twenty primary leukaemias, with a representative range of clinical, biological and cytogenetic features, were used to assess the range of activity of 33 molecules.

4.2. Generation and optimisation of RTK inhibitor library screen assay

A library of 33 TKIs was purchased from Selleck Chemicals (Boston, MA, USA), which targeted a total of at least 43 putative kinase targets. The TKIs and their putative kinase targets are shown on table 2.5.

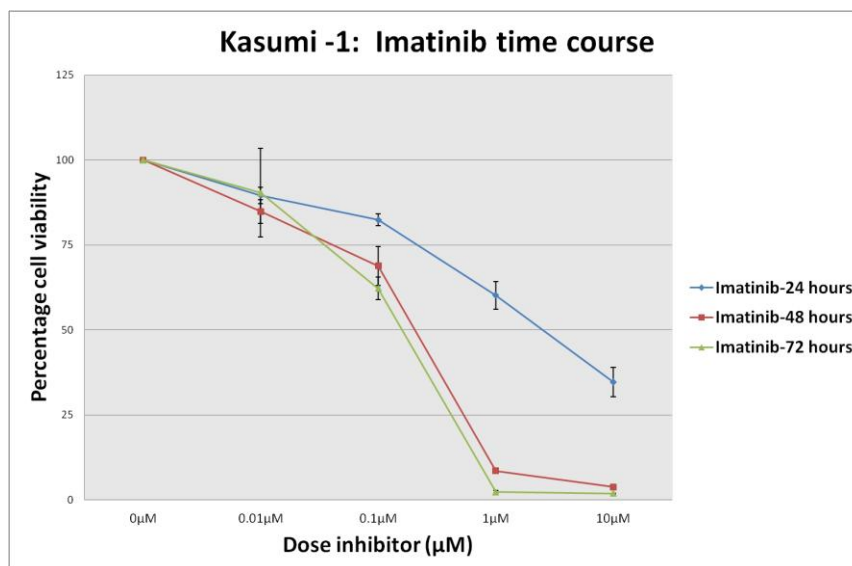
The ATP – based metabolic assay, Promega CellTiter – Glo® (Madison, WA, USA) was used to measure cell viability of cell lines and primary ALL samples after treatment with the TKIs (Methods 2.11). Using this method, at least 50% reduction in cell viability after treatment was selected as the margin to indicate activity of the novel TKIs.

Three aspects of the assay were optimised before using it in the TKI screen. These aspects were: (i) the duration of treatment, (ii) the concentrations of the drugs, and (iii) the culture medium in which the primary ALL cells were screened. A series of preliminary experiments were performed, using the myeloid Kasumi – 1 cell line, which possesses t(8;21) and an activating *KIT* mutation (Asn822Lys). Inhibition of this KIT activity by what the tyrosine kinase inhibitor SU5614 reduces proliferation and induces apoptosis in Kasumi-1 cells (376).

(i) Establishing optimal drug exposure time to leukaemia cells

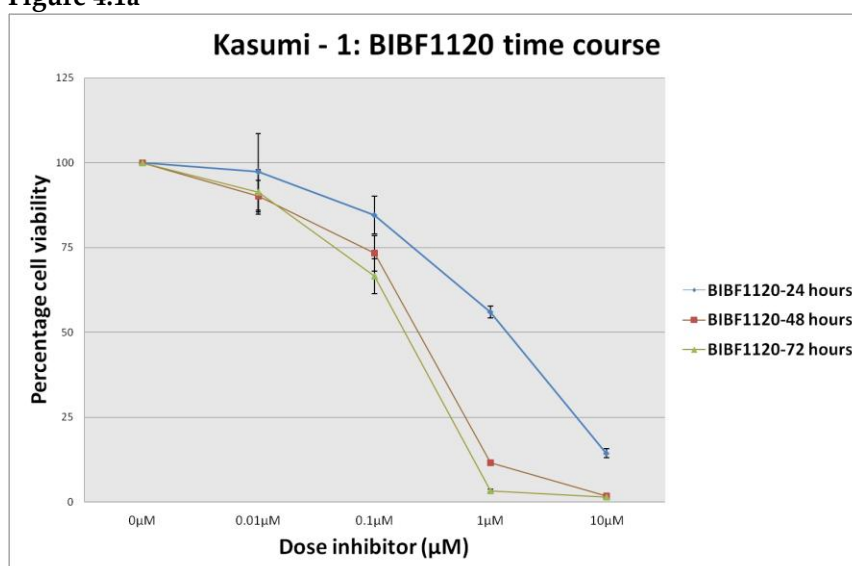
Using Kasumi-1 cells as a positive control for the assay, the optimal duration of drug exposure to detect activity was assessed with a time course experiment with 2 KIT inhibitors from the library. These inhibitors were imatinib (Abl/CSF-1R/KIT/PDGFR) and BIBF1120 (FGFR/FLT3/KIT/PDGFR/VEGFR). The effect on cell viability was assessed after 24, 48 and 72 hours. With both inhibitors, the percentage of surviving cells decreased with increasing drug exposure up to 72 hours (figs 4.1a and b). The IC₅₀ for both imatinib and BIBF1120 decreased with increased duration of treatment. The IC₅₀ at 24 hour exposure for imatinib was 1.11µM compared to 0.161µM with 72 hour exposure. Similarly, with BIBF1120, the IC₅₀ was 0.977µM and 0.052µM following 24 hour and 72 hour exposure respectively. The IC₅₀ measured at 72 hours for both imatinib and BIBF1120 are consistent

with published data (339, 377) therefore validating this system. There was little difference in cell kill following the 48 and 72 hour exposures, which is important in applying the assay to primary ALLs, since prolonged *in vitro* incubation of primary ALL cells can significantly reduce cell viability because of their propensity to undergo spontaneous apoptosis (378).



| IC ₅₀ | Imatinib |
|------------------|---------------------|
| 24h | 1.11 μM |
| 48h | 0.262 μM |
| 72h | 0.161 μM |

Figure 4.1a



| IC ₅₀ | BIBF1120 |
|------------------|---------------------|
| 24h | 0.977 μM |
| 48h | 0.077 μM |
| 72h | 0.052 μM |

Figure 4.1b

Figure 4.1 Incubation of Kasumi – 1 cell line with Kit – inhibitors demonstrate a time dependent reduction in cell viability. Both (a) imatinib and (b) BIBF1120 demonstrated maximal inhibition of cell viability by 72 hours. In keeping with published data both TKI induced responses at nanomolar concentrations. The difference in reduction of cell viability was minimal in cells incubated for 48 hours or 72hours.

(ii) Establishing optimal drug concentrations

While detailed incremental dose response evaluation is the ideal method to elucidate the potency of each drug, the number of concentrations applied in this screen is limited by the quantity of primary ALL material available. Therefore an upper dose limit was selected, based on the well – established NCI – 60 DTP Human Tumor Cell Line Screen. This screen uses a single dose of 10 μ M to investigate the activity of new compounds (379, 380). An additional lower dose was also included, to enable detection of low-dose activity and to establish dose – dependent efficacy of the TKIs to be established. To identify what a suitable lower dose, the Kasumi – 1 cell line was treated with 8 TKIs, 5 of which inhibit Kit (imatinib, nilotinib, dasatinib, axitinib and sunitinib), and 3 of which do not (gefitinib [EGFR/HER2], brivanib [VEGFR/FGFR] and NVPAEW541 [IR/IGF – 1R]). While all 5 KIT inhibitors induced a 50% reduction in cell viability a dose of 1 μ M, only 2 caused this reduction at a dose of 0.1 μ M (fig 4.2). Since none of the 3 TKIs which do not target Kit induced a greater than 50% reduction in viability at a dose of 1 μ M, these data indicate that 1 μ M drug is likely to be discriminatory in determining an active dose.

Thus, for this study, a compound of interest was defined as a TKI exhibiting a greater than 50% reduction in cell viability at 1 μ M and demonstrating a further response at 10 μ M.

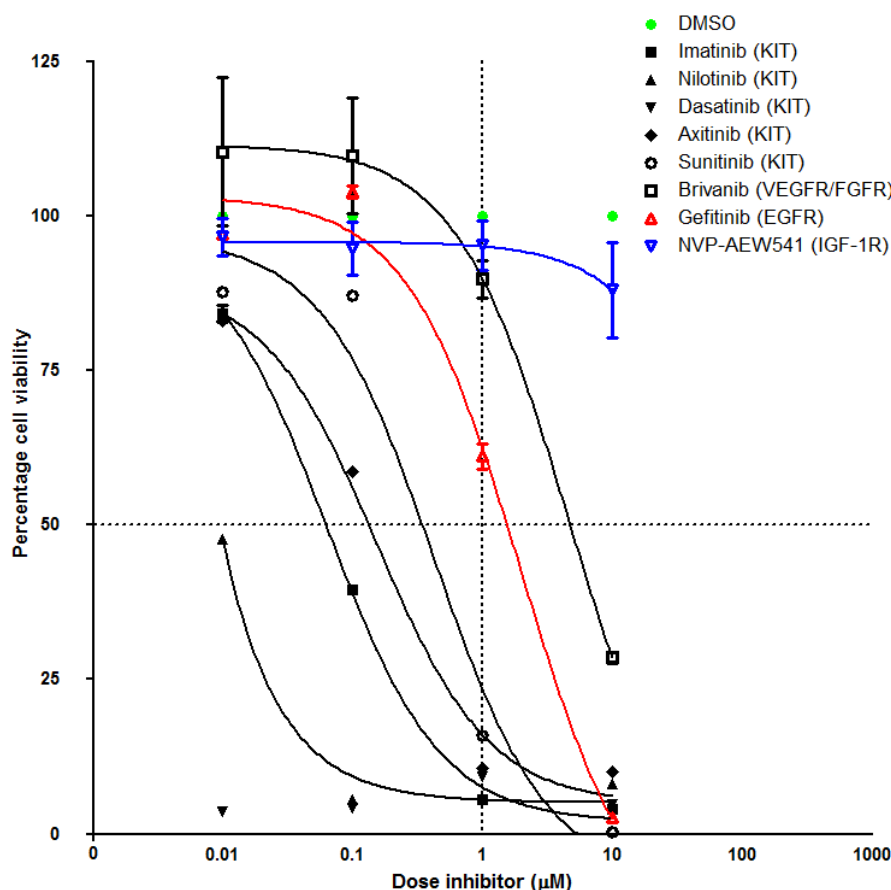


Figure 4.2 Selective response to Kit – inclusive inhibitors in demonstrated in Kasumi – 1 cell lines when tested with a panel of 8 TKI. All Kit – inclusive inhibitors demonstrated nanomolar activity. The Kit – inclusive inhibitors imatinib, nilotinib dasatinib, axitinib and sunitinib demonstrated nanomolar activity in the Kasumi – 1 cell line. Brivanib, gefitinib and NVP - AEW541 did not induce significant cell death at nanomolar concentration. The concentration of 1 μ M was most discriminatory to identify possible Kit inhibitors.

(iii) Establishing optimal culture conditions for ALL primary cells

Primary ALL cells have limited viability when cultured *in vitro*. The reducing agent β – mercaptoethanol (BME) has been reported to improve the *in vitro* viability of lymphocytes in cell culture, by reducing oxidative stress and maximising the ability of lymphocytes to utilise essential amino acids (381). To optimise the culture media for *in vitro* incubation of the primary ALL cells for study of drug activity, the effects of BME on cell viability were investigated. Serial dilutions of primary ALL cells from ALL-36 were incubated either in RPMI/10%FCS/1%pen/strep alone or with 50 μ M BME for 48 hours and the cell viability compared. Consistent with published data, it was confirmed that viability of the cells

cultured with BME was consistently higher than cells cultured without BME (fig 4.3a and b). BME was subsequently included in the primary cell cultures during drug screening.

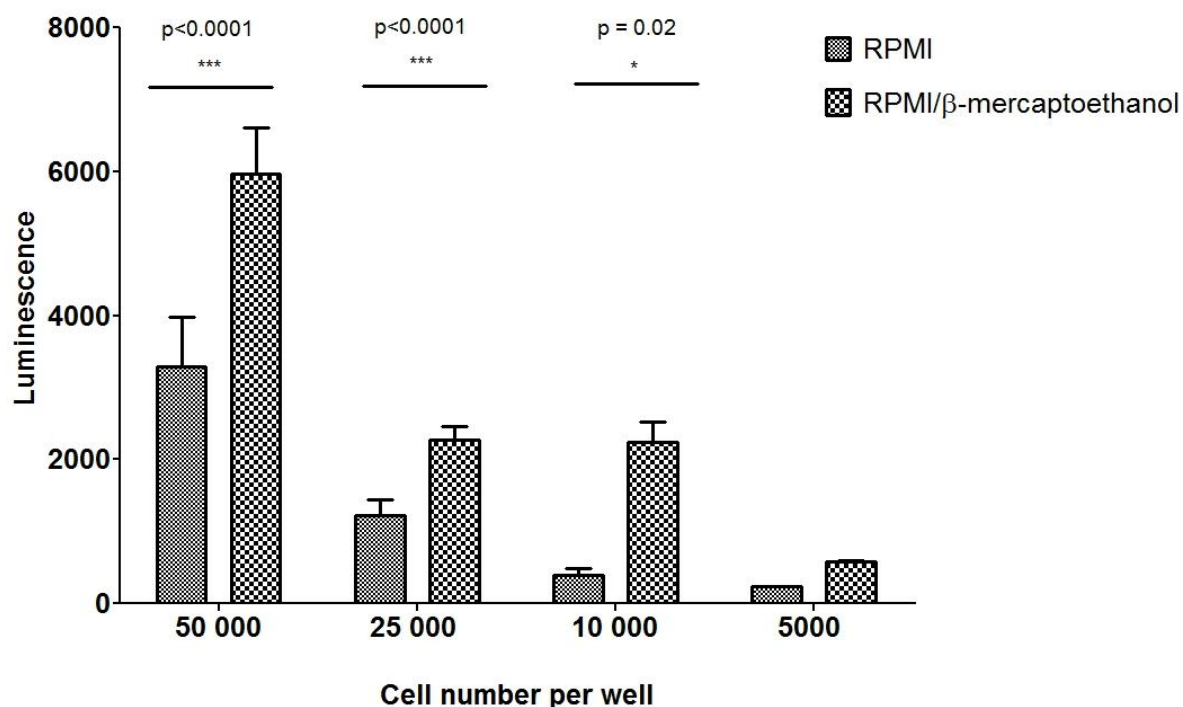


Figure 4.3a

| Cells per well | Ratio of luminescence RPMI BME/RPMI |
|----------------|-------------------------------------|
| 50 000 | 1.68 |
| 25 000 | 1.77 |
| 50 000 | 1.94 |
| 25 000 | 1.95 |
| 10 000 | 1.5 |

Figure 4.3b

Figure 4.3 Correlation of relative luminescence with cell density and culture media. (a) The relative luminescence ratio of cells culture in RPMI and RPMI with 50 μ M BME was determined. The relative luminescence was directly related to cell number, but addition of BME demonstrated a statistically significant increase in cell viability. (b) Luminescence was persistently higher in the RPMI/BME cultured primary cells at all concentrations of cells per well, except 5000 cells per well.

4.3. Proof of principle of TKI screen in a primary myeloid leukaemia (AML – 2)

Optimisation of the TKI library screening method had been performed using cell lines. Before initiating the TKI library screen in the primary ALL samples, the optimised TKI library method was tested in primary myeloid leukaemia cells (AML – 2) carrying a specific, defined RTK – abnormality, *FLT3 – ITD*, which was expected to exhibit sensitivity to FLT3 inhibition.

The activity of 20 TKIs was tested against AML – 2 using the optimised method. A reduction in cell viability of greater than 50% was observed at 1 μ M in 10 of the 20 TKIs screened (fig 4.4). Six of these TKIs (BIBF1120, CEP – 701, dovitinib, foretinib, sorafenib and sunitinib) are known to be FLT3 inhibitors and therefore the effect was predicted. The remaining active compounds were PHA739358 (Aurora kinase/Abl/RET), bosutinib (Abl/Src/Axl/Trk) and the EGFR/HER-2 inhibitors CI-1033 and BIBW-2992. No effect was induced by the remaining inhibitors at 1 μ M, of which only the dual Aurora kinase/FLT3 inhibitor VX-680 is active against FLT3 (347). These data, therefore, show that the optimised TKI library screen is able to target and distinguish molecules and pathways involved in disease pathology. This method, if used in a larger cohort of primary ALLs, could be used to identify useful novel therapeutic targets and drugs.

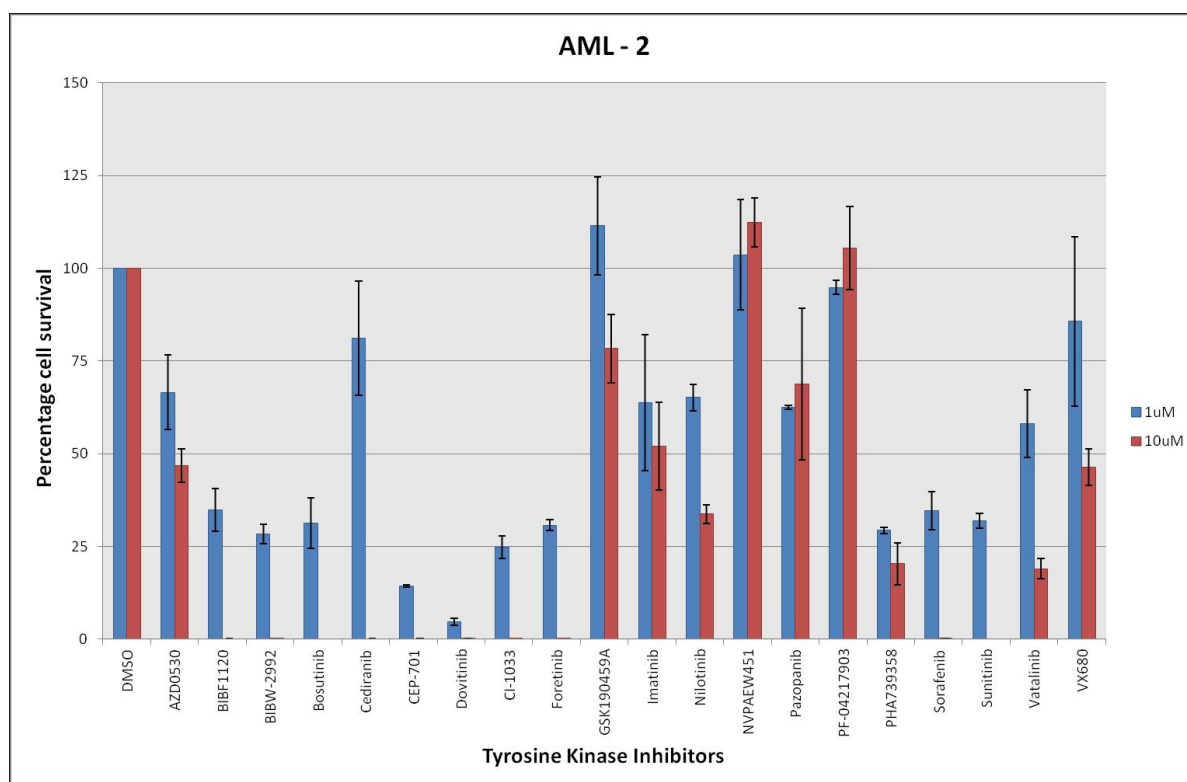


Figure 4.4 Bar chart demonstrating activity of TKIs against AML – 2 at 1 and 10 μM. Ten FLT3 – inclusive inhibitors demonstrate activity in the FLT3 mutated AML – 2 cells at 1 μM. The experiment was performed once, with triplicate wells. Data plotted is the mean of the 3 wells, error bars are standard deviation of triplicate wells.

4.4. Screen of B – precursor ALL cell lines with expanded TKI library

Following the optimisation and proof of principle evaluation of the TKI library assay, a cohort of ALL cell lines (n=5) were screened and a cohort of primary ALLs (n=20) were evaluated (table 4.1). Compounds of interest which were defined as TKIs causing a greater than 50% reduction in cell viability at 1 μM and a further response at 10 μM were identified from a panel of 33 molecules.

| TKI | Putative primary targets |
|--|---|
| JAK inhibitors | |
| AG490 | JAK 2 – 3, EGFR |
| CP690550 | JAK 1 – 3 |
| IGF-1R/Insulin inhibitors | |
| GSK1904529A | IGF – 1R/Insulin |
| NVPAEW541 | IGF – 1R/Insulin |
| Irreversible EGFR/HER2 | |
| BIBW-2992 | EGFR/HER2 |
| CI – 1033 | EGFR/HER2/HER4 |
| Restricted spectrum inhibitors | |
| AZD0530 | Abl/Src/EGFR |
| Bosutinib | Abl/Src/Axl/EGFR/Trk |
| Dasatinib | Abl/Src/CSF-1R/Kit/PDGFR $\alpha\beta$ |
| Imatinib | Abl/CSF-1R/Kit/PDGFR $\alpha\beta$ |
| Masitinib | Kit/PDGFR $\alpha\beta$ |
| Nilotinib | Abl/Kit/PDGFR $\alpha\beta$ |
| PF-04217903 | Met |
| PF-2341066 | Met/ALK |
| PHA739358 | Aurora kinase A – C/Abl/Src/RET |
| AMG – TIE-2 – 1 | Tie – 2 |
| Multikinase inhibitors (VEGFR/PDGFR) | |
| Axitinib | VEGFR 1 – 3/PDGFR $\alpha\beta$ /CSF – 1R/Kit/FGFR 1 |
| Brivanib | VEGFR 1 -3/FGFR 1 – 3 |
| Cediranib | VEGFR 1 – 3/PDGFR $\alpha\beta$ /CSF – 1R/Kit/FGFR 1 |
| Motesanib | VEGFR 1 – 3/PDGFR α /Kit/RET |
| Pazopanib | VEGFR 1 – 3/PDGFR $\alpha\beta$ /CSF – 1R/Kit/FGFR 1, 3 and 4 |
| Vandetanib | VEGFR 1 -3/EGFR/RET |
| Vatalinib | VEGFR 1 – 3/PDGFR β /Kit |
| Multikinase inhibitors with FLT3 activity | |
| ABT-869 | FLT3/VEGFR 1 – 3/PDGFR β /CSF – 1R/Kit |
| BIBF1120 | FLT3/VEGFR 1 – 3/PDGFR $\alpha\beta$ /FGFR 1 – 4/Src |
| CEP-701 | FLT3/VEGFR 1 – 2/PDGFR β /RET/TrkA |
| Dovitinib | FLT3/VEGFR 1 – 3/PDGFR $\alpha\beta$ /CSF – 1R/Kit/FGFR 1 and 3 |
| Foretinib | FLT3/VEGFR 1 – 3/PDGFR $\alpha\beta$ /CSF – 1R/Kit/FGFR 1/Ron/Axl/Tie – 2 |
| NVPTAE684 | FLT3/Met/ALK |
| Sorafenib | FLT3/VEGFR 2 -3/PDGFR β /Kit/B – raf |
| Sunitinib | FLT3/VEGFR 1 – 3/PDGFR $\alpha\beta$ /CSF – 1R/Kit/RET/FGFR1 |
| Tandutinib | FLT3/PDGFR $\alpha\beta$ /Kit |
| VX-680 | FLT3/Aurora kinase A – C/Abl |

Table 4.1 Expanded tyrosine kinase inhibitor library, with primary putative targets TKIs were chosen to cover the kinome. The inhibitors have been grouped together by principle activity: (i) Jak inhibitors, (ii) IR/IGF – 1R, (iii) EGFR/HER2 inhibitors, (iv) restricted inhibitors with no FLT3 activity, (v) multikinase inhibitors with no FLT3 activity and (vi) multikinase inhibitors with FLT3 activity.

4.4.1. Characteristics of ALL cell line panel for TKI library screen

The 5 cell lines screened were representative of the heterogeneity of ALL with respect to cytogenetic variety and drug sensitivity (Table 4.2). As a proxy for chemosensitivity the cell lines were characterised for apoptotic response to IR – induced DNA damage (chapter 3.1). Three patterns of damage were identified. Nalm 17 and SupB15, were apoptosis proficient (suggesting chemosensitivity), while REH and SD - 1 were apoptosis defective (suggesting chemoresistance). Nalm 6 exhibited an intermediate response, with limited cleavage of procaspases and PARP – 1 after irradiation. This pattern of response is interpreted as a leukaemia with a moderate degree of chemoresistance. Normal accumulation of p53 in response to IR was present in all cell lines as previously described (315).

| Cell line | Cytogenetics | Apoptotic response to IR – induced DNA damage |
|-----------|------------------|---|
| Nalm 6 | t(5;12) | Intermediate |
| Nalm 17 | Normal karyotype | Apoptosis proficient |
| REH | t(12;21) | Apoptosis defective |
| SD – 1 | t(9;22) | Apoptosis defective |
| Sup – B15 | t(9;22) | Apoptosis proficient |

Table 4.2 Characteristics of B – cell precursor ALL cell lines. The 5 ALL cell lines were characterised for apoptotic response to IR – induced DNA damage. Cells were considered proficient if there was evidence of intrinsic apoptosis, demonstrated by activation of p53 with cleavage of PARP – 1 and procaspases 7. The cell lines Nalm17 and SupB15 demonstrated proficient apoptotic responses, while REH and SD – 1 were apoptosis defective. The t(5;12) cell line Nalm 6 demonstrated an intermediate response, with activation of p53 and limited PARP – 1 and procaspase cleavage.

4.4.2. Sensitivity of cell lines to TKIs at 1 μ M and 10 μ M

There was significant heterogeneity of response of the 5 cell lines to many of the TKIs. Sixteen of the 33 TKIs demonstrated activity at 1 μ M, while 26/33 demonstrated activity in at least 1 cell line at 10 μ M. Table 4.3 summarises the mean percentage of remaining viable cells at 1 μ M, with active TKIs, highlighted in green. The response of SupB15 to PHA739358 (Aurora kinase/FLT3) is highlighted in yellow because, while a reduction in cell viability greater than 50% was detected at 1 μ M, an increase was observed to above 50% at 10 μ M. This drug was thus not considered a compound of interest.

| Tyrosine Kinase Inhibitors | | Nalm 6 | Nalm 17 | REH ^a | SD-1 ^{ab} | SupB15 ^b |
|--|---|---------|---------|------------------|--------------------|---------------------|
| JAK inhibitors | | | | | | |
| AG490 | JAK 2 – 3, EGFR | 91 (12) | 94(5) | 88(19) | 74(7) | 108(14) |
| CP690550 | JAK 1 – 3 | 103(35) | 96(3) | 107(15) | 80(5) | 106(7) |
| IGF-1R/Insulin inhibitors | | | | | | |
| GSK1904529A | IGF – 1R/Insulin | 90(8) | 104(8) | 96(3) | 97(39) | 106(26) |
| NVPAEW541 | IGF – 1R/Insulin | 96(15) | 91(12) | 104(3) | | 103(10) |
| EGFR/HER2 Quinazoline | | | | | | |
| BIBW-2992 | EGFR/HER2 | 88 (28) | 68(45) | 42(14) | 35(16) | 92(20) |
| CI – 1033 | EGFR/HER2/HER4 | 77(4) | 77(27) | 41(10) | 22(17) | 98(6) |
| Restricted spectrum | | | | | | |
| AZD0530 | Abl/Src/EGFR | 95 (32) | 94(3) | 91(29) | 45(6) | 64(10) |
| Bosutinib | Abl/Src/Axl/EGFR/Trk | 35(7) | 23(15) | 38(0) | 23(20) | 30(11) |
| Dasatinib | Abl/Src/CSF-1R/Kit/PDGFRαβ | 67(29) | 70(22) | 76(3) | 32(15) | 22(10) |
| Imatinib | Abl/CSF-1R/Kit/PDGFRαβ | 80(16) | 88(14) | 91(2) | 73(12) | 60(11) |
| Masitinib | Kit/PDGFRαβ | 113(45) | 102(8) | 83(6) | 56(9) | 53(13) |
| Nilotinib | Abl/Kit/PDGFRαβ | 97(14) | 94(5) | 88(2) | 72(9) | 55(8) |
| PF-04217903 | Met | 91(16) | 94(8) | 89(11) | 82(12) | 109(15) |
| PF-2341066 | Met/ALK | 70(3) | 72(36) | 46(3) | 35(5) | 14(8) |
| PHA739358 | Aurora kinase A – C/Abl/Src/RET | 73(22) | 66(22) | 66(14) | 27(9) | 25(12) |
| TIE-2 | Tie – 2 | 68(25) | 94(3) | 89(4) | 52(22) | 60(18) |
| Multikinase inhibitors (VEGFR/PDGFR) | | | | | | |
| Axitinib | VEGFR 1 – 3/PDGFRαβ/CSF – 1R Kit/FGFR 1 | 99(19) | 85(13) | 52(30) | 70(24) | 46(13) |
| Brivanib | VEGFR 1 -3/FGFR 1 – 3 | 71(12) | 94(8) | 97(13) | 88(17) | 113(9) |
| Cediranib | VEGFR 1 – 3/PDGFRαβ/CSF – 1R Kit/FGFR 1 | 93(3) | 92(2) | 89(15) | 65(5) | 103(12) |
| Motesanib | VEGFR 1 – 3/PDGFRα/Kit/RET | 113(19) | 102(8) | 85(1) | 99(30) | 103(13) |
| Pazopanib | VEGFR 1 – 3/PDGFRαβ/CSF – 1R Kit/FGFR 1, 3 and 4 | 93(13) | 92(15) | 91(0) | 64(20) | 105(34) |
| Vandetanib | VEGFR 1 -3/EGFR/RET | 71(11) | 84(20) | 92(12) | 70(23) | 60(15) |
| Vatalinib | VEGFR 1 – 3/PDGFRβ/Kit | 105(28) | 101(5) | 76(16) | 85(6) | 101(4) |
| Multikinase inhibitors with FLT3 activity | | | | | | |
| ABT-869 | FLT3/VEGFR 1 – 3/PDGFRβ/CSF – 1R/Kit | 125(36) | 95(5) | 87(12) | 2(2) | 88(3) |
| BIBF1120 | FLT3/VEGFR 1 – 3/PDGFRαβ/FGFR 1 – 4/Src | 64(26) | 86(31) | 83(6) | 42(4) | 43(4) |
| CEP-701 | FLT3/VEGFR 1 – 2/PDGFRβ/RET/TrkA | 25(7) | 12(6) | 35(16) | 10(4) | 19(5) |
| Dovitinib | FLT3/VEGFR 1 – 3/PDGFRαβ/CSF – 1R Kit/FGFR 1 and 3 | 34(15) | 35(15) | 11(1) | 19(8) | 1(1) |
| Foretinib | FLT3/VEGFR 1 – 3/PDGFRαβ/CSF – 1R/Kit/FGFR 1/Ron/Axl/Tie – 2 | 77(20) | 35 (9) | 19(5) | 12(15) | 8(4) |
| NVPTAE684 | FLT3/Met/ALK | 112(24) | 68(38) | 62(15) | 35(10) | 80(38) |
| Sorafenib | FLT3/VEGFR 2 -3/PDGFRβ/Kit/B – raf | 81(2) | 82(2) | 90(5) | 53(9) | 77(17) |
| Sunitinib | FLT3/VEGFR 1 – 3/PDGFRαβ/CSF – 1R/Kit/RET/FGFR1 | 85(7) | 79(19) | 65(0) | 62(26) | 107(29) |
| Tandutinib | FLT3/PDGFRαβ/Kit | 82(12) | 95(10) | 107(8) | 64(25) | 109(10) |
| VX-680 | FLT3/Aurora kinase A – C/Abl | 86(13) | 88(32) | 64(5) | 36(7) | 22(13) |

Key:

a – Apoptosis defective in response to IR – induced DNA damage

b – Philadelphia positive cell line

Table 4.3 Summary of inhibitors grouped by putative targets which demonstrated greater than 50% reduction in viability at 1μM in cell lines. Mean percentage of remaining viable cells at 1μM of 3 separate experiments in triplicate with standard deviation in parentheses. TKIs with activity in cell lines are highlighted in green. PHA739358 is highlighted in yellow, despite reducing cell viability >50% at 1μM, there was no further decrease at 10μM.

Three of 33 compounds were able to induce $\geq 50\%$ reduction in viability at $1\mu\text{M}$ in all 5 cell lines (fig 4.5). These inhibitors were dovitinib (VEGFR/PDGFR/FGFR/FLT3), CEP – 701 (FLT3/Ret/Trk/VEGFR2), and bosutinib (Abl/Src/Axl/EGFR/Trk). A further multikinase inhibitor, foretinib (Axl/CSF – 1R/FLT3/ Met/PDGFR/Ron/Tie – 2/VEGFR), inhibited 4/5 cell lines; only Nalm 6 was resistant at $1\mu\text{M}$. PF – 2341066 (Met/ALK) was active in 3/5 cell lines, while the Abl inhibitors, dasatinib and VX – 680, inhibited only the 2 t(9;22) cell lines.

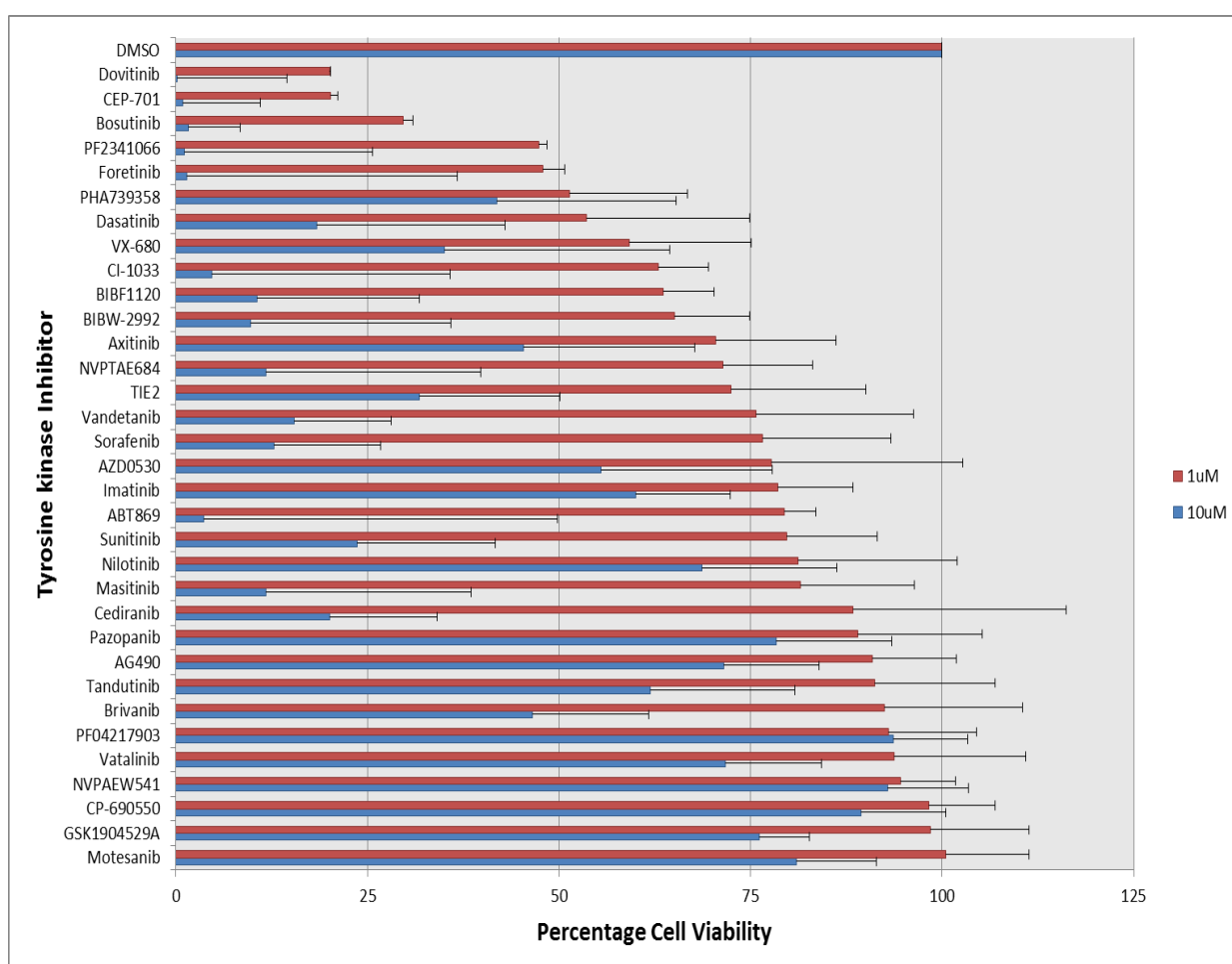


Figure 4.5 Summary of mean responses of cell lines to individual TKIs. Percentage viability documented is the mean of the 5 cell lines, with error bars as standard deviation. The TKIs which were most potent in 4 or 5 cell lines were dovitinib, CEP-701, foretinib and bosutinib. While the mean reduction of cell viability was $>50\%$ in response to PF – 2341066, it demonstrated activity in only 3 of the 5 cell lines.

To investigate whether the 4 TKIs bosutinib, CEP – 701, dovitinib and foretinib work through a single pathway the putative targets of the drugs were compared (fig 4.6).

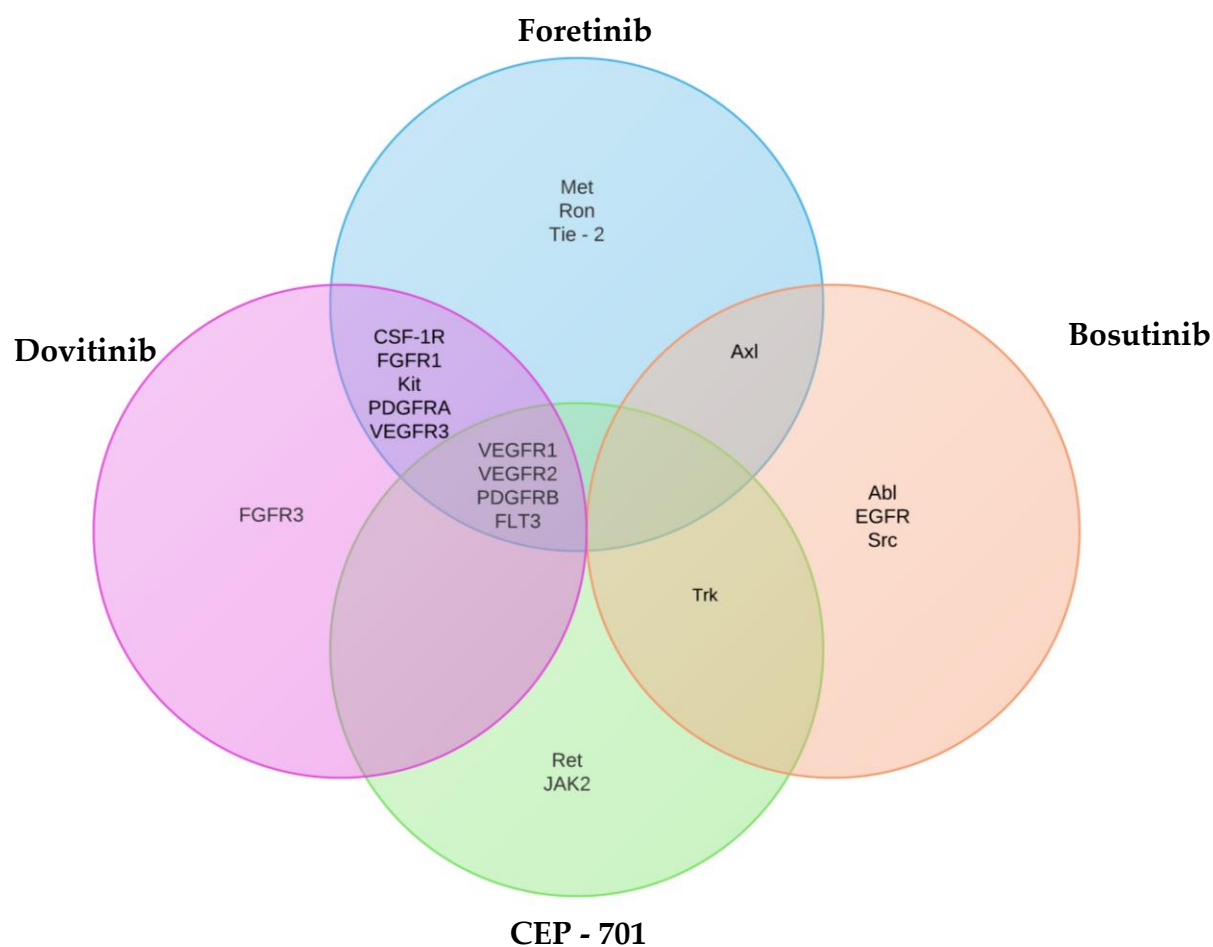


Figure 4.6 Venn diagram demonstrating shared putative targets of bosutinib, CEP – 701, dovitinib, and foretinib. No unifying putative target was shared by the 4 TKIs. Three of the 4 TKIs demonstrate *in vitro* activity against FLT3, PDGFR β and VEGFR RTKs.

Three of these four compounds, CEP – 701, dovitinib and foretinib, are multikinase inhibitors with activity against common targets FLT3, VEGFR1, VEGFR2 and PDGFR β . Bosutinib was initially designed as a dual non - receptor tyrosine Abl/Src inhibitor and has a more restricted spectrum of activity, with no identified activity against FLT3, FGFR, or PDGFR families; at nanomolar concentrations its principal targets include Axl, EGFR and Trk (323).

CEP – 701, dovitinib and foretinib do not have activity against Abl or Abl mutants, but yet reduced the viability of both t(9;22) Abl – dependent cell lines (SupB15 and SD – 1). This

finding would suggest that at least one of their primary targets (including Axl, CSF – 1R, FGFR1/3, FLT – 3, Kit, Met, PDGFR α/β , Ret, Ron, Trk or VEGFR1 – 3) is important in the cell survival of t(9;22) cell lines, SupB15 and SD – 1.

In summary, while a common target was not shared by the 4 most active TKIs against the panel of cell lines, common patterns were noted. RTKs common to at least 2/4 inhibitors included Axl, CSF-1R, FGFR1, Kit, PDGFR α , Trk A and VEGFR3. Four RTKs, FLT3, PDGFR β , VEGFR1 and VEGFR2, were common targets for 3 inhibitors. It is possible that these TKIs target a combination of TKs which leads to reduced viability. Alternatively, the inhibitors may act against ‘off – target’ molecular sites which have not yet been identified.

4.4.3. Sensitivity of cell lines to TKIs with activity in all cell lines at 10 μ M

To minimise the chance that potentially important pathways were excluded by the definition of active compounds used in this study, the spectra of the TKIs which demonstrated a significant reduction in cell viability by greater than 50% at 10 μ M in all 5 cell lines were assessed.

Of the 33 TKIs tested 14 compounds were effective in all 5 cell lines at 10 μ M (fig 4.7). These were: (i) FLT3 – inclusive multikinase inhibitors (ABT – 869, BIBF1120, CEP – 701, dovitinib, foretinib, NVPTAE684, sorafenib and sunitinib), (ii) EGFR/HER2 inhibitors (BIBW-2992 and CI – 1033) and (iii) more restricted inhibitors bosutinib (Abl/Axl/EGFR/Trk), vandetanib (VEGFR/EGFR/RET), masitinib (Kit/PDGFR) and PF -2340166 (Met/ALK). The additional potential targets were therefore ALK, FGFR 2 and HER2 (fig 4.8).

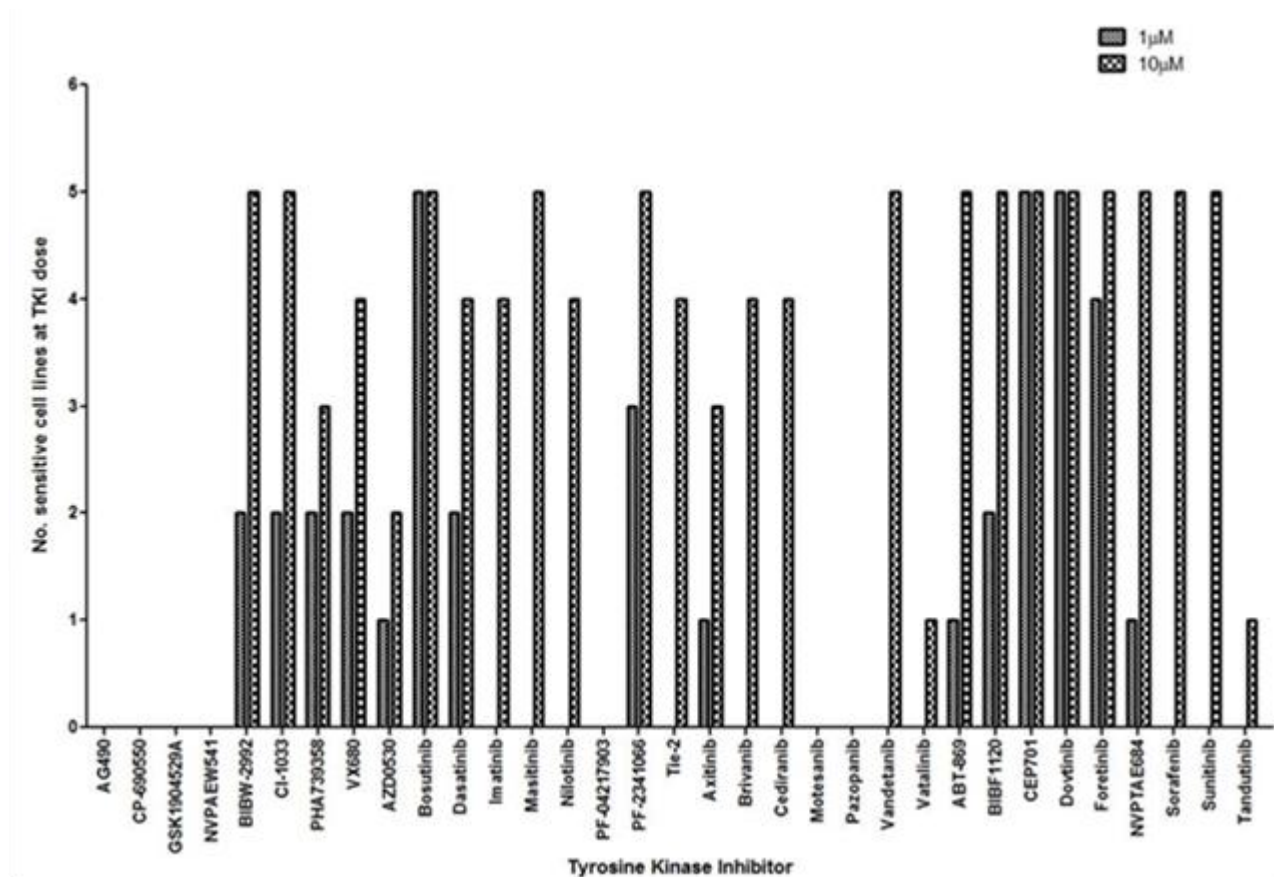


Figure 4.7 Fourteen TKIs induced greater than 50% reduction in cell viability in all 5 cell line at 10µM. Cell viability was potently affected in all 5 cell lines by the inhibitors bosutinib, CEP – 701 and dovitinib at 1µM. A further 10 TKIs (BIBW – 2992, CI – 1033, masitinib, PF – 2341066, vandetanib, ABT – 869, BIBF1120, NVPTAE684, sorafenib and sunitinib) induced a global inhibition of all 5 cell lines at 10µM.

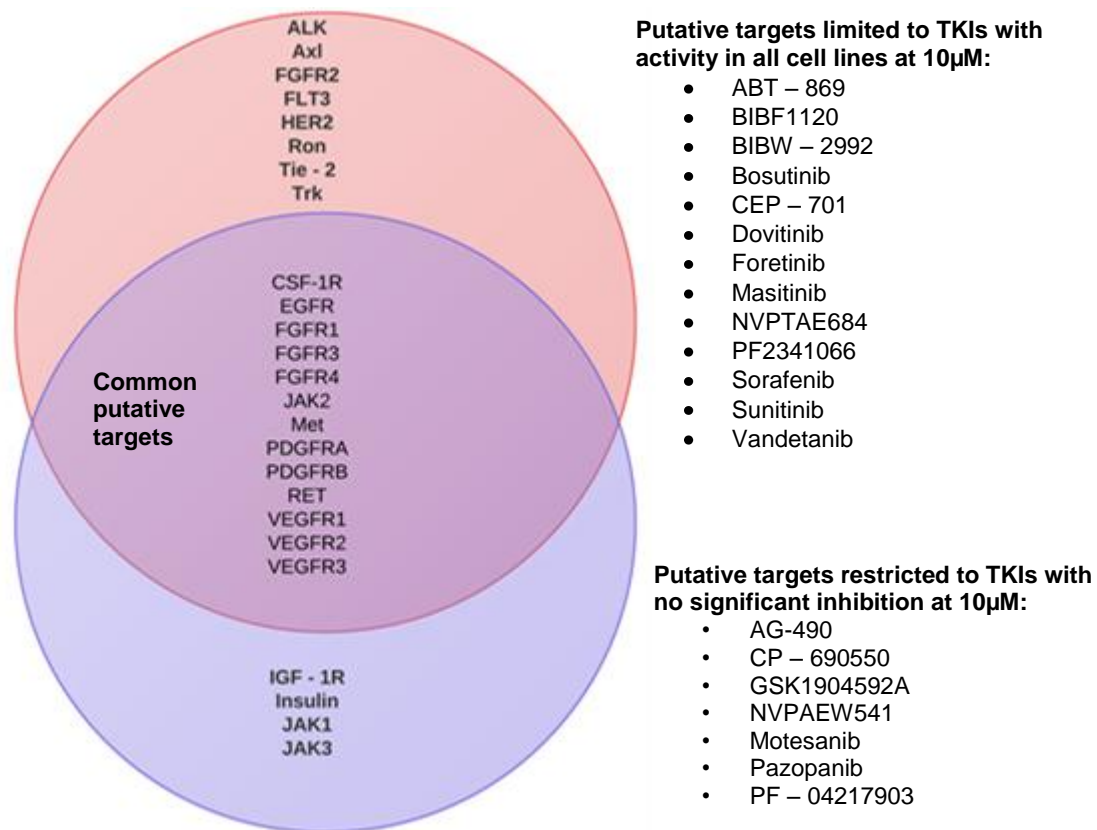


Figure 4.8 Venn Diagram comparing possible targets of TKIs with activity at 10µM and those with no significant activity at 10µM. The JAK, Insulin/IGF – 1R, Met, PDGFR and VEGFR pathways do not appear vital to the survival of childhood ALL blasts in this study.

In summary, the patterns of putative targets of TKIs which demonstrate activity at 1µM and 10µM are very similar in the cell lines. The inclusion of the putative targets ALK, FGFR2 and HER2 at 10µM could be associated with on – or ‘off – target’ effects at this higher concentration.

4.4.4. Sensitivity of cell lines with defective apoptotic responses to IR – induced DNA damage to TKIs

The greatest clinical need in drug development for childhood ALL is for treatment resistant sub-groups. A defective apoptotic response to IR – induced DNA damage *in vitro*, has been shown to be a proxy marker of chemoresistance (315). The pattern of sensitivity to the TKI panel in the apoptosis defective cell lines, REH and SD – 1 was therefore compared to TKI sensitivity in apoptosis proficient Nalm 17 and Sup B15 or the intermediate responding Nalm 6.

Of the 33 TKIs tested, 2 revealed a differential effect on cell survival relating to apoptotic response to IR. These were the structurally related pan – EGFR inhibitors, CI-1033 and BIBW2992 (fig 4.9). Whilst all the cell lines responded to CI-1033 and BIBW2992 at the 10 μ M level, it was the apoptosis defective cell lines, REH and SD – 1 that had the greatest response at the 1 μ M level.

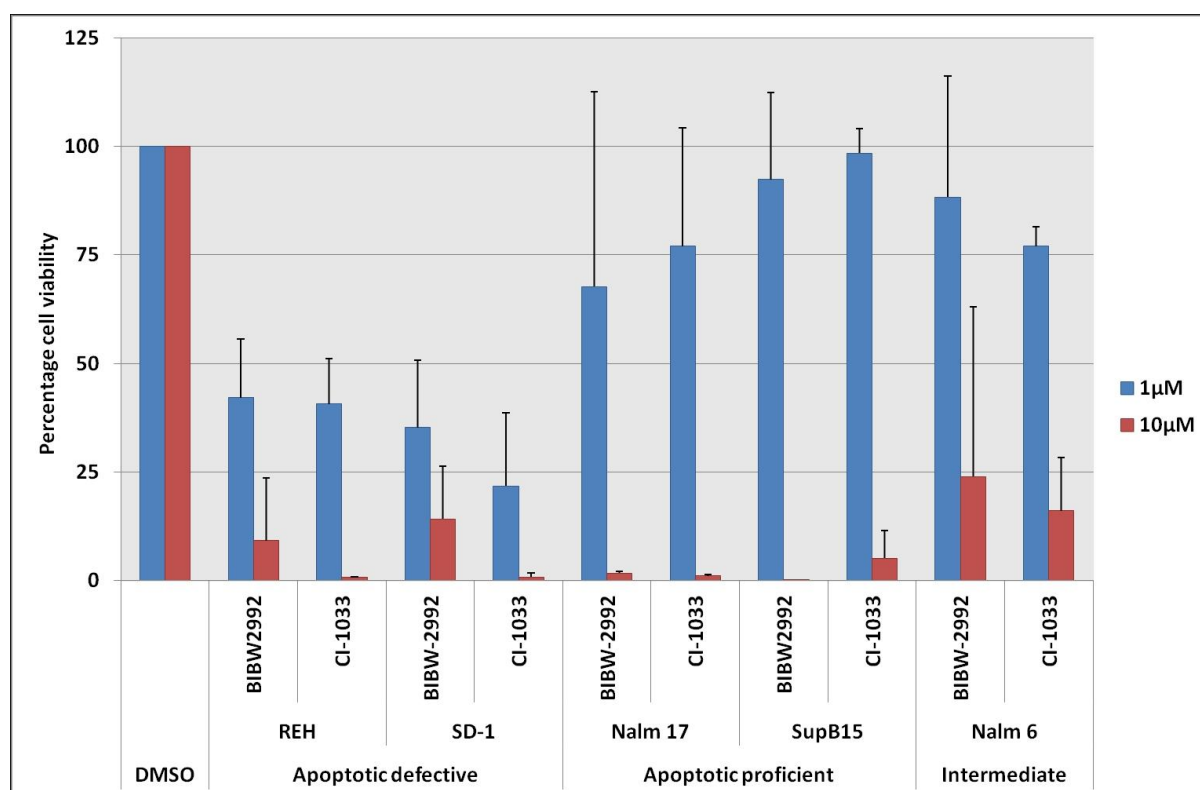


Figure 4.9 Differential response demonstrated by apoptotic defective cell lines, REH and SD – 1, to the irreversible quinazoline inhibitors BIBW – 2992 and CI – 1033. These 2 TKIs demonstrated significant potency against the apoptotic deficient cells lines, REH and SD – 1, and thus may be important in the treatment of chemoresistant ALL.

EGFR inhibitors have been shown to induce differentiation in myeloid leukaemias (382), this study is the first to investigate the activity in B – precursor ALL. To investigate whether the activity was due to EGFR/HER2 inhibition or an ‘off – target’ effect REH and SD-1 cell were treated with 2 additional EGFR/HER2 inhibitors, gefitinib and BMS – 599626, that were not included in the original TKI library screen. Gefitinib is a structurally related quinazoline inhibitor, but unlike BIBW-2992 or CI – 1033 does not bind irreversibly to the ATP – pocket of the receptors. BMS – 599626 is an unrelated pyrrolotriazine analogue. Both of these inhibitors demonstrate nanomolar activity in cell – based assays where EGFR or HER2 are overexpressed or activated (155, 383, 384).

The nanomolar activity of BIBW – 2992 and CI – 1033 was confirmed in both the apoptosis defective cell lines, REH and SD1 (fig 4.10a and b), however neither gefitinib nor BMS –

599626 exhibited sufficient activity against SD – 1 or REH to generate an IC_{50} below $10\mu M$, suggesting inhibition of EGFR/HER2 is not the mechanism of action of CI – 1033 and BIBW – 2992. The absence of a response to all EGFR family of inhibitors tested, would suggest the activity of BIBW-2992 and CI-1033 in these cell lines is due to higher affinity to the target or an ‘off – target’ effect, for example FLT3. A recent series of reports have implicated FLT3 as an unexpected kinase target of CI – 1033 (385, 386). Both REH and SD – 1 exhibited sensitivity to the FLT3 – inclusive multikinase inhibitors, CEP – 701, dovitinib and foretinib (table 4.3).

The restricted activity of the quinazoline inhibitors in the apoptosis defective cell lines, REH and SD – 1, suggests that this family of inhibitors may be active in chemoresistant leukaemias however, the mechanism of action is uncertain. It may be through FLT3, but this needs further investigation.

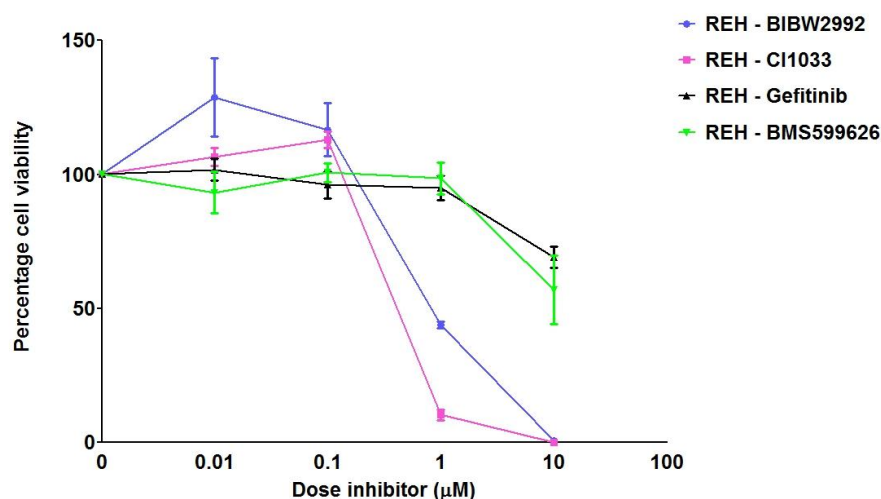


Figure 4.10a

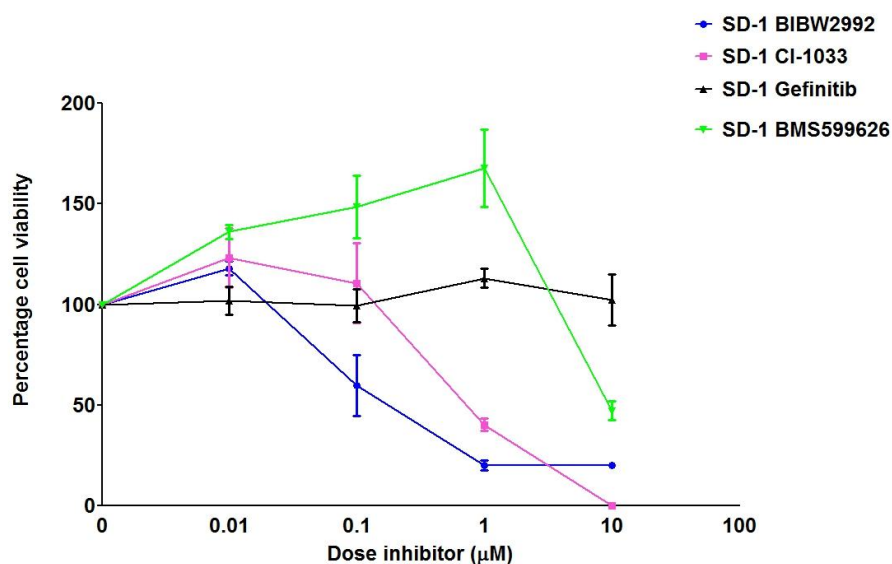


Figure 4.10b

| | REH | SD-1 |
|------------------|----------|---------------|
| BIBW-2992 | 0.861μM | 0.100 μM |
| CI-1033 | 0.472μM | 0.789 μM |
| Gefitinib | 13.85 μM | Not converged |
| BMS599626 | >10 μM | Not converged |

Figure 4.10c

Figure 4.10 Significant nanomolar activity is limited to the irreversible quinazoline inhibitors BIBW – 2992 and CI – 1033 in (a) REH and (b) SD – 1 cell lines. The EGFR/HER2 inhibitors gefitinib and BMS – 599626 did not demonstrate any activity against the REH and SD – 1 cell lines. These data suggest the activity of BIBW-2992 and CI-1033 may not be via these axes in the childhood ALL cell lines investigated in this study.

4.4.5. TKI sensitivity in Philadelphia positive cell lines

Ph⁺ leukaemias are generally chemoresistant and historically have a poor prognosis. The use of Bcr/Abl inhibitors in conjunction with chemotherapy has improved survival, but resistance to inhibitors is a concern. To investigate whether additional pathways could be targeted in Ph⁺ cell lines, the responses of the Ph⁺ ALL cell lines SupB15 and SD – 1 to the 33 TKI panel were analysed.

SupB15 and SD – 1, demonstrated sensitivity to the largest number of TKIs, 9 and 14 compounds respectively. Of these inhibitors, 3 with activity in SupB15 and 5 with activity in SD – 1, were known Abl inhibitors (table 4.4). The absence of nanomolar response to imatinib and nilotinib is consistent with published data (387).

| | | Ph+ cell lines | | Non – Ph+ cell lines | | |
|----------------------|--------------------------------|---------------------|---------------------|----------------------|---------|-----|
| | Putative targets | SD – 1 ^a | SupB15 ^a | Nalm 6 | Nalm 17 | REH |
| Abl inhibitors | | | | | | |
| Imatinib | Abl/CSF-1R/Kit/PDGFR | - | - | - | - | - |
| Nilotinib | Abl/CSF-1R/Kit/PDGFR | - | - | - | - | - |
| Dasatinib | Abl/Src/CSF-1R/Kit/PDGFR | + | + | - | - | - |
| Bosutinib | Abl/Src/Axl/EGFR/TrkA | + | + | + | + | + |
| AZD0530 | Abl/Src | + | - | - | - | - |
| VX – 680 | Aurora/Abl/FLT3 | + | + | - | - | - |
| PHA739358 | Aurora/Abl/RET | + | -* | - | - | - |
| Non – Abl inhibitors | | | | | | |
| ABT – 869 | VEGFR/PDGFR/CSF-1R/FLT3/KIT | + | - | - | - | - |
| BIBF1120 | VEGFR/PDGFR/FLT3/FGFR/Src | + | + | - | - | - |
| BIBW – 2992 | EGFR/HER2 | + | - | - | - | + |
| CI – 1033 | EGFR/HER2 | + | - | - | - | + |
| CEP – 701 | FLT3/VEGFR/RET/Trk | + | + | + | + | + |
| Dovitinib | VEGFR/PDGFR/FLT3/FGFR | + | + | + | + | + |
| Foretinib | VEGFR/PDGFR/FLT3/Met/Axl/Tie-2 | + | + | - | + | + |
| NVPTAE684 | Met/ALK/FLT3 | + | - | - | - | - |
| PF – 2341066 | Met/ALK | + | + | - | - | + |

*PHA739358 demonstrated >50% reduction in viability in SupB15 at 1µM but no further reduction at 10µM



TKI with activity limited to Ph⁺ cell lines

Table 4.4 Summary of inhibitors which demonstrated activity in Ph⁺ cell lines at 1µM and 10µM. In addition to the recognised Abl – inhibitors BIBF1120 revealed activity restricted to the Ph⁺ ALL cells at 1µM.

The Ph⁺ ALL cell lines were sensitive to a range of TKIs. Of note, the activity of the multikinase inhibitor BIBF1120 (VEGFR/PDGFR/FGFR/FLT3) was restricted to the Ph⁺ cell lines only (table 4.4). BIBF1120 is not a recognised Abl inhibitor but has extended activity against FGFR 1 – 4 and the Src family. The central role of Src family kinases in Ph⁺ ALL has been described (388, 389) and thus the activity may be mediated through Src – inhibition in Ph⁺ cells.

Activity of 3 further non – Abl TKIs was observed in the Ph⁺ cell lines. These were the broad spectrum inhibitor ABT – 869 (VEGFR/FLT3/Kit/ PDGFR β /CSF-1R) and NVPTAE684 (Met/ALK/FLT3), which were active against SD – 1, and the multikinase inhibitor axitinib (VEGFR/PDGFR $\alpha\beta$ /CSF1R/Kit/FGFR1), which was only effective against SupB15. There was no single target common to all TKIs shown to be active in the Ph⁺ ALL cell lines, although common targets for at least 2 of the inhibitors included FLT3, Met, PDGFR α/β and VEGFR.

In summary, the differential activity of the Abl inhibitors dasatinib and VX – 680 in Ph⁺ ALL was expected. The profound inhibition induced by BIBF1120 in both Ph⁺ cell lines implicates possible alternative RTK targets to Abl could be exploited in the treatment of Ph⁺ disease and warrant validation in a larger cohort of cell lines and/or primary ALLs.

4.5. RT q-PCR analysis of expression of putative targets of active TKIs

To identify if putative targets of the TKIs which demonstrated activity in the cell lines were present in the cell lines tested, the presence of target transcripts was quantified by RT q-PCR and the level of expression was then correlated with responses to the TKIs. The expression levels are presented as threshold cycle (Ct) values for each target gene normalised to actin expression for each cell line (table 4.5). Transcript for *FGFR1* was the only receptor to be expressed in all cell lines and *FLT3* was expressed in 4 of the 5 cell lines. The relationship between expression of the target mRNA and with TKI activity at (i) the 1µM concentration, (ii) the 10µM concentration only, (iii) activity in apoptosis resistant and (iv) Ph⁺ cell lines was explored. Results were obtained for all TKI targets except *TIE2*, for which mRNA could not be successfully amplified because of technical difficulties.

(i) Expression of targets unique to TKIs active in at least 4 cell lines at 1µM

The targets of dovitinib, foretinib, bosutinib and CEP – 701, the TKIs which demonstrated activity at 1µM in at least 4 cell lines, were *AXL*, *CSF1R*, *EGFR*, *FLT3*, *FGFR1*, *FGFR3*, *KIT*, *MET*, *PDGFRA/B*, *RET*, *RON*, *TIE2*, *TRKA* and *VEGFR 1 – 3*. Only *FGFR1* transcript was present in all cell lines but is the target of only 2 inhibitors, foretinib and dovitinib. The presence of *FLT3* and *VEGFR1* transcript in 4/5 cell lines could identify these RTKs as the potential targets of inhibition by dovitinib, foretinib and CEP – 701. The only cell line not to express *FLT3* and *VEGFR1* was Nalm 6. *TRKA* was expressed in 3/5 cell lines and may represent one target for bosutinib, since the lack of *AXL* and *EGFR* precludes these as targets. The absence of *AXL*, *EGFR*, *MET*, *RET*, *VEGFR2* transcript in all 5 cell lines, excludes these RTKs as viable targets. *TIE2* mRNA could not be successfully amplified because of technical difficulties.

| | Nalm 6 | Nalm 17 | REH | SD1 | SupB15 |
|---------------------------------|--------|---------|--------|--------|--------|
| <i>ALK</i> | Absent | Absent | Absent | Absent | Absent |
| <i>AXL</i> | Absent | Absent | Absent | Absent | Absent |
| <i>CSF-1R</i> | Absent | Absent | 16 | 14 | 12 |
| <i>EGFR</i> | Absent | Absent | Absent | Absent | Absent |
| <i>HER2</i> | Absent | Absent | Absent | Absent | 16 |
| <i>HER3</i> | Absent | Absent | Absent | Absent | Absent |
| <i>HER4</i> | Absent | Absent | Absent | Absent | Absent |
| <i>FGFR1</i> | 11 | 6 | 8 | 10 | 9 |
| <i>FGFR2</i> | Absent | Absent | Absent | Absent | Absent |
| <i>FGFR3</i> | Absent | 11 | 16 | 16 | Absent |
| <i>FGFR4</i> | Absent | 16 | 13 | Absent | Absent |
| <i>FLT3</i> | Absent | 16 | 8 | 16 | 7 |
| <i>KIT</i> | Absent | 17 | 17 | Absent | Absent |
| <i>MET</i> | Absent | Absent | Absent | Absent | Absent |
| <i>PDGFRα</i> | Absent | Absent | Absent | Absent | 11 |
| <i>PDGFRβ</i> | Absent | 17 | 13 | Absent | 16 |
| <i>RON</i> | 16 | 14 | Absent | Absent | Absent |
| <i>RET</i> | Absent | Absent | Absent | Absent | Absent |
| <i>TIE2</i> | Failed | Failed | Failed | Failed | Failed |
| <i>TRKA</i> | Absent | 17 | 14 | Absent | 16 |
| <i>VEGFR1</i> | Absent | 14 | 15 | 16 | 11 |
| <i>VEGFR2</i> | Absent | Absent | Absent | Absent | Absent |
| <i>VEGFR3</i> | 16 | Absent | Absent | Absent | Absent |

Table 4.5 Transcript levels for each RTK expressed as Ct value – normalised – to – actin. Transcript for *FGFR1* was the only putative target expressed in all 5 cell lines. No definitive signature was observed in the mRNA expression of the 5 ALL cell lines.

(ii) Expression of targets specific to drugs active in all cell lines at 10 μ M

Similarly, the targets limited to the TKIs that demonstrate activity in all 5 cell lines at 10 μ M (ABT – 869, BIBF1120, BIBW – 2992, CI – 1033, masitinib, NVPTAE684, PF-2340166, sorafenib, sunitinib and vandetanib) were *ALK*, *AXL*, *CSF1R*, *EGFR*, *FGFR1 – 4*, *FLT3*, *HER2*, *HER3*, *HER4*, *PDGFRA/B*, *RET*, *RON*, *TRKA*, *TIE2* and *VEGFR1 – 3*. The presence of *FLT3* and *VEGFR 1* transcript in 4/5 cell lines may identify these RTKs as a potential target of inhibition. The absence of transcript for *ALK*, *AXL*, *EGFR*, *FGFR2*, *MET*, *RET* and *VEGFR2* in all cell lines exclude these RTKs as possible targets. The restricted expression of *HER2* (SupB15), *RON* (Nalm 6 and 17) and *TRKA* (Nalm 17, REH and SD – 1) reflects either the limited involvement of these pathways in survival or ALL heterogeneity.

(iii) Expression of targets of the pan – EGFR quinazoline inhibitors (BIBW – 2992 and CI – 1033) targeting apoptosis defective leukaemias

The drugs BIBW – 2992 and CI – 1033 exhibited activity to the apoptosis defective cell lines, REH and SD – 1. BIBW – 2992 and CI-1033 target the EGFR family, EGFR and HER 2 – 4, however neither REH nor SD – 1 expressed transcript from any of the *EGFR* family members. The only cell line to do so was SupB15 (expressing *HER2*) which did not demonstrate sensitivity at the 1 μ M level to either quinazoline. These results suggest that the activity of BIBW – 2992 and CI-1033 was not mediated through inhibition of EGFR family members. FLT3 has recently been identified as a novel target of BIBW – 1992 and CI – 1033 (385, 386) and expression of its transcript could be detected in both REH and SD – 1 by RT – qPCR supporting FLT3 as a target of these drugs. Conversely, Nalm 17 and SupB15 also expressed *FLT3* transcript at similar levels but were not sensitive to either drug. A possible explanation for the lack of concordance between *FLT3* expression and the TKI activity is that the level of mRNA expression of a target does not necessarily equate to activation of the RTK, which is a post – translational event. A second explanation could be that a higher concentration of BIBW – 2992 and CI – 1033 is required to inhibit FLT3 in Nalm 17 and Sup B15, as demonstrated by the reduction in cell viability at 10 μ M only (section 4.3.4).

(iv) Targets of TKIs active against Ph+ cell lines

The targets of the TKIs which demonstrated activity at 1 μ M in the Ph+ ALL cells lines SD – 1 and SupB15 (ABT – 869, bosutinib, BIBF1120, BIBW – 2992, CEP – 701, CI – 1033, dasatinib, dovitinib, foretinib, NVPTAE684, PF – 2341066, PHA739358 and VX – 680) were *ALK*, *AXL*, *CSF1R*, *EGFR*, *FLT3*, *FGFR1*, *FGFR3*, *KIT*, *MET*, *PDGFRA/B*, *RET*, *RON*, *TIE2*, *TRKA* and *VEGFR 1 – 3*. Both the Ph+ cell lines expressed transcript for *CSF – 1R*, *FGFR1*, *FLT3* and *VEGFR1*, possible targets of BIBF1120, CEP – 701, dovitinib and foretinib. Of all the 5 cell lines, only SupB15 expressed transcript for *HER2* and *PDGFRA*. However, TKIs with EGFR/HER2 activity did not demonstrate any activity against the cell line and no TKI individually targeted PDGFR α .

In summary, no relationship was evident between the level of transcript expression of a single RTK and response to a TKI. This expression analysis, however, does not exclude the possibility that a cell line expressing a target may not be sensitive to a corresponding TKI because of underlying mechanisms of resistance such as an increased expression of efflux pumps or the upregulation of additional survival pathways.

Overall, the TKI library screen of the cell lines has revealed 3 patterns of response. Firstly, the multikinase inhibitors with anti-FLT3 activity, CEP- 701, dovitinib and foretinib, displayed activity against multiple cell lines and thus could be a useful therapy for a variety of ALL subtypes. Secondly, the irreversible quinazoline inhibitors, BIBW – 2992 and CI – 1033, demonstrated activity in apoptosis defective cell lines which could suggest a potential role in the treatment of resistant leukaemias with defects in apoptosis. Finally, BIBF1120 which is not recognised to act through a Bcr/Abl mechanism exhibited activity in the high risk Ph+ leukaemia cell lines, and therefore may provide a mechanism to explore for the treatment of Ph+ ALL.

4.6. Screen of primary B – cell precursor ALL cohort with expanded TKI library

The sensitivity of 20 primary ALL samples to the same library of 33 TKIs was investigated. MRD status at the end of induction therapy was used as a proxy for clinical chemosensitivity. The primary leukaemia cells were treated with 1 μ M and 10 μ M of each TKI for 48 hours, after which cell viability was assessed using the Promega CellTiter-Glo[®] assay. As for the cell line experiments, inhibitors were defined as active and of potential interest by their ability to reduce cell viability by greater than 50% at 1 μ M and exhibit a further cell viability reduction at 10 μ M.

| Sample code | Age (yrs) | Sex | WCC (x10 ⁹ /L) | Cytogenetics | Response | Flow MRD | Molecular MRD |
|-------------|-----------|-----|---------------------------|---|----------|----------|---------------|
| ALL16 | 3.5 | M | 3.4 | t(12;21) | GER | HR | HR |
| ALL20 | 12 | F | 109 | 46XX, t(3;10) t(9;16) +8 biallelic del p16 | GER | Ind | SR |
| ALL21 | 12 | F | 8 | t(12;21) | GER | NK | NK |
| ALL22 | 2 | F | 20 | Normal | GER | SR | SR |
| ALL23 | 9.5 | M | 24 | 45XY, der19, t(1;19) | GER | HR | SR |
| ALL24 | 11 | M | 59.7 | 46XY, del9p21p21, monoallelic CDKN2A loss, 13q14 loss | PER | HR | HR |
| ALL25 | 3 | M | 12.7 | No report | GER | HR | HR |
| ALL26 | 0.5 | M | 110 | t(9;11) | GPR | NK | SR |
| ALL27 | 9.5 | M | 26 | 46XY | GER | HR | HR |
| ALL28 | 8.5 | M | 4 | Hyperdiploid | GER | HR | SR |
| ALL29 | 3 | F | 5 | t(12;21) | GER | SR | SR |
| ALL30 | 10.5 | F | 83 | 47XX, t(12;21) | GER | SR | SR |
| ALL31 | 11 | F | 73 | 46XX, der 19 , t(1;19) | GER | SR | SR |
| ALL32 | 0.5 | F | 44.7 | t(4;11) | GPR | NK | SR |
| ALL33 | 3 | M | 43 | Hyperdiploid | GER | SR | SR |
| ALL34 | 10 | M | 15.8 | t(12;21) | GER | HR | NK |
| ALL35 | 2 | F | 41 | Hyperdiploid | GER | HR | HR |
| ALL36 | 16 | F | 60 | 46XX, t(2;12), p1p13(8) | GER | HR | HR |
| ALL37 | 2 | F | 45 | Hyperdiploid | GER | HR | HR |
| ALL38 | 5 | F | 15 | Normal | GER | HR | SR |

Key:**CR:** Complete Remission**GER:** Good early response (<25% blasts at day 8/15)**PER:** Poor early response (>25% blasts at day 8/15)**HR:** High Risk (leukaemia cells detected >0.01%)**SR:** Standard Risk (leukaemia cells not detected at 0.01%)**Ind:** Indeterminate**NK:** Not known

Table 4.6 Clinical and biological characteristics of primary ALL panel

4.6.1 Sensitivity of primary ALLs to TKIs at 1 μ M and 10 μ M

Consistent with results from the cell line screen, there was heterogeneity in response to the inhibitors. Tables 4.7a and b summarise the responses of the 20 primary ALLs to each TKI at the 1 μ M concentration. A total of 23/33 compounds reduced cell viability by greater than 50% in 15 primary samples at 1 μ M and 25/33 reduced viability by greater than 50% at 10 μ M. Fig 4.11 demonstrates the number of primary leukaemias responding to each inhibitor at 1 μ M and the increase in responders at 10 μ M.

| | ALL16 | ALL20 | ALL21 | ALL22 | ALL23 | ALL24 | ALL25 | ALL26 | ALL27 | ALL28 |
|-------------|---------|---------|---------|---------|---------|---------|---------|---------|---------|---------|
| ABT869 | 95(5) | 26(4) | 106(54) | 98(7) | 129(11) | 112(1) | 138(51) | 132(2) | 106(31) | 100(13) |
| AG-490 | 121(4) | 72(4) | 112(5) | 89(8) | 106(3) | 115(8) | 77(20) | 90(5) | 67(17) | 102(16) |
| Axitinib | 128(10) | 57(4) | 107(23) | 97(14) | 141(4) | 133(8) | 91(27) | 146(2) | 73(20) | 131(30) |
| AZD0530 | 134(11) | 80(7) | 87(40) | 104(3) | 110(11) | 193(13) | 95(3) | 106(2) | 139(10) | 193(18) |
| BIBF1120 | 80(5) | 48(6) | 92(5) | 72(4) | 100(5) | 152(26) | 52(14) | 76(6) | 57(3) | 100(37) |
| BIBW-2992 | 38(4) | 23(3) | 54(14) | 51(3) | 67(2) | 71(9) | 66(10) | 88(5) | 58(21) | 47(7) |
| Bosutinib | 132(2) | 20(3) | 93(3) | 110(15) | 91(11) | 176(12) | 91(6) | 59(2) | 66(5) | 104(15) |
| Brivanib | 107(9) | 86(1) | 107(11) | 79(7) | 99(6) | 148(21) | 128(10) | 99(3) | 88(6) | 103(13) |
| Cediranib | 122(11) | 59(9) | 116(6) | 93(17) | 119(6) | 133(4) | 112(14) | 124(2) | 110(39) | 319(50) |
| CEP-701 | 45(3) | 16(6) | 84(8) | 82(14) | 100(4) | 148(6) | 64(12) | 66(4) | 34(9) | 100(16) |
| CI-1033 | 34(1) | 52(5) | 60(6) | 40(4) | 83(4) | 118(5) | 80(15) | 108(9) | 62(14) | 44(2) |
| CP690550 | 114(8) | 67(6) | 112(12) | 60(13) | 99(4) | 133(7) | 104(3) | 87(4) | 113(22) | 100(5) |
| Dasatinib | 159(8) | 15(7) | 106(9) | 202(6) | 94(8) | 243(44) | 76(10) | 94(3) | 156(52) | 382(72) |
| Dovitinib | 57(1) | 9(1) | 66(8) | 55(7) | 51(3) | 121(10) | 68(11) | 14(1) | 60(8) | 49(7) |
| Foretinib | 13(2) | 18(5) | 73(5) | 46(4) | 76(1) | 55(3) | 63(13) | 140(14) | 20(3) | 75(10) |
| GSK1904592A | 114(4) | 99(2) | 126(12) | 88(10) | 97(5) | 105(12) | 109(35) | 95(11) | 97(22) | 99(6) |
| Imatinib | 108(8) | 60(4) | 107(19) | 95(10) | 92(8) | 157(28) | 94(38) | 76(2) | 95(22) | 106(4) |
| Masitinib | 126(4) | 42(2) | 96(11) | 82(2) | 98(2) | 149(17) | 78(25) | 104(11) | 136(36) | 142(13) |
| Motesanib | 108(8) | 57(2) | 115(17) | 85(12) | 95(3) | 163(31) | 95(9) | 76(4) | 116(22) | 120(7) |
| Nilotinib | 114(11) | 100(2) | 103(9) | 110(8) | 81(9) | 132(34) | 120(15) | 97(8) | 64(17) | 87(10) |
| NVPAEW541 | 116(5) | 108(19) | 155(44) | 101(7) | 104(10) | 134(12) | 87(6) | 84(4) | 144(37) | 113(2) |
| NVPTAE684 | 17(3) | 21(4) | 92(7) | 76(4) | 104(12) | 111(3) | 126(18) | 44(5) | 42(13) | 66(26) |
| Pazopanib | 119(9) | 53(9) | 92(4) | 87(11) | 98(13) | 210(44) | 96(16) | 84(7) | 171(36) | 89(8) |
| PF-04217903 | 107(9) | n/a | 119(15) | 96(8) | 107(3) | 129(13) | 121(31) | 90(8) | 89(11) | 113(10) |
| PF-2341066 | 41(3) | 41(5) | 77(9) | 64(5) | 96(4) | 74(9) | 78(3) | 111(12) | 197(51) | 73(13) |
| PHA739358 | 109(10) | 107(30) | 113(2) | 92(8) | 98(14) | 150(12) | 122(35) | 46(2) | 110(22) | 88(4) |
| Sorafenib | 122(3) | 77(7) | 101(3) | 103(18) | 108(15) | 150(9) | 53(12) | 193(21) | 53(6) | 105(4) |
| Sunitinib | 90(11) | 16(2) | 97(8) | 68(13) | 105(10) | 65(5) | 77(14) | 44(3) | 96(7) | 87(2) |
| Tandutinib | 126(9) | 70(9) | 110(2) | 75(8) | 104(4) | 124(13) | 86(12) | 70(11) | 102(10) | 97(17) |
| TIE2 | 114(8) | 36(2) | 104(4) | 87(13) | 91(12) | 65(4) | 106(23) | 175(21) | 49(6) | 108(11) |
| Vandetanib | 117(52) | 52(3) | 93(6) | 95(3) | 96(9) | 188(22) | 82(17) | 90(3) | 164(37) | 91(6) |
| Vatalinib | 109(1) | 65(15) | 101(12) | 71(3) | 96(3) | 97(10) | 109(10) | 87(8) | 46(11) | 92(9) |
| VX680 | 98(8) | 63(5) | 102(14) | 106(9) | 107(13) | 84(4) | 137(24) | 82(8) | 118(7) | 95(17) |

Key:

Percentage of cell viability at 1µM ≤50% = TKI of interest



Percentage of cell viability at 1µM <50% but no further reduction at 10µM



Percentage of cell viability at 1µM >50%



Technical failure



Primary ALL which did not demonstrate sensitivity to any TKI

Table 4.7a Summary of responses of primary ALLs to TKI panel at 1µM. The percentage of cell viability of primary ALLs after 48 hours incubation with 1µM of TKI is expressed in this table. It is the mean reading of cells in triplicate, with standard deviation in parentheses. The highlighted data are those TKIs which demonstrate over 50% cell killing in specific cell lines.

| | ALL29 | ALL30 | ALL31 | ALL32 | ALL33 | ALL34 | ALL35 | ALL36 | ALL37 | ALL38 |
|-------------|---------|---------|--------|----------|---------|---------|---------|---------|--------|---------|
| ABT869 | 66(31) | 84(10) | 59(1) | 93(7) | 109(13) | 150(9) | 78(10) | 88(17) | 87(11) | 101(5) |
| AG-490 | 125(16) | 55(17) | 50(14) | 87(10) | 107(34) | 100(4) | 90(8) | 101(13) | 91(13) | 100(14) |
| Axitinib | 124(26) | 91(2) | 59(7) | 259(255) | 136(9) | 231(31) | 151(24) | 70(4) | 108(9) | 79(22) |
| AZD0530 | 58(22) | 101(69) | 50(3) | 85(20) | 117(54) | 142(14) | 104(7) | 100(31) | 92(10) | 144(13) |
| BIBF1120 | 76(11) | 41(16) | 58(7) | 98(28) | 41(14) | 63(8) | 107(19) | 49(10) | 66(11) | 31(10) |
| BIBW-2992 | 9(3) | 59(17) | 36(6) | 92(10) | 123(31) | 25(2) | 69(10) | 57(3) | 62(7) | 30(4) |
| Bosutinib | 49(6) | 94(4) | 57(5) | 95(9) | 94(32) | 108(20) | 123(5) | 61(8) | 83(2) | 33(1) |
| Brivanib | 116(28) | 73(16) | 49(6) | 101(5) | 123(17) | 99(17) | 105(7) | 85(17) | 106(1) | 87(6) |
| Cediranib | 110(9) | 74(13) | 70(10) | 94(8) | 101(12) | 146(22) | 147(7) | 102(11) | 102(7) | 78(10) |
| CEP-701 | 45(4) | 60(10) | 74(12) | 77(16) | 45(12) | 32(13) | 78(3) | 54(7) | 60(4) | 26(5) |
| CI-1033 | 6(1) | 79(82) | 37(4) | 73(10) | 59(15) | 17(1) | 83(3) | 42(20) | 50(3) | 63(7) |
| CP690550 | 110(9) | 59(13) | 51(7) | 94(9) | 118(23) | 113(70) | 121(7) | 126(42) | 93(5) | 140(22) |
| Dasatinib | 34(8) | 85(9) | 67(5) | 93(1) | 306(45) | 165(11) | 266(21) | 68(9) | 139(2) | 155(32) |
| Dovitinib | 28(5) | 76(18) | 34(3) | 64(2) | 89(1) | 41(3) | 43(3) | 69(15) | 29(1) | 65(8) |
| Foretinib | 20(5) | 56(4) | 37(1) | 78(8) | 57(31) | 33(5) | 88(13) | 82(7) | 64(1) | 18(2) |
| GSK1904592A | 141(19) | 94(8) | 58(1) | 92(17) | 72(31) | 112(31) | 112(21) | 84(5) | 98(2) | 117(27) |
| Imatinib | 111(18) | 109(10) | 57(6) | 134(68) | n/a | 128(33) | 102(4) | 94(21) | 101(2) | 104(9) |
| Masitinib | 104(2) | 91(11) | 58(6) | 96(6) | 105(9) | 102(7) | 130(20) | 91(19) | 98(4) | 112(13) |
| Motesanib | 118(15) | 60(11) | 53(4) | 91(16) | n/a | 120(25) | 115(12) | 100(13) | 104(3) | 113(12) |
| Nilotinib | 107(19) | 132(19) | 44(4) | 104(13) | 83(17) | 122(8) | 169(4) | 57(3) | 92(1) | 66(3) |
| NVPAEW541 | 142(15) | 110(9) | 52(5) | 108(22) | 106(11) | 95(5) | 105(12) | 112(32) | 102(8) | 99(14) |
| NVPTAE684 | 51(6) | 45(11) | 48(4) | 67(35) | 175(38) | 26(1) | 53(1) | 103(44) | 59(2) | 37(7) |
| Pazopanib | 141(27) | 145(31) | 44(5) | 91(2) | 114(25) | 151(19) | 122(9) | 82(9) | 103(6) | 96(31) |
| PF-04217903 | 159(26) | 104(17) | 46(4) | 118(35) | 94(8) | 90(6) | 104(3) | 99(10) | 103(3) | n/a |
| PF-2341066 | 57(11) | 46(6) | 49(4) | 69(35) | 76(10) | 23(20) | 88(10) | 59(6) | 75(5) | 39(3) |
| PHA739358 | 87(11) | 80(4) | 50(1) | 94(5) | 78(8) | 80(3) | 70(1) | 92(8) | 94(4) | 150(41) |
| Sorafenib | 97(12) | 106(6) | 77(8) | 97(12) | 71(12) | 143(30) | 153(6) | 71(6) | 92(2) | 34(8) |
| Sunitinib | 93(4) | 117(12) | 54(4) | 106(9) | 116(4) | 67(6) | 67(8) | 105(6) | 77(6) | 53(10) |
| Tandutinib | 137(16) | 99(17) | 58(5) | 99(13) | 91(14) | 116(27) | 104(12) | 93(6) | 91(1) | 130(22) |
| TIE2 | 50(7) | 78(15) | 60(3) | 94(17) | 95(19) | 61(5) | 155(29) | 72(11) | 76(1) | 33(9) |
| Vandetanib | 71(6) | 83(9) | 56(4) | 86(16) | 79(20) | 113(5) | 145(15) | 89(7) | 92(3) | 93(13) |
| Vatalinib | 89(14) | 58(36) | 65(4) | 99(2) | 82(27) | 81(16) | 82(6) | 84(4) | 87(3) | 72(14) |
| VX680 | 104(10) | 142(72) | 71(7) | 103(8) | 110(40) | 101(13) | 89(2) | 112(11) | 89(3) | 79(7) |

Key:

Percentage of cell viability at 1µM ≤50% = TKI of interest



Percentage of cell viability at 1µM <50% but no further reduction at 10µM



Percentage of cell viability at 1µM >50%



Technical failure



Primary ALL which did not demonstrate sensitivity to any TKI

Table 4.7b Summary of responses of primary ALL cells to TKI panel at 1µM. The percentage of cell viability of primary ALLs after 48 hours incubation with 1µM of TKI is expressed in this table. It is the mean reading of cells in triplicate, with standard deviation in parentheses. The highlighted data are those TKIs which demonstrate over 50% cell killing in specific cell lines.

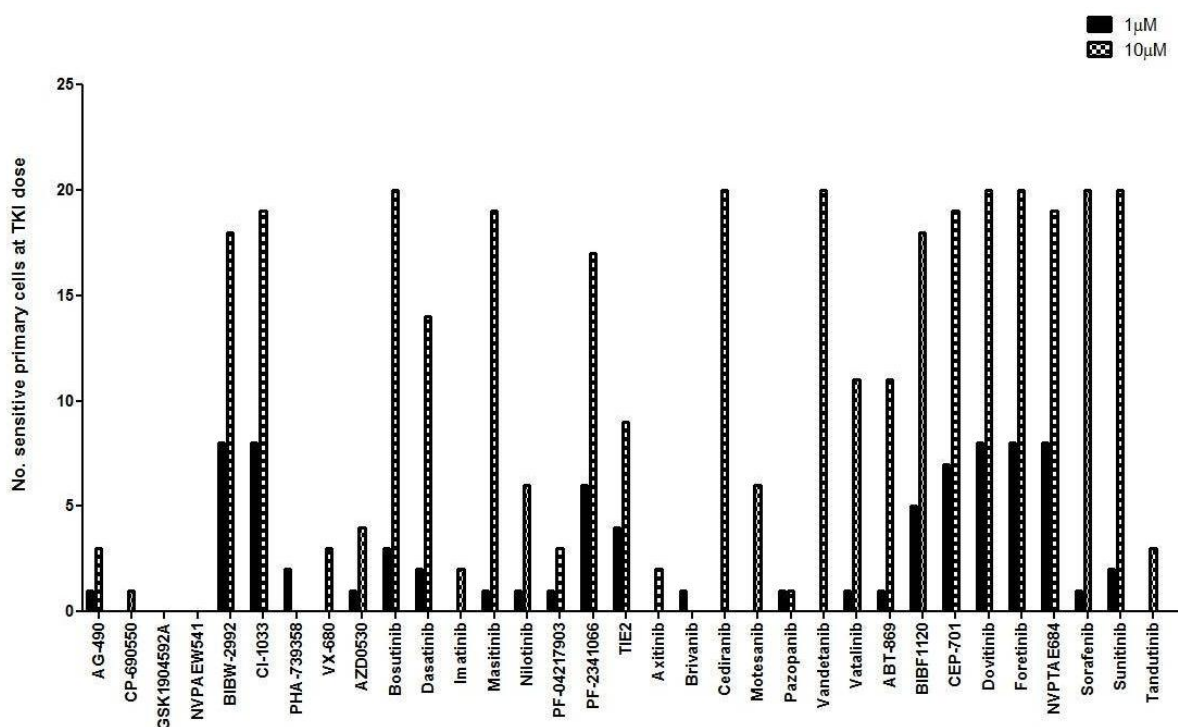


Figure 4.11 Number of primary cells demonstrating activity at 1μM reveals no global inhibition by a single TKI. Dose – dependent reduction in viability in primary cells was induced by 25/33 TKI when inhibitor concentration was increased to 10 μM.

Overall, 15/20 primary leukaemias exhibited sensitivity to any of the TKIs at 1μM, of which 14 responded to ≥ 2 compounds. As expected, given the heterogeneity of ALL, there were no inhibitors were active against all primary ALLs at 1μM. This finding was in contrast to the cell line experiments previously performed, where bosutinib, CEP-701 and dovitinib inhibited viability in all 5 cell lines. Two of these agents, CEP – 701 and dovitinib, had the broadest activity in the primary ALLs, inhibiting 8 and 7 ALL respectively. Bosutinib, in contrast, demonstrated limited inhibition in only 3/20 primary ALLs. At 10μM, all of the primary ALLs demonstrated sensitivity to a range of TKIs, with each ALL responding to an average of 17 different inhibitors (range 8 – 25).

| TKI | Putative targets | Primaries | Cell lines |
|---------------|---|-------------------|------------|
| Foretinib | VEGFR1 -3, PDGFR $\alpha\beta$, CSF1R, FLT3, KIT, FGFR1, Tie -2, Met, Ron, Axl | 8/20 | 4/5 |
| Dovitinib | VEGFR1 -3, PDGFR $\alpha\beta$, CSF1R, KIT, FGFR1, FLT-3 | 8/20 | 5/5 |
| NVPTAE684 | ALK, FLT3 | 8/20 | 1/5 |
| CI-1033 | EGFR/HER2 | 8/20 | 2/5 |
| BIBW2992 | EGFR/HER2 | 7/20 | 2/5 |
| CEP-701 | FLT3, VEGFR1 -2, TrkA, RET | 7/20 | 5/5 |
| PF-2341066 | Met, ALK | 6/20 | 3/5 |
| BIBF1120 | VEGFR1 -3, PDGFR $\alpha\beta$, CSF1R, KIT, FGFR1 - 4, FLT3 | 5/20 | 2/4 |
| TIE2 | Tie-2 | 4/20 | 0/5 |
| Bosutinib | Axl, Abl, Src | 3/20 | 2/5 |
| Dasatinib | PDGFR $\alpha\beta$, CSF1R, KIT, Abl, Src | 2/20 | 2/5 |
| PHA739358 | Aurora kinase, RET | 2/20 ^a | 2/5 |
| Sunitinib | VEGFR1 -3, PDGFR $\alpha\beta$, CSF1R, FLT3, KIT | 2/20 | 0/5 |
| ABT869 | VEGFR1 -3, PDGFR $\alpha\beta$, CSF1R, FLT3, KIT | 1/20 | 1/5 |
| Brivanib | VEGFR1 -3, PDGFR $\alpha\beta$, CSF1R, KIT | 1/20 | 0/5 |
| Vatalinib | VEGFR1 -3, PDGFR $\alpha\beta$, CSF1R, KIT | 1/20 | 0/5 |
| Sorafenib | VEGFR1 -3, PDGFR $\alpha\beta$, CSF1R, FLT3, KIT | 1/20 | 0/5 |
| Pazopanib | VEGFR1 -3, PDGFR $\alpha\beta$, CSF1R, KIT | 1/20 ^b | 0/5 |
| Nilotinib | PDGFR $\alpha\beta$, CSF1R, KIT | 1/20 | 0/5 |
| Masatinib | PDGFR $\alpha\beta$, KIT | 1/20 | 0/5 |
| PF – 04217903 | Met | 1/20 | 0/5 |
| AZD0530 | Abl, Src, EGFR | 1/20 | 1/5 |
| AG-490 | JAK2, EGFR | 1/20 | 0/5 |

a – PHA739358 demonstrated >50% reduction in cell viability at 1 μ M in ALL26 – GFER and ALL31 – KMER but did not demonstrate a further reduction at 10 μ M

b – Pazopanib demonstrated >50% reduction in cell viability at 1 μ M in but did not demonstrate a further reduction at 10 μ M

Table 4.8 Summary of TKI which demonstrated \geq 50% reduction at 1 μ M and further reduction at 10 μ M in 20 primary samples. The TKIs highlighted in grey demonstrate activity in at least 5/20 primary ALLS.

Table 4.8 ranks the TKIs exhibiting activity in the primary ALLs at 1 μ M and compares with the effect in the cell lines. Consistent with the responses observed in the cell lines, the 8 most active TKIs could be categorised into 3 groups: (i) multikinase inhibitors with FLT3 activity (foretinib, CEP701, dovitinib and BIBF1120), (ii) EGFR/HER2 quinazoline irreversible inhibitors (BIBW-2992 and CI - 1033) and (iii) combined Met/ALK inhibitors (NVPTAE684 and PF – 2341066). The greatest number of primary samples affected by a single TKI at nanomolar doses was 8 leukaemias. Four TKIs induced a significant amount of cell killing in the most ALL samples (n=8 for all four drugs); these included foretinib

(FLT3/Met/ PDGFR/VEGFR), dovitinib (FGFR/FLT3/PDGFR/VEGFR), NVPTAE684 (Met/ALK/FLT3) and CI – 1033 (EGFR/HER2).

The TKIs which had the broadest effect across the primary ALLs were those including FLT3 – inhibitory activity; foretinib (n=8), dovitinib (n=8), CEP – 701 (n=7) and BIBF1120 (n=5). BIBF1120, which demonstrated activity restricted to Ph+ cell lines, was active in 5/20 primary leukaemias; none of the cohort were Ph+.

NVPTAE684 (ALK/Met/FLT3) and CI – 1033 (pan – EGFR) also exhibited broad activity, inhibiting 8/20 leukaemias. This was in contrast to the cell line screen, in which the activity of CI – 1033 and NVPTAE684 was limited.

The characteristics of the primary ALLs that were most sensitive and most resistant to the 8 TKIs (foretinib, dovitinib, NVPTAE684, CI – 1033, BIBW – 2992, CEP – 701, PF – 2341066 and BIBF1120) selected as having the greatest activity against the full panel were compared to assess whether any features might correlate with response. No statistically significant differences between these 2 groups were found when comparing age, WCC, cytogenetics, MRD status determined by flow and PCR techniques (table 4.9).

In summary, in the TKI library used in this study, compounds with activity against EGFR RTK families or FLT3/PDGFR/FGFR/VEGFR (multikinase) demonstrated the broadest activity in primary ALLs. This spectrum of activity was comparable to that observed in the cell line screen.

| TKI | | Age (year) | WCC (x10 ⁹ /L) | Cytogenetics | | | | | | Flow MRD | | | Molecular MRD | | |
|--------------|----------------------|---------------|------------------------------|-----------------------|----------------|--------------|---------|--------|-----|----------|----|----|---------------|----------|----|
| | | | | Non – contributory | t(12:21) | Hyperdiploid | t(1:19) | CDK2NA | MLL | SR | HR | NK | SR | HR | NK |
| Foretinib | Sensitive (N=8) | 6.99 (4.01) | 33.4 (37.55) | 4 | 3 | 0 | 1 | 0 | 0 | 4 | 2 | 2 | 6 | 2 | 0 |
| | Resistant (n=12) | 6.53 (5.27) | 44.58 (31.11) | 2 | 2 | 4 | 1 | 1 | 2 | 3 | 7 | 2 | 6 | 5 | 1 |
| | Statistical analysis | p = 0.84 | p = 0.48 | | p = 0.22 (Chi) | | | | | p = 0.33 | | | | p = 0.46 | |
| Dovitinib | Sensitive (N=8) | 6.11 (4.68) | 50.33 (43.11) | 1 | 2 | 3 | 1 | 0 | 1 | 2 | 3 | 3 | 5 | 3 | 0 |
| | Resistant (n=12) | 7.11 (4.87) | 33.29 (24.7) | 5 | 3 | 1 | 1 | 1 | 1 | 5 | 6 | 1 | 7 | 4 | 1 |
| | Statistical analysis | p = 0.65 | p = 0.27 | | p = 0.52 | | | | | p = 0.83 | | | | p = 1 | |
| NVPtAE684 | Sensitive (N=8) | 7.93 (3.82) | 43.14 (39.2) | 4 | 3 | 0 | 1 | 0 | 1 | 4 | 2 | 2 | 6 | 2 | 0 |
| | Resistant (n=12) | 5.91 (5.2) | 38 (30.5) | 1 | 2 | 4 | 1 | 1 | 1 | 3 | 7 | 2 | 6 | 5 | 1 |
| | Statistical analysis | p = 0.36 | p = 0.74 | | p = 0.14 | | | | | p = 0.97 | | | | p = 0.99 | |
| CI – 1033 | Sensitive (N=8) | 6.99 (5.15) | 28.28 (27.41) | 2 | 3 | 2 | 1 | 0 | 0 | 4 | 3 | 1 | 5 | 3 | 0 |
| | Resistant (n=12) | 6.35 (4.6) | 48 (35.66) | 4 | 2 | 2 | 1 | 1 | 2 | 3 | 6 | 3 | 7 | 4 | 1 |
| | Statistical analysis | p = 0.83 | p = 0.2 | | p = 0.67 | | | | | p = 0.99 | | | | p = 1 | |
| BIBW – 2992 | Sensitive (N=7) | 7.56 (3.69) | 32.17 (41.81) | 2 | 3 | 1 | 1 | 0 | 0 | 3 | 2 | 2 | 6 | 1 | 0 |
| | Resistant (n=13) | 6.26 (5.24) | 45.91 (29.51) | 4 | 2 | 3 | 1 | 1 | 2 | 4 | 7 | 2 | 6 | 6 | 1 |
| | Statistical analysis | p = 0.57 | p = 0.45 | | p = 0.64 | | | | | p = 0.91 | | | | p = 1 | |
| CEP – 701 | Sensitive (N=7) | 6.56 (3.8) | 31 (36.9) | 3 | 3 | 1 | 0 | 0 | 0 | 3 | 2 | 2 | 2 | 5 | 0 |
| | Resistant (n=13) | 6.8 (5.26) | 45 (31.7) | 3 | 2 | 3 | 2 | 1 | 2 | 7 | 4 | 2 | 7 | 5 | 1 |
| | Statistical analysis | p = 0.92 | p = 0.39 | | p = 0.44 | | | | | p = 0.99 | | | | p = 0.99 | |
| PF – 2341066 | Sensitive (N=6) | 8.65 (3.51) | 49.86 (43.97) | 2 | 3 | 0 | 1 | 0 | 0 | 3 | 1 | 2 | 5 | 1 | 0 |
| | Resistant (n=14) | 5.89 (5) | 35.93 (28.61) | 4 | 2 | 4 | 1 | 1 | 2 | 4 | 8 | 2 | 7 | 6 | 1 |
| | Statistical analysis | p = 0.24 | p = 0.41 | | p = 0.35 | | | | | p = 0.94 | | | | p = 0.99 | |
| BIBF1120 | Sensitive (N=5) | 9.3 (5.28) | 63 (36.13) | 3 | 1 | 1 | 0 | 0 | 0 | 2 | 2 | 1 | 4 | 1 | 0 |
| | Resistant (n=15) | 5.85 (4.34) | 32.81 (30.12) | 3 | 4 | 3 | 2 | 1 | 2 | 4 | 1 | 0 | 8 | 6 | 1 |
| | Statistical analysis | p = 0.16 | p = 0.09 | | p = 0.59 | | | | | p = 1 | | | | p = 1 | |
| Tie – 2 | Sensitive (N=4) | 7.38 (4.11) | 38.73 (47.61) | 3 | 1 | 0 | 0 | 0 | 0 | 1 | 2 | 1 | 3 | 1 | 0 |
| | Resistant (n=16) | 6.55 (4.94) | 40.45 (30.89) | 3 | 4 | 4 | 2 | 1 | 2 | 6 | 7 | 3 | 9 | 6 | 1 |
| | Statistical analysis | p = 0.76 | p = 0.93 | | p = 0.34 | | | | | p = 1 | | | | p = 0.99 | |

Table 4.9 Correlation of TKIs responses to the clinical and biological features of leukaemias. No significant correlations were observed between response to TKI and biological or clinical parameters.

4.6.2 Resistance of primary ALLs to TKI at 1 μ M and 10 μ M

Table 4.10 shows the 16/33 TKIs screened in the primary samples which did not reduce cell viability by greater than 50% at 1 μ M and 10 μ M. All primary ALLs tested were resistant to both JAK inhibitors at 1 μ M and furthermore, 18/20 did not respond to AG – 490 and 18/19 were resistant to pan – JAK inhibitor CP – 690550 at 10 μ M. Similarly, all primary ALLs were resistant to both IR/IGF – 1R inhibitors, GSK1904592A and NVPAEW541, at 10 μ M.

| TKI | Putative Targets | No. Primary cells not responding |
|---|---|----------------------------------|
| IR/IGF – 1R inhibitor | | |
| NVPAEW541 | IGF-1R/Insulin | 20/20 |
| GSK1904592A | IGF-1R/Insulin | 20/20 |
| JAK inhibitor | | |
| AG-490 | JAK2 and JAK3, EGFR | 18/20 |
| CP-690550 | JAK 1 – 3 | 18/19* |
| Aurora kinase inhibitor | | |
| PHA739358 | Aurora A – C, Abl, Src, RET | 20/20 |
| VX-680 | Aurora, Abl, Src, FLT3 | 18/20 |
| Multikinase inhibitors with no FLT3 – activity | | |
| Pazopanib | VEGFR1 –3, PDGFR β , CSF1R, Kit, FGFR1 | 19/20 |
| Axitinib | VEGFR1 –3, PDGFR α/β , CSF1R, Kit, FGFR1 | 18/19* |
| Brivanib | VEGFR 1 – 3, FGFR1 – 3 | 19/20 |
| Motesanib | VEGFR 1 – 3, PDGFR α , Kit, RET | 14/20 |
| Restricted inhibitors | | |
| Imatinib | Kit, Abl, Arg, PDGFR α/β , CSF – 1R | 18/19* |
| Nilotinib | Abl, Arg, PDGFR β , Kit | 14/20 |
| AZD0530 | Src, Kit, EGFR | 16/20 |
| PF04217903 | Met | 15/18* |
| FLT3 – specific inhibitor | | |
| Tandutinib | FLT3, Kit, PDGFR β | 17/20 |

*Reduced denominators because of technical failures.

Table 4.10 Summary of 16 TKIs which did not induce greater than 50% reduction in viability at 10 μ M. All TKIs tested against 20 primary cells unless otherwise stated.

The aurora kinase inhibitors VX680 and PHA739358 did not show any high level of activity in the primary ALL panel. Only 3/20 primary ALLs responded to VX680 at the 10 μ M concentration and none of the 20 primary ALLs demonstrated any response to PHA739358. This lack of Aurora Kinase inhibitor activity is consistent with the cell line results, where Aurora Kinase inhibitor activity was demonstrated only in the Ph⁺ cell lines. As none of the

primary ALLs was Ph+ this activity of the Aurora Kinase inhibitors could not be confirmed in primary cells.

Other relatively inactive TKIs included pazopanib (CSF-1R/FGFR/Kit / PDGFR/VEGFR), axitinib (CSF-1R/FGFR /Kit/PDGFR/VEGFR) and brivanib (FGFR/VEGFR). These 3 inhibitors, originally designed as anti – angiogenic agents, demonstrate activity against FGFR and VEGFR. Inhibitors with dominant activity limited to the IGF-1R, JAK and Met pathways were amongst the least active against cell lines and the primary ALLs, suggesting that these pathways are not major targets for the primary ALL cohort screened in this study.

Primary ALLs were highly sensitive to the multikinase TKIs foretinib, dovitinib and CEP – 701 which all target FLT3. Activity against FLT3 has not been demonstrated in kinase assays at doses under 1 μ M for axitinib (331) or 20 μ M for pazopanib (390). These data are consistent with FLT3 being an important target for primary ALL. Contrary to this, the more restricted FLT3 inhibitor tandutinib, failed to reduce viability in 17/20 primary ALL screened, even at 10 μ M. Twelve of these 17 demonstrated inhibition by other putative FLT3 inhibitors at 1 μ M (table 4.7a and b). Resistance to tandutinib was also evident in the cell lines, with only SD – 1 exhibiting an appreciable response at 10 μ M. The discrepancy in activity exhibited by the FLT3 – inclusive multikinase TKIs and tandutinib may be due to the differing capabilities of these drugs to inhibit wild type and mutant receptors (338), with tandutinib more active against FLT3 mutant receptors.

4.6.3 Comparison of putative targets of most and least active inhibitors in primary ALLs

To further elucidate which targets may have therapeutic value in ALL, putative targets of the 9 most active inhibitors were compared with the targets of the 12 TKIs which did not inhibit viability greater than 50% at 10 μ M in at least 17/20 primary leukaemias (see fig 4.12).

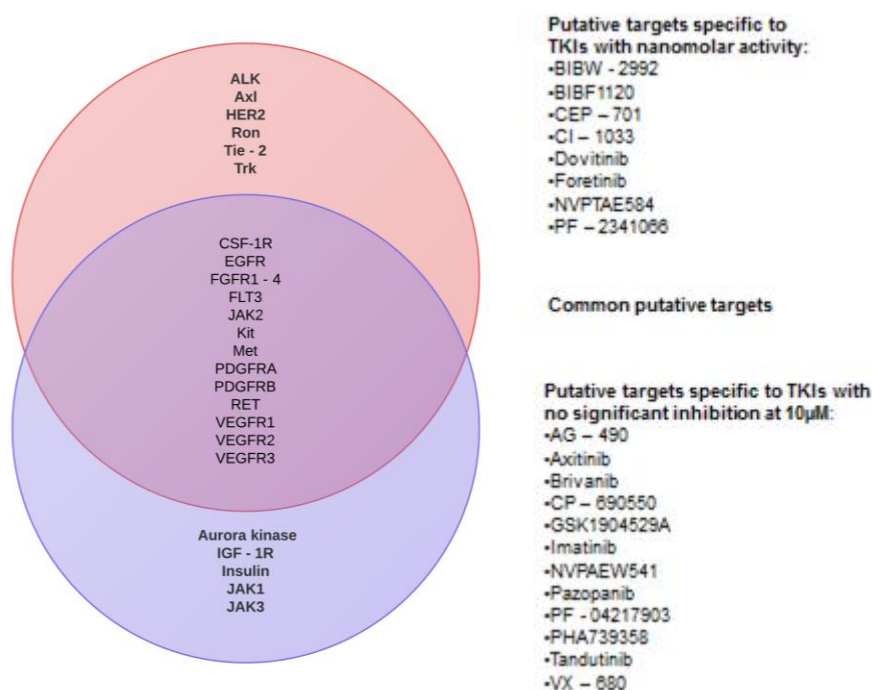


Figure 4.12 Venn diagram comparing putative targets of TKIs with activity at 1 μ M to those with no significant activity at 10 μ M in primary ALL samples. Similar patterns of activity were demonstrated in the cell line and primary ALL experiments, with limited impact on survival from TKIs inhibiting the JAK, Insulin/IGF – 1R and Aurora kinase pathways.

The putative targets limited to the TKIs with activity at 1 μ M included ALK, Axl, HER2, Ron and Tie – 2, while the targets limited to those inhibitors which did not induce responses at 10 μ M were JAK 1/3, Insulin/IGF1-R and Aurora kinases (fig 4.15). The targets which were common to both TKI responses were the same as those present in the cell lines.

To date, there is only limited published evidence of the relevance of HER2, Trk and Axl in ALL. The protein expression of HER2 in chemoresistant ALL has been demonstrated in

small studies (391, 392) and surface expression Trk family members in adult ALL has recently been reported (268). The overexpression of Axl in leukaemias with normal cytogenetics and *MLL* – rearrangements was reported in a study defining the gene expression profiles of adult leukaemias(223), but has not been reported in childhood ALL. ALK, Ron and Tie – 2 over-expression have not been reported in childhood ALL.

In summary, these results suggest a limited role for JAK, Aurora kinases, IGF – 1R, and Abl as targets in the treatment of paediatric non – Ph + ALL, whereas Axl, ALK, HER2, Ron, Tie – 2 or Trk A may play a role.

4.6.4 Sensitivity of primary ALLs to TKIs with activity at 10µM alone

To ensure that no potentially important targets were omitted the spectra of activity of the TKIs which demonstrated a significant dose – dependent response, reducing cell viability greater than 50% at 10 µM in all 20 primary cells, were assessed. Of the 33 TKIs, a total of 6 TKIs fulfilled these criteria, namely bosutinib, dovitinib and foretinib, the FLT3 – inhibitor sorafenib (B – Raf/FLT3/Kit/PDGFR β /VEGFR2 – 3) and the VEGFR inhibitors, cediranib (VEGFR1-3/CSF-1R/PDGFR α / β /Kit/FGFR1) and vandetanib (VEGFR1-3/EGFR/RET). A further 8 TKIs demonstrated activity in 18 or more of the primary cells, and these were the: (i) FLT3 – inclusive inhibitors (BIBF1120, CEP – 701, NVPTAE684 and sunitinib), (ii) the EGFR/HER2 quinazolines (BIBW – 2992 and CI – 1033) and (iii) the restricted inhibitors masatinib (Kit/PDGFR) and PF – 2341066 (Met/ALK). Therefore, apart from B – Raf, no additionally potentially active targets were identified (fig 4.13).

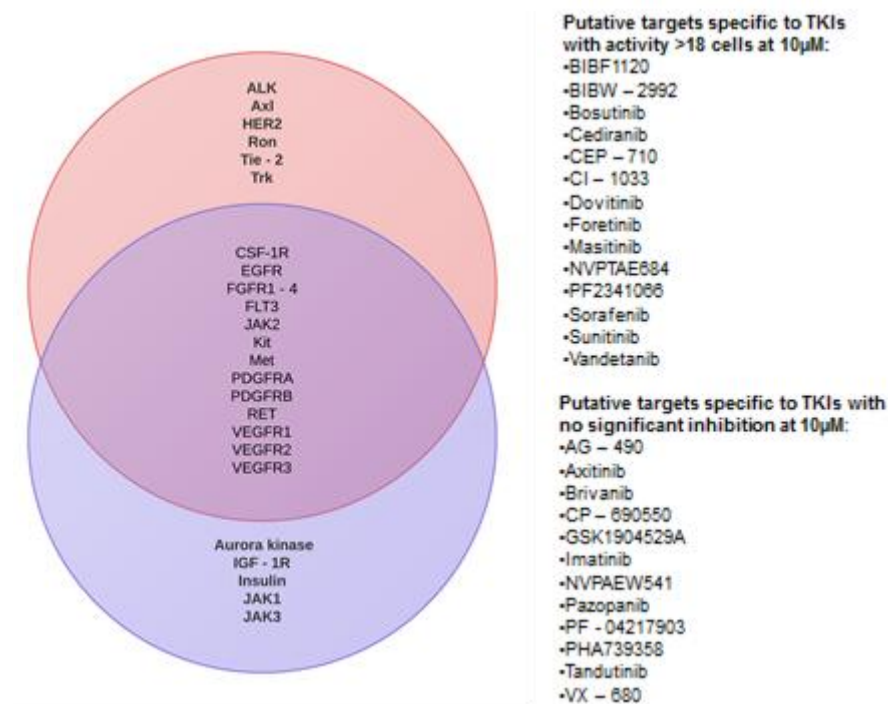


Figure 4.13 Venn diagram comparing putative targets of TKIs with activity only at 10µM to those with no significant activity at 10µM in primary ALL samples. Similar patterns of activity were demonstrated in the cell line and primary ALL experiments, with limited impact on survival from TKIs inhibiting the JAK, Insulin/IGF – 1R and Aurora kinase pathways.

4.6.5 Association of clinical features of leukaemias sensitive to TKI

The relationship between the specific targets identified in the primary leukaemia as sensitive to TKIs and clinical features of the primary cells, including MRD status, cytogenetics, age and white cell count was investigated.

4.6.5.1 Association of MRD status with proportion of leukaemias sensitive to TKIs

Details of flow MRD status were available for 16 samples and molecular MRD status for 19 samples. The samples were stratified by high and standard MRD risk. No significant association was observed between the MRD status, either detected by flow cytometry or PCR, and responses to TKIs (table 4.11).

| TKI | Flow MRD | | | Fisher's exact (p-value) | Molecular MRD | | | Fisher's exact (p-value) |
|------------|---------------------------|-----------------------|-----------------------|-----------------------------|----------------------------|-----------------------|-----------------------|-----------------------------|
| | Standard risk (n=7) | High risk (n=9) | Not known (n=4) | | Standard risk (n=12) | High risk (n=7) | Not known (n=1) | |
| ABT-869 | 0 | 0 | 1 | n/a | 1 | 0 | 0 | 1 |
| AG-490 | 1 | 0 | 0 | 0.44 | 1 | 0 | 0 | 1 |
| AZD0530 | 1 | 0 | 0 | 0.44 | 1 | 0 | 0 | 1 |
| BIBF1120 | 2 | 2 | 1 | 1 | 4 | 1 | 0 | 0.6 |
| BIBW-2992 | 3 | 2 | 2 | 0.6 | 6 | 1 | 0 | 0.17 |
| Bosutinib | 1 | 1 | 1 | 1 | 3 | 0 | 0 | 0.26 |
| Brivanib | 1 | 0 | 0 | 0.44 | 1 | 0 | 0 | 1 |
| CEP-701 | 3 | 2 | 2 | 0.6 | 5 | 2 | 0 | 0.66 |
| CI-1033 | 4 | 3 | 1 | 0.62 | 5 | 3 | 0 | 1 |
| Dasatinib | 1 | 0 | 1 | 0.44 | 2 | 0 | 0 | 0.51 |
| Dovitinib | 2 | 3 | 3 | 1 | 5 | 3 | 0 | 1 |
| Foretinib | 4 | 2 | 2 | 0.30 | 6 | 2 | 0 | 0.63 |
| Masitinib | 0 | 0 | 1 | n/a | 1 | 0 | 0 | 1 |
| Nilotinib | 1 | 0 | 0 | 0.44 | 1 | 0 | 0 | 1 |
| NVPTAE684 | 3 | 2 | 3 | 0.60 | 6 | 2 | 0 | 0.63 |
| Pazopanib | 1 | 0 | 0 | 0.44 | 1 | 0 | 0 | 1 |
| PF04217903 | 1 | 0 | 0 | 0.44 | 1 | 0 | 0 | 1 |
| PF2341066 | 3 | 1 | 2 | 0.26 | 5 | 1 | 0 | 0.33 |
| PHA739358 | 1 | 0 | 1 | 0.44 | 2 | 0 | 0 | 0.51 |
| Sorafenib | 0 | 1 | 1 | 1 | 1 | 0 | 0 | 1 |
| Sunitinib | 0 | 0 | 2 | n/a | 2 | 0 | 0 | 0.51 |
| Tie – 2 | 1 | 2 | 1 | 1 | 3 | 1 | 0 | 1 |
| Vatalinib | 0 | 1 | 0 | 1 | 0 | 1 | 0 | 0.39 |

Table 4.11 Association of MRD risk category with proportion of cells displaying sensitivity to a TKI at 1 μ M. No direct associations were identifiable between MRD status and response to specific TKIs.

4.6.5.2 Association of cytogenetic finding with sensitivity to TKIs

Cytogenetic data was available on 20 ALL (table 4.12). No correlation was demonstrable between the cytogenetic characteristics and TKI sensitivity. The FLT3 inhibitors, dovitinib, sunitinib and NVPTAE684 demonstrated activity in the *MLL* – rearranged infant ALL.

| TKI | TEL/AML (n=5) | Complex (n=1) | Non-contributory (n=6) | t(1;19) (n=2) | Hyperdiploid (n=4) | MLL (n=2) | p – value (Chi square) |
|--|------------------|------------------|---------------------------|------------------|-----------------------|--------------|---------------------------|
| JAK inhibitors | | | | | | | |
| AG-490 | 0 | 0 | 0 | 1 | 0 | 0 | 1 |
| CP690550 | 0 | 0 | 0 | 0 | 0 | 0 | 1 |
| Insulin/IGF-1R inhibitors | | | | | | | |
| GSK1904592A | 0 | 0 | 0 | 0 | 0 | 0 | 1 |
| NVPAEW541 | 0 | 0 | 0 | 0 | 0 | 0 | 1 |
| EGFR/HER2 inhibitors | | | | | | | |
| BIBW-2992 | 3 | 0 | 2 | 1 | 1 | 0 | 0.64 |
| CI-1033 | 3 | 0 | 2 | 1 | 1 | 0 | 0.67 |
| Restricted spectrum inhibitors | | | | | | | |
| AZD0530 | 0 | 0 | 0 | 0 | 0 | 0 | 1 |
| Bosutinib | 1 | 0 | 2 | 0 | 0 | 0 | 1 |
| Dasatinib | 1 | 0 | 1 | 0 | 0 | 0 | 1 |
| Imatinib | 0 | 0 | 0 | 0 | 0 | 0 | 1 |
| Masitinib | 0 | 0 | 1 | 0 | 0 | 0 | 1 |
| Nilotinib | 0 | 0 | 0 | 1 | 0 | 0 | 1 |
| PF-04217903 | 0 | 0 | 0 | 1 | 0 | 0 | 1 |
| PF-2341066 | 3 | 0 | 2 | 1 | 0 | 0 | 0.35 |
| PHA739358 ^a | 0 | 0 | 0 | 0 | 0 | 1 | 1 |
| TIE-2 | 1 | 0 | 3 | 0 | 0 | 0 | 1 |
| Multikinase inhibitor with no FLT3 activity | | | | | | | |
| Axitinib | 0 | 0 | 0 | 0 | 0 | 0 | 1 |
| Brivanib | 0 | 0 | 0 | 1 | 0 | 0 | 1 |
| Cediranib | 0 | 0 | 0 | 0 | 0 | 0 | 1 |
| Motesanib | 0 | 0 | 0 | 0 | 0 | 0 | 1 |
| Pazopanib ^a | 0 | 0 | 0 | 1 | 0 | 0 | 1 |
| Vandetanib | 0 | 0 | 0 | 0 | 0 | 0 | 1 |
| Vatalinib | 0 | 0 | 1 | 0 | 0 | 0 | 1 |
| Multikinase inhibitor with FLT3 activity | | | | | | | |
| ABT – 869 | 0 | 0 | 1 | 0 | 0 | 0 | 1 |
| BIBF1120 | 1 | 0 | 3 | 0 | 1 | 0 | 0.59 |
| CEP-701 | 3 | 0 | 3 | 0 | 1 | 0 | 0.44 |
| Dovitinib | 2 | 0 | 1 | 1 | 3 | 1 | 0.52 |
| Foretinib | 3 | 0 | 4 | 1 | 0 | 0 | 0.22 |
| NVPTAE684 | 3 | 0 | 3 | 1 | 0 | 1 | 0.14 |
| Sorafenib | 0 | 0 | 1 | 0 | 0 | 0 | 1 |
| Sunitinib | 0 | 0 | 1 | 0 | 0 | 1 | 1 |
| Tandutinib | 0 | 0 | 0 | 0 | 0 | 0 | 1 |
| VX680 | 0 | 0 | 0 | 0 | 0 | 0 | 1 |

a- A reduction in cell viability >50% was detected at 1µM, no dose – dependent response was observed.

Table 4.12 Association of cytogenetics and responses to individual TKIs. No significant relationship was identified between the response of leukaemias to TKIs and the somatic cytogenetic findings. The cohort consisted of 20 leukaemia samples of which 4 had normal cytogenetic analyses, 2 ‘non – contributory’ cytogenetic abnormalities, 5 t(12;21), 4 hyperdiploid, 2 *MLL* – rearranged infant leukaemias, 2 t(1;19) and 1 sample had 46XY, del9p21p21, monoallelic *CDKN2A* loss, 13q14 loss. Of the 2 leukaemias with ‘non – contributory’ cytogenetic findings, one had 46XX, t(2;12), p1p13(8) 46XX (2) *ETV6* neg and the other was 46XX, t(3;10) t(9;16) +8 biallelic del p16.

4.6.5.3 Association of NCI/Rome criteria with TKI sensitivity

The panel of primary ALLs was stratified by NCI/Rome age risk criteria (standard risk <10 years and adverse risk >10 years) and the relationship with TKI sensitivity analysed. Two of twenty samples were infant ALL and were excluded from analysis as they represent a separate risk group. No statistically significant difference was demonstrated.

| TKI | Targets | Age | | p – value (Fisher's) |
|-------------|--------------------------|---------------|-----------|----------------------|
| | | 1 – 10 (n=12) | >10 (n=6) | |
| Foretinib | VEGFR/Met/PDGFR/Ron/FLT3 | 6 | 2 | 0.64 |
| CI-1033 | EGFR/HER2 | 6 | 2 | 0.64 |
| CEP-701 | FLT3/VEGFR/PDGFR/RET/Trk | 6 | 1 | 0.32 |
| BIBW-2992 | EGFR/HER2 | 5 | 2 | 1 |
| Dovitinib | FLT3/VEGFR/PDGFR/FGFR | 5 | 2 | 1 |
| NVPTAE684 | ALK/Met/FLT3 | 4 | 3 | 0.63 |
| PF-2341066 | Met/ALK | 3 | 3 | 0.34 |
| BIBF1120 | VEGFR/PDGFR/FGFR/FLT3 | 2 | 3 | 0.27 |
| TIE-2 | Tie – 2 | 3 | 1 | 1 |
| Bosutinib | Abl/Src/Axl/EGFR/Trk | 2 | 1 | 1 |
| Dasatinib | Abl/Src/CSF-1R/Kit/PDGFR | 1 | 1 | 1 |
| Sorafenib | VEGFR/PDGFR/FLT3 | 1 | 0 | 1 |
| Vatalinib | VEGFR/PDGFR | 1 | 0 | 1 |
| ABT-869 | VEGFR/PDGFR/FLT3 | 0 | 1 | 0.34 |
| AG-490 | JAK | 0 | 1 | 0.34 |
| AZD0530 | Abl/Src | 0 | 1 | 0.34 |
| Brivanib | VEGFR/PDGFR | 0 | 1 | 0.34 |
| Masitinib | Kit | 0 | 1 | 0.34 |
| Nilotinib | Abl/Src/CSF-1R/Kit/PDGFR | 0 | 1 | 0.34 |
| Pazopanib | VEGFR/PDGFR | 0 | 1 | 0.34 |
| PF-04217903 | Met | 0 | 1 | 1 |
| PHA739358 | Aurora/RET | 0 | 1 | 0.34 |
| Sunitinib | VEGFR/PDGFR/Kit/FLT3 | 0 | 1 | 0.33 |

a- A reduction in cell viability >50% was detected at 1µM, no dose – dependent response was observed

Table 4.13 Association of NCI/Rome age risk criteria with proportion of cells responding to individual TKIs (excluding 2 Infant ALL). TKIs highlighted in grey demonstrated activity in ≥5/20 samples. No significant relationships were identified between response to TKI and NCI/Rome risk criteria. Fisher's exact test was used to analyse the proportion of primary ALLs sensitive to each TKI when samples were stratified by age.

Finally, the WCC at the time of presentation was assessed to determine if there was relationship with the proportion of responses to the TKIs. NCI/Rome adverse WCC features were present in 6 of the leukaemias studied. No statistically significant difference was noted in the samples responding to each TKI.

| TKI | Targets | WCC (x 10 ⁹ /L) | | Fisher's exact test (p-value) |
|-------------|----------------------------------|-------------------------------|-----------|----------------------------------|
| | | <50 (n=14) | >50 (n=6) | |
| CEP-701 | FLT3/VEGFR1-2/PDGFR/RET/Trk | 6 | 1 | 0.35 |
| CI-1033 | EGFR/HER2 | 6 | 2 | 1 |
| Foretinib | FLT3/VEGFR/PDGFR/Axl/Ron/Met | 6 | 2 | 1 |
| BIBW-2992 | EGFR/HER2 | 5 | 2 | 1 |
| Dovitinib | FLT3/VEGFR/PDGFR/CSF-1R/Kit/FGFR | 5 | 3 | 0.64 |
| NVPTAE684 | FLT3/Met/ALK | 4 | 4 | 0.32 |
| PF-2341066 | Met/ALK | 3 | 3 | 0.30 |
| TIE-2 | Tie – 2 | 3 | 1 | 1 |
| BIBF1120 | FLT3/VEGFR/PDGFR/FGFR/Src | 2 | 3 | 0.13 |
| Bosutinib | Abl/Src/Axl/EGFR/Trk | 2 | 1 | 1 |
| Dasatinib | Abl/Src/CSF-1R/Kit/PDGFR | 1 | 1 | 0.52 |
| Sorafenib | FLT3/VEGFR | 1 | 0 | 1 |
| Vatalinib | VEGFR | 1 | 0 | 1 |
| ABT-869 | FLT3/CSF-1R/Kit/VEGFR/PDGFR | 0 | 1 | 0.3 |
| AG-490 | JAK/EGFR | 0 | 1 | 0.3 |
| AZD0530 | Abl/Src | 0 | 1 | 0.3 |
| Brivanib | VEGFR/FGFR | 0 | 1 | 0.3 |
| Masitinib | CSF-1R/Kit/PDGFR | 0 | 1 | 0.3 |
| Nilotinib | Abl/CSF-1R/Kit/PDGFR | 0 | 1 | 0.3 |
| Pazopanib | VEGFR/PDGFR | 0 | 1 | 0.3 |
| PF-04217903 | Met | 0 | 1 | 0.3 |
| PHA739358 | Aurora/Abl/Src/RET | 0 | 2 | 0.08 |
| Sunitinib | FLT3/CSF-1R/Kit/PDGFR/VEGFR | 0 | 2 | 0.08 |

Table 4.14 Association of WCC standard and adverse risk criteria with proportion of TKIs displaying nanomolar activity to individual TKIs. TKIs highlighted in grey demonstrated activity in $\geq 5/20$ samples. No significant relationships were identified between response to TKI and NCI/Rome risk criteria.

Overall the TKI library screen of the 20 primary ALLs revealed multikinase inhibitors with FLT3 activity (foretinib, dovitinib, CEP – 701, NVPTAE684) and the irreversible quinazoline pan – EGFR inhibitors (BIBW – 2992 and CI – 1033) displayed broad activity across the ALL panel. The sensitivity to TKIs was not related to clinical and biological parameters.

4.7 Discussion

In this study, ALL cell lines and primary cells were screened using a kinase inhibitor library to identify compounds which reduce cell viability, to candidate kinase therapeutic targets and infer pathways involved in ALL cell survival and proliferation. The library of inhibitors was constructed from drugs in early phase trial development to cover as much of the kinome as possible. The putative targets of the inhibitors in the library were based on the published recognised targets of the inhibitors, typically from *in vitro* kinase assays.

A drug screening approach assessing the viability of treated cells was adopted because cryopreserved cells are of sufficient quality for interrogation and the system is flexible enough to include newly available molecules, with the aim of quickly identifying clinically applicable compounds for translation into early phase clinical trials.

An alternative screening approach has been described, using siRNA to interrogate freshly harvested leukaemias (263). A limiting factor for this method is the need to obtain fresh bone marrow as thawed aliquots of cryopreserved marrow are not of sufficient quality to undertake reliable screening (personal communication Dr M. Loriaux, Oregon Health & Sciences University). Much like a drug screen, this screening approach is confounded by false positive and negatives, through off – targets effects and technical difficulties (393).

Not unexpectedly, no individual TKI was identified which globally inhibited all of the primary and cell line leukaemias. Three categories of TKI demonstrated activity in subsets of the cell lines and primary cells studied: (i) multikinase inhibitors with FLT3 activity (BIBF1120, CEP – 701, dovitinib and foretinib), (ii) the aniline – quinazoline group of EGFR inhibitors (BIBW – 2992 and CI – 1033) and (iii) combined Met/ALK inhibitors (NVPTAE684 and PF – 2341066). The putative targets of these 3 categories were diverse, including the EGFR, FGFR, PDGFR and VEGFR families and related classes of RTKs such as CSF – 1R, FLT3 and KIT. In the cell line experiments FLT3 was the common target for TKIs which demonstrated activity at 1 μ M. Although limited to a small cell line panel, the results could not demonstrate a relationship between expression of a single RTK transcript and

sensitivity to a TKI. This could suggest TKIs are likely to be most effective by simultaneously targeting multiple TKs rather than acting on individual kinases.

(i) Multikinase inhibitors with FLT3 activity (BIBF1120, CEP – 701, dovitinib and foretinib)

In both cell lines and primary cells the activity of the FLT3 – inclusive multikinase inhibitors (BIBF1120, CEP – 701, dovitinib and foretinib) is of interest as FLT3 is almost universally expressed in B – precursor ALL (394, 395). Activating mutations are present in 3 – 5% of the ALL population (396) with a predominance in the hyperdiploid (8 - 25%) and *MLL* – rearranged infant leukaemias (3 - 20%) (371, 397-399). Furthermore, increased activity in these leukaemias may be due to overexpression of wild type receptors (220, 221, 252).

The role of FLT3 as a therapeutic target has been investigated in childhood ALL. Sensitivity to nanomolar concentrations of the FLT3 inhibitors, CEP – 701 and PKC412/midostaurin, was demonstrated in ALL cells with high expression of wild type FLT3 transcript (hyperdiploid and *MLL* – rearranged leukaemias) while higher concentrations did not inhibit cell lines or primary cells with low FLT3 expression (397, 398, 400).

In this study anti – leukaemic activity was demonstrated by FLT3 – inhibitors in cytogenetic subtypes of ALL which have not previously reported, namely ALL with normal karyotype and t(12;21). Unfortunately due to limited material the FLT3 status of these leukaemias could not be determined. A possible explanation for this unexpected activity is the doses used in this study exceed those used in previous *in vitro* studies by 10 to 20 – fold (397, 398, 400). A second reason may be the chemical structure and properties of the investigated inhibitors are different to those previously investigated in ALL and may thus bind irreversibly to the receptors leading to more potent inhibition and activity. Third, the higher doses of the FLT3 – inclusive inhibitors may have additional off – target effects which could contribute to their efficacy. The secondary kinase profiles of some of the FLT3

targeting TKIs used in this study (dovitinib, foretinib, BIBF1120) are different to the inhibitors previously investigated in ALL. Concomitant inhibition of FLT3 with other RTKs could lead to a reduced viability of the tumour cells. The FLT3 – inclusive inhibitor CEP – 701 has an extended kinase inhibitory profile against the Trk family of receptors, which have recently been implicated in leukaemogenesis. Expression of Trk A – C has been demonstrated in adult myeloid and lymphoid leukaemias (268) and phosphorylated Trk A and B were recently identified in childhood ALL (362). Trk may play a role in chemoresistance as receptor stimulation increased survival in response to IR – induced damage and inhibition abrogated this anti – apoptotic effect. The confirmation of Trk A transcript in Nalm 17, REH and SupB15 and the activity of bosutinib (Abl/Src/Axl/Trk) in a limited number of non – Ph+ primary cells warrants further investigation.

In contrast to the broad spectrum activity demonstrated by the FLT3 – inclusive multikinase inhibitors, the FLT3/Kit/PDGFR inhibitor tandutinib demonstrated limited activity at 10µM in the primary cells; only 3/20 were sensitive at this dose in addition each of these samples demonstrated sensitivity to at least one other FLT3 inhibitor at nanomolar concentrations. This restricted activity may be due to the fact that tandutinib preferentially inhibits mutant FLT3 receptors (338, 401) which may suggest that these 3 samples may possess mutant receptors. The other 12 samples which were sensitive to FLT3 – inclusive multikinase inhibitors were not sensitive to tandutinib.

Overall, the data from this primary screen suggests that there may be role for further research into the role of FLT3 – inclusive multikinase TKIs in ALL, in leukaemias that are not limited to the hyperdiploid and infant ALL categories.

(ii) Aniline – quinazoline group of EGFR inhibitors (BIBW – 2992 and CI – 1033)

The second group of TKIs which were active in the cell lines and primary leukaemias were the irreversible aniline – quinazoline inhibitors (BIBW-2992 and CI – 1033). The selective inhibition of the apoptosis defective cell lines REH and SD -1 initially supported a role for

EGFR or HER2 in chemoresistance, but this differential activity did not extend to the primary leukaemias, where activity was not restricted to MRD positive leukaemias. While HER2 has been described in both adult and paediatric ALL and was associated with poor responses to chemotherapy, gene expression of *HER2* and *EGFR* in childhood leukaemias is at relatively low levels (391, 392) (chapter 3). The low level of EGFR family expression, together with the absence of response to other EGFR/HER2 inhibitors in the cell line screen supports the idea of off – target activity by the quinazolines. Further evidence is supplied by recent publications reporting the induction of cell cycle arrest and intrinsic apoptosis in AML and Jurkat cell lines by CI - 1033, neither of which expresses EGF family receptors at protein level (386, 402). These data are in conflict with the initial *in vitro* kinase assays, which demonstrated highly restricted activity of CI – 1033 against the EGFR family of kinases (320, 403). Fabian *et al.* has demonstrated CI – 1033 is significantly more promiscuous than originally thought (404), binding up to 36 kinases including members of the Abl, Src and Eph receptor family. It is possible that more of these targets are involved in cell line biology compared with primary cells. Another possible mechanism of action of these TKIs in the ALL cell lines and primary cells could be through FLT3 inhibition as Nordigarden *et al.* (385) demonstrated CI – 1033 induced cell death in primary *FLT3 – ITD* AML cells *in vitro* and in a murine xenograft model. These data are consistent with the original proof of principle experiment with AML – 2 (section 4.2), as both of these inhibitors reduced viability of the *FLT3 – ITD* primary at 1µM. Thus, the broad activity of CI-1033 and BIBW – 2992 in the primary cell may be due to FLT3 inhibition, which is corroborated by the significant degree of overlap demonstrated by the FLT3 – inclusive multikinase and the quinazoline inhibitors. Further work will be required to investigate whether other mechanisms of action exist in pre – B ALL.

(iii) Combined Met/ALK inhibitors (NVPTAE684 and PF – 2341066).

The third group of active inhibitors was the combined Met/ALK inhibitors, NVPTAE684 and PF – 2341066 which were active in 8 and 6 primary ALL samples respectively. All 6 primary leukaemias which were sensitive to PF-2341066 were also sensitive to

NVPTAE684, suggesting a possible common target. In the cell lines, NVPTAE684 was active in only in SD – 1, while REH, SD – 1 and SupB15 were sensitive to PF-2341066. Neither ALK nor Met were expressed at mRNA level in the cell lines investigated. While NVPTAE684 demonstrates activity against FLT3, PF-2341066 does not have recognised anti – FLT3 activity. The primary target of PF-2340166 is Met and expression of this receptor has been reported in ALL, most abundantly in t(12;21) ALL (276). However, contrary to providing a survival advantage, stimulation of the receptor by the cognate ligand Hepatocyte Growth Factor (HGF) increases sensitivity to doxorubicin – induced apoptosis in t(12;21) leukaemia cells. It would appear in the context of t(12;21) it is unlikely that Met play an important role in cell survival in ALL. The notion that Met has no significant survival role in the ALLs in this study is supported by the limited activity of the restricted and potent Met inhibitor, PF – 04217903, in the cell lines and primary cells.

A pro – apoptotic role for the over-expressed wild type ALK receptor has been demonstrated in the T – ALL cell line, Jurkat (405) whereas, the NPM – ALK mutation recurrently present in anaplastic lymphoma is a constitutively activate kinase with anti – apoptotic properties (218). This mutant form has not been described in ALL, however the mechanism of action of NVPTAE684 and PF – 2341066 in this leukaemia screen remains uncertain. More detailed kinase profiling of this drug may elucidate the mechanisms of action.

Inhibitors to which cell lines and primary cells were resistant to at 10µM

The cell line and primary screen defined 3 categories of TKIs with limited activity at 10µM concentrations suggesting these are not viable targets for treating ALLs in this study. These 3 groups of TKIs included: (i) IGF – 1R inhibitors, (ii) JAK family inhibitors and (iii) the Aurora kinase inhibitors.

(i) IR/IGF – 1R inhibitors

The lack of response exhibited by the leukaemias in this study to treatment with IR/IGF – 1R inhibitors correlates with limited activity demonstrated previously in murine preclinical

models of ALL and solid tumours (406, 407). However, recent publications have suggested that IGF - 1R provides a survival advantage to ALL cells *in vitro* (408). Furthermore, growth inhibition and induction of apoptosis was also reported in the pre - B ALL cell lines Nalm 6, REH and SupB15 after IGF-1R inhibition (409). A reason for this discrepancy could be the concentrations of IGF - 1R inhibitor required to achieve growth reduction or apoptosis were higher than those utilised in this study. The demonstration of a limited dose - dependent reduction in viability in 5 primary samples from patients with adverse features or outcome, including *CDKN2A* deletion, *MLL* - rearrangement, a relapse of t(12;21) disease and a death from disease, may yet support IGF - 1R as a possible target in childhood ALL.

(ii) JAK inhibitors

The JAK inhibitors also demonstrated limited response in both the cell lines and primary cells. Recent description of JAK activation in DS - ALL and high risk leukaemias has piqued interest in this pathway. The lack of activity in the primary cell panel to JAK inhibitors in this study may due to the primary cells not overexpressing *CRLF2* or possessing activating *JAK* mutations, both of which are relatively rare events in paediatric ALL, only 3% in the unselected ALL population (222).

(iii) Aurora kinase inhibitors (AKIs)

While investigation of the role of Aurora kinases is not central to this study, the dual Aurora kinase/RTK inhibitors, PHA739358 and VX-680, were included in the drug library for their putative RTK target inhibition. The lack of activity in both cell lines and primary cells by these 2 inhibitors in this study is contradictory to a recent publication, which reported the novel Aurora kinase inhibitor, MLN8237, demonstrated activity in murine ALL xenografts (410). Although MLN8237 is not in the drug library investigated in this study, it has a similar profile of Aurora kinase inhibition to VX - 680 and PHA739358 (Aurora A - C). The lack of activity in this study may be because the leukaemias assayed do

not overexpress the Aurora kinases or they may possess the T217D mutation in Aurora A, recognised to induce resistance to AKIs (411).

Overall, in summary of this chapter, while it was not possible to identify an inhibitor which uniformly inhibited the cell line and primary leukaemias or implicate a single common RTK in the proliferation or survival of ALL, 3 groups of TKIs which demonstrated significant activity in cell lines and primary cells were identified. Of the candidate TKIs identified in this screen, a decision was made to further explore the compounds foretinib and dovitinib in preclinical studies. This decision was in part based on the broad spectrum of activity of foretinib and dovitinib demonstrated in the cell line and primary screens. Both compounds demonstrated activity in all cell lines which was not restricted by cytogenetic or apoptotic phenotype. In the primary cells, these TKIs were active against the most number of samples (n=8). As demonstrated in this study the TKIs with the most promiscuous spectra appear to be most effective and these TKIs have broad inhibitory profiles. Despite this promiscuity, early clinical trials have demonstrated these drugs are well tolerated and safe (412, 413). The predominant side effects in adult studies are nausea, fatigue and hypertension. In addition, previous experience in adults may expedite the transfer of these inhibitors to clinical trials in childhood leukaemias.

5 Preclinical investigation of the multikinase inhibitors, foretinib and dovitinib

5.1. Introduction

The results from the preceding chapter identified 6 TKIs that were candidates for further investigation, foretinib (FLT3/Met/PDGFR/VEGFR), dovitinib (FGFR/FLT3/PDGFR/VEGFR), NVPTAE684 (ALK /FLT3/Met), CI – 1033, BIBW2992 (EGFR/HER2) and CEP – 701(FLT3/Trk A/VEGFR). These TKIs were selected because they all were active at 1 μ M, in at least 7/20 primary ALL samples.

From these candidates, foretinib and dovitinib were chosen for further investigation based on the combined evidence of anti – leukaemic activity in the cell lines and primary cell studies and evidence that these TKIs are well tolerated in adult clinical studies and the lack of published literature for their use in paediatric ALL.

Foretinib and dovitinib were designed as anti – angiogenic agents, with the principal targets PDGFR and VEGFR families (table 5.1). Foretinib was specifically designed to target Met, an RTK associated with invasive tumours (414). Foretinib was the first in class Met inhibitor entering clinical trials and has completed phase 1 investigation (413). Dovitinib has an extended FGFR spectrum of activity, another RTK family associated with angiogenesis.

| Kinase | Dovitinib | Foretinib |
|---------|-----------|-----------|
| Axl | - | 11 |
| CSF-1R | 36 | - |
| FGFR1 | 8 | 660 |
| FGFR3 | 8 | - |
| FLT3 | 1 | 3.6 |
| KIT | 2 | 6.7 |
| Met | - | 0.4 |
| PDGFRA | 200 | 3.6 |
| PDGFRB | 27 | 9.6 |
| Ron | - | 3 |
| Tie – 2 | - | 1.1 |
| VEGFR 1 | 10 | 6.8 |
| VEGFR 2 | 13 | 0.86 |
| VEGFR 3 | 8 | 2.8 |

Table 5.1 Kinase targets of foretinib and dovitinib with biochemical IC₅₀ values (nmol/L) (297, 415)

Both TKIs are currently being investigated in clinical trials. Dovitinib is being investigated in phase 2 trials in FGFR1 – expressing breast cancer (416), melanoma (417) and urothelial cancer (418). Phase 2 trials are currently underway to investigate the efficacy of foretinib in squamous cell carcinoma of head and neck (419) and ‘triple negative’ breast cancer (420). Neither of these two TKIs has been investigated in childhood ALL.

5.2. Assessment of responses of ALL cell lines and primary cells to TKIs

In the cell line screen, both foretinib and dovitinib demonstrated activity against the Philadelphia positive cell lines, SD – 1 and SupB15. Foretinib and dovitinib also inhibited 8/20 primary leukaemias, none of which possessed the chromosome translocation t(9;22). The possibility that foretinib and dovitinib might also inhibit Bcr/Abl led to the inclusion of a third Ph⁺ cell line, TOM – 1; any novel agent demonstrating activity against this inherently resistant leukaemia is worthy of further investigation. Assessment of the putative RTK targets by RT q – PCR revealed TOM – 1 expressed transcript for *FGFR1*, *FLT3*, *PDGFRB* and *VEGFR1* at comparable levels to the other cell lines.

To further investigate the potency of these agents, both drugs were re – tested against the 6 cell lines, Nalm6, Nalm 17, REH, SD – 1, SupB15 and TOM – 1 to detail their dose –

response curves. Serial 8 point dilutions of foretinib and dovitinib covering the concentration range 0.001 - 10 μ M were tested. Cell viability was assessed after 72 hours by determining alterations in luminescence with Promega CellTite – Glo® (section 2.11). The data presented are the mean of three separate experiments, each repeated in triplicate, with error bars representing standard deviation. The dose response curves from the mean of the 3 experiments were analysed, and the IC₅₀ of the cell lines were calculated by non – linear regression using Graphpad Prism *vers5*.

5.2.1. Foretinib dose response assessment in cell lines

Fig 5.1 shows the sensitivity profiles of the 6 cell lines investigated. Nalm 17 (IC₅₀ 0.43 μ M), REH (IC₅₀ 0.19 μ M), SD – 1 (IC₅₀ 0.27 μ M) and SupB15 (IC₅₀ 0.27 μ M) all demonstrated sensitivity to foretinib at doses under 1 μ M. Both the t(9;22) cell line TOM – 1 and t(5;12) Nalm 6 were less sensitive to foretinib, although responded at low micromolar concentrations.

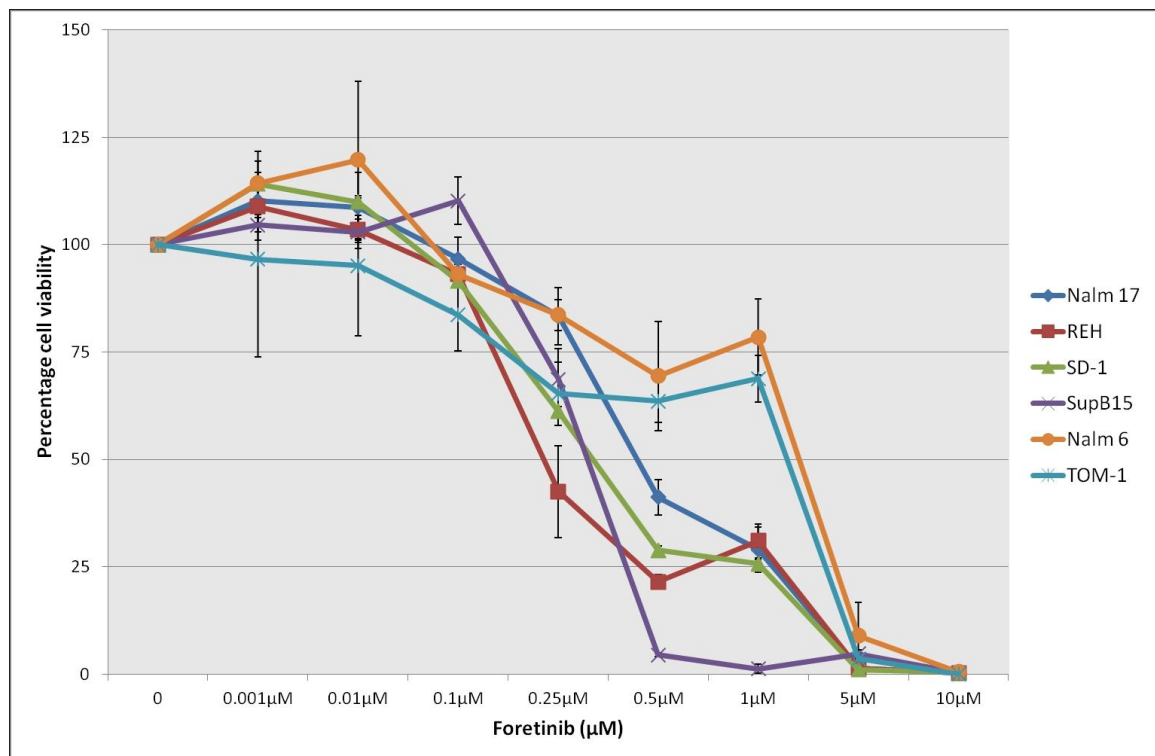


Figure 5.1 Dose response curves of the 6 pre – B ALL cell lines against foretinib. Four of the 6 cell lines investigated demonstrated responses to foretinib at nanomolar concentrations, REH (0.19μM), SD – 1 (0.27μM), SupB15 (0.27μM) and Nalm 17 (0.43μM). The cell lines Nalm 6 and TOM – 1 demonstrated low micromolar responses, IC₅₀ 1.96μM and 1.84μM respectively. Data presented are the mean of 3 experiments, performed in triplicate. Error bars are standard deviations for the mean of the 3 experiments. Curves were analysed with Graphpad Prism 5 software to determine the calculated IC₅₀.

5.2.2. Dovitinib dose response assessment in cell lines

Fig 5.2 shows the dose response curves for the cell lines treated with increasing concentrations of dovitinib. All 6 cell lines demonstrated greater than 50% reduction in cell viability at 1μM. The most sensitive cell line SupB15 exhibited an IC₅₀ 0.19μM, whereas the most resistant cell lines were Nalm 6 and TOM – 1, with IC₅₀ 0.84μM and 0.5μM, respectively.

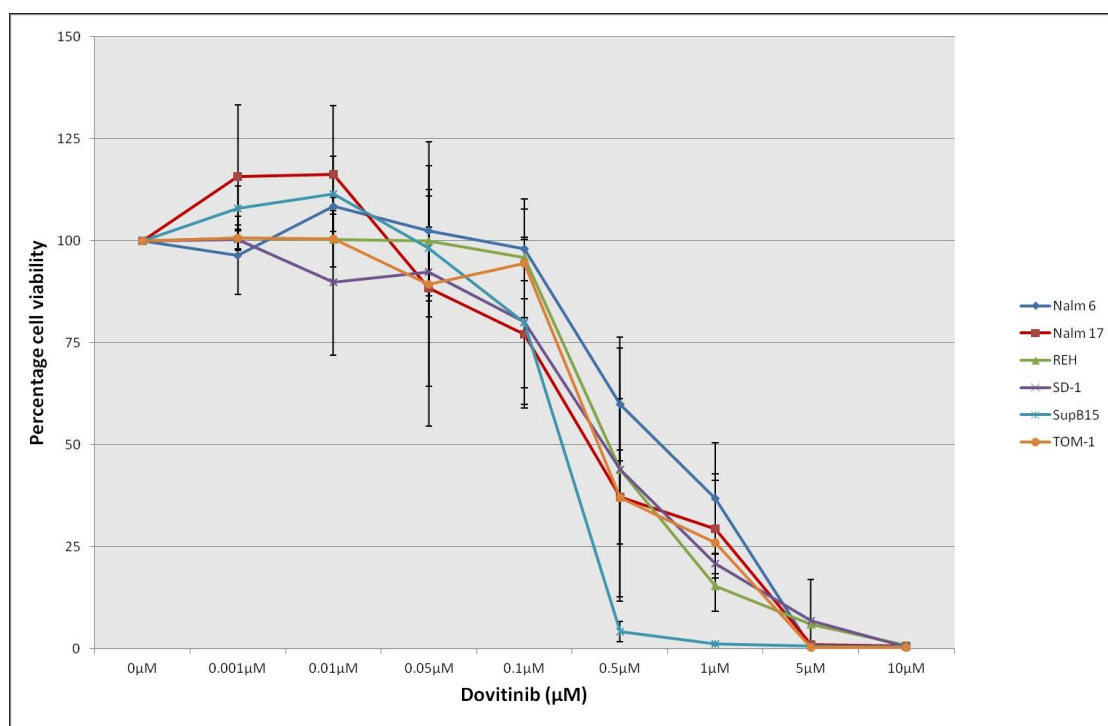


Figure 5.2 Dose response curves of the 6 pre – B ALL cell lines against dovitinib. All 6 cell lines investigated demonstrated responses to dovitinib at nanomolar concentrations, SupB15 (0.19μM), SD – 1 (0.2μM), REH (0.23μM), and Nalm 17 (0.28μM). The cell lines Nalm 6 and TOM – 1 demonstrated low micromolar responses, IC₅₀ 0.84μM and 0.5μM respectively. Data presented are the mean of 3 experiments, performed in triplicate and plotted. Error bars are standard deviations for 3 experiments. Curves were analysed with Graphpad Prism 5 software to determine the calculated IC₅₀.

In summary, the potent nanomolar activity observed in the original library screen was confirmed for both TKIs. Response to foretinib or dovitinib was not limited to a specific cytogenetic subtype or apoptotic phenotype. In general, dovitinib was more potent, except in REH, which exhibited a slightly lower IC₅₀ in response to foretinib (0.19 μM cf. 0.23μM).

5.2.3. TKI activity in ALL primary cells (ALL – 20)

Dose response curves over a dose range 0.01 – 10μM for the sample ALL – 20 which had exhibited a response to foretinib and dovitinib at 1μM in the primary cell screen, were then determined. Primary cells were incubated with DMSO (0.1% - 0.0001%) to ensure that the viability of the primary cells would not be negatively affected by the diluent. No alteration in viability was present at DMSO concentration of 0.1% (fig 5.3a). ALL – 20 was slightly more sensitive to foretinib (IC₅₀ 0.129μM) compared to dovitinib (IC₅₀ 0.133μM fig 5.3b).

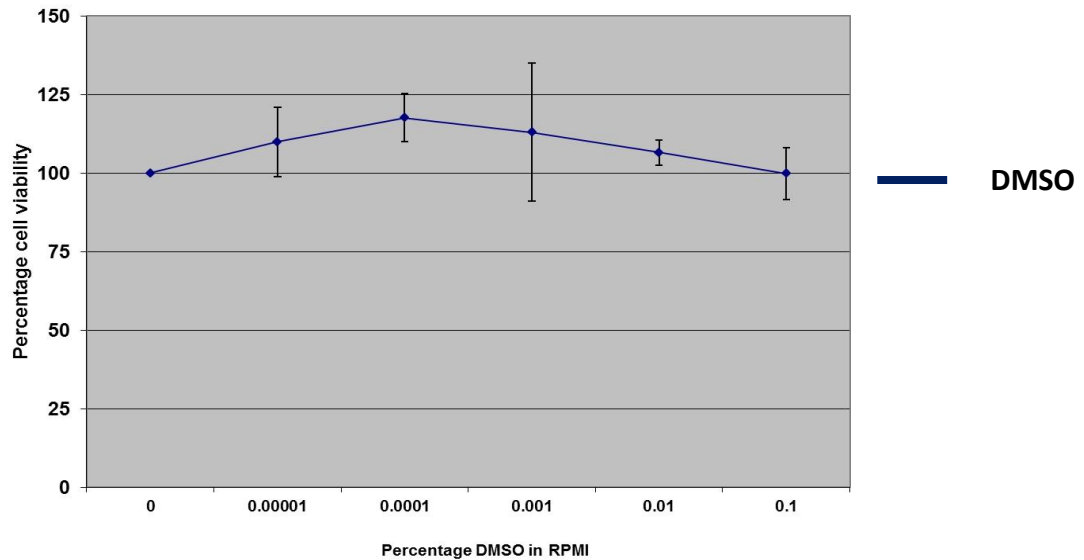


Figure 5.3a

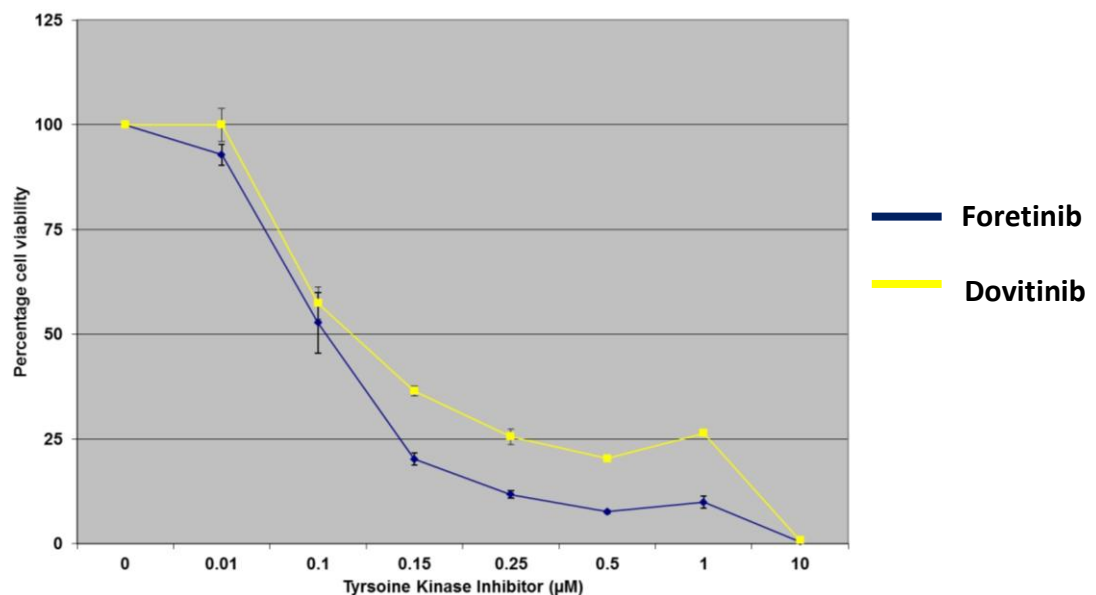


Figure 5.3b

Figure 5.3 Dose response curves were determined for DMSO, dovitinib and foretinib in primary ALL cells. (a) The TKIs were dissolved in DMSO. To assess whether DMSO would have any impact on primary ALL viability a dose curve was determined for primary sample ALL – 20 ALL – 20 cells were incubated with increasing concentration of DMSO 0.00001 – 0.1% and cell viability estimated by Promega CelTitre – Glo® at 48h. DMSO did not reduce cell viability of ALL – 20. (b) Dose response curves were determined for ALL – 20 against dovitinib and foretinib (0.01 - 10μM). The experiments were performed in triplicate and error bars are standard deviation of mean.

In summary, foretinib and dovitinib demonstrated *in vitro* anti – leukaemic activity in both cell lines and primary ALL at nanomolar concentrations, which was not restricted by cytogenetic subgroup.

5.3. Effects of TKIs on cell cycle profiles of ALL cell lines

The effects of foretinib and dovitinib on the cell cycle profiles of 6 cell lines were investigated.

5.3.1. Effects of foretinib on cell cycle profiles

Cells were treated with 3 concentrations of foretinib, 0.15 μ M, 0.5 μ M and 1 μ M, and alterations in the cell cycle profile assessed at 24, 48 and 72 hours. These concentrations were chosen to assess whether the effects were dose – dependent. The lowest dose was sub – IC₅₀ for all cell lines, while 0.5 μ M and 1 μ M were above the IC₅₀ of Nalm 17, REH, SD -1 and SupB15. The 2 most resistant cell lines, Nalm 6 and TOM -1, with micromolar IC₅₀ were treated with 5 μ M foretinib for 48 and 72 hours to further characterise the effects of foretinib. All cells were treated with a corresponding concentration of DMSO to act as control.

Significant alterations in the cell cycle profile were present in all 6 cell lines at all concentrations of foretinib tested. Three patterns of response were observed with foretinib concentrations up to 1 μ M.

The first pattern of response was exhibited by the cell lines REH and SupB15 and demonstrated an arrest at G2/M by 24 hours followed by subsequent cell death.

After the initial cell cycle arrest, there was a reduction in the G2/M peak and subsequent accumulation of cells in sub – G1. This finding is consistent with the induction of cell death. Cell death increased from 48 to 72 hours and the magnitude of accumulation was dose dependent. Some differences in the detail of the pattern of response existed between the 2 cell lines.

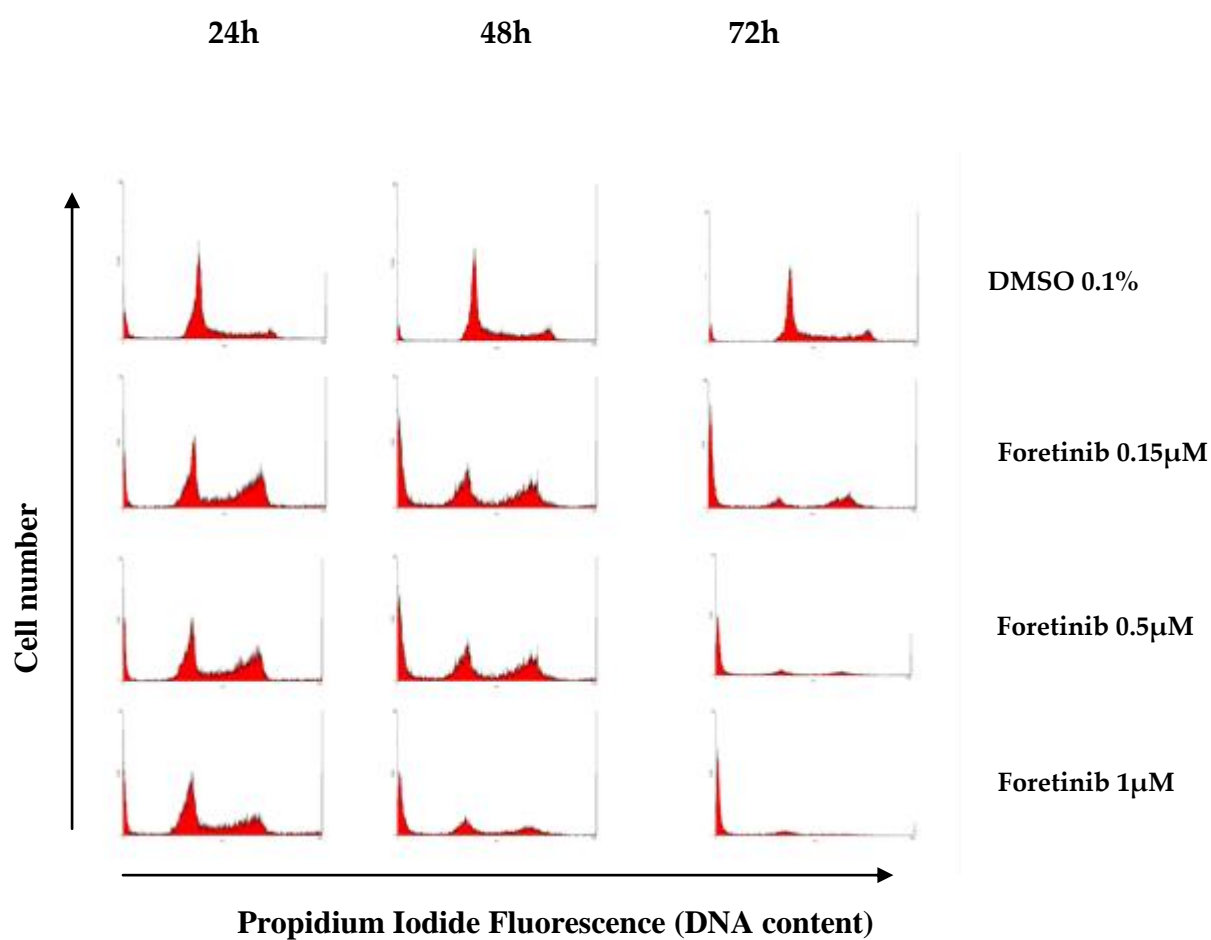


Figure 5.4 Foretinib induces significant changes in the cell cycle profile of the REH t(12;21) cell line. Incubation with foretinib induces G2/M arrest followed by accumulation of sub – G1 (cell death) in a dose – and time – dependent manner. Experiments were performed 3 times, in triplicate. Cell numbers are on y – axis and intensity of Propidium Iodide fluorescence is expressed on the x – axis.

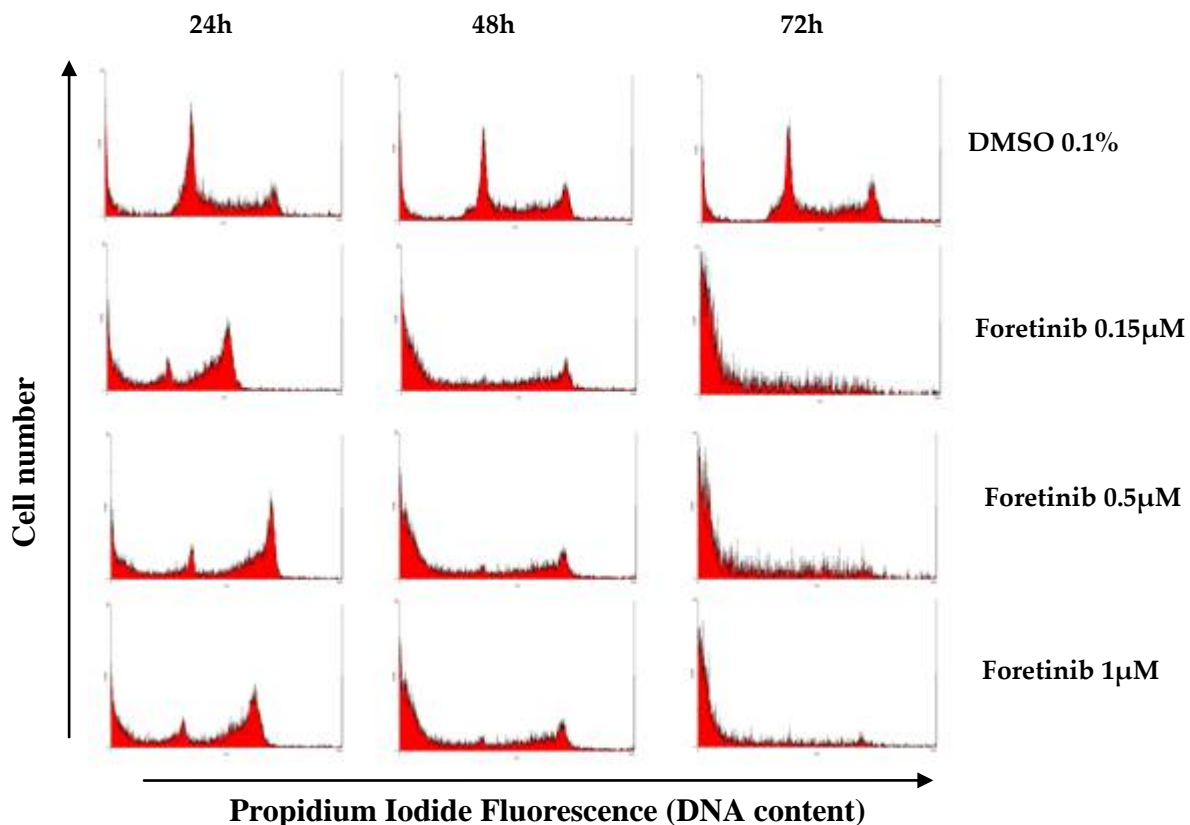


Figure 5.5 Foretinib induces significant changes in the cell cycle profile of the SupB15 t(9;22) cell line. Incubation with foretinib induces G2/M arrest followed by accumulation of cells in G1 (cell death) in a dose – and time – dependent manner. Experiments were performed 3 times, in triplicate. Cell numbers are on y – axis and intensity of Propidium Iodide fluorescence is expressed on the x – axis.

The second pattern of response was exhibited by the cell lines, Nalm 17 and SD – 1. Following treatment with foretinib, cells accumulated in sub – G1 by 24 hours, with a reduction in G1 and S – phases (fig 5.6). Unlike the cell lines, REH or SupB15, there was no concomitant G2/M arrest. Accumulation of sub – G1 cells in the SD – 1 cell line increased as the concentration increased from 0.15μM to 1μM, as early as 24 hours. Cell death in response to foretinib in SD – 1 was both time – and concentration – dependent.

The induction of cell death in Nalm 17 appeared relatively dose – independent, with a similar pattern of cells accumulating in sub – G1 at all time-points (fig 5.7). A similar reduction in G1, S and G2/M occurred at all time – points and concentrations. The induction of cell death was time – dependent.

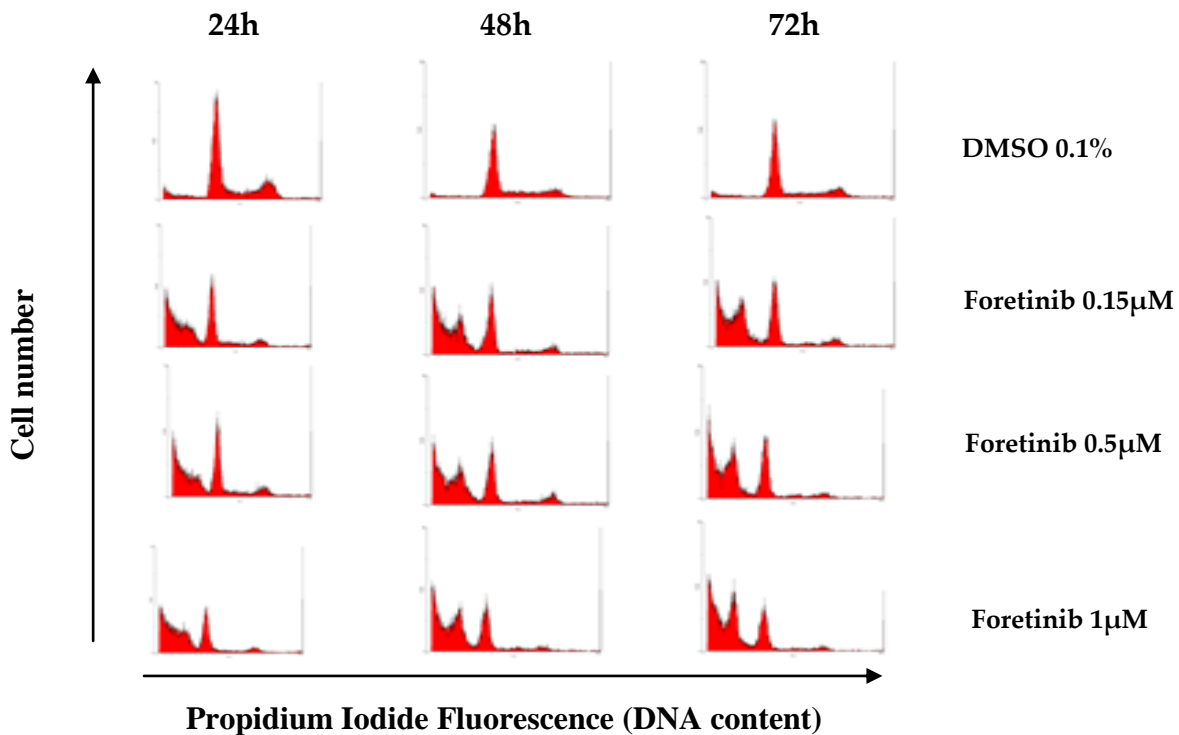


Figure 5.6 Foretinib induces significant changes in the cell cycle profile of the SD – 1 t(9;22) cell line. Incubation with foretinib induces accumulation of cells in the sub – G1 phase (cell death) in a dose- and time – dependent manner. Experiments were performed 3 times, in triplicate. Cell numbers are on y – axis and intensity of Propidium Iodide fluorescence is expressed on the x – axis.

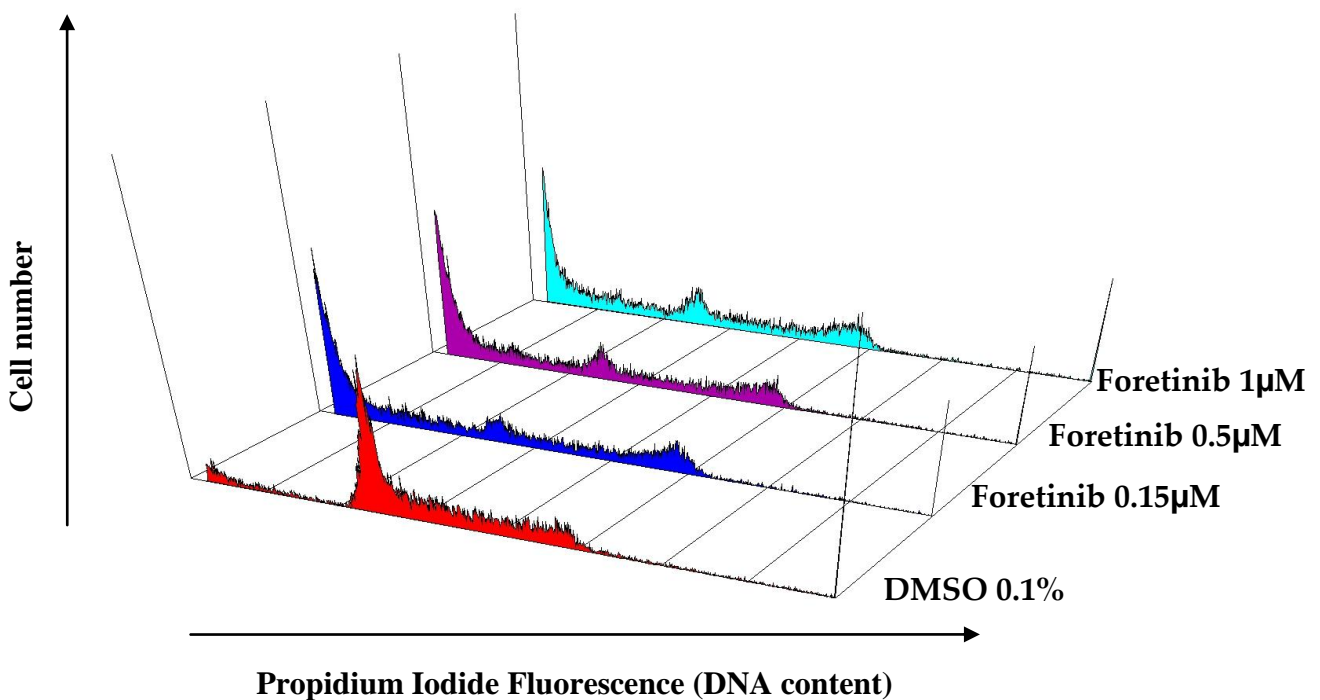


Figure 5.7 Foretinib induces reduction in G1 and S – phase of Nalm 17 cell lines at all concentration by 24h. Foretinib induces significant accumulation of cells in sub – G1 (cell death) by 24h. Experiments were performed 3 time times, in triplicate. Cell numbers are on y – axis and intensity of Propidium Iodide fluorescence is expressed on the x – axis.

The third pattern was observed in the 2 most foretinib – resistant cell lines, Nalm 6 and TOM – 1. Neither of these cell lines exhibited significant cell death in concentrations of foretinib up to 1 μ M (fig 5.8a and 5.9a). Both cell lines demonstrated a reduction in the proportion of cells in G1 with a concomitant accumulation of cells in G2/M. The induction of G2/M arrest was present by 24 hours at all 3 concentrations of foretinib. Subsequent to the cell cycle arrest, a population displaying polyploidy is detectable after 48 hours treatment. Foretinib 1 μ M induced a degree of cell death in Nalm 6, but not TOM – 1.

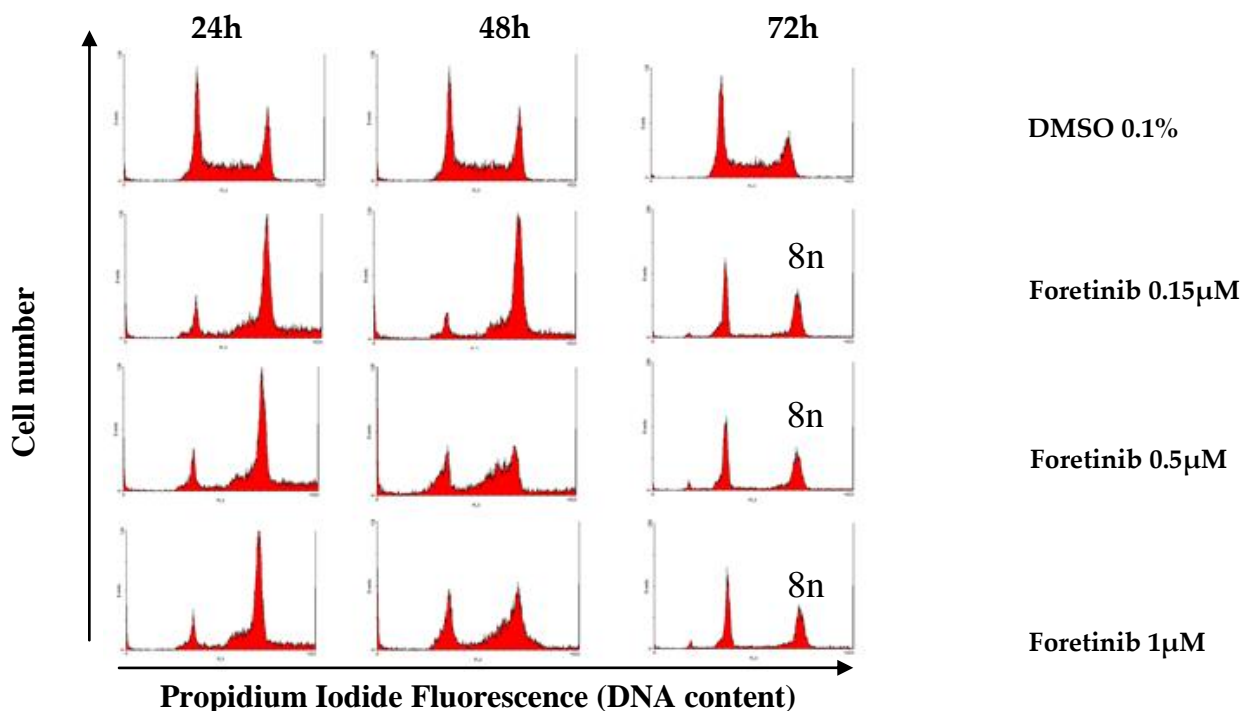


Figure 5.8a

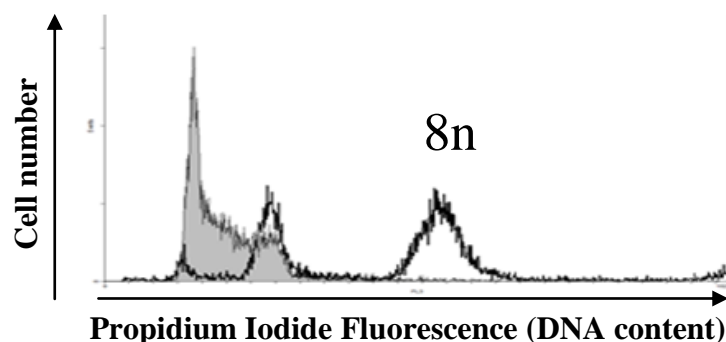


Figure 5.8b

Figure 5.8a Foretinib induced significant alterations in TOM – 1 t(9;22) cell line at all concentrations 0.15 - 1 μ M. (a) Foretinib induced G2/M arrest in all concentrations, but no increase in cells in the sub – G1 phase, at 72h incubation the emergence of a polyploid population (8n) was obvious (b) Foretinib induced the accumulation of a 8n population of cells (polyploidy) in the TOM – 1 cell line after 24h incubation at all concentration. Baseline control cell profile at 24h is described in grey, with alterations in revealed in white.

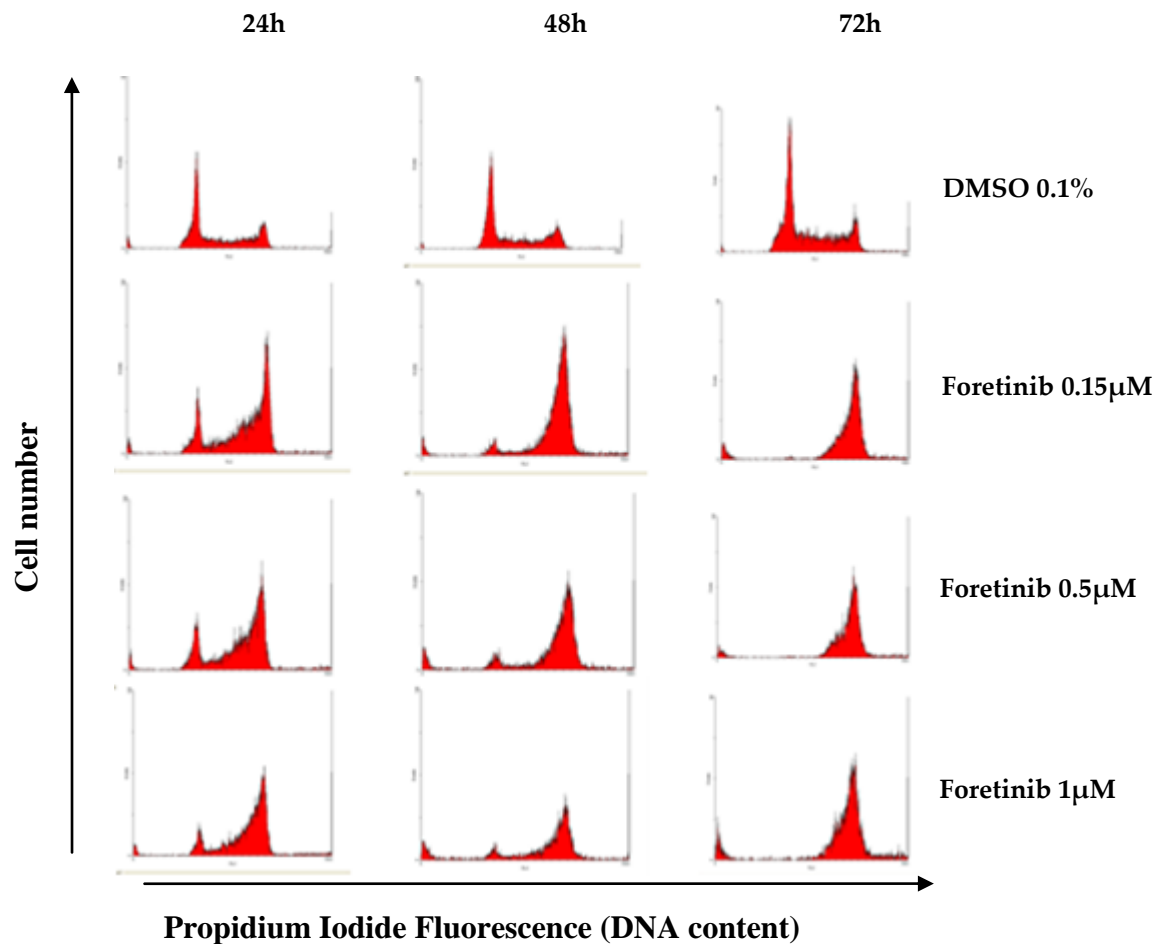


Figure 5.9a

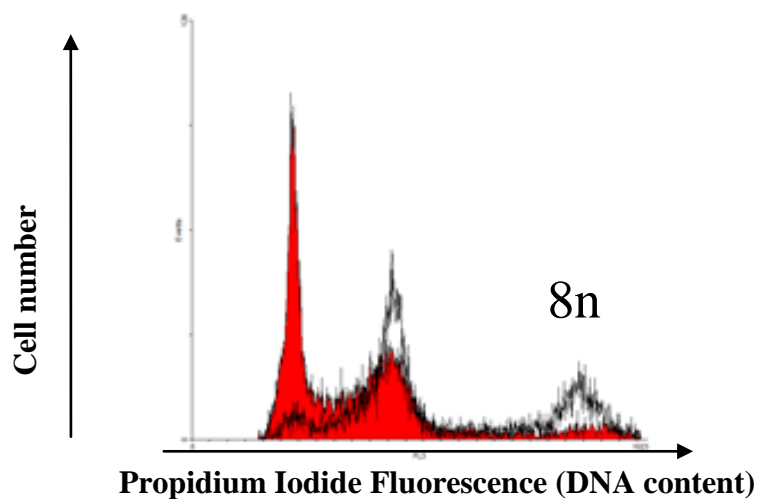


Figure 5.9b

Figure 5.9 Foretinib induced significant alterations in Nalm 6 t(5;12) cell line at all concentrations 0.15 - 1µM. (a) Foretinib induced G2/M arrest in all concentrations, but no increase in cells in the sub - G1 phase **(b)** Foretinib induced the accumulation of a 8n population of cells (polyploidy) in the Nalm 6 cell line after 24h incubation at all concentration. Baseline control cell profile at 24h is described in red, with alterations in revealed in white.

To assess whether doses in excess of the IC₅₀ would induce cell death in these cell lines, Nalm 6 and TOM – 1 were treated with 5 μ M foretinib. Fig 5.10a and 5.10b show the accumulation of cells in sub – G1 at 48 hours in Nalm 6 but not in TOM - 1. By 48 hours, Nalm 6 growth was abrogated while TOM -1 demonstrates persistent accumulation of G2/M.

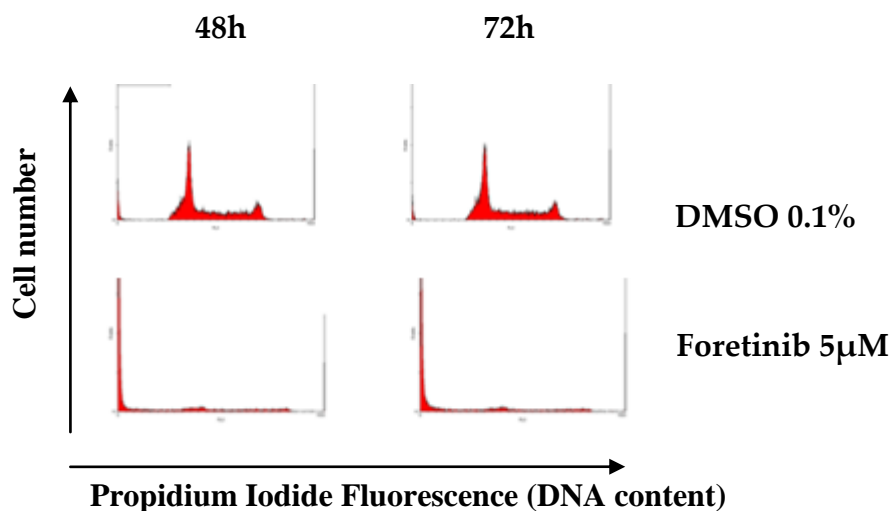


Figure 5.10a

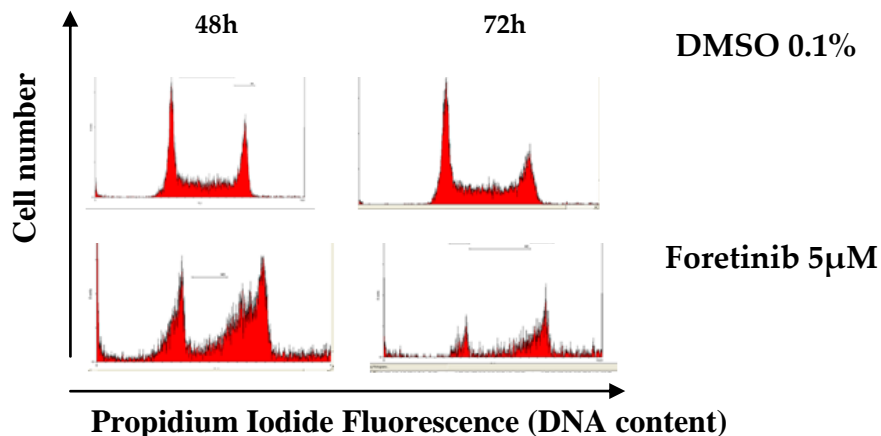


Figure 5.10b

Figure 5.10 Higher doses of foretinib (5 μ M) revealed different impacts on the Nalm 6 and TOM – 1 cell lines. (a) Nalm 6 treated with foretinib 5 μ M demonstrated accumulation of dead cells by 72h. (b) TOM – 1 cells treated with foretinib 5 μ M demonstrated G2/M arrest, but no accumulation of sub – G1 cells by 72h.

In summary, foretinib induces significant alterations in the cell cycle profiles in all cell lines investigated. The induction of cell death was demonstrated in Nalm 17, REH, SD – 1 and SupB15 at nanomolar concentrations, while Nalm 6 required micromolar concentrations.

TOM – 1 exhibited significant alterations the G2/M transition, with associated polyploidy but no cell death. These data are consistent with the dose response curves in 5.2.1. A possible explanation for the heterogeneous patterns of response is foretinib does not work through a single target in the cell lines investigated.

5.3.1.1 Emergent population in Nalm 6 and TOM - 1 confirms polyploidy

To investigate the nature of the polyploid population which was induced by foretinib 1 μ M in Nalm 6 and TOM - 1, the nuclei of these cell lines were stained with DAPI to evaluate nuclear changes after 72 hours of foretinib 1 μ M. Fig 5.11 and 5.12 demonstrate the increase in size and the nuclear aggregations seen in nuclei of both Nalm 6 and TOM – 1, consistent with polyploidy. The DAPI staining is consistent with the increase in nuclear content demonstrated on flow cytometry.

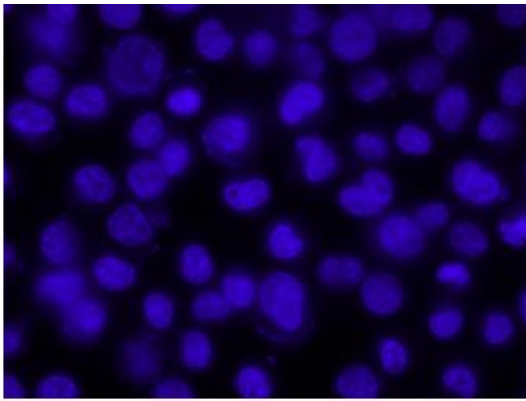


Figure 5.11a

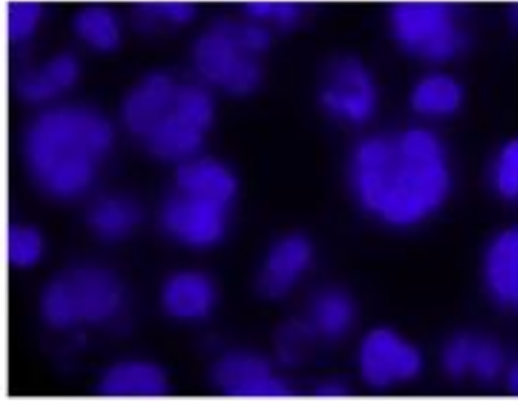


Figure 5.11b

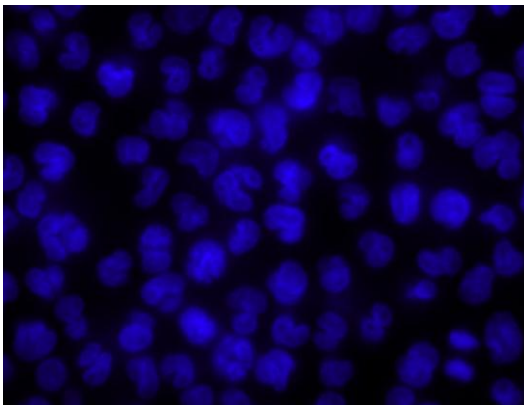


Figure 5.11c

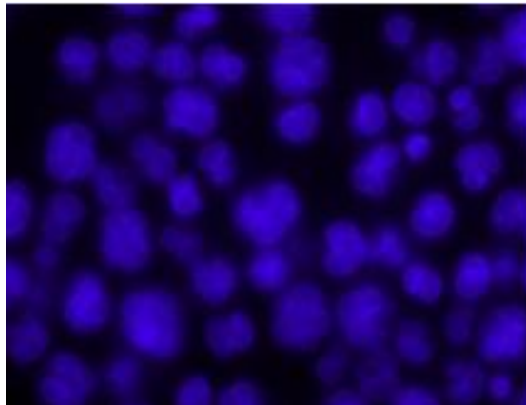


Figure 5.11d

Figure 5.11 Foretinib 1 μ M induces alterations in nuclear size and aggregation in Nalm 6 and TOM – 1 cell lines by 72h. The nuclei increase in size from (a) Nalm 6 control to (b) Nalm 6 Foretinib 1 μ M 72h and (c) TOM -1 control to (d) TOM – 1 1 μ M 72h.

5.3.2. Effects of dovitinib on cell cycle profiles

The effect of dovitinib was studied in the 6 cell lines at a single concentration, 1 μ M, and changes in cell cycle profile assessed at 24, 48 and 72 hours. Significant alterations were observed in the cell cycle profiles of all cell lines by 24 hours. Dovitinib induced significant cell death in Nalm 17, REH, SD – 1 and SupB15 as early as 24 hours (figs 5.12 and 5.13) and progressed in time – dependent manner.

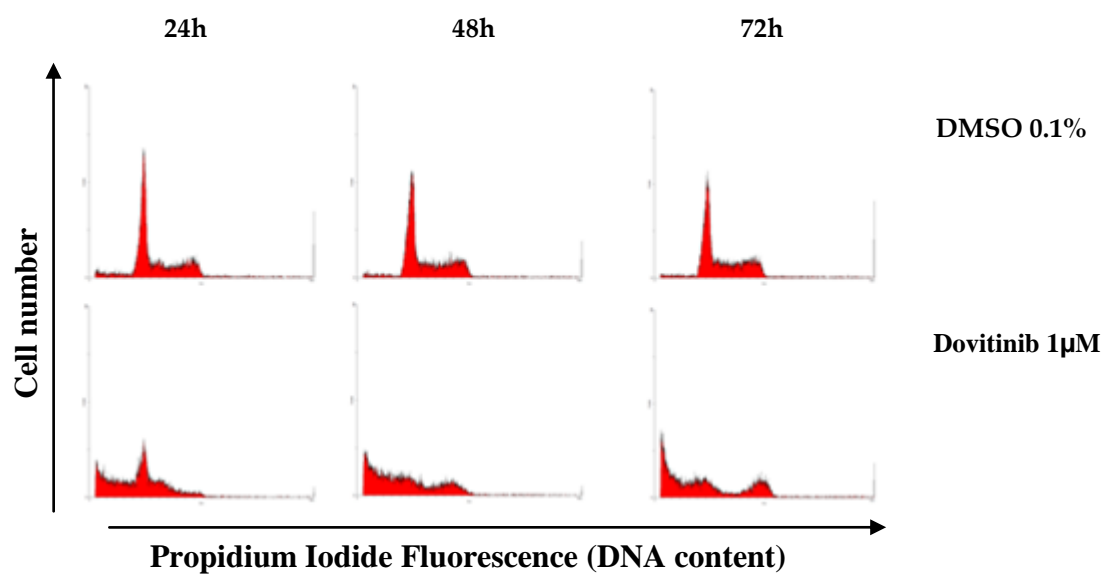


Figure 5.12a

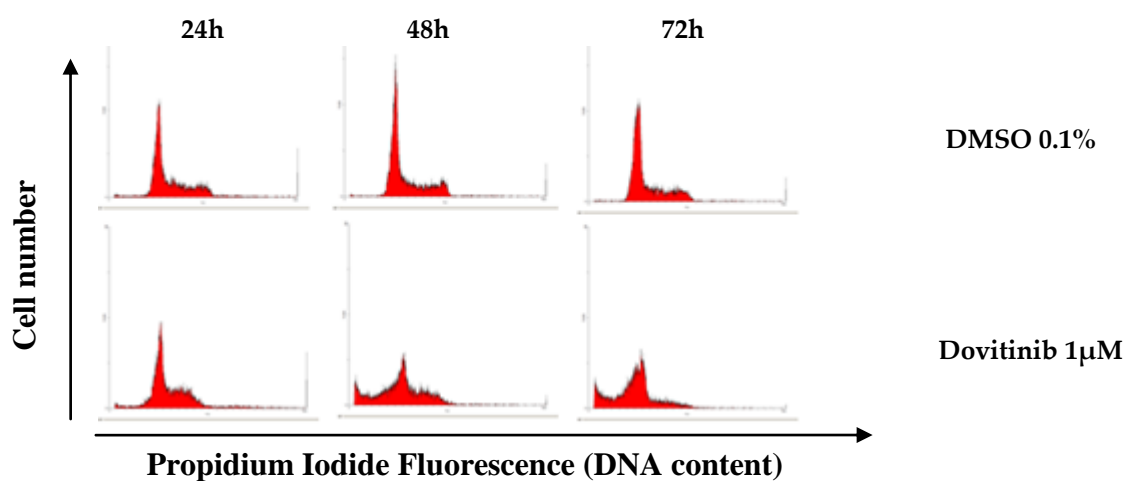


Figure 5.12b

Figure 5.12 Dovitinib induced significant alterations in Nalm 17 and REH cell lines at 1 μ M. (a) Dovitinib induced profound accumulation of dead cells (sub – G1) in (a) Nalm 17 and (b) REH cell lines.

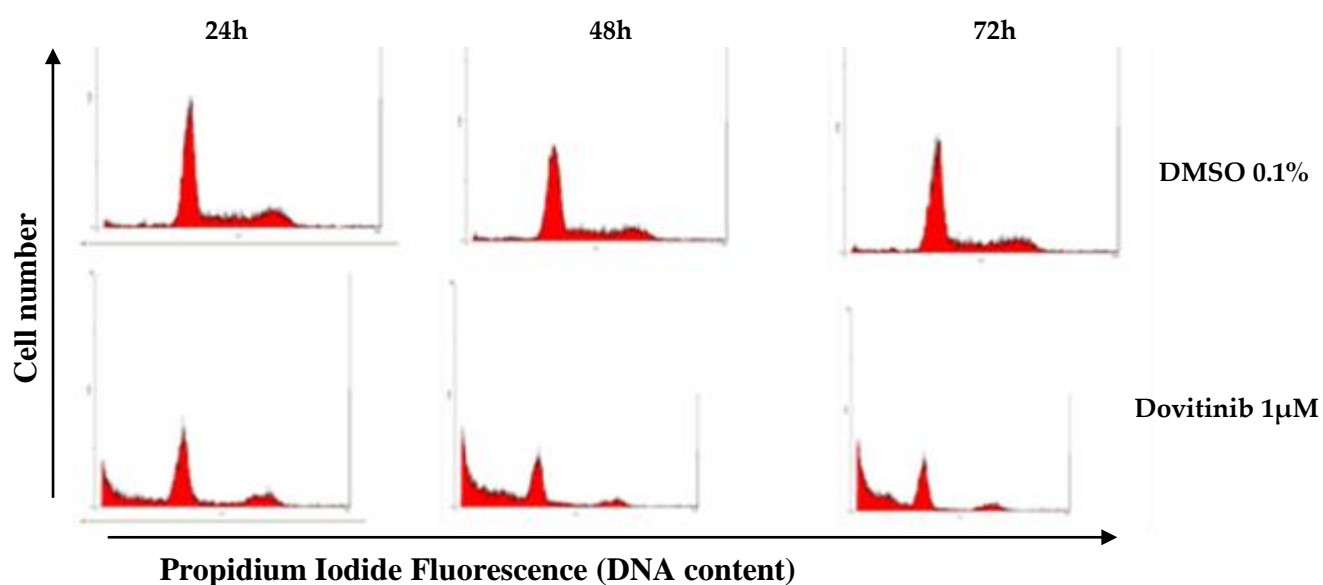


Figure 5.13a

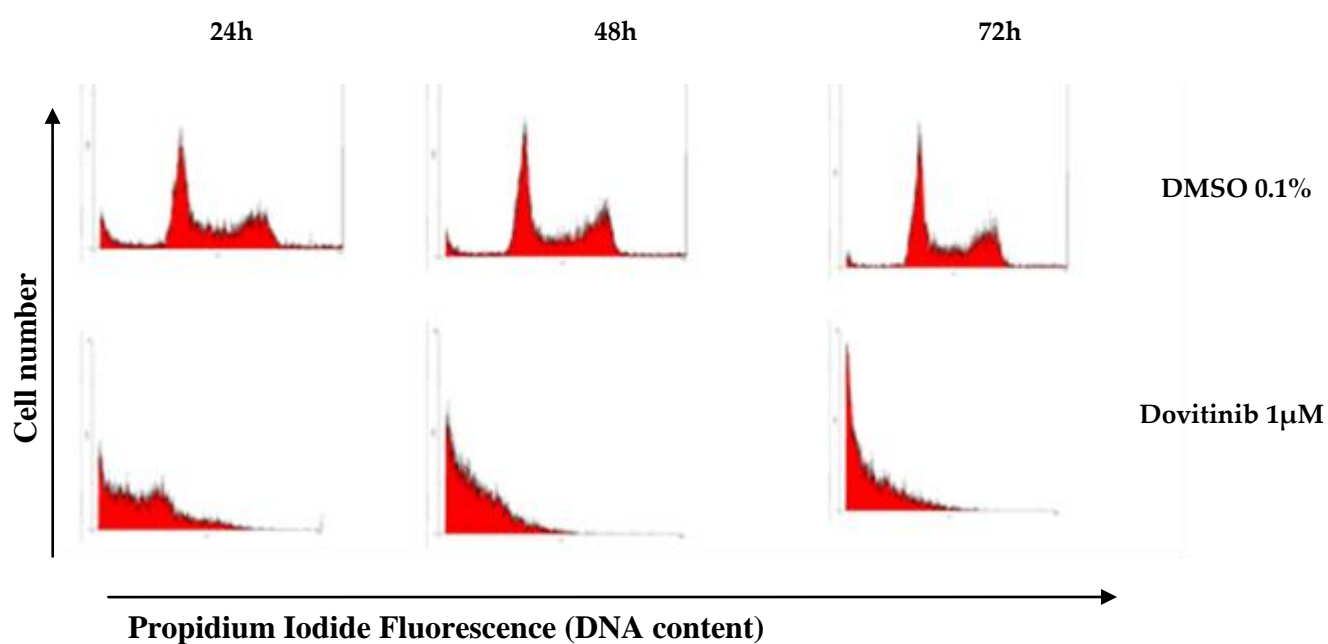


Figure 5.13b

Figure 5.13 Dovitinib induced significant alterations in SD – 1 and SupB15 cell lines at 1μM. (a) Dovitinib induced profound accumulation of dead cells (sub – G1) in (a) SD -1 and (b) SupB15 cell lines.

The G2/M arrest exhibited in response to foretinib was not present in REH or SupB15, but was present in Nalm 6 and TOM -1. Despite the nanomolar IC₅₀ of Nalm 6 and TOM -1, no significant cell death was induced at 1μM. The G2/M arrest induced by dovitinib in Nalm 6 and TOM -1 did not result in the polyploidy noted in response to foretinib (fig 5.15).

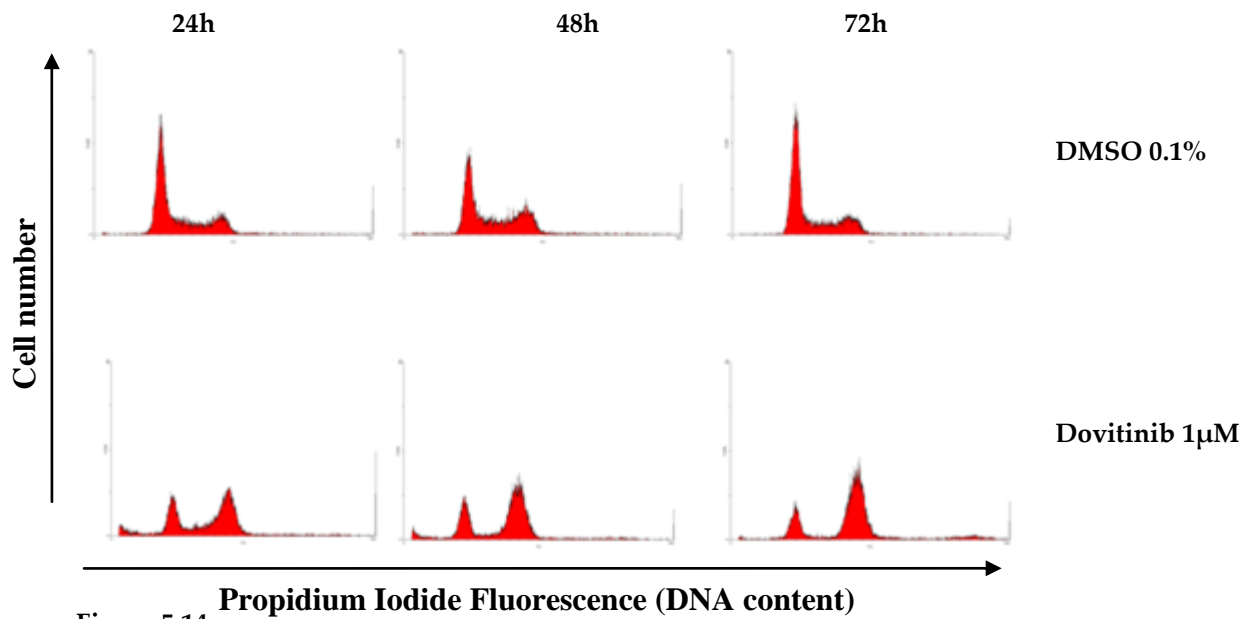


Figure 5.14a

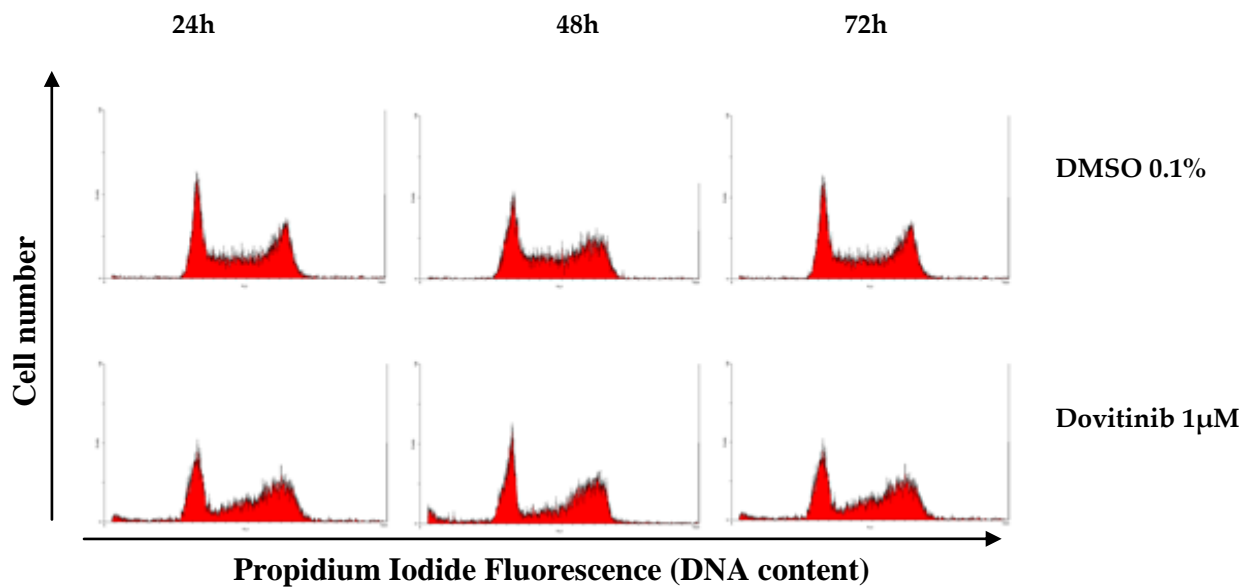


Figure 5.14b

Figure 5.14 Dovitinib induced significant alterations in Nalm 6 t(5;12) and TOM - 1 t(9;22) cell lines at 1 μ M. Dovitinib induced G2/M arrest in (a) Nalm 6 and (b) TOM - 1 by 24h. No increase in cells in the sub - G1 phase was induced in either cell line.

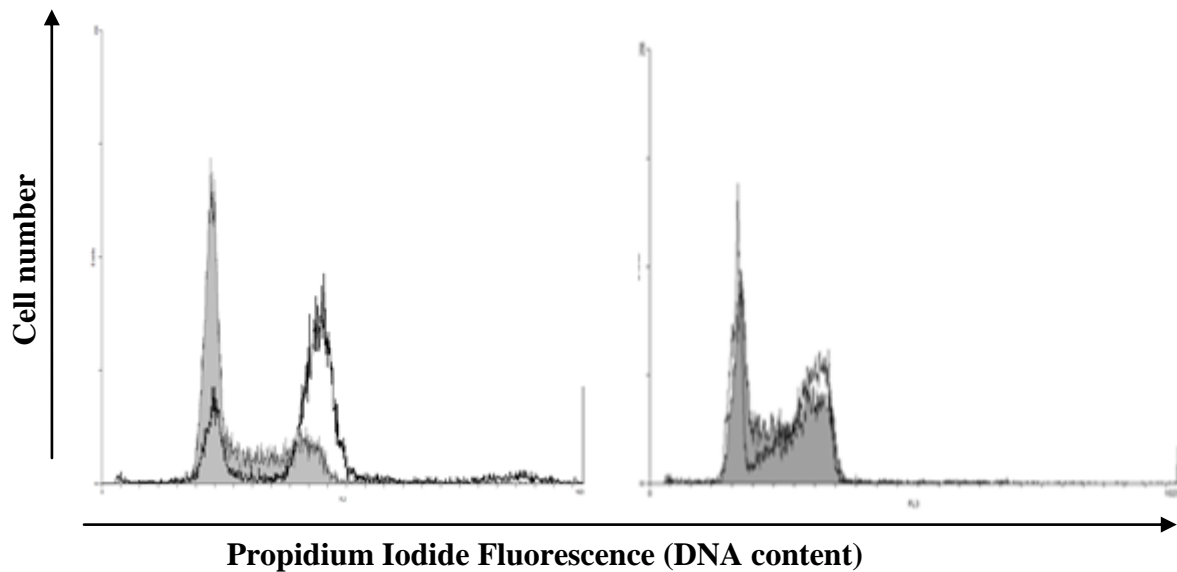


Figure 15.5a

Figure 15.5b

Figure 5.15 Dovitinib does not induce polyploidy in (a) Nalm 6 or (b) TOM – 1 after 72h incubation. Population of cells shaded in grey represent cell line treated with DMSO 0.1% at 24h. Alterations in cell cycle, G2/M, are induced in both cell lines by dovitinib, represented by the white population.

In summary, dovitinib induced profound cell death in 4/6 cell lines and cytostasis in the remaining 2 at a single concentration. These data are consistent with the dose response curves described in 5.2.2, where the Nalm 6 and TOM – 1 cell lines were least sensitive to dovitinib.

5.4. Characterisation of changes in cyclin B1 after foretinib – treatment

Next the effect of foretinib on proteins involved in the G2/M transition was investigated. Normal progression through mitosis requires the accumulation of cyclin B1 and for it to bind to cdc2. The cdc2 – cyclin B1 complex is involved in early mitotic events, such as chromosomal condensation, dissolution of the nuclear envelope and assembly of spindle poles (421). The G1, S and G2/M checkpoints of the cell cycle are governed by p53 and its downstream effector p21, the universal cyclin – dependent kinase inhibitor. The responses of cyclin B1, p53 and p21 were characterised by Western Blot to investigate the alterations induced by foretinib induced in cell cycle.

Cell lines were treated with foretinib 1 μ M and 30 μ g of cell lysate subjected to SDS – PAGE, followed by immunoblotting for cyclin B1 and p53.

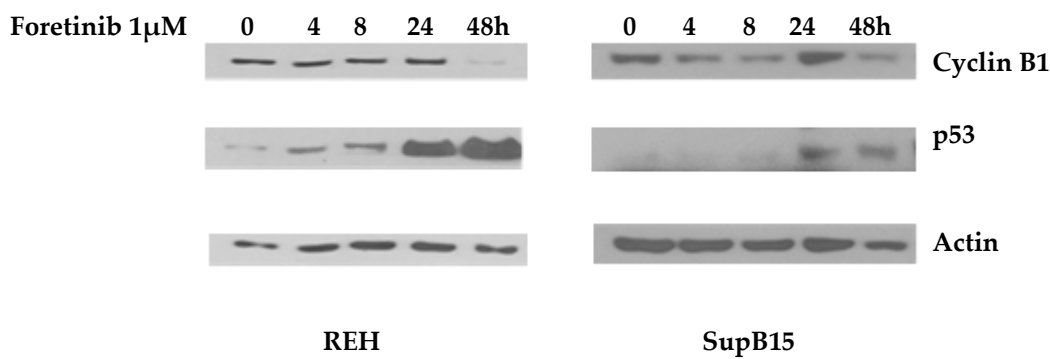


Figure 5.16 Foretinib 1 μ M induces the reduction in cyclin B1 and variable p53 accumulation in the sensitive cell lines, REH and SupB15. Western Blot analysis demonstrated foretinib induced the accumulation of p53 and decrease in cyclin B1 in a time – dependent manner in REH and SupB15. Both cell lines demonstrated G2/M arrest at 24h, the peak of cyclin B1 expression.

Fig 5.16 shows changes in the expression of cyclin B1 in the 2 cell lines, REH and SupB15, following treatment with foretinib, both of which displayed G2/M arrest followed by cell death in the cell cycle profile experiments. Foretinib induces a reduction in cyclin B1 expression in SupB15 as early as 4 hours and expression continues below baseline at 48 hours. The expression of cyclin B1 in REH remains stable until 24 hours thereafter it decreases significantly. In both cell lines foretinib significantly induced the accumulation of total p53 by 24 hours. The increase in p53 correlated with the decreased expression of cyclin B1.

In the 2 cell lines which did not demonstrate G2/M arrest, Nalm 17 and SD – 1, cyclin B1 expression was variable. In Nalm 17, cyclin B1 expression did not alter with foretinib treatment up to 48 hours (fig 5.17). The accumulation of p53 in the Nalm 17 cell line was delayed until 48 hours. SD – 1 demonstrated a rapid reduction in expression of cyclin B1 by 8 hours of treatment, with disappearance by 48 hours. SD – 1 did not exhibit a significant accumulation of p53 in response to foretinib. Maximal p53 expression was evident by 24 hours, which coincided with the degradation of cyclin B1. The level of total p53 decreased thereafter.

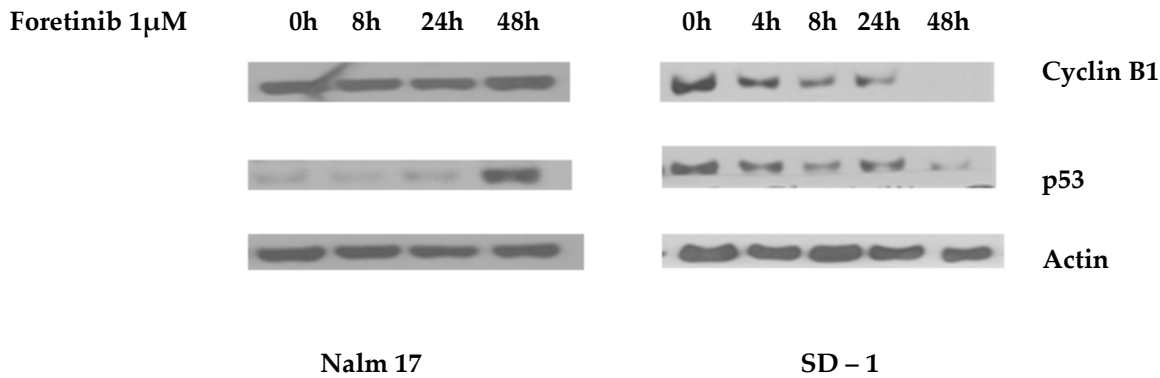


Figure 5.17 Foretinib 1μM induces the variable responses in cyclin B1 and p53 accumulation in the sensitive cell lines, Nalm 17 and SD -1. Western Blot analysis reveals foretinib induced accumulation of p53 in Nalm 17 at 48h, but not in SD -1. Neither cell line demonstrated G2/M arrest after incubation with foretinib.

The cell lines most resistant to foretinib, Nalm 6 and TOM-1, both demonstrated an initial increase in cyclin B1, with maximal expression present at 24 hours (fig 5.18). Subsequently, the expression decreased below baseline expression by 72 hours. Both Nalm 6 and TOM -1 exhibited marked accumulation of p53 by 24 hours. Nalm 6 exhibited a subsequent reduction in intensity with a return to just above baseline levels at 72 hours. The expression of p53 in TOM -1 continued to increase in intensity until 72 hours.

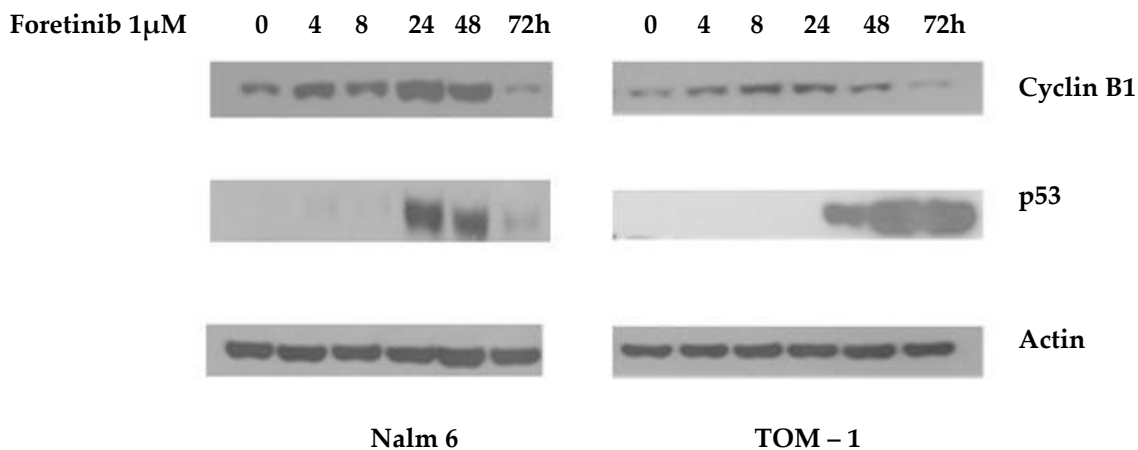


Figure 5.18 Foretinib 1μM induces the accumulation and subsequent reduction in cyclinB1 Nalm6 and TOM -1. Western Blot analysis demonstrated foretinib induced G2/M arrest in both cell lines. Significant p53 accumulation was present in both cell lines in response to foretinib.

Western Blots were performed to assess whether the accumulation of p53 lead to an increase in the downstream effector p21. Nalm 6, Nalm 17, REH and TOM -1 (all which displayed significant accumulation of p53) were treated with 1 μ M foretinib and cells were harvested after 24, 48 and 72 hours of treatment. Nalm 6, REH and TOM-1 showed induction of p21 after treatment with foretinib, but Nalm 17 did not.

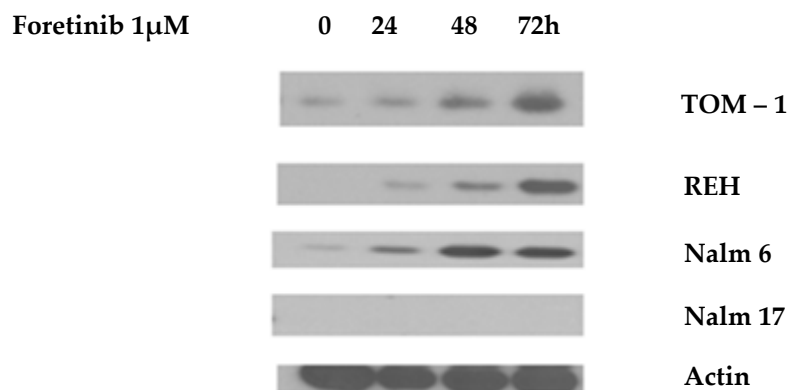


Figure 5.19 Foretinib treatment induces the expression of p21 in a time dependent manner in the cell lines which demonstrate G2/M arrest. Western Blot analysis reveals the foretinib – sensitive cell lines Nalm 17 and REH demonstrated differing patterns of p21 accumulation on response to treatment. Both Nalm 6 and TOM – 1 demonstrated obvious accumulation of p21 on treatment, despite the lack of cell death at the same dose.

5.5. Accumulation of p53 is not due to foretinib – induced DNA damage

To exclude DNA damage as a mechanism of p53 accumulation, γ H2AX foci, a marker of DNA double stranded breaks (DSB), were counted after immunofluorescence staining. This was evaluated in the Nalm 17 cell line, which accumulated p53 by 48 hours, as the rate of proliferation was sufficiently slow to allow visualisation of the γ H2AX foci. Nalm 17 cells were exposed to 3 conditions: (i) untreated, (ii) irradiation with 2Gy IR to induce DNA DSB to act as positive controls and harvested after 2h or (iii) treated with foretinib 1 μ M for 24h. Cells were prepared as described in methods and materials (section 2.15). One hundred cells from 3 separate wells were counted for each condition. The degree of DSB, reflected as the percentage of cells with greater than 10 γ H2AX foci present assessed. The experiment was performed twice. Fig 5.20 shows the increase in γ H2AX foci visualised after IR in

comparison with the baseline Nalm 17 cells. The fraction of cells that exhibited >10 foci increased from 14% (± 4.3) to 89% (± 9.2) ($p = 0.00001$) after IR – induced DNA damage.

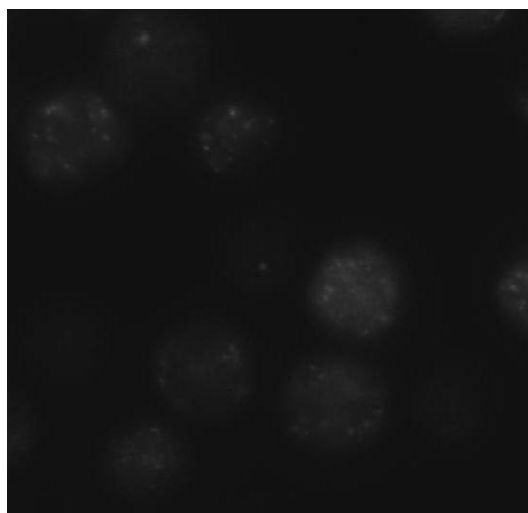


Figure 5.20a

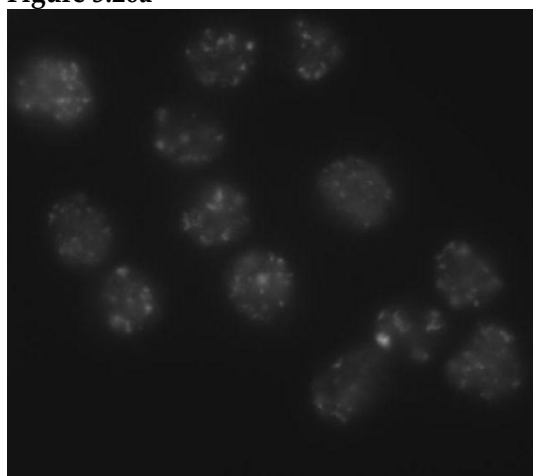


Figure 5.20b

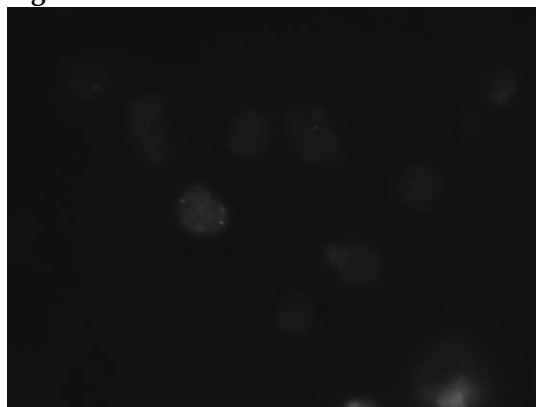


Figure 5.20c

Figure 5.20 Visualisation of γ H2AX foci reveals accumulation of p53 in response to foretinib is not due to DNA DSB. Foci are demonstrated in (a) the untreated Nalm 17 cell line. (b) IR induced significant increases in the number of foci in Nalm 17 cells exposed to 2Gy irradiation. (c) No increase in γ H2AX foci is evident in the Nalm 17 cells treated with foretinib 1 μ M at 24h.

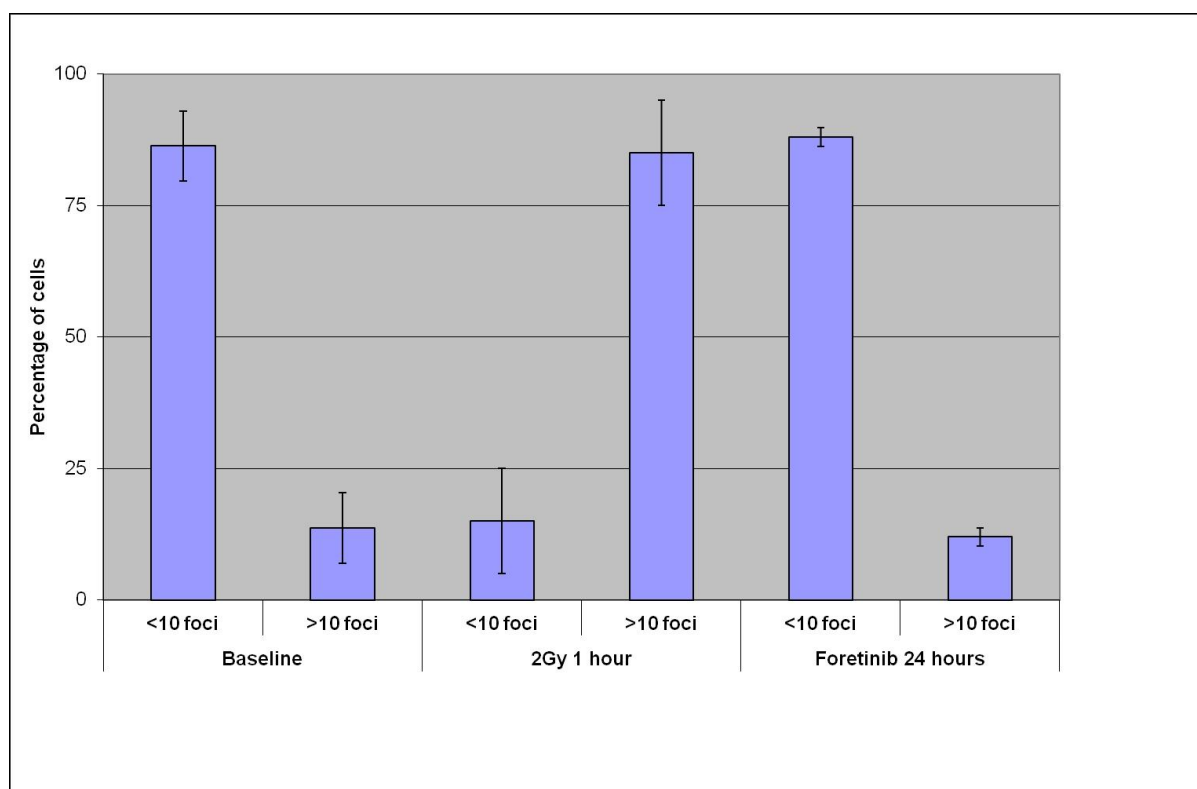


Figure 5.21 The number of cells with greater than 10 γ H2AX foci increases after exposure to 2Gy IR, but not foretinib 1 μ M 24h. The cell line, Nalm 17, revealed a significant increase in the number of γ H2AX foci after 2Gy irradiation, but not after treatment with foretinib. The experiment data presented is the mean of 2 experiments, performed in triplicate; error bars are standard deviation.

| | Baseline | | 2Gy 1h | | Foretinib 24h | |
|--------------------|----------|-----|--------|-----|---------------|-----|
| γ H2AX foci | <10 | >10 | <10 | >10 | <10 | >10 |
| Percentage | 86 | 14 | 11 | 89 | 86 | 15 |
| Std dev | 4.3 | 4.3 | 9.2 | 9.2 | 3.5 | 3.5 |

Table 5.2 Significant increases in γ H2AX foci were induced by IR but not foretinib. Cells with greater than 10 foci increased from 14% to 89% after IR exposure ($p = 0.00001$) and 14% to 15% after foretinib ($p = 0.947$)

There was no significant increase in the proportion of cells with >10 foci after 24 hours treatment with foretinib (14% (± 4.3) to 15% (± 3.5), $p = 0.947$). The lack of accumulation of γ H2AX foci excluded induction of DNA damage by foretinib as a mechanism of p53 accumulation.

5.6. Foretinib inhibits the pro – survival Akt pathway

The Akt pathway regulates anti – apoptotic and pro – survival functions. To assess whether foretinib inhibited the Akt axis, the Nalm and REH 17 cell lines, which are constitutively Akt phosphorylated, were treated with foretinib. Cells were treated with foretinib at IC₅₀ (Nalm 17 0.43μM and REH 0.19μM) and 1μM and harvested at 24h. A reduction in the level of phosphorylation was evident, which was not associated with a reduction in total Akt. This reduction in p-Akt preceded the accumulation of p53.

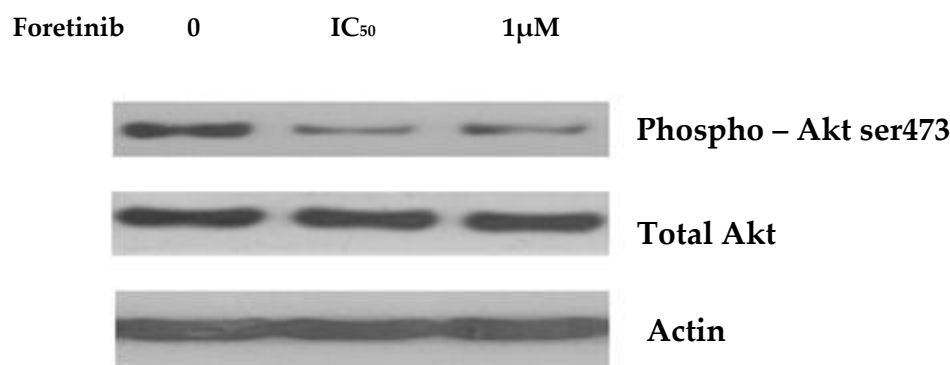


Figure 5.22a

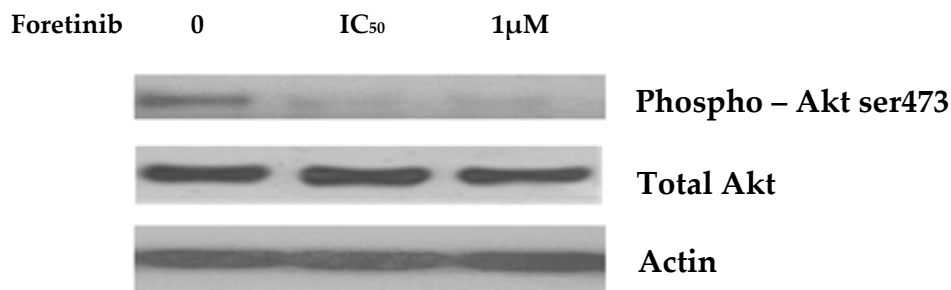


Figure 5.22b

Figure 5.22 Foretinib induces alteration in the p – Akt status of the constitutively activated cell lines Nalm 17 and REH. Reduction in p – Akt is demonstrated at both IC₅₀ and 1μM in (a) Nalm 17 and (b) REH cell lines.

In summary, foretinib induced changes in the cell cycle profiles of all cell lines. These alterations were reflected in differing patterns of accumulation of cyclinB1, p53 and p21. Foretinib leads to the reduction of Akt phosphorylation at IC₅₀ concentrations.

5.7. TKIs mediate anti – leukaemic effect via apoptosis

Next, the mechanism of cell death identified in the cell cycle profiles was studied in cell lines after treatment with foretinib and dovitinib.

5.7.1. Foretinib induces apoptosis in cell lines

The ability of foretinib to induce apoptosis in the t(9;22) cell lines SD – 1 and SupB15 was evaluated by assessing for DNA fragmentation (354) (section 2.14). Cells were treated with foretinib 1 μ M and harvested at 24, 48 and 72 hours. Apoptosis was confirmed by the presence of 100bp DNA fragments (fig 5.23).

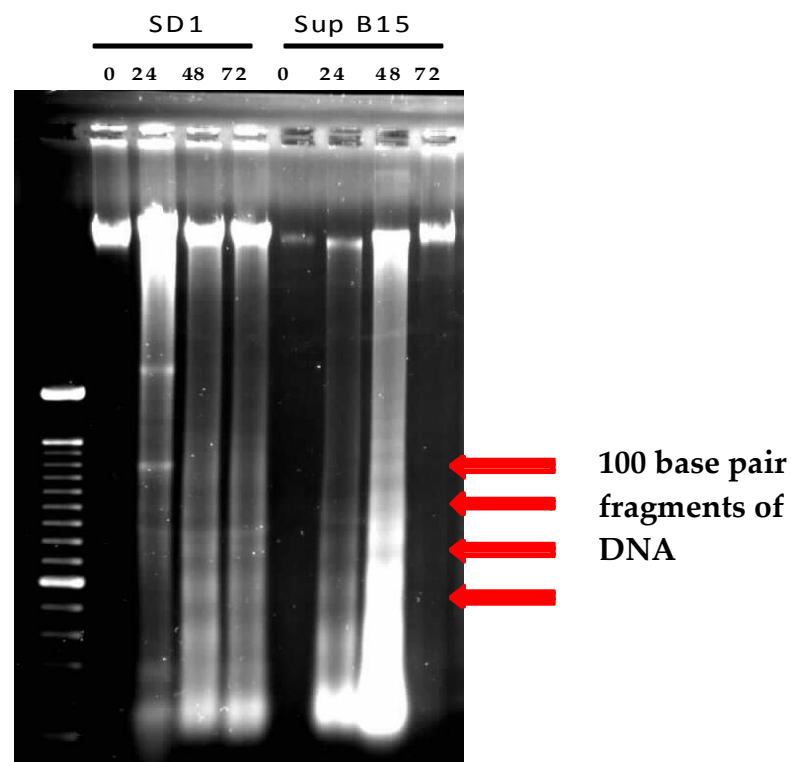


Figure 5.23 Foretinib 1 μ M induces apoptotic DNA fragmentation in SD – 1 and SupB15. Apoptosis is demonstrated by the induction of the 100bp DNA fragments after incubation with foretinib.

To investigate whether the intrinsic or extrinsic apoptotic pathways were activated immunoblotting for PARP – 1 cleavage was characterised in cell lines treated with foretinib. Cells were incubated with foretinib 1 μ M and harvested at 24, 48 and 72 hours. The cleavage of the PARP -1 protein into its 89kDa and 116kDa fragments confirmed that the cell death

was induced by intrinsic pathway apoptosis. Apoptosis was induced in Nalm 17, REH, SD – 1 and SupB15, while neither Nalm 6 nor TOM -1 demonstrated cleavage of PARP – 1 protein (fig 5.24a and b).

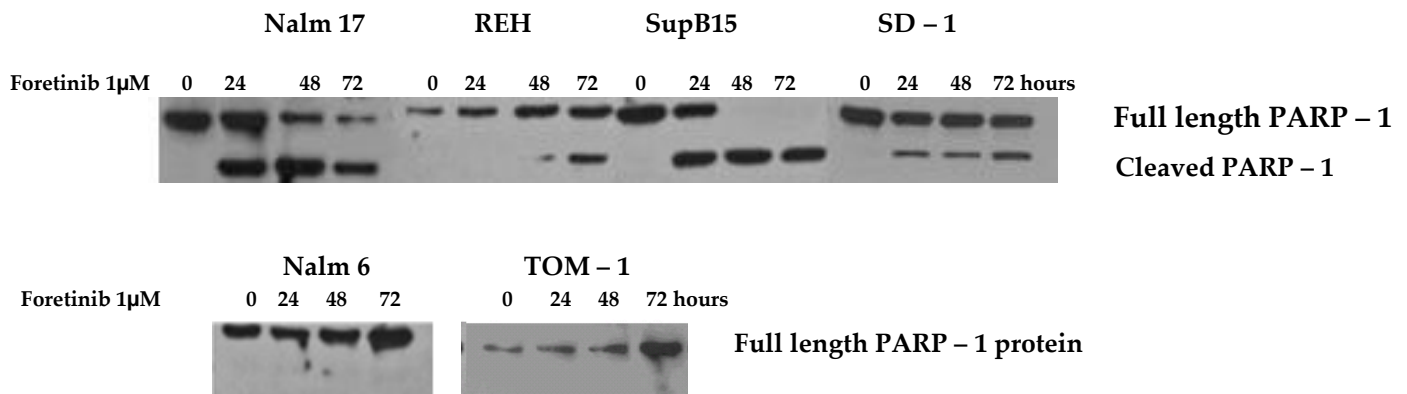


Figure 5.24a

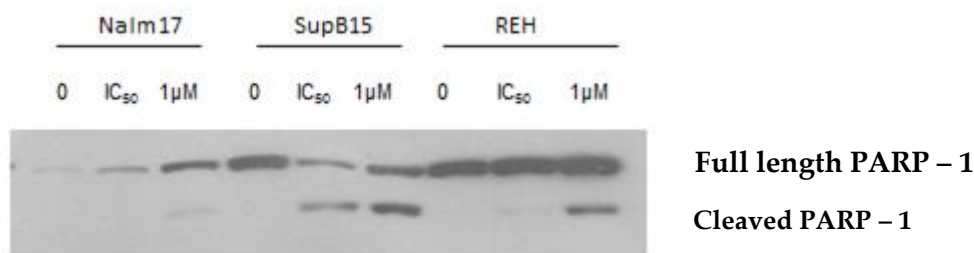


Figure 5.24b

Figure 5.24 Foretinib induced PARP – 1 cleavage in pre – B ALL cell lines. (a) Foretinib 1 μM induces the intrinsic apoptotic pathway in Nalm 17, REH, SupB15 and SD – 1 cell lines. No evidence of intrinsic apoptosis was observed in the Nalm 6 and TOM -1 cell lines. These findings correlate with alterations noted in the cell cycle profiles. (b) PARP -1 cleavage is induced in the sensitive cell lines Nalm 17, REH and SupB15 at lower doses and shorter time courses.

To investigate whether IC₅₀ concentrations of foretinib could induce apoptosis, the cell lines Nalm 17, REH and SupB15 were treated with concentrations of foretinib for 24 hours and then assessed for PARP-1 cleavage by immunoblotting (fig 5.24b). REH and SupB15 demonstrated foretinib – induced apoptosis at IC₅₀ concentrations by 24 hours however Nalm 17 did not demonstrate cleavage at the lower dose at the earlier time course.

5.7.2. Dovitinib induces apoptosis in SupB15 t(9;22) cell line

To assess the mechanism of cell death in response to dovitinib, a dose response course was performed on the cell line SupB15. Cells were harvested after 4 hours incubation with dovitinib 0.01 – 1 μ M and immunoblotted for cleavage of PARP – 1 protein. The dose response course in SupB15 cells reveals PARP – 1 cleavage was present at concentrations as low as 0.01 μ M after 4 hours.

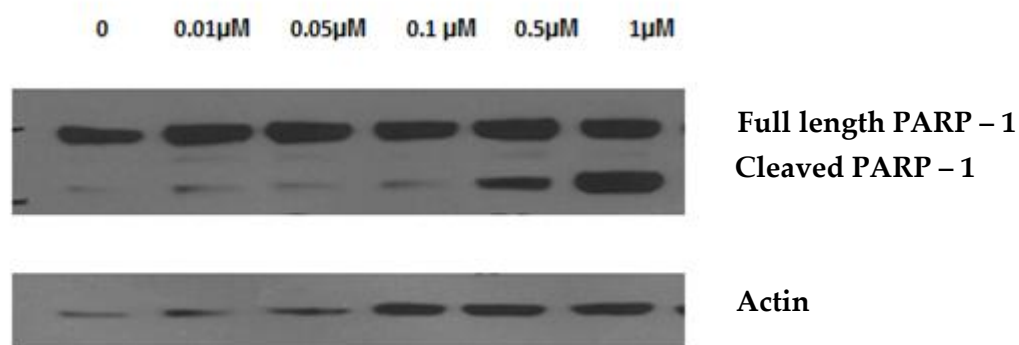


Figure 5.25 Dovitinib dose course in the SupB15 t(9;22) cell line demonstrated cleavage of PARP – 1 protein. Western Blot analysis demonstrates apoptosis was evident at 4h in doses as low as 0.01 μ M, by the cleavage of PARP - 1. The amount of apoptosis increased in a dose – dependent manner.

In summary both foretinib and dovitinib induces apoptotic cell death in childhood ALL cell lines at nanomolar concentrations.

5.8. TKIs demonstrate synergy when combined with conventional chemotherapy

Because TKIs would not be used as monotherapy in clinical practice the question whether the drug could sensitise ALL cells to conventional chemotherapeutic agents used in the induction and maintenance phases of current ALL protocols was assessed. The agents investigated were the steroid dexamethasone, the anti – metabolites methotrexate, cytarabine and fludarabine, DNA – damaging agents (doxorubicin and mitoxantrone) and the mitotic spindle poison, vincristine. While fludarabine and mitoxantrone are not used in frontline therapy, they are both components in relapse and refractory chemotherapy protocols; therefore, modelling interactions may yield clinically significant information.

Foretinib was tested in combination with all 7 chemotherapeutic agents, while dovitinib was tested with the agents, dexamethasone, doxorubicin and vincristine, which are used in remission – induction regimens.

Interactions between the TKIs and chemotherapy were assessed using the Median Effect model of drug – dose effect, as described by Chou – Talalay (351, 352). Combination indices (CI) were calculated using the Calcosyn (BIOSOFT, Cambridge, UK) algorithm and the combinations were evaluated as synergistic, additive or antagonistic. A CI < 1 indicated synergy, CI = 1 indicated additivity and a CI >1 indicated antagonistic effects.

5.8.1. Foretinib combinations with cytotoxics demonstrate synergy

To assess the effect of combining TKIs with chemotherapy, dose response curves for each cell line were generated for: (i) foretinib/dovitinib alone, (ii) conventional chemotherapy alone and (iii) the combination of a fixed sub – IC₅₀ dose of foretinib/dovitinib with an increasing dose of chemotherapy.

A concentration for each cell line was established by a dose-finding experiment which would reduce cell viability but no more than 50%. Cell lines which exhibited a nanomolar IC₅₀ were treated with dose range 0.1 – 0.5µM to establish a suitable concentration. Nalm 6 and TOM – 1 were treated with foretinib 0.1 - 5µM. Fig 5.26a and 5.26b show the dose response curves for the cell lines.

The foretinib concentrations for co-treatment were 0.125µM for SD – 1 and SupB15, 0.175µM for REH and 0.25µM for Nalm 6, Nalm 17 and TOM-1.

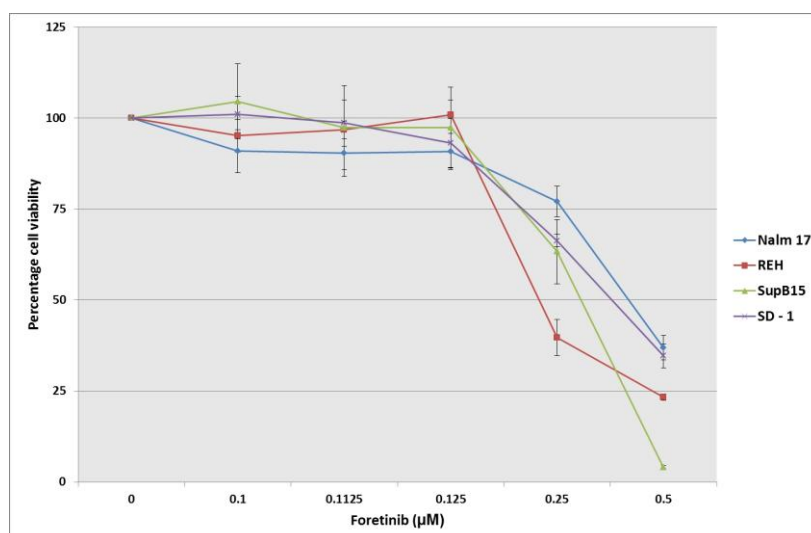


Figure 5.26a

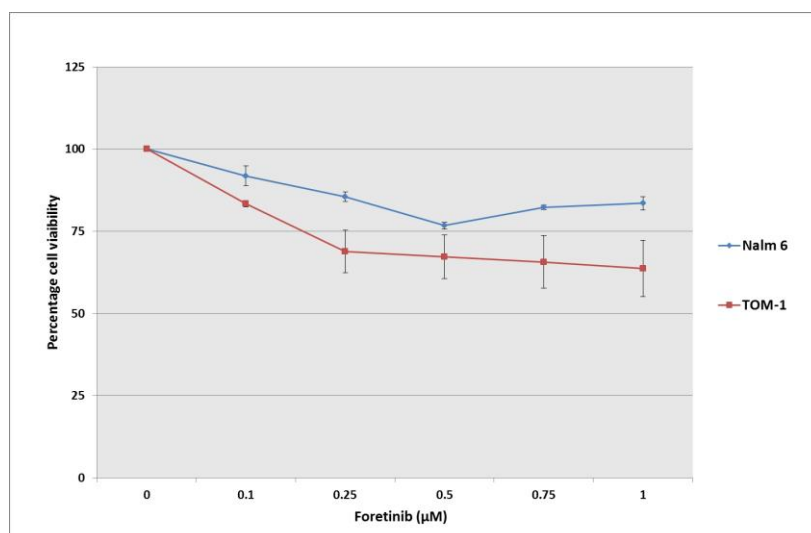


Figure 5.26b

Figure 5.26 Dose finding response curves for the combination therapy for cell lines (a) Nalm 17, REH, SupB15, SD – 1 and (b) Nalm 6 and TOM – 1. Dose response curves were repeated to determine a dose at which the TKI induced less than a 50% reduction of cell viability.

Dose response curves were subsequently generated for serial dilutions of chemotherapy alone and in combination with fixed dose of foretinib.

5.8.1.1 Foretinib in combination with dexamethasone

Table 5.3 illustrates foretinib was able to sensitise all 6 lines to dexamethasone, with CI <1 in all cell lines. The cell lines Nalm 6, REH and SD – 1 demonstrated resistance to dexamethasone monotherapy in concentrations up to 10 μ M (fig 5.27a - c). Antagonistic interactions were observed in Nalm 6, SD – 1 and SupB15, but only at combined concentrations of foretinib and dexamethasone which had already reduced cell viability greater than 50%.

The most significant results were the sensitisation of the steroid – resistant cell lines Nalm 6, REH and SD – 1 to low concentrations of DXM, 0.01 - 1 μ M. Marked changes in cell viability were observed Nalm 17, REH and SupB15, with the combination of foretinib and 0.001 μ M dexamethasone reducing cell viability greater than 50% (fig 5.27).

| Drug | | Nalm 6 | Nalm17 | REH | SD-1 | Sup B15 | TOM-1 |
|-------------------|-------|-----------------------------|--------|-------|-------|---------|-------|
| | | Combination index | | | | | |
| | | Foretinib (μM) | | | | | |
| | | 0.25 | 0.25 | 0.175 | 0.125 | 0.125 | 0.25 |
| Dexamethasone | 0.001 | 0.1 | 0.6 | 0.7 | 0.4 | 0.4 | 7.9 |
| (μM) | 0.01 | 0.1 | 0.5 | 0.7 | 0.3 | 0.6 | 0.0 |
| | 0.1 | 0.1 | 0.4 | 0.7 | 0.3 | 4.6 | 0.1 |
| | 1 | 0.8 | 0.3 | 0.7 | 0.5 | 44.4 | 0.1 |
| | 10 | 6.8 | 0.3 | 0.7 | 2.2 | 442.4 | 0.1 |
| | | Interaction | | | | | |
| | | Foretinib (μM) | | | | | |
| | | 0.25 | 0.25 | 0.175 | 0.125 | 0.125 | 0.25 |
| Dexamethasone | 0.001 | +++++ | +++ | ++ | +++ | +++ | ---- |
| (μM) | 0.01 | +++++ | +++ | ++ | +++ | +++ | +++++ |
| | 0.1 | ++++ | +++ | ++ | +++ | ---- | ++++ |
| | 1 | ++ | +++ | ++ | +++ | ---- | ++++ |
| | 10 | ---- | +++ | ++ | --- | ----- | ++++ |

Key:




| | |
|---|--------------------------|
|  | Synergistic interaction |
|  | Antagonistic interaction |
|  | Additive interaction |

Table 5.3 Summary of the responses of combination therapy for foretinib and dexamethasone described as Combination Indices. Predominant interactions between foretinib and dexamethasone were synergistic in the 6 cell lines.

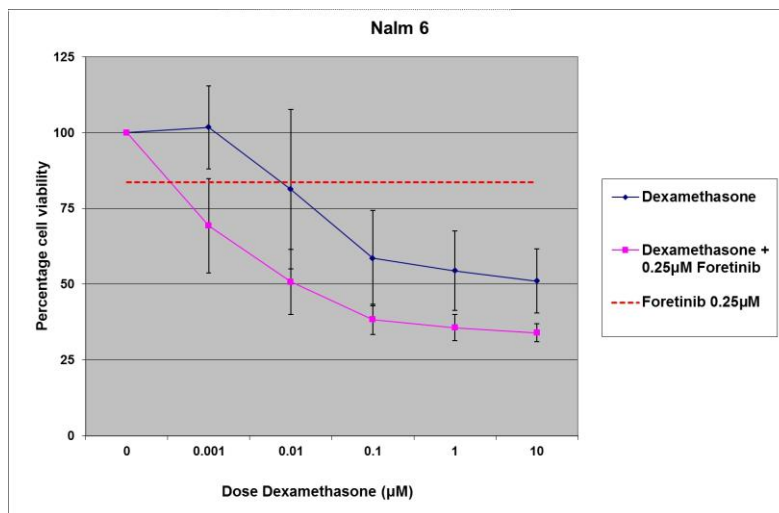


Figure 5.27a

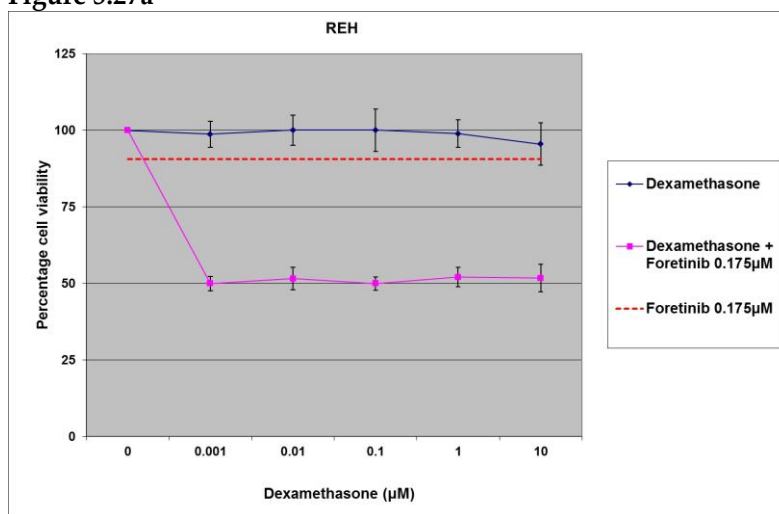


Figure 5.27b

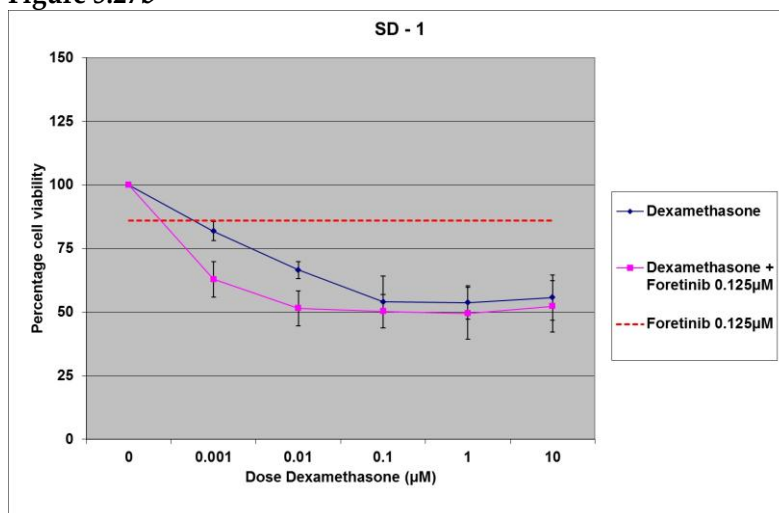


Figure 5.27c

Figure 5.27 Foretinib sensitises the steroid – resistant cell lines Nalm 6, REH and SD -1. The red line demonstrates the percentage cell viability induced by foretinib alone. For combinations to be synergistic, the reduction in viability needs to be below the chemotherapy alone and the red line. Steroid resistant cell lines (a) Nalm 6, (b) REH and (c) SD – 1 are sensitised to DXM by foretinib. Points represent the mean of 3 experiments performed in triplicate, with error bars representing standard deviation.

5.8.1.2 Foretinib in combination with the anti – metabolites

As a class, anti – metabolite monotherapy, demonstrated significant anti – leukaemic activity. Only SD – 1 displayed resistance to any of the anti – metabolic chemotherapies, with cell viability remaining at greater than 50% in response to fludarabine 10 μ M. The impact of concurrent treatment with foretinib and the anti - metabolites was predominantly synergistic (CI<1) (tables 5.4a and b). The exceptions were the combination with cytarabine in REH and with methotrexate in SD – 1. The effects of concurrent treatment did not appear to be class – dependent, as differences in quality of interaction were drug – specific.

SD – 1 displayed disparate responses to each of the drugs (see fig 5.28a – c). Foretinib sensitised the fludarabine – resistant cell line to 10 μ M and displayed synergy with cytarabine at concentrations 0.001 – 0.1 μ M. However, SD – 1 demonstrated no effect on the sensitivity to methotrexate at all dose levels.

| Drug | | Nalm 6 | Nalm17 | REH | SD-1 | Sup B15 | TOM-1 |
|------------|-------|-------------------|--------|-------|-------|---------|-------|
| | | Combination index | | | | | |
| | | Foretinib (μM) | | | | | |
| | | 0.25 | 0.25 | 0.175 | 0.125 | 0.125 | 0.25 |
| Cytarabine | 0.001 | 0.1 | 0.5 | 0.8 | 0.5 | 0.3 | 0.3 |
| (μM) | 0.01 | 0.3 | 0.5 | 1.7 | 0.7 | 0.4 | 0.4 |
| | 0.1 | 0.4 | 0.5 | 6.7 | 0.6 | 0.8 | 0.4 |
| | 1 | 0.7 | 0.5 | 12.5 | 1.1 | 2.7 | 0.5 |
| | 10 | 2.7 | 1.9 | 10.6 | 1.6 | 25.6 | 1.4 |
| | | Interaction | | | | | |
| | | Foretinib (μM) | | | | | |
| | | 0.25 | 0.25 | 0.175 | 0.125 | 0.125 | 0.25 |
| Cytarabine | 0.001 | +++++ | +++ | ++ | +++ | +++ | ++++ |
| (μM) | 0.01 | +++ | +++ | --- | ++ | +++ | +++ |
| | 0.1 | +++ | +++ | ---- | +++ | ++ | +++ |
| | 1 | ++ | +++ | ----- | ± | --- | +++ |
| | 10 | --- | --- | ----- | --- | ----- | --- |

| Drug | | Nalm 6 | Nalm17 | REH | SD-1 | Sup B15 | TOM-1 |
|--------------|-------|-------------------|--------|-------|-------|---------|-------|
| | | Combination index | | | | | |
| | | Foretinib (μM) | | | | | |
| | | 0.25 | 0.25 | 0.175 | 0.125 | 0.125 | 0.25 |
| Methotrexate | 0.001 | 0.1 | 0.4 | 0.7 | 2.3 | 0.3 | 0.7 |
| (μM) | 0.01 | 0.1 | 0.4 | 0.6 | 1.1 | 0.3 | 1.1 |
| | 0.1 | 0.2 | 0.4 | 0.4 | 1.9 | 0.2 | 0.2 |
| | 1 | 0.9 | 0.4 | 1.2 | 16.6 | 0.8 | 0.3 |
| | 10 | 7.7 | 0.3 | 9.6 | 152.8 | 4.7 | 1.5 |
| | | Interaction | | | | | |
| | | Foretinib (μM) | | | | | |
| | | 0.25 | 0.25 | 0.175 | 0.125 | 0.125 | 0.25 |
| Methotrexate | 0.001 | +++++ | +++ | ++ | --- | ++++ | ++ |
| (μM) | 0.01 | +++++ | +++ | +++ | ± | ++++ | ± |
| | 0.1 | ++++ | +++ | +++ | --- | ++++ | ++++ |
| | 1 | + | +++ | --- | ----- | ++ | ++++ |
| | 10 | ----- | +++ | ----- | ----- | ----- | --- |

Key:



Synergistic interaction



Antagonistic interaction



Additive interaction

Table 5.4a Summary of the responses of combination therapy for foretinib and the anti – metabolites described as Combination Indices. Data is presented for interactions of foretinib in combination with cytarabine and methotrexate. Interactions represent the mean of 3 experiments performed in triplicate.

| Drug | | Nalm 6 | Nalm17 | REH | SD-1 | Sup B15 | TOM-1 |
|-------------|-------|-------------------|--------|-------|-------|---------|-------|
| | | Combination index | | | | | |
| | | Foretinib (μM) | | | | | |
| | | 0.25 | 0.25 | 0.175 | 0.125 | 0.125 | 0.25 |
| Fludarabine | 0.001 | 0.1 | 0.5 | 0.7 | 0.5 | 0.3 | 0.3 |
| (μM) | 0.01 | 0.1 | 0.5 | 0.1 | 0.6 | 0.3 | 0.0 |
| | 0.1 | 0.1 | 0.5 | 1.2 | 0.6 | 0.3 | 0.3 |
| | 1 | 0.5 | 0.4 | 1.0 | 0.6 | 0.3 | 0.4 |
| | 10 | 3.0 | 1.7 | 0.8 | 0.3 | 1.4 | 1.5 |
| | | Interaction | | | | | |
| | | Foretinib (μM) | | | | | |
| | | 0.25 | 0.25 | 0.175 | 0.125 | 0.125 | 0.25 |
| Fludarabine | 0.001 | +++++ | +++ | ++ | +++ | +++ | +++ |
| (μM) | 0.01 | +++++ | +++ | ++++ | +++ | ++++ | ++++ |
| | 0.1 | ++++ | +++ | - | +++ | ++++ | ++++ |
| | 1 | +++ | +++ | ± | +++ | +++ | +++ |
| | 10 | --- | --- | ++ | +++ | --- | --- |

Key:




| | |
|---|--------------------------|
|  | Synergistic interaction |
|  | Antagonistic interaction |
|  | Additive interaction |

Table 5.4b Summary of the responses of combination therapy for foretinib and the anti – metabolite fludarabine, described as Combination Indices. Data is presented for interactions of foretinib in combination with fludarabine. Interactions represent the mean of 3 experiments performed in triplicate

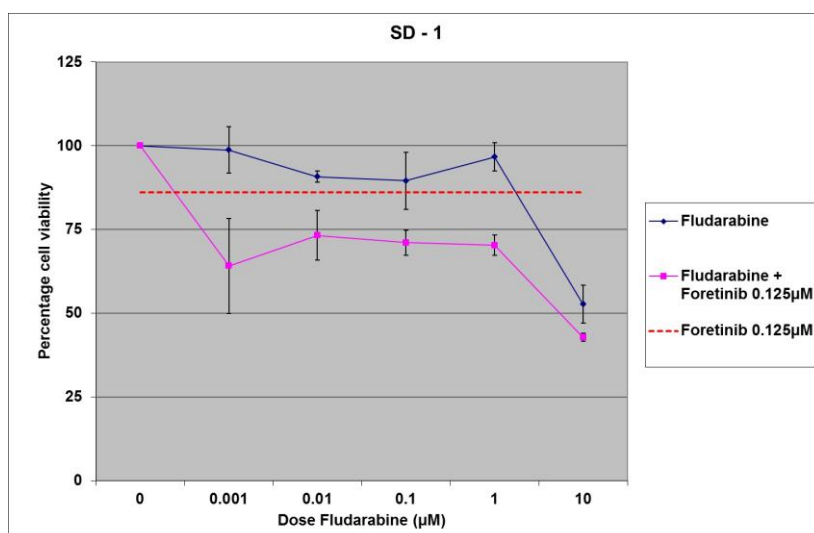


Figure 5.28a

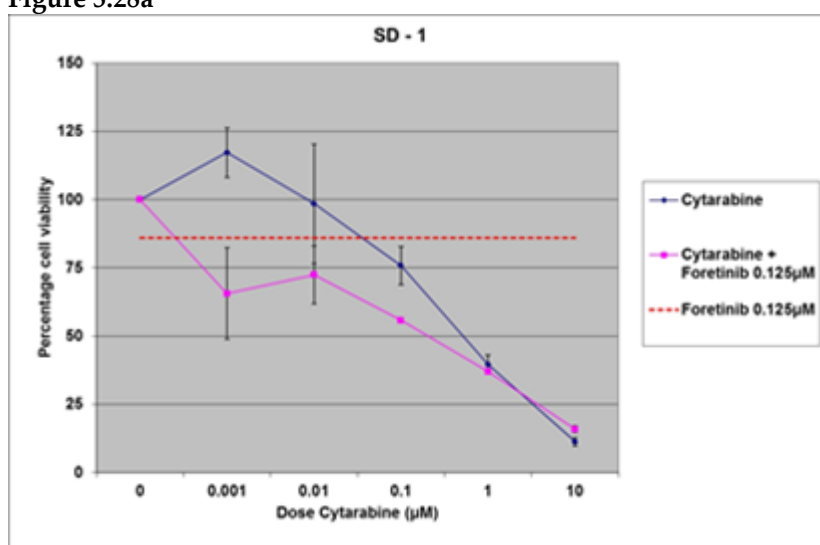


Figure 5.28b

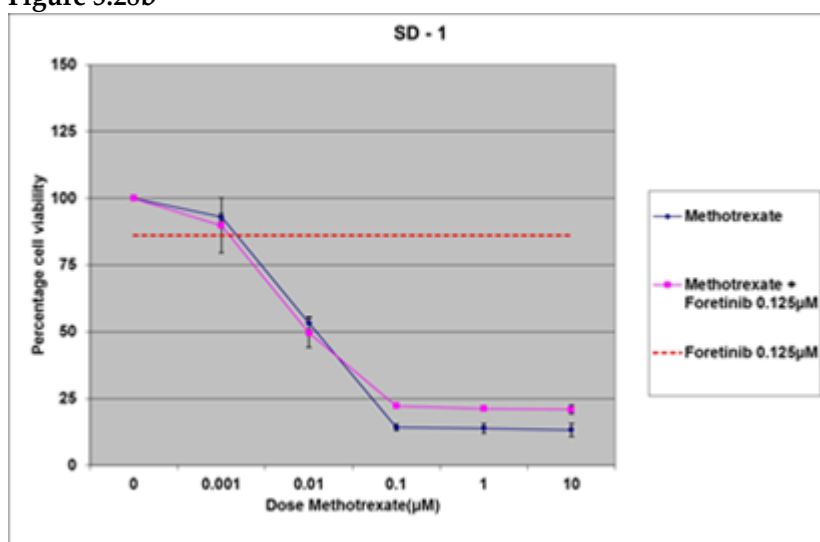


Figure 5.28c

Figure 5.28 Combination of foretinib with anti – metabolites demonstrates differing responses in SD – 1 (a) synergy in combination with fludarabine and (b) cytarabine, but (c) no effect on the methotrexate response curve. Points represent the mean of 3 experiments performed in triplicate; error bars Std deviation.

REH exhibited an early synergistic response to cytarabine with a reduction in cell viability to 50% at 0.001 μ M, while higher doses demonstrated antagonism. Foretinib exhibited synergy when combined with methotrexate and fludarabine in REH (fig 5.29).

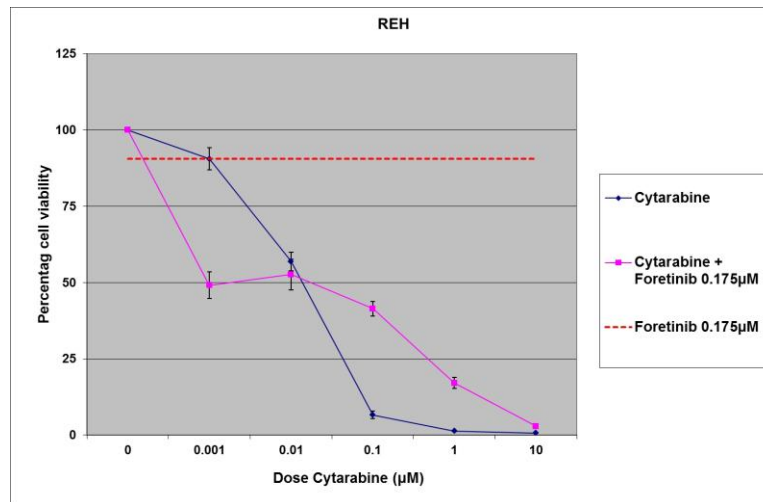


Figure 5.29 Foretinib demonstrates early synergy and late antagonism in combination with cytarabine in the REH cell line. Points represent the mean of 3 experiments performed in triplicate, with error bars representing standard deviation.

While the Chou – Talalay modelling of interactions of foretinib and the anti – metabolites was synergistic in TOM -1 ($CI < 1$), the dose response curves did not appear to support these results. Fig. 5.30a - c show the reduction in viability when foretinib was combined with cytarabine (0.001 – 0.01 μ M), methotrexate (0.001 – 0.1 μ M) and fludarabine (0.001 – 0.1 μ M) were either equal to or less than foretinib alone. This would suggest that despite the mathematical modelling, these were antagonistic interactions.

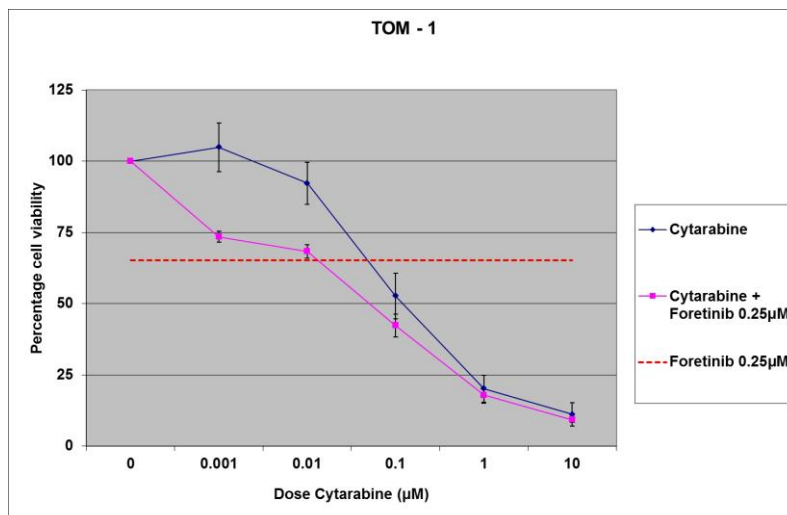


Figure 5.30a

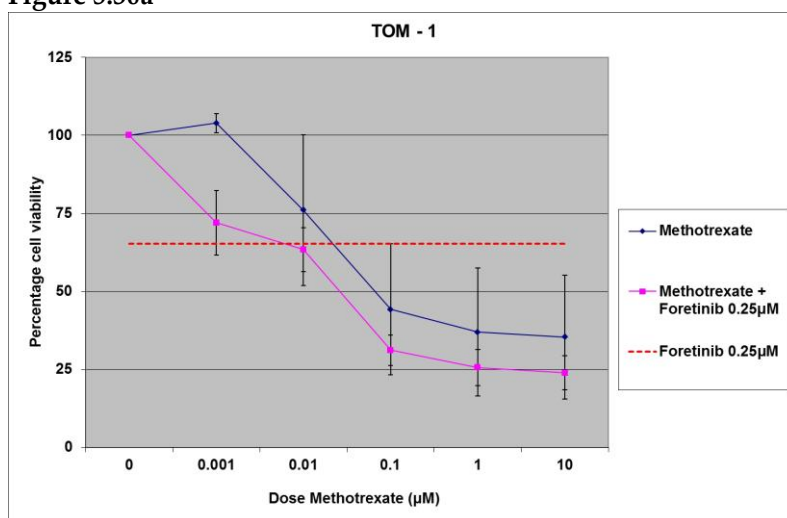


Figure 5.30b

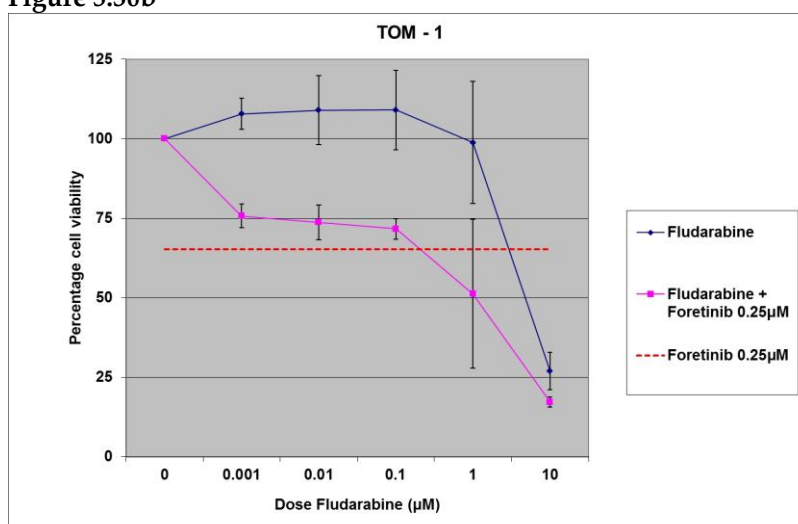


Figure 5.30c

Figure 5.30 Combination therapy with foretinib and anti – metabolites in cell line TOM – 1 result in reduced cell viability (a) cytarabine, (b) methotrexate and (c) fludarabine. Interactions between foretinib and the anti – metabolites appear antagonistic. Points represent the mean of 3 experiments performed in triplicate, with error bars representing standard deviation.

The most marked reduction in cell viability in response to low doses of cytarabine, fludarabine and methotrexate (0.001 – 0.1 μ M) was observed in Nalm 17 and SupB15. These interactions were strongly to moderately synergistic at these doses. In both cell lines concurrent treatment with foretinib (0.25 μ M and 0.125 μ M respectively) with 0.001 μ M of the 3 anti – metabolite cytotoxic agents resulted in a >50% reduction in cell viability at 72 hours.

5.8.1.3 Foretinib in combination with DNA – damaging agents

Treatment with doxorubicin and mitoxantrone as single agents resulted in profound loss of viability in all cell lines. Both mitoxantrone and doxorubicin exhibited strong synergistic interactions (CI<1) when combined with foretinib in all cell lines (table 5.5). Antagonism was present in SD – 1 and SupB15, however the cell viability has reduced >50% at these concentrations (0.1 - 1 μ M fig 5.31).

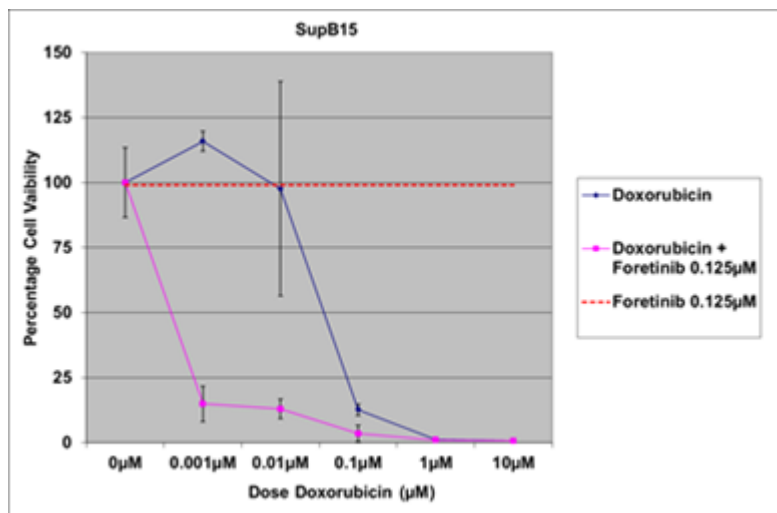


Figure 5.31 a

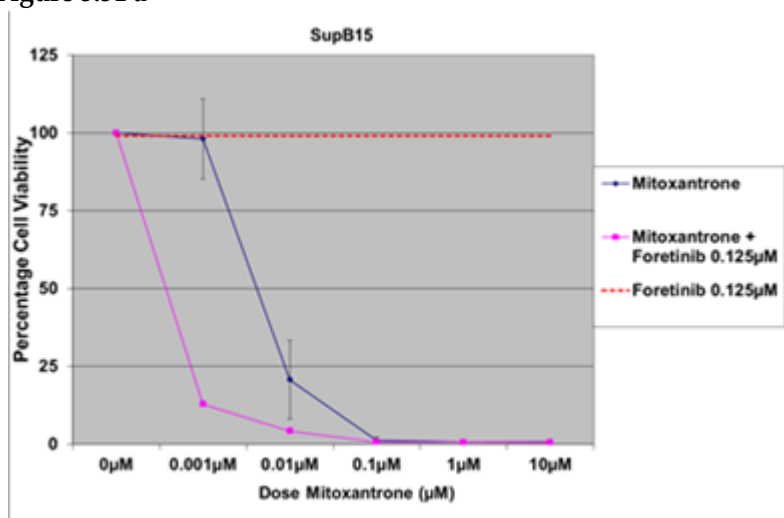


Figure 5.31 b

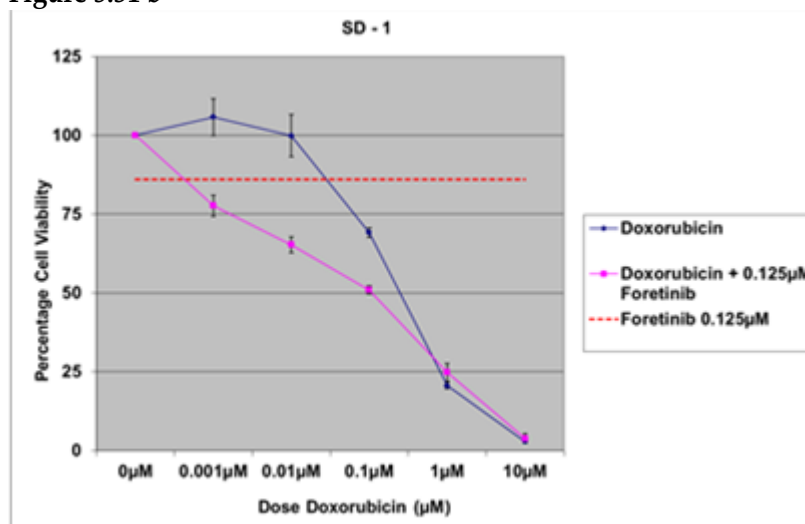


Figure 5.31 c

Figure 5.31 Combination of foretinib and DNA – damaging agents in SupB15 and SD -1 cell lines. Interactions between foretinib and (a) doxorubicin and (b) mitoxantrone in SupB15 demonstrate significant reduction in cell viability. (c) Combination of doxorubicin and foretinib in SD -1 reveal significant reduction in cell viability. Points represent the mean of 3 experiments performed in triplicate, with error bars representing standard deviation.

| Drug | | Nalm 6 | Nalm17 | REH | SD-1 | Sup B15 | TOM-1 |
|-------------|--------|-------------------|--------|-------|-------|---------|-------|
| | | Combination index | | | | | |
| | | Foretinib (μM) | | | | | |
| | | 0.25 | 0.25 | 0.175 | 0.125 | 0.125 | 0.25 |
| Doxorubicin | 0.0001 | 0.1 | 0.5 | 0.7 | 0.7 | 0.3 | 0.2 |
| (μM) | 0.001 | 0.1 | 0.7 | 0.8 | 0.5 | 0.3 | 0.8 |
| | 0.01 | 0.1 | 0.9 | 1.5 | 0.5 | 0.4 | 0.3 |
| | 0.1 | 0.3 | 0.4 | 0.7 | 1.0 | 1.1 | 0.6 |
| | 1 | 0.9 | 1.6 | 2.2 | 1.6 | 9.3 | 0.1 |
| | | Interaction | | | | | |
| | | Foretinib (μM) | | | | | |
| | | 0.25 | 0.25 | 0.175 | 0.125 | 0.125 | 0.25 |
| Doxorubicin | 0.0001 | ++++ | +++ | +++ | +++ | ++++ | ++++ |
| (μM) | 0.001 | ++++ | +++ | ++ | +++ | ++++ | ++ |
| | 0.01 | ++++ | + | --- | +++ | +++ | +++ |
| | 0.1 | +++ | +++ | ++ | ± | ± | +++ |
| | 1 | + | --- | --- | --- | ---- | ++++ |

| Drug | | Nalm 6 | Nalm17 | REH | SD-1 | Sup B15 | TOM-1 |
|--------------|-------|-------------------|--------|-------|-------|---------|-------|
| | | Combination index | | | | | |
| | | Foretinib (μM) | | | | | |
| | | 0.25 | 0.25 | 0.175 | 0.125 | 0.125 | 0.25 |
| Mitoxantrone | 0.001 | 0.2 | 0.4 | 0.7 | 0.5 | 0.4 | 0.639 |
| (μM) | 0.01 | 0.4 | 0.3 | 0.7 | 1.1 | 1.0 | 0.4 |
| | 0.1 | 0.7 | 0.2 | 1.8 | 1.7 | 8.7 | 1.0 |
| | 1 | 1.9 | 1.8 | 6.1 | 0.2 | 85.8 | 0.1 |
| | | Interaction | | | | | |
| | | Foretinib (μM) | | | | | |
| | | 0.25 | 0.25 | 0.175 | 0.125 | 0.125 | 0.25 |
| Mitoxantrone | 0.001 | ++++ | +++ | +++ | +++ | +++ | ++ |
| (μM) | 0.01 | +++ | ++++ | ++ | ± | ± | +++ |
| | 0.1 | ++ | ++++ | --- | --- | ---- | ± |
| | 1 | --- | --- | ---- | ++++ | ----- | ++++ |

Key:




| | |
|---|--------------------------|
|  | Synergistic interaction |
|  | Antagonistic interaction |
|  | Additive interaction |

Table 5.5 Summary of the responses of combination therapy for foretinib and the DNA – damaging agents described as Combination Indices. Data is presented for interactions of foretinib in combination with (a) doxorubicin and (b) mitoxantrone. Interactions represent the mean of 3 experiments performed in triplicate.

5.8.1.4 Foretinib in combination with vincristine

The effect of foretinib and vincristine was predominantly synergistic at lower doses (table 5.6). However, antagonism was present in REH and TOM – 1 and the degree of antagonism increased with vincristine concentration (fig 5.32).

| Drug | | Nalm 6 | Nalm17 | REH | SD-1 | Sup B15 | TOM-1 |
|-------------|--------|-------------------|--------|-------|-------|---------|-------|
| | | Combination index | | | | | |
| | | Foretinib (μM) | | | | | |
| | | 0.25 | 0.25 | 0.175 | 0.125 | 0.125 | 0.25 |
| Vincristine | 0.0001 | 0.1 | 0.5 | 0.8 | 0.5 | 0.2 | 0.32 |
| (μM) | 0.001 | 0.1 | 0.5 | 2.0 | 0.7 | 0.8 | 1.3 |
| | 0.01 | 0.5 | 0.7 | 5.7 | 1.4 | 6.1 | 8.4 |
| | 0.1 | 4.2 | 2.9 | 17.9 | 16.7 | 49.6 | 54.0 |
| | | Interaction | | | | | |
| | | Foretinib (μM) | | | | | |
| | | 0.25 | 0.25 | 0.175 | 0.125 | 0.125 | 0.25 |
| Vincristine | 0.0001 | ++++ | +++ | +++ | +++ | ++++ | +++ |
| (μM) | 0.001 | ++++ | +++ | --- | ++ | ++ | -- |
| | 0.01 | +++ | +++ | ---- | --- | ---- | ---- |
| | 0.1 | ---- | --- | ----- | ----- | ----- | ----- |

Key:


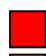

| | |
|---|--------------------------|
|  | Synergistic interaction |
|  | Antagonistic interaction |
|  | Additive interaction |

Table 5.6 Summary of the responses of combination therapy for foretinib and vincristine described as Combination Indices. Combination therapy demonstrates a predominantly synergistic effect at lower vincristine doses, but antagonism predominates as vincristine concentration increases. Interactions represent the mean of 3 experiments performed in triplicate.

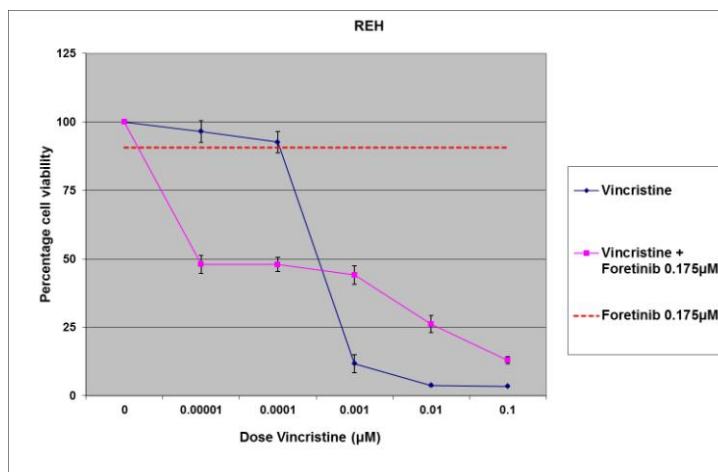


Figure 5.32a

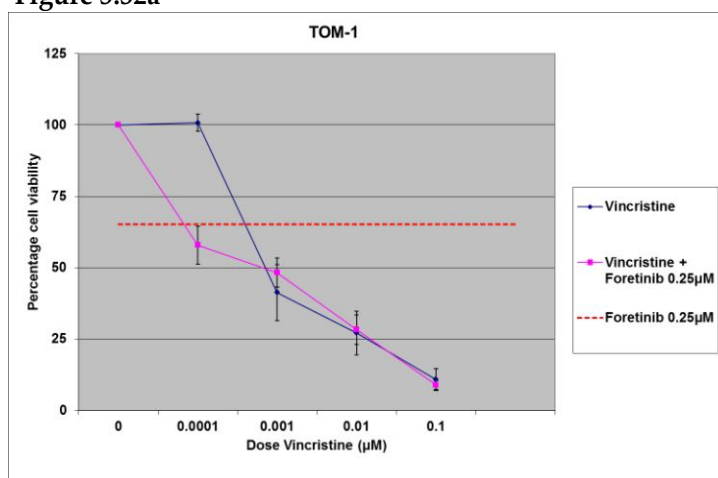


Figure 5.32b

Figure 5.32 Combination of foretinib with vincristine demonstrates synergy at low doses in both (a) REH and (b) TOM – 1 cell lines. Points represent the mean of 3 experiments performed in triplicate, with error bars representing standard deviation.

In summary, the dominant impact of foretinib in combination with cytotoxic agents was one of synergy. In particular foretinib was able to sensitise resistant cell lines to chemotherapy and it did so in cell lines which did not display a significant response to foretinib alone.

5.8.2 Assessment of combination of foretinib and cytotoxics in primary ALL – 20

To determine whether foretinib was able to sensitise the primary leukaemia ALL – 20 to chemotherapeutic agents, cells were treated the cells with a fixed sub – IC₅₀ dose of foretinib 0.0075 μ M, in combination with dexamethasone, doxorubicin, mitoxantrone, cytarabine, methotrexate or vincristine. ALL – 20 demonstrated profound *in vitro* resistance to methotrexate monotherapy. An increase in cell viability corresponded with dose increments up to 1 μ M, twice that of baseline (fig 5.33).

Significant sensitisation was exhibited in response to combination therapy of foretinib with all classes of chemotherapy. Table 5.7 summarises the responses to combination therapy. In particular, the methotrexate resistance was negated (fig 5.33); low doses of methotrexate induced a significant reduction in viability, >75% with 0.001 μ M methotrexate and 0.075 μ M foretinib.

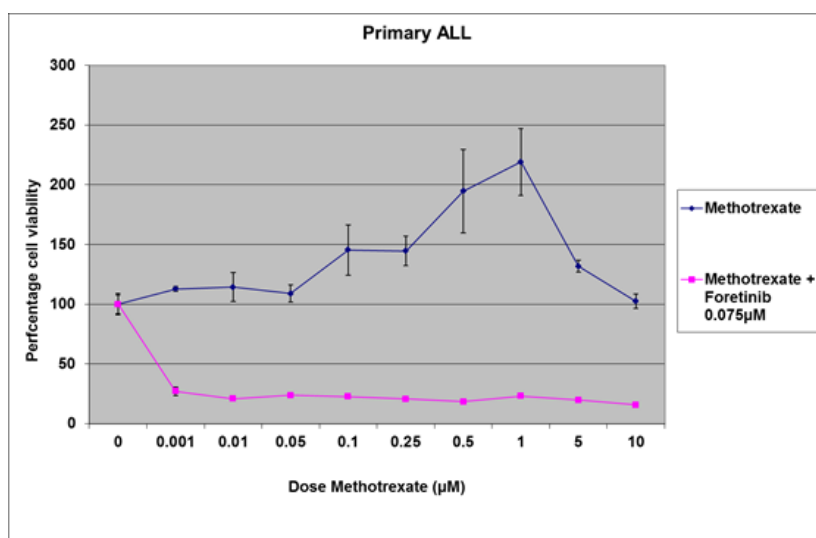


Figure 5.33 Methotrexate resistance in primary sample ALL -20 is abrogated by sub – IC₅₀ dose of foretinib. Foretinib demonstrates potent ability to reverse methotrexate resistance in primary cells (ALL – 20).

| | Dose | CI | Interaction |
|---------------------------------|---------|-----|-------------|
| Dexamethasone (μM) | 0.001 | 0.3 | +++ |
| | 0.01 | 0.3 | +++ |
| | 0.1 | 0.5 | +++ |
| | 0.25 | 0.9 | \pm |
| | 0.5 | 1.3 | -- |
| Cytarabine (μM) | 0.001 | 0.4 | +++ |
| | 0.01 | 0.4 | +++ |
| | 0.1 | 0.3 | +++ |
| | 1 | 0.2 | ++++ |
| | 10 | 0.2 | ++++ |
| Methotrexate (μM) | 0.001 | 0.7 | +++ |
| | 0.01 | 0.8 | ++ |
| | 0.1 | 0.8 | ++ |
| | 1 | 0.8 | ++ |
| | 10 | 0.9 | \pm |
| Vincristine (μM) | 0.0001 | 0.5 | +++ |
| | 0.001 | 0.5 | +++ |
| | 0.01 | 0.5 | +++ |
| | 0.1 | 0.7 | ++ |
| Doxorubicin (μM) | 0.00001 | 0.5 | +++ |
| | 0.0001 | 0.5 | +++ |
| | 0.001 | 0.5 | +++ |
| | 0.01 | 0.9 | \pm |
| | 0.1 | 1.3 | --- |
| Mitoxantrone (μM) | 0.00001 | 0.4 | +++ |
| | 0.0001 | 0.4 | +++ |
| | 0.001 | 0.5 | +++ |
| | 0.01 | 0.8 | ++ |
| | 0.1 | 6.0 | ---- |

Key:




| | |
|---|--------------------------|
|  | Synergistic interaction |
|  | Antagonistic interaction |
|  | Additive interaction |

Table 5.7 Foretinib demonstrates ability to sensitise the primary ALL sample (ALL – 20) to a wide variety of chemotherapeutic agents. The predominant interaction is synergistic with Combination Indices less than 1 (CI <1).

5.8.3 Dovitinib combinations with cytotoxics demonstrate synergy in cell lines

The interaction of dovitinib with the induction agents, dexamethasone, doxorubicin and vincristine was then examined. Cell lines were co – treated with fixed sub – IC₅₀ dovitinib doses. Dovitinib predominantly demonstrated synergy in combination with dexamethasone in all 6 cell lines (tables 5.8a and b).

| Drug | | Nalm 6 | Nalm17 | REH | SD-1 | Sup B15 | TOM-1 |
|---------------|--------|-------------------|--------|-------|-------|---------|-------|
| | | Combination index | | | | | |
| | | Dovitinib (µM) | | | | | |
| | | 0.25 | 0.1 | 0.1 | 0.075 | 0.075 | 0.1 |
| Dexamethasone | 0.001 | 0.7 | 0.4 | 0.6 | 1.3 | 1.4 | 1.9 |
| (µM) | 0.01 | 0.3 | 0.4 | 0.6 | 0.4 | 0.0 | 0.2 |
| | 0.1 | 0.2 | 0.3 | 0.6 | 0.3 | 0.1 | 0.2 |
| | 1 | 0.3 | 0.6 | 0.9 | 0.5 | 0.9 | 0.5 |
| | 10 | 0.2 | 3.4 | 3.5 | 3.2 | 9.1 | 3.8 |
| | | Interaction | | | | | |
| | | Dovitinib (µM) | | | | | |
| | | 0.1 | 0.1 | 0.075 | 0.075 | 0.1 | 0.25 |
| Dexamethasone | 0.001 | ++ | +++ | +++ | -- | --- | --- |
| (µM) | 0.01 | ++++ | +++ | +++ | +++ | ++++ | ++++ |
| | 0.1 | ++++ | +++ | +++ | +++ | ++++ | ++++ |
| | 1 | ++++ | +++ | ± | +++ | ± | +++ |
| | 10 | ++++ | --- | --- | --- | --- | --- |
| Drug | | Nalm 6 | Nalm17 | REH | SD-1 | Sup B15 | TOM-1 |
| | | Combination index | | | | | |
| | | Dovitinib (µM) | | | | | |
| | | 0.25 | 0.1 | 0.1 | 0.075 | 0.075 | 0.1 |
| Doxorubicin | 0.0001 | 0.6 | 0.5 | 0.8 | 1.0 | 171000 | 2.2 |
| (µM) | 0.001 | 2.4 | 0.5 | 0.7 | 0.5 | 0.8 | 0.8 |
| | 0.01 | 3.0 | 0.3 | 0.4 | 0.5 | 0.2 | 0.2 |
| | 0.1 | 3.8 | 0.2 | 1.0 | 1.0 | 0.4 | 0.6 |
| | 1 | 0.3 | 0.7 | 5.4 | 5.1 | 4.1 | 3.0 |
| | | Interaction | | | | | |
| | | Dovitinib (µM) | | | | | |
| | | 0.1 | 0.1 | 0.075 | 0.075 | 0.1 | 0.25 |
| Doxorubicin | 0.0001 | +++ | +++ | ++ | ± | ----- | --- |
| (µM) | 0.001 | --- | +++ | +++ | +++ | ++ | ++ |
| | 0.01 | --- | +++ | +++ | +++ | ++++ | ++++ |
| | 0.1 | ---- | ++++ | ± | ± | +++ | +++ |
| | 1 | ++++ | +++ | ----- | ----- | ----- | --- |

Key:



Synergistic interaction



Antagonistic interaction



Additive interaction

Table 5.8a Summary of the responses of combination therapy for dovitinib and cytotoxic agents described as Combination Indices. Data is presented for interactions of dovitinib in combination with (a) dexamethasone and (b) doxorubicin. Interactions represent the mean of 3 experiments performed in triplicate.

| Drug | | Nalm 6 | Nalm17 | REH | SD-1 | Sup B15 | TOM-1 |
|-------------|---------|-------------------|--------|--------|-------|----------|-------|
| | | Combination index | | | | | |
| | | Dovitinib (µM) | | | | | |
| | | 0.25 | 0.1 | 0.1 | 0.075 | 0.075 | 0.1 |
| Vincristine | 0.00001 | 0.8 | 0.4 | 3385.0 | 1.2 | 171000.0 | 3.4 |
| (µM) | 0.0001 | 2.8 | 0.4 | 1881.0 | 0.5 | 0.9 | 1.5 |
| | 0.001 | 1.7 | 0.2 | 28.3 | 0.2 | 0.2 | 0.2 |
| | 0.01 | 1.2 | 0.6 | 7.4 | 0.5 | 1.1 | 0.5 |
| | 0.1 | 0.9 | 4.8 | 7.4 | 4.7 | 6.5 | 3.4 |
| | | Interaction | | | | | |
| | | Dovitinib (µM) | | | | | |
| | | 0.1 | 0.1 | 0.075 | 0.075 | 0.1 | 0.25 |
| Vincristine | 0.00001 | ++ | +++ | ---- | - | ---- | ---- |
| (µM) | 0.0001 | --- | +++ | ---- | +++ | ± | --- |
| | 0.001 | --- | ++++ | ---- | ++++ | ++++ | ++++ |
| | 0.01 | --- | +++ | ---- | +++ | ± | +++ |
| | 0.1 | ± | ---- | ---- | ---- | ---- | ---- |

Key:




| | |
|--|--------------------------|
|  | Synergistic interaction |
|  | Antagonistic interaction |
|  | Additive interaction |

Table 5.8b Summary of the responses of combination therapy for dovitinib and cytotoxic agents described as Combination Indices. Data is presented for interactions of dovitinib in combination with vincristine. Interactions represent the mean of 3 experiments performed in triplicate.

Dovitinib sensitised the steroid – resistant cell lines, Nalm 6, SD – 1 and REH to dexamethasone. The cell line Nalm 17 developed steroid resistance while in culture; despite this finding, dovitinib co – treatment sensitised the cells to dexamethasone (fig 5.34).

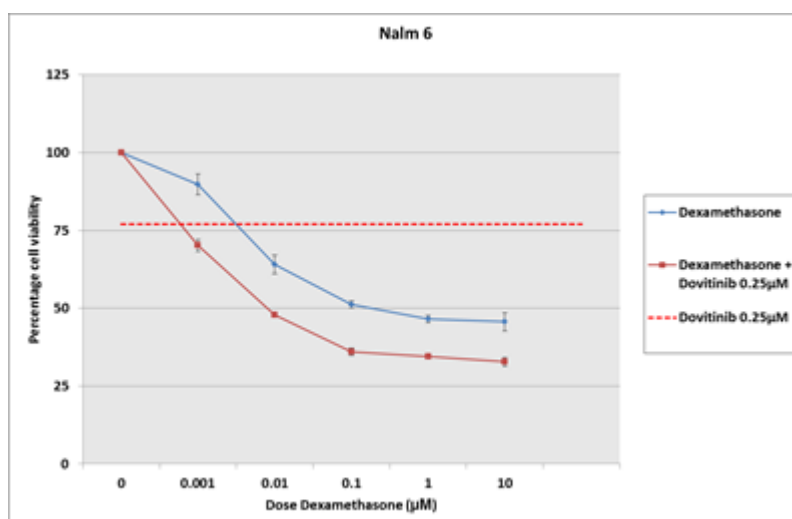


Figure 5.34a

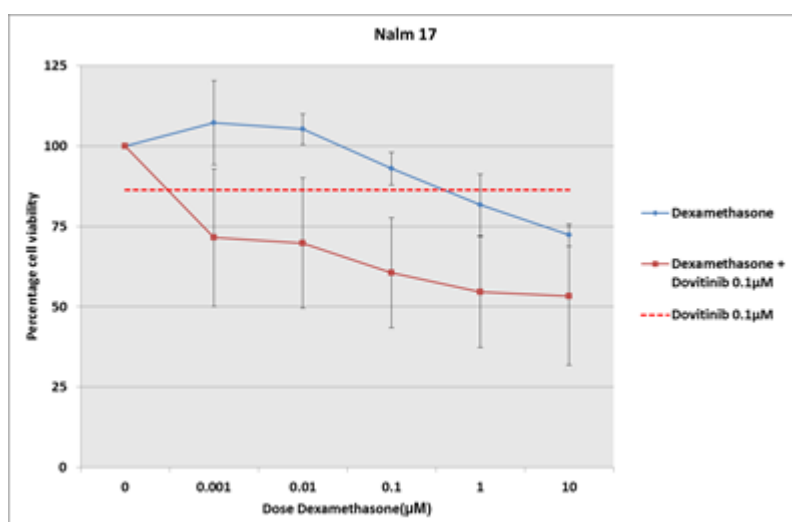


Figure 5.34b

Figure 5.34 Dovitinib sensitises the steroid – resistant cell lines Nalm 6 and Nalm 17. The red line demonstrates the percentage cell viability induced by dovitinib alone. For combinations to be synergistic, the reduction in viability needs to be below the chemotherapy alone and the red line. Steroid resistant cell lines (a) Nalm 6 and (b) Nalm 17 are sensitised to DXM by foretinib. Data presented is the mean of 2 experiments, undertaken in triplicate. Error bars are standard deviation.

The impact of dovitinib on doxorubicin was found to be generally synergistic (table 5.8a). Antagonism was displayed in Nalm 6 at concentrations 0.001 – 0.1 μM and REH 0.01 - 1 μM. Despite the $CI > 1$ exhibited in these 2 cell lines, the reduction in cell viability of the combination was always more than either the TKI alone or doxorubicin.

Finally, the effect of dovitinib and vincristine was largely antagonistic, with Nalm 6 and REH exhibiting $CI > 1$ for most concentrations (table 5.8b). The only cell line to demonstrate synergy at concentrations 0.0001 – 0.01 μM was Nalm 17.

Overall, these data indicate foretinib and dovitinib are able to sensitise ALL cell lines to conventional chemotherapeutic agents. The combination of dexamethasone and TKI (either foretinib or dovitinib) induced the most reliable synergy. While some evidence of antagonism is present these interactions are limited to individual cell lines and specific chemotherapies.

5.8.4 Steroid sensitisation induced by foretinib in REH cell line is not due to apoptosis

The cell line REH is profoundly resistant to glucocorticoid induced cell death (422). The strong synergy demonstrated by foretinib and dexamethasone in REH was investigated to determine whether the synergy arose because of an increase in apoptosis. Cellular responses to co-treatment with foretinib and dexamethasone were assessed using an Annexin V/PI assay. REH cells were treated with dexamethasone 0.1 μ M alone, foretinib 0.25 μ M alone and in combination with dexamethasone, and then assayed for Annexin positive cells at 24, 48 and 72 hours (fig 5.35). Dexamethasone alone did not induce significant apoptosis at the three time points (p values = 0.69, 0.56 and 0.15 respectively). An apoptotic response to foretinib was seen at all time-points. No appreciable difference between the apoptosis induced by foretinib alone or in combination with dexamethasone was identified (p – values = 0.49, 0.63 and 0.8 at 24, 48 and 72 hours respectively) (fig 5.34).

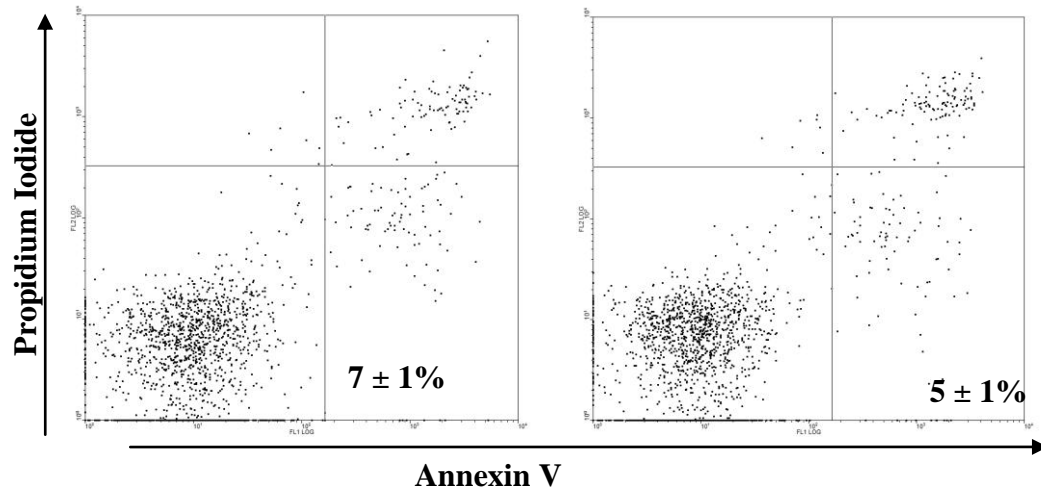


Figure 5.34a

Figure 5.34b

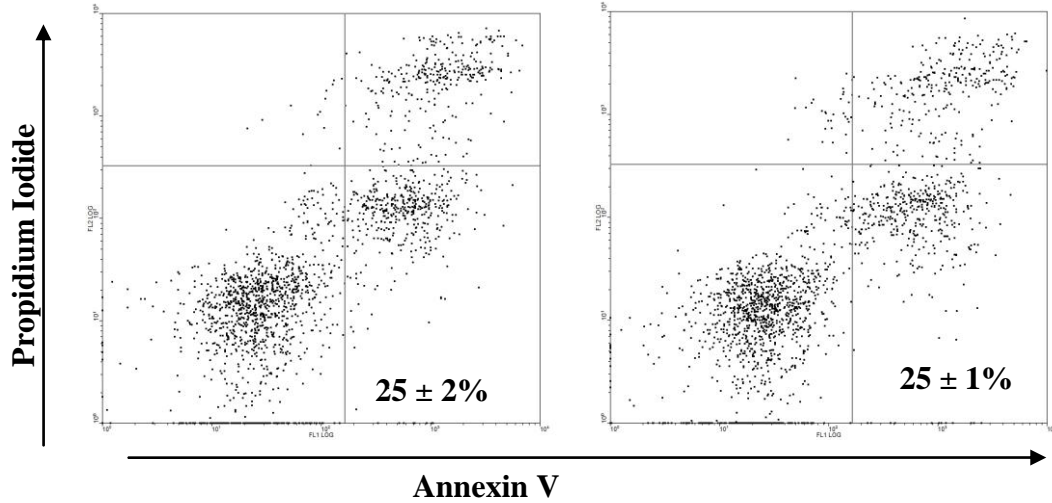


Figure 5.34c

Figure 5.34 d

Figure 5.35 Combination of foretinib and dexamethasone in REH cell line does not induce an increase in apoptosis after 72 hours treatment. Assessment of foretinib to induce apoptosis was assessed in the dexamethasone – resistant REH cell line. Cells were exposed to different conditions, (a) DMSO 0.1% (b) dexamethasone monotherapy (c) foretinib 0.25 μ M monotherapy (d) dexamethasone 0.1 μ M and foretinib 0.25 μ M. Percentage expressed are the population of apoptotic cells under each condition after 72 hours treatment.

| | | Percentage of population | | |
|----------|---|--------------------------|----------------|----------------|
| | | Live | Apoptotic | Dead |
| 24 hours | DMSO 0.1% control | 90 (± 4) | 6 (± 3) | 4 (± 2) |
| | Dexamethasone (DXM) 0.1 μ M | 90 (± 3) | 6 (± 3) | 4 (± 1) |
| | Foretinib 0.250 μ M | 76 (± 1) | 13 (± 1) | 10 (± 1) |
| | DXM 0.1 μ M + Foretinib 0.250 μ M | 77 (± 3) | 13 (± 2) | 9 (± 1) |
| 48 hours | DMSO 0.1% control | 88 (± 5) | 7 (± 3) | 4 (± 2) |
| | DXM 0.1 μ M | 87 (± 4) | 9 (± 3) | 4 (± 1) |
| | Foretinib 0.250 μ M | 74 (± 1) | 15 (± 1) | 11 (± 1) |
| | DXM 0.1 μ M + Foretinib 0.250 μ M | 74 (± 1) | 16 (± 3) | 10 (± 1) |
| 72 hours | DMSO 0.1% control | 83 (± 4) | 7 (± 1) | 10 (± 3) |
| | DXM 0.1 μ M | 87 (± 1) | 5 (± 1) | 7 (± 1) |
| | Foretinib 0.250 μ M | 60 (± 1) | 25 (± 2) | 14 (± 2) |
| | DXM 0.1 μ M + Foretinib 0.250 μ M | 58 (± 2) | 25 (± 1) | 16 (± 1) |

Table 5.9 Percentage of apoptotic cells in response to dexamethasone, foretinib or combination. Percentage given is the mean experiments performed in triplicate, with standard deviation in parentheses.

5.9 Assessment of *in vivo* efficacy of foretinib and dovitinib in murine primagraft model

To investigate the *in vivo* impact of the TKIs, a murine xenograft model of the primary B – precursor leukaemia ALL – 20 was established. Immune deficient mice were inoculated with leukaemia cells (section 2.19) obtained from a diagnostic B – precursor ALL bone marrow sample, with the adverse NCI/Rome risk criteria for WCC ($109 \times 10^9/l$) and age (12yrs) (table 2.2). The experiments were planned by Dr Wilson and carried out by Dr Wilson and Mrs Tracey Perry, laboratory technician to the Kearns Group. Mrs Perry helped with inoculation of mice, gavaging of TKIs, bleeding of mice and harvesting of mice. Dr Wilson harvested mice and prepared blood and organ samples for flow cytometry. Dr Wilson and Mrs Perry performed flow cytometry as described in section 2.16.

5.9.1 Engraftment kinetic experiments for ALL – 20

Fluorescent – activated cell sorting (FACS) immunophenotyping, performed at Birmingham Children's Hospital (BCH) as part of the routine diagnostic service, demonstrated ALL – 20 as a B – cell precursor ALL, demonstrating surface markers CD45 (pan – leukocyte) 80%, CD19 (pan – B) 90%, CD10 (common ALL antigen) 87%, and CD34 8%. Four per cent of cells expressed Tdt and cytoplasmic μ was present in 14%. These data

support the diagnosis of common ALL that was made on morphological grounds by study of bone marrow smears. The maturity of the leukaemia population in the murine xenograft was defined according to CD45, CD34, CD19 and CD10 expression. The panel of fluorochromes used for the xenograft model (table 2.8) demonstrated concordance with the original BCH findings in the leukaemia sample prior to injection, with 73% of total cells staining for human CD45 (hCD45+) of which 93% were CD19+/CD10+ , confirming B – cell origin and an immature B – cell precursor phenotype. Fewer than 1% of the cells were CD34+, indicating the leukaemia was not stem cell – like in origin (fig 5.36a).

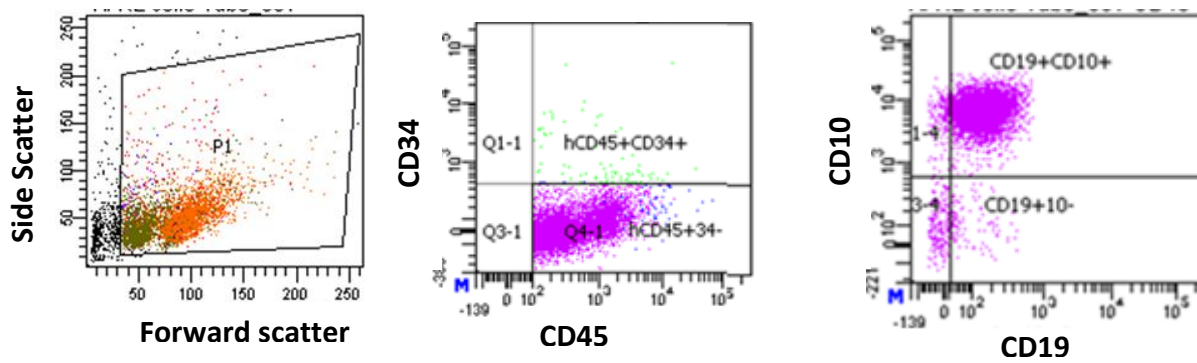


Figure 5.36a

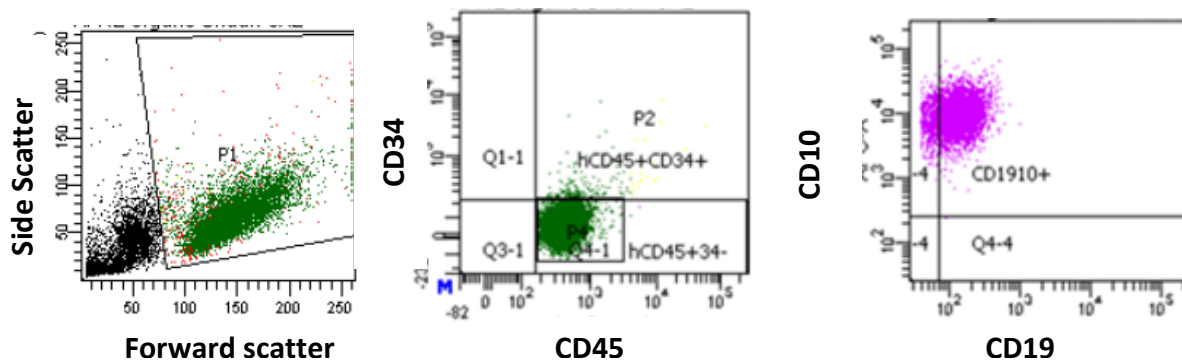


Figure 5.36b

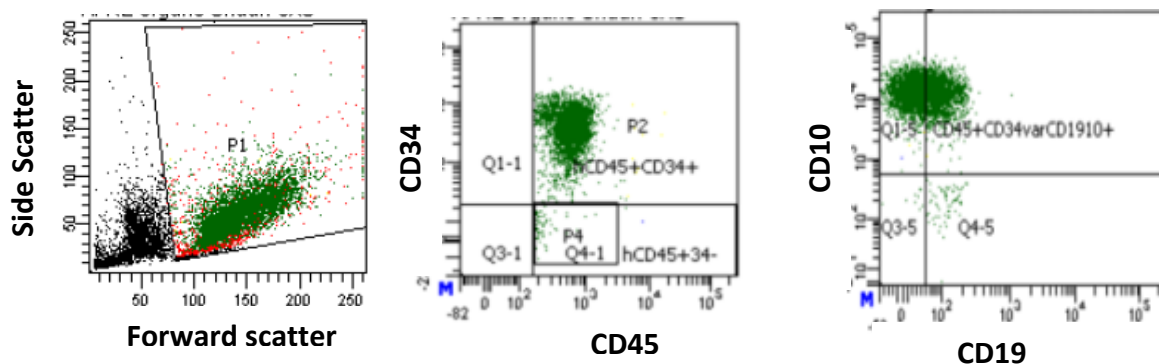


Figure 5.36c

Figure 5.36 Immunophenotyping of ALL – 20 cells with the fluorochrome panel. (a) ALL – 20 cells labelled with the fluorochrome panel prior to injection revealed a phenotype consistent with the original diagnostic investigations performed at BCH, CD45+CD34-CD19+CD10+. (b) Representative FACS analysis from passaged ALL – 20 harvested from the liver of mouse 5. Engrafted cells demonstrate a similar original immunophenotype, CD45+CD34-CD19+CD10+. (c) FACS analysis of cells engrafted in spleen of mouse 5 displayed evolution of a CD34+ more stem – like sub - clone. The leukaemia infiltrating the liver and bone marrow however were CD34-CD1910+.

Leukaemia cells were washed, counted and suspended in 1ml PBS prior to injection. 1×10^6 cells per mouse were injected via lateral tail vein into 8 immune deficient (NOD/Scid/IL2r γ NOG) mice (all male) and the presence of human leukaemia blasts were assessed by sampling of murine blood. Engraftment was defined as the presence of at least 1% of all live cells staining for hCD45+ cells in the peripheral murine blood (423). Engraftment of ALL – 20 was rapid, with all 8 mice exhibiting greater than 1% hCD45+ cells in murine blood by day 15, mean 14.2 % (SD \pm 7.1%). There was an insignificant reduction ($p = 0.65$) in peripheral hCD45+ at day 28, with mean engraftment 12.5% (SD \pm 7.5%) (fig 5.37).

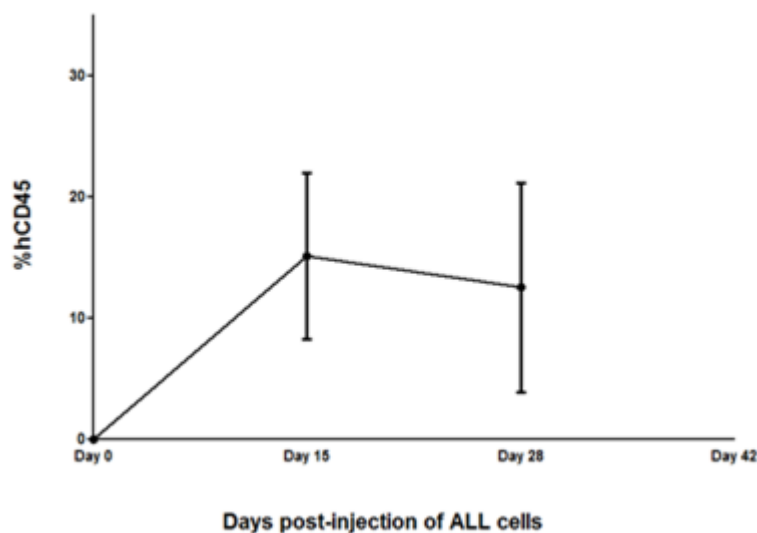


Figure 5.37 Initial engraftment kinetics experiments revealed rapid engraftment of the ALL – 20 sample. Peripheral engraftment of hCD45 cells was evident in peripheral murine blood samples by day 15. Each time point is the mean engraftment of all mice alive at the time of sampling. Error bars are standard deviations.

The median survival of the mice was 34 days. Two of eight corpses were macerated and could not be analysed. Infiltration of bone marrow and spleen was assessed in the remaining 6 mice. Infiltration of the livers in 4 mice by FACS analysis, which confirmed significant engraftment of ALL – 20 in all organs. The mean percentage of CD45+ infiltrating all harvested murine organs was 77.31% (SD \pm 10.48%). Table 5.10 shows the initial engraftment, percentage of tumour infiltration of each organ at death and survival for each of the mice.

| | Percentage human CD45 (%) | | | | Survival |
|-------|---------------------------|-----------------|-----------------|-----------------|----------|
| Mouse | Day 8 blood | Bone marrow | Liver | Spleen | Days |
| 1 | 18 | 58.5 | 90.9 | 86.6 | 36 |
| 2 | 24.8 | No viable cells | No viable cells | No viable cells | 36 |
| 3 | 19.2 | No viable cells | No viable cells | No viable cells | 34 |
| 4 | 13.1 | 61.6 | 84.7 | 72.7 | 36 |
| 5 | 17.5 | 73.3 | 92.5 | 79.1 | 34 |
| 6 | 2.6 | 57.4 | 90.9 | 80.9 | 34 |
| 7 | 9.4 | 69 | Not done | 70.9 | 34 |
| 8 | 8.9 | 71.9 | Not done | 75.8 | 34 |

Table 5.10 Summary of hCD45 engraftment in peripheral blood and murine organs at terminal cull from the initial experiment to determine the engraftment kinetics of ALL – 20. High levels of engraftment were present in evaluable murine organs. No viable cells were present in mouse 2 and mouse 3 as the corpses were macerated and analysis was not possible.

The scatter plot Fig. 5.38a reveals a greater mean tumour load in the liver ($89.8 \pm 3.5\%$) than the bone marrow ($65.3 \pm 7\%$) or spleen ($77.7 \pm 5.8\%$), which was statistically significant higher ($p < 0.0001$ by one – way ANOVA).

FACS analysis of the composition of the xenograft leukaemia confirmed the recapitulation of the original phenotype. Fig 5.37b shows the relative engraftment of CD34+ and CD34- cells. One outlier is present, with evidence of a sub – clone developing in the spleen of mouse 5. The predominant immunophenotype in mouse 5 spleen was CD45+CD34+ CD19+.

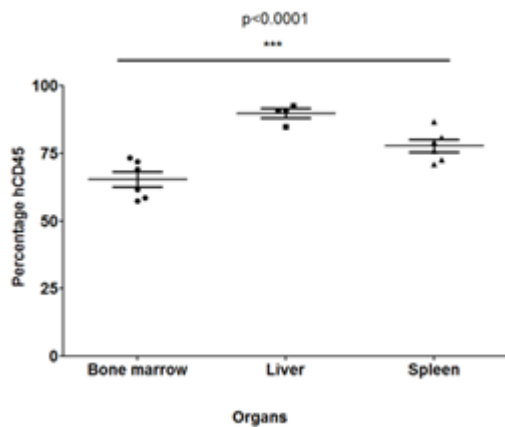


Figure 5.38a

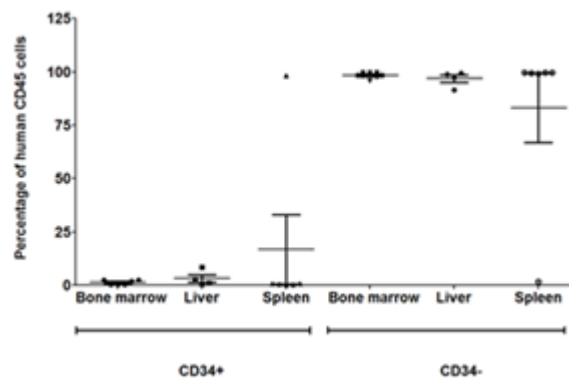


Figure 5.38b

Figure 5.38 The murine xenograft demonstrates the hepatotropic nature of ALL – 20 which reconstituted the original CD45+CD34-19+10+ phenotype. (a) Significantly higher tumour load was present in all livers harvested from evaluable mice (ANOVA one – way $p < 0.0001$). (b) The engrafted leukaemia recapitulated original CD45+CD34-19+10+ phenotype. The emergence of a CD34+ clone was evident in the spleen of mouse 5.

To assess the stability of the ALL – 20 xenograft, the VDJ gene rearrangements in the original primary tumour and leukaemia harvested from bone marrow, liver and spleen from mice were examined. PCR was performed using primers for framework region 3A (Fr3A) and J1H heavy chain joining fragment (J1H) regions. Products were visualised on a 4% agarose gel (fig 5.39), extracted and sequenced. Sequencing of these rearrangements revealed identical products in all cells. In summary, the ALL – 20 xenograft model demonstrates rapid and reliable engraftment, with recapitulation of the original immunophenotype and clonal stability.

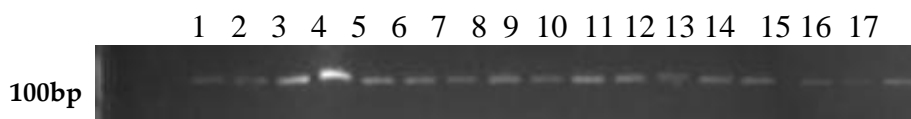


Figure 5.39 Stability of VDJ rearrangements of ALL – 20 is demonstrated in the expression of the identical product from diagnostic sample and samples harvested from mouse livers and spleens. Utilising the primers for Fr3A and J1H, the PCR product was run on 4% agarose gel. The product visualised in Lane 1 is the VDJ product from the original diagnostic bone marrow sample for ALL – 20. The products in lane 2 – 5 were derived from the spleen and liver harvested from mouse 1, products in lane 6 – 7 derived from the liver of mouse 7, products in lane 8 – 11 the spleen and liver from mouse 2 and the products in lane 12 – 17 from the bone marrow, spleen and liver harvested from mouse 3.

5.9.2 Assessment of *in vivo* activity of foretinib

After establishing the characteristics of the ALL – 20 xenograft; the efficacy of foretinib was investigated in this xenograft model. Ten immunodeficient mice were used in this experiment, with 5 in each cohort. Two cycles of foretinib 30mg/kg/day by oral gavage, 5 days on and 9 days off were administered to the treatment group, while control group were treated with an equal volume (100µl) of DMSO by oral gavage. The following criteria, based on the PPTP model, were used to initiate treatment and assess responses (423, 424):

- Peripheral engraftment of leukaemia was defined as the presence of >1% human CD45 cells (hCD45) in peripheral murine blood and the trigger for commencing TKI treatment;
- The presence of >25% hCD45 cells in peripheral murine blood was classified as an event and the efficacy of the drug was calculated until that point.

1x10⁶ cells were injected via lateral tail vein. Engraftment at day 8 was confirmed by blood sampling, with hCD45 cells in the range 2.5 – 19%. Treatment was commenced in 5 mice. There was no difference in the engraftment level between treatment and control groups 11.7±6.2% vs. 12.7±5.4% respectively ($p = 0.79$). The first cycle of foretinib was administered on days 8 to 12 and the second cycle days 21 to 25 after inoculation.

Early deaths occurred at day 9, when a control mouse was sacrificed because of poor health. A treatment cohort mouse also died at day 9 after the third treatment gavage (4.4), and thus had received only 2 full doses of foretinib. The organs of both mice were harvested and engraftment analysed by FACS. Engraftment was present in both bone marrows, 58.9% engraftment in the control compared with 10% in the treated mouse. The peripheral engraftment was comparable on day 8, 13.5% (vehicle) compared with 17.3% (foretinib). Preferential engraftment was present in the liver of the treated mouse, with 45.8% hCD45+ cells compared to the 9.2% in the spleen.

After completion of the first cycle of treatment (day 8 to 12), engraftment increased from 12.7 to 19.5% at day 15 in the control cohort (n=4 after early loss) and from 11.7% to 25% in the foretinib – treated cohort (n=4 after early loss). The level of engraftment at day 15 in each cohort was not significantly different ($p=0.34$ fig 5.40).

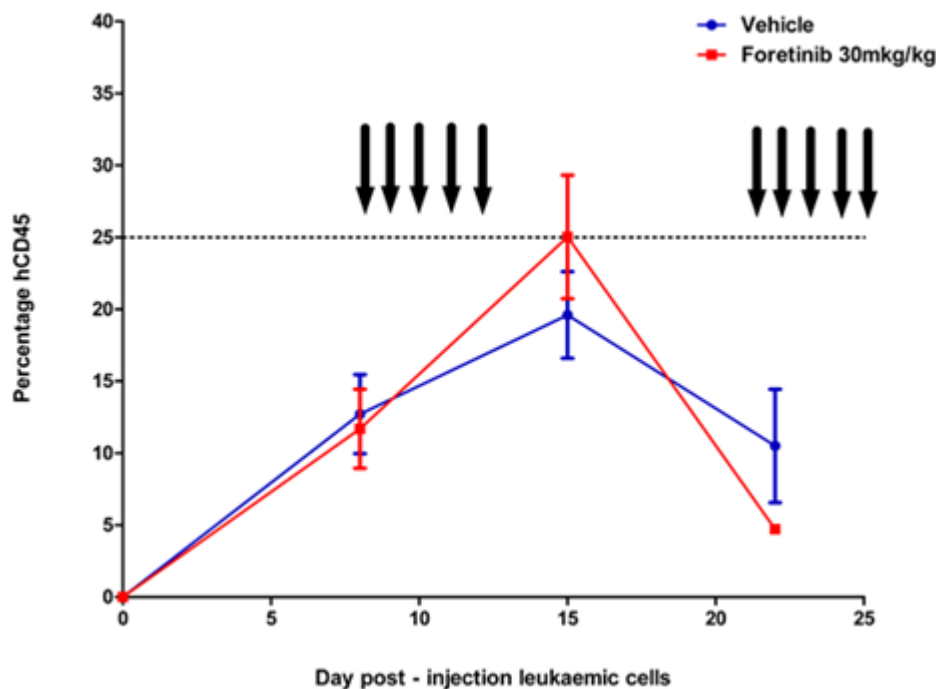


Figure 5.40 Peripheral engraftment of hCD45 cells in murine blood did not demonstrate a significant difference between the control and foretinib – treated cohorts. Each point is the mean engraftment of the mice alive at the time point, error bars are standard deviation.

By the PPTP criteria for assessing response to therapy, the foretinib cohort reached an “event” (>25% of murine peripheral consisting of human leukaemia cells) while the control cohort did not. There was no significant difference in the level of engraftment of hCD45 cells in murine peripheral blood at day 21 (control group 10.5%, foretinib treated 4.7%, $p=0.27$), but there was a statistically significant reduction in engraftment after the first course of treatment, mean $25 \pm 8.6\%$ reduced to $4.7 \pm 0.02\%$ ($p=0.04$, paired t - test). The reduction in hCD45 engraftment present in the control cohort was not significant ($p=0.17$ paired t - test). Fig. 5.41 shows the survival curves for the 2 cohorts, with median survival in the vehicle – treated cohort 36 days compared to 30 days (p - value = 0.269 Log – Rank test).

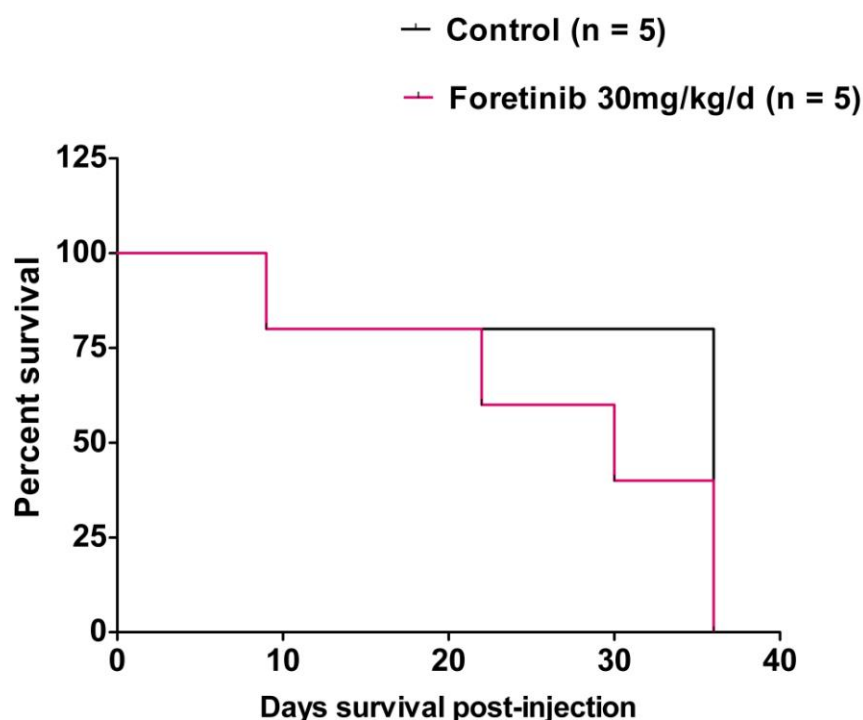


Figure 5.41 Kaplan – Meier curve for foretinib – treated mice compared to vehicle mice. No statistically significant difference in the median survival was demonstrated between the 2 cohorts. The median survival for mice treated with foretinib was 30 days in comparison with 36 days for the control mice.

| | Blood hCD45 (%) | Terminal engraftment hCD45 (%) | | | Survival |
|-----------------------------------|-----------------|--------------------------------|-------|-------------|----------|
| Mouse | Day 7 | Spleen | Liver | Bone marrow | Days |
| Control cohort | | | | | |
| 1.1 | 11.4 | 71.9 | | 68.9 | 36 |
| 1.2 | 4.9 | 71.95 | 68.73 | 17.9 | 36 |
| 2.3 | 13.89 | 61.9 | 49.67 | 53.3 | 36 |
| 2.4 | 13.53 | - | 71.95 | 58.85 | 9 |
| 2.5 | 19.86 | 63.13 | - | - | 36 |
| Foretinib – treated cohort | | | | | |
| 3.1 | 11.36 | 74.85 | 75.53 | 48.1 | 36 |
| 3.2 | 9.92 | 10.75 | 68.25 | 18.93 | 30 |
| 4.3 | 2.5 | 65.15 | 28.89 | 28.52 | 36 |
| 4.4 | 17.33 | 9.21 | 75.11 | 10.05 | 9 |
| 4.5 | 17.37 | 1.92 | 45.76 | 3.57 | 22 |

Table 5.11 Summary of hCD45 engraftment in peripheral blood at time of starting foretinib and murine organs at terminal cull from control and foretinib – treated cohorts.

A second foretinib – treated mouse died post – gavage on day 21, but by then it had received all doses in the first cycle of treatment and the first dose of the second cycle. The bone marrow, liver and spleen did not have a significant tumour load, with engraftment of

hCD45 at 1.1%, 3.5% and 1.9% respectively. Peripheral engraftment for this mouse had remained stable post the first course of treatment, day 8 (17.4%) and day 15 (17.2%).

A third, moribund mouse from the treated cohort was sacrificed, after receiving 2 full cycles, on day 30. The liver and spleen were haemorrhagic and there was limited infiltration of bone marrow, liver and spleen, with hCD45 counts of 16.5%, 28.2% and 10.1% respectively.

The remaining 2 treatment and 4 vehicle mice were culled at day 36 because of poor health and bone marrow, liver and spleen harvested. Comparison of the 4 control mice which survived to day 36 to the treated cohort demonstrated higher average infiltration of hCD45 in bone marrow, 46.6% compared to 38.3%. The tumour load in the liver (63.8% control; to 71.6% treated) and the spleen (68.6% control; 70% treated) was lower in the control cohort.

The majority of the hCD45 population in each of the organs in the control mice were a recapitulation of the original B – precursor leukaemia, with a mean CD34-CD19+10+ cell count of 70.95% (± 16.4) in the bone marrow, 69.1% (± 16.4) liver and 92.85% (± 0.63) in the spleen. Treated mice displayed mean CD34-19+10+ cell counts of 75% in the bone marrow and 78% in the spleen, but only 47% in the liver. Mouse 3.1 had only 28% of the CD45+CD34- cells that were CD1910+ despite a single CD10+ population.

The efficacy of the current treatment schedule for foretinib was not proven. There was survival advantage in this study. However, a statistically significant reduction in peripheral engraftment was observed after the first cycle of treatment.

5.9.3 Assessment of *in vivo* activity of dovitinib

Using the ALL – 20 model the *in vivo* efficacy of dovitinib was assessed. Eleven immune deficient mice (NOD/Scid) were used in this experiment, 6 dovitinib – treated mice and 5 control mice. 1×10^6 cells per mouse were inoculated via the lateral tail vein on day 1. The treatment cohort was planned to receive 3, 5 – day cycles of 65mg/kg/d dovitinib by oral gavage on days 7 – 11, 14 – 18 and 20 – 24

Peripheral engraftment was assessed on day 4 post – inoculation because of early engraftment, with a mean hCD45+ cell counts of engraftment 0.61% (SD \pm 0.82%), range 0 – 2.9%. Therapy was unable to start at a weekend and thus treatment was started at day 7. Engraftment in the randomised control group of 5 mice was 1.02% (SD \pm 1.1%) and in the 6 treatment mice was 0.32% (SD \pm 0.25%). There was no statistically significant difference between the two groups (p = 0.25 t – test).

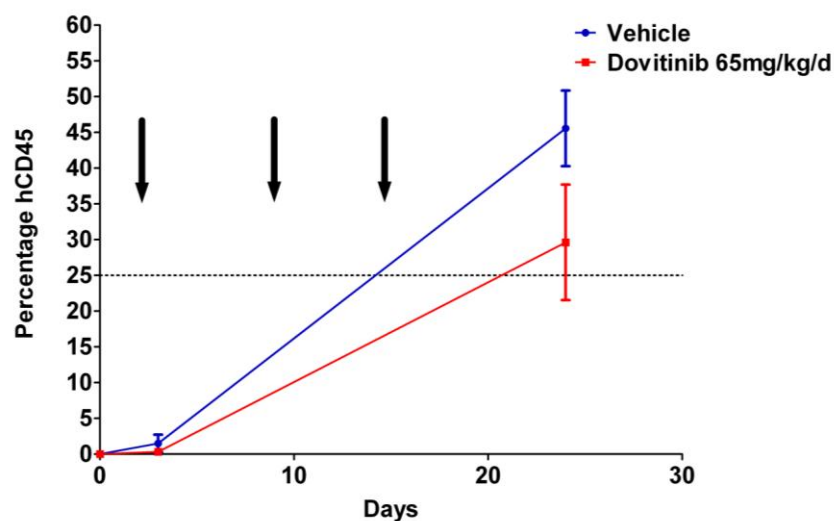


Figure 5.42 Peripheral engraftment of hCD45 in murine blood in response to dovitinib treatment. Each point is the mean engraftment of the mice alive at the time point, error bars are standard deviation. No difference was present between the 2 cohorts at time of commencing dovitinib therapy.

Peripheral engraftment in the murine blood at day 24 (after the third cycle of treatment) demonstrated a lower CD45+ cell count in the dovitinib treatment cohort (n=5), mean peripheral hCD45 29.62% (SD \pm 8%) compared to the control 45.56% (SD \pm 5.28%), p=0.012 t –

test (fig 5.42). Peripheral sampling was only possible in 3/5 vehicle mice because of high blood viscosity. Despite the reduced engraftment in the treatment group, according to PPTP classification an event had occurred ($hCD45 > 25\%$), and so objective response could be documented.

The median survival for the control group was 26 days and the dovitinib – treated cohort 29 days (fig 5.43, $p=0.08$ by log – rank Mantel – Cox test). The median survival was not related to the level of engraftment, with the 4 shortest survivals (day 25) displaying a wide range of day 4 engraftment, 0.1% - 2.9% (table 5.12).

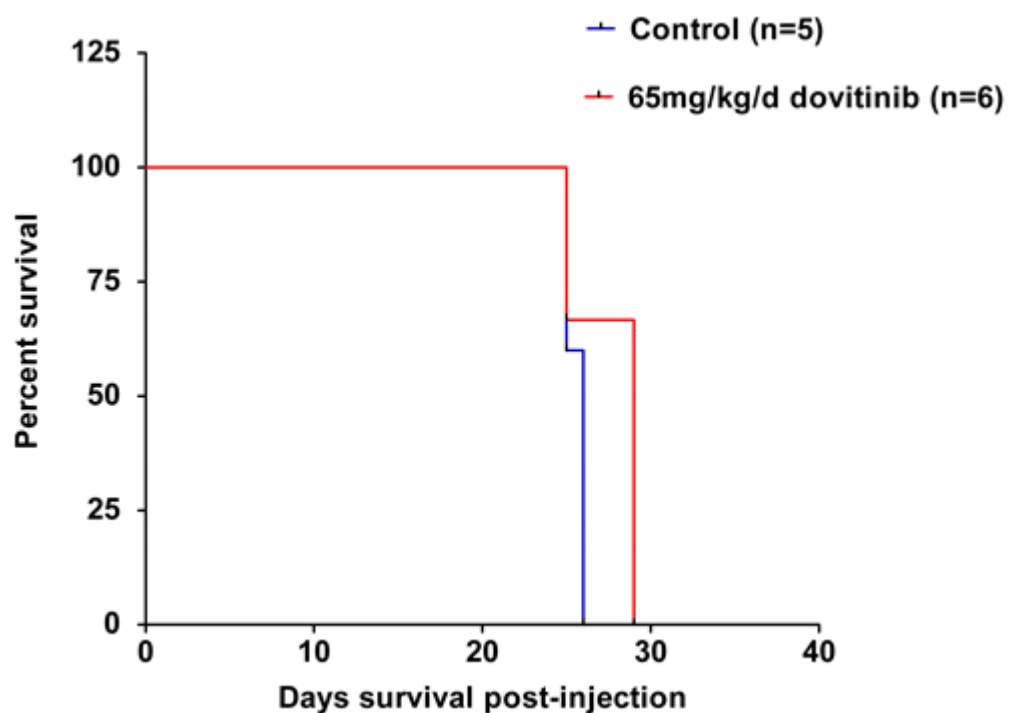


Figure 5.43 Kaplan – Meier curve for dovitinib compared to vehicle mice. No statistically significant difference was demonstrated between the 2 cohorts. The median survival for mice treated with dovitinib was 29 days in comparison with 26 days for the control mice.

Tumour load was estimated by weighing the harvested organs and tumour infiltration was measured by FACS analysis. A statistically significant difference in spleen weight was observed with 0.3g (± 0.09 g) in the control cohort and only 0.115g (± 0.069 g) in the treated group ($p = 0.0029$, t – test) (fig 5.44). No difference in liver mass was observed (2.3 g compared to 2.1g, t – test $p=0.59$).

Four of the five control mice (2.1, 3.3, 4.2, 4.5) and 1 dovitinib – treated mouse (4.4) died during a weekend; consequently, the organs were haemorrhagic and necrotic at time of analysis. No viable cells were evaluable for control mouse 4.5, which was excluded from FACS analysis.

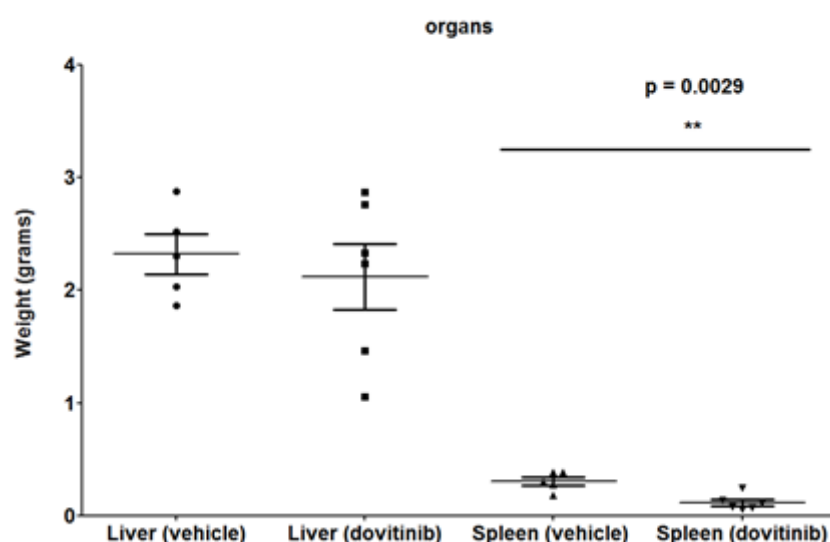


Figure 5.44 Spleens harvested from mice in the control group were significantly heavier than the dovitinib – treated cohort ($p = 0.0029$).

| | Blood hCD45 (%) | Terminal engraftment hCD45 (%) | | | Survival |
|------------------|-----------------|--------------------------------|-----------------|-----------------|----------|
| Mouse | Day 4 | Spleen | Liver | Bone marrow | Days |
| Control cohort | | | | | |
| 1-3 | 0.9 | 92.2 | 95 | 42.6 | 25 |
| 2-1 | 2.9 | 24.2 | 97 | 39.4 | 25 |
| 3.3 | 0.6 | 100 | 66.7 | 23.8 | 26 |
| 4-2 | 0 | 66.6 | 8 | No viable cells | 29 |
| 4-5 | 0.7 | No viable cells | No viable cells | No viable cells | 26 |
| Treatment cohort | | | | | |
| 1-1 | 0.1 | 91.1 | 70.9 | 99.2 | 25 |
| 1-2 | 0.4 | 88.1 | 89.7 | 57.4 | 29 |
| 3-2 | 0 | 86 | 97.3 | 69 | 29 |
| 4-1 | 0.6 | 54.4 | 97.1 | 36.6 | 29 |
| 4-3 | 0.5 | 90.2 | 80 | 51.8 | 29 |
| 4-4 | 0.1 | No viable cells | 54 | 17.1 | 25 |

Table 5.12 Summary of hCD45 engraftment in peripheral blood and murine organs at terminal cull from control and dovitinib – treated mouse cohorts. The bone marrow of the control mice 4.2, all organs from mouse 4.5 and the spleen of treated mouse 4.4 were necrotic at time of FACS analysis.

Fig 5.45a - c shows the hCD45 engraftment of the dovitinib – treated and control cohorts at time of terminal cull. Mean engraftment was lower in the control group in bone marrow (26% vehicle cf. 55% dovitinib) and liver (61% cf. 82%), but higher in the spleen (71% cf. 68%).

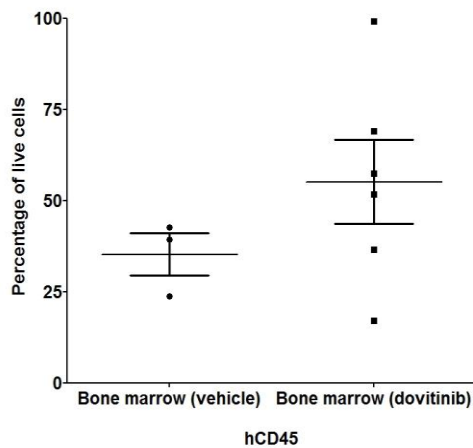


Figure 5.45a

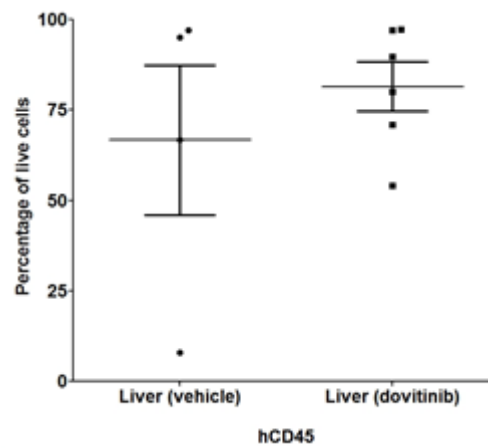


Figure 5.45b

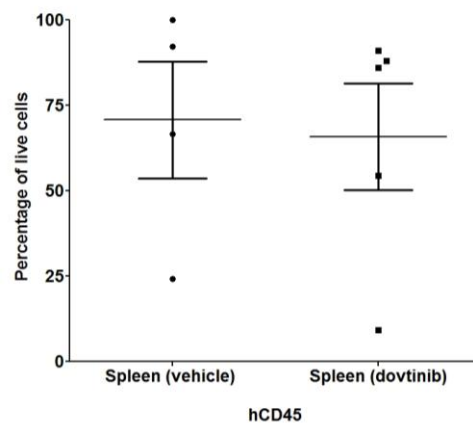


Figure 5.45c

Figure 5.45 FACS analysis of organs at terminal cull in control and dovitinib – treated cohorts. No statistically significant differences in the tumour load were identified in the organs of mice treated with DMSO or dovitinib.

Analysis of the levels of engraftment did not reveal a difference in liver ($p = 0.63$) or spleen ($p = 0.83$), however there was a trend to reduced hCD45 engraftment in the bone marrow ($p = 0.07$) of the vehicle cohort. The composition of the infiltrating leukaemia recapitulated the CD45+CD34-leukaemia in all organs. Evaluation of the maturity of the cells depended on the degree of cell death present in the organs, with CD45+CD34-CD19+CD10+ cells the major population in each mouse.

In summary, in this aggressive ALL xenograft model 65mg/kg/day, dovitinib does not offer a survival advantage. However, the level of peripheral engraftment at day 24 was significantly different. Evaluation of the level of engraftment was difficult because of necrosis of the murine organs, which reflects major infiltration and necrosis. Further dosing schedules for both TKIs warrant further exploration.

5.10 Discussion

In this study the *in vitro* and *in vivo* anti – leukaemic properties of the 2 candidate TKIs, foretinib and dovitinib, identified as potential therapeutic candidates in the cell line and primary cell screens have been investigated. Both TKIs profoundly affected the expression of cell cycle – regulating proteins, induced apoptosis and sensitised leukaemic cells to conventional chemotherapeutic agents. While the effects of these TKIs are well documented in solid tumours, this study is the first to investigate the role of foretinib or dovitinib in childhood acute lymphoblastic leukaemia.

The results demonstrate that both foretinib and dovitinib exert a significant anti – leukaemic effect at nanomolar concentrations in cell lines and primary cells. Of the 2 TKIs, dovitinib demonstrated a lower IC₅₀ in 5/6 cell lines; whereas foretinib was more potent in REH and the primary cells, ALL – 20.

The differences in potency might arise because the two drugs act against different RTKs, although they include a similar spectrum, VEGFR, PDGFR, Kit and FLT3 (table 5.1). Whether the difference in molecular structure or the avidity for the RTKs explains the differences in response were not assessed in this study. Dovitinib is more potent when assessed by *in vitro* kinase assay against FLT3 and FGFR1 (415). It has additional activity against CSF – 1R and FGFR3, which is not reported in foretinib. Foretinib, in turn, possesses activity against Met, Ron and Tie – 2. As observed in the previous chapter, all the cell lines express *FGFR1* mRNA transcript but the level of expression did not predict sensitivity to the TKI. This lack of correlation with a specific receptor in the cell lines investigated could indicate that numerous pathways are targeted by the TKIs. The wide range of

concentrations required to inhibit the cell lines is consistent with the possibility that anti – leukaemic effects are mediated through different pathways in different leukaemias.

The difference in potency was evident in the cell cycle profiles when cells were treated with 1µM of either drug. While both TKIs induced accumulation of sub – G1 cells in 4/6 cell lines dovitinib induced more cell death in Nalm 17, REH, SD – 1 and SupB15, at an earlier time point. Dovitinib did not induce the G2/M arrest present in REH and SupB15, which supports the notion that TKIs do not affect the cells through identical mechanisms of action.

The induction of G2/M arrest in cancer cells has been reported in response to treatment with foretinib (425-427) and dovitinib (428) . The G2/M transition of eukaryotic cells into mitosis is governed by Plk-1, cyclin B1 and Cdc25; and the checkpoint is regulated by the cyclin – kinase inhibitor p21. The accumulation and subsequent degradation of cyclin B1 is required for cells to progress successfully through mitosis. In hepatic, ovarian and CML cell lines, foretinib – induced G2/M arrest has been reported with associated reduction in cyclin B1 (426, 427). In the present study, 4 cell lines, REH, SupB15, Nalm 6 and TOM – 1 demonstrated G2/M arrest, although differing patterns of expression of cyclin B1 were identified.

In REH and SupB15, the G2/M arrest was associated with an early reduction in cyclin B1 expression, followed by apoptosis. This pattern of arrest and apoptosis has been reported in the CML cell line, K562 (425). Dufies *et al.* reported foretinib – induced reduction of cyclin B1 mediated via JNK – dependent mechanisms which lead to degradation of the mitotic transitional proteins, Plk – 1, cyclin B1 and Cdk1 (cdc2), resulting in G2/M arrest, polyploidy and apoptotic death by mitotic catastrophe (425). The group found that caspase inhibition reduced the accumulation of cells in sub – G1 and was associated with an increase in polyploid cell numbers. In the current study, a reduction in cyclin B1, G2/M arrest and apoptosis was present in REH and SupB15 but neither cell line displayed increased polyploid cell numbers in response to foretinib treatment.

G2/M arrest and polyploidy was present in Nalm 6 and TOM – 1, although these cell lines did not demonstrate significant cell death. Here, cell cycle arrest was preceded by an accumulation of cyclin B1, similar to that seen in the cell lines which did undergo apoptosis.

A similar phenomenon of G2/M arrest and polyploidy associated with an increase in cyclin B1 has been reported with the cyclin – dependent kinase inhibitor, butyrolactone (429). Butyrolactone is cdc2 inhibitor in non – synchronised cells. It binds to the kinase, interfering with the ability form the cyclinB1 – cdc2 complex and hence progress through normal mitosis. This finding suggests that the accumulation of polyploid cells in Nalm 6 and TOM -1 was likely due to foretinib – induced disruption of the cyclin B1 – cdc2 complex. The failure of cyclin B1 degradation, normally required for the exit of cell from mitosis, results in cells skipping mitosis and the accumulation of a population of cells with increased DNA content (8n). The decrease in cyclin B1 correlates with the progression of cells through a new cell cycle. These data suggest that the inhibition of the G2/M is not complete, and some cells slip through mitosis.

The cells lines in which G2/M arrest was induced also demonstrated an early accumulation of p53 after 24 hours of foretinib treatment, with induction of p21. The 2 cell lines in which G2/M arrest was not induced (Nalm17 and SD -1) did not demonstrate significant early p53 accumulation. Both p53 and p21 are involved in the regulation of the G2/M checkpoint, with p53 reducing cyclin B1 production by inactivating the cyclin B1 promoter (430); p21 directly inactivates the cyclinB1 – cdc2 complex thus inhibiting mitosis (431).

These data suggest the effect of foretinib on the cell cycle may be protean, and will depend on the cellular context. Foretinib may inhibit the cyclinB1 – cdc2 complex directly through cdc2 inhibition or via p53 – mediated mechanisms or possess the ability to induce JNK – activated degradation of cyclin B1 followed by cell death. The mechanism of arrest and possible cell death will need further investigation.

The G2/M arrest induced by dovitinib in Nalm 6 and TOM -1 has been reported in a FGFR1 – expressing hepatocellular carcinoma (HCC) cell line and was associated with a reduction in cyclin B1 (428). The lack of G2/M arrest in REH and SupB15 might be due to the high concentration of dovitinib used for the cell cycle profiling or alternatively that it exerts its effect through different pathways. Dovitinib induces G1 arrest in FGFR3 expressing Waldenström Macroglobulinaemia (432); thus the effect of the TKIs on the cell cycle most likely reflects the particular target it inhibits and is not a function of the drug itself. This notion was highlighted by Odgerel *et al.* (433), who reported differential cell cycle patterns in AML cell lines with constitutively activated FLT3 after treatment with the FLT3 inhibitor, PKC412. Cell lines with FLT3 mutations underwent apoptosis, while those with wild type receptor arrested in G2/M.

The accumulation of p53 after foretinib – treatment was not DNA damage related, as demonstrated by the lack of increase in γ H2AX foci. Increased expression of p53 can result from a myriad of stressors, mutations, hypoxia, loss of repression by MDM2, inhibition of ubiquitin, deregulation oncogene expression and release from Akt inhibition. The accumulation of the tumour suppressor may be explained by the release of p53 repression imposed by phospho – Akt when the cell lines are treated with foretinib, as observed in Nalm 17.

The accumulation of cells in sub – G1 indicates that the effects of both TKIs were not solely due to cell cycle arrest. Both foretinib and dovitinib induced apoptosis as demonstrated PARP– 1 protein cleavage, even at low doses of TKI. Caspase – dependent apoptosis induced by treatment by dovitinib and foretinib as seen in this study has been reported in AML and ovarian cell lines (427, 434). While the TKIs induced apoptosis in susceptible leukaemias, it is unlikely that a single agent TKI will be effective in eradicating the disease in a patient.

The impact of combined treatment was assessed since any novel drug would be included in a multi – agent regimen in clinical practice. The ultimate goal for the use of TKIs in the treatment of cancer is twofold. First, in high risk or relapsed disease, the addition of a TKI to an established chemotherapy regimen could sensitise the tumour to the conventional cytotoxics. Second, in lower risk disease a successful combination might allow for dose reduction of particularly toxic agents. To this end cells were treated with both TKIs in combination with a variety of cytotoxic drugs. Significant synergy was found when foretinib was combined with 7 different conventional cytotoxics in both cell lines and primary cells. Notably, synergy was observed in cell lines that did not demonstrate significant response to the TKI alone. The impact of dovitinib on combination therapy was more variable.

The precise mechanisms by which the TKIs sensitise malignancies to conventional chemotherapy are uncertain, but the inhibition of pro – survival pathways should result in increased susceptibility to chemotherapy. Successful inhibition of RTKs and their pro – survival intracellular signalling cascades, such as activated AKT/PKB, and sensitisation to conventional cytotoxics has been reported with combinations of IGF-1R inhibitors and chemotherapy in Ewing’s sarcoma (435) and multiple myeloma (436).

Concurrent treatment of the leukaemias with both TKIs and dexamethasone was strongly synergistic in all cell lines, including the steroid – resistant Nalm 6, SD -1 and REH, despite the latter lacking a glucocorticoid receptor (422) . Bachman *et al* reported the sensitisation of a steroid – resistant primary xenograft to dexamethasone with the inhibitor multikinase inhibitor SU11657, although not in the cell lines investigated here (422) .

One possible mechanism of sensitisation to steroids is TKI – induced expression of pro – apoptotic Bcl – 2 family members. Huynh *et al* (426) reported foretinib induced the expression of Bim in hepatocellular xenografts and this protein is essential for the induction of GC – induced apoptosis (422, 437). Thus alteration in Bcl-2 proteins may tip the balance

in favour of cell death. Sensitisation may also occur through GC receptor – independent mechanisms, since the reduction in viability induced by foretinib and dexamethasone co – treatment in REH was not via apoptosis, as demonstrated by the lack of increase in Annexin V – staining cells or increased PARP – 1 cleavage in comparison with foretinib alone. The lack of GR expression in REH supports potentiation via GR – independent mechanism, unless the TKI itself induces the expression of the receptor protein.

The interaction between foretinib and dovitinib in combination with the DNA – damaging agents is of significant clinical interest. Foretinib sensitised cells to mitoxantrone, which is used in the re – induction phase in relapsed ALL (438). The synergy displayed between foretinib and the anthracyclines might allow a reduction in the dose of anthracycline required for patients who have received a significant cumulative dose of cardiotoxic drugs. However, TKI – induced cardiotoxicity in adults is well described (439), which could limit the use of TKIs in combination with anthracycline/anthraquinones.

The impact of sequential exposure to TKI and chemotherapy was not explored in this study, although timing of administration might affect the quality of the interaction. Brown *et al.* (397) demonstrated the sequence – specific nature of the FLT3 inhibitor CEP – 701 and conventional cytotoxic in childhood ALL. Cells which were pre – treated with CEP – 701 and followed by chemotherapy demonstrated significantly less response compared to the samples initially treated with chemotherapy and subsequent exposure to CEP – 701. It has been suggested the sequence – specificity is due to the effect CEP – 701 exerts on the cell cycle, which might interfere with subsequent cell – phase specific chemotherapy. In general the addition of FLT3 inhibitors prior to chemotherapy induces antagonism, whereas the addition of the TKIs after or at the same time as the conventional cytotoxic results in a synergistic interaction (440, 441). The sequential timing of dovitinib in relationship to chemotherapy could be realised as it has a half – life of 13 hours (417), which would allow flexibility in dosing. The half – life of foretinib is approximately 40 hours (413), which would diminish the feasibility of meaningful sequential dosing.

The synergy observed between dovitinib and DNA – damaging agents or dexamethasone has previously been described in Waldenström's macroglobulinemia cells (432), where melphalan and dexamethasone exerted a moderate synergistic effect. The results described here are the first evidence of interaction between foretinib and conventional chemotherapeutic agents.

To investigate the *in vivo* efficacy of both TKIs, a murine xenograft of an *in vitro* sensitive primary cell was created. While the *in vivo* experiments did not confirm an objective response to the TKIs, foretinib induced a statistically significant reduction in peripheral hCD45 cells and dovitinib demonstrated a trend to increased survival ($p = 0.08$).

A reason for this lack of objective response may be the aggressive nature of the ALL - 20 xenograft model. The rapid rates of engraftment might have led to too great a tumour load by the time treatment started. The *in vivo* efficacy of dovitinib has been investigated in a xenograft model of the myeloid FLT3 - ITD cell line MV4;11 (434). The myeloid leukaemia took 23 days to engraft in comparison to the 4 – 8 days in this study. The MV4;11 control mice displayed a median survival time of 51 days with median survival 134 days in the dovitinib – treated mice. The untreated mice in the present study survived for 25 – 36 days. The engraftment in the untreated mice was also low, 2 – 19% at day 51, while up to 95% engraftment reported here. The effects of dovitinib in slower engrafting models might be more promising. Foretinib has not been examined in a leukaemic model.

Another limiting factor in this study was the small numbers of mice in each cohort and attrition because of misgavage of the TKIs. The decision to continue with oral treatment was based on the lack of evidence for administration of either agent by the intraperitoneal route. The further loss of viable organs for FACS analysis limits the veracity of tumour load comparison in the dovitinib experiment. It seems likely though, that the necrosis was due to thrombosis and haemorrhage induced by massive tumour infiltration. Using the

untreated and vehicle cohorts of the foretinib and kinetics experiment as historical controls, the level of hCD45 engraftment is similar to that of the dovitinib – treated mice.

The dose schedule used for the dovitinib experiments (65mg/kg/day) has demonstrated good responses in myeloid and solid tumour xenografts (428, 434). The dose chosen for foretinib, 30mg/kg/day, has been used in solid tumour xenografts with good response (297, 426), although it was given daily. The 5 days on/ 9 days off schedule was identified as the maximum tolerated dose (MTD) in a recent phase 1 study in adult solid tumours. Excellent pharmacodynamic activity was demonstrated (413), with significant post – exposure reduction in phosphorylated RTKs. The limited response in this study may be attributable to an inadequate dosing schedule and a higher dose given continuously might have provided a better response. Neither foretinib nor dovitinib significantly altered the maturity of the engrafting population. The bulk cell population after treatment were still the CD34-CD1910+ B – precursor, thus indicating that these TKIs do not induce differentiation in *in vivo* models.

In conclusion, *in vitro* efficacy of 2 TKI as single agents and in combination with conventional chemotherapies has been demonstrated in the childhood ALLs in this study. Objective responses to either TKI could not be in an established and validated primagraft model. However, further exploration within the murine xenograft with continuous dosing and possibly slower engrafting leukaemias would be justified to fully investigate the potential clinical use of these agents.

6 Conclusions and future work

The work undertaken in this study has demonstrated that further investigation into the use of TKIs in treating childhood ALL is warranted. Using the complementary approaches of phospho – protein arrays and an inhibitor library numerous possible targets have been identified.

The phospho – RTK array data demonstrated heterogeneous phosphorylation of a significant number RTKs in primary ALLs. Data from the R&D array system was consistent with published literature in demonstrating increased FLT3 phosphorylation in the hyperdiploid ALLs. Novel data included the identification of increased EphA2 phosphorylation in ALL with normal cytogenetics, increased phosphorylation signals of Mer and FGFR2 in ALLs with high white cell count at diagnosis and the presence of increased PDGFR β in ALLs with MRD detectable by flow cytometry at the end of induction. In contrast to published data, the Raybiotech array identified increased phosphorylation of Axl in primary ALLs with proficient responses to IR – induced apoptosis. The hypothesis that (R)TKs are activated in apoptotic defective leukaemias was not demonstrated in this study. Further validation these potential targets is required.

The inhibitor library screen of cell lines and primary ALL revealed heterogeneous activity of the TKIs screened. While no single inhibitor was active in all samples investigated, 4 inhibitors (bosutinib, CEP – 701, dovitinib and foretinib) were active in 4 of the 5 cell lines screened. These 3 drugs have activity against common targets FLT3, VEGFR – 1 and 2 and PDGFR β . Similarly, in the primary ALL screen TKIs with multikinase activity against FLT3, VEGFR and PDGFR families were the most potent. From the data in this study, the inhibitors with a broad spectrum of activity were most active. Other candidate inhibitors with a reportedly narrower spectrum of activity included the Met/ALK inhibitors and the irreversible EGFR inhibitors. The most likely mechanism of action for these drugs were via off – target effects.

The 2 candidates, dovitinib and foretinib taken forward for further preclinical investigations demonstrated nanomolar activity in cell line and primary ALL assays. Both drugs inhibited cell growth, either via the induction of apoptosis or cytostasis, and revealed a predominantly synergistic effect when combined with conventional cytotoxics. The most notable interaction was the potent sensitisation of steroid – resistant cell lines to dexamethasone when incubated with dovitinib or foretinib. In the murine primagraft dovitinib and foretinib did not extend median survival, but limitations to the model have been identified.

These data support the on-going investigation into the use of TKIs in non – Ph+ ALL. As reported in this study, inhibitors demonstrated significant activity in cell lines resistant to conventional chemotherapy and potent sensitisation of cell lines to steroids. The sensitisation of REH to dexamethasone via GR – independent mechanisms highlights the potential of TKIs to exploit novel pathways to treat resistant leukaemias. The activity of non – Abl inhibitors in the Ph+ ALL cell lines, SD – 1 and SupB15 is of particular interest as resistance to TKIs is a particular concern in the management of Ph+ ALL. Further investigation into the action of the non – Abl identified in this study would be of interest as alternate targets may be identified.

A limitation of the data presented in this study is the lack of evidence demonstrating the inhibitors work through the putative targets. In the EGFR/HER2 inhibitors, BIBW – 2992 and CI – 1033, the mechanism of action is most likely due to off – target effects. In clinical practice it could be argued that if the goal of any therapy is the eradication of leukaemia, it is debatable whether the concept of on – and off – target is vital, if the drug achieves cell death. However, the identification of pathways is important to understand potential toxicities, interactions with other drugs in multi – agent regimens and ultimately define the “true” targets to understand a drugs mechanism of action.

While this study did not identify particular targets, evidence from the arrays and inhibitor screen suggest further investigation into the role of RTKs in leukaemias is warranted. Approaches to further validate and identify targets include:

6.1 Validation of phosphorylated RTKs identified by phospho – RTK arrays

The identification of the phosphorylated RTKs, Axl, EphA2, FLT3, FGFR2 and Mer by the phospho – RTK arrays need to be validated because inhibitors for all of these RTKs are available or coming through the pharmaceutical pipeline. While this project has demonstrated a screening approach based on arrays and cell viability can identify candidate RTKs and compounds, it has not identified or validated targets. The goal of this work would be to confirm the presence of the proposed targets. To fully characterise the potential targets, mRNA transcript and protein should be undertaken in original samples used in the study, identifying the total and phosphorylated forms of the RTKs. Unfortunately, because of limited amount of sample this will not be achievable. If sufficient sample were present and this could be performed, validation in a second cohort would be vital.

6.2 Genomic characterisation of primaries at baseline and in response to TKIs

To date, projects undertaking sequencing of the tyrosine kinome have not identified obvious gain – of – function mutations in ALL (442). Although very few specific gene mutations have been identified leading to kinase activation, investigation of the molecular pathways affected by TKIs may identify susceptible gene expression profiles. Microarray analysis of the alterations in the gene expression profiles of primary leukaemias in response to TKIs identified in the library screen may elucidate the signalling modules/pathways involved in determining sensitivity or resistance. The establishment of gene expression profiles of primary cells at baseline and after treatment with candidate inhibitors may uncover both on – and off – target mechanisms of action.

6.3 Target Deconvolution: Identification of protein targets

The large number of activated RTKs identified by the arrays in this study and the lack of universal response of the samples to a single inhibitor suggests that, unlike CML, ALL does not express one individual specific activated tyrosine kinase. Alterations in the leukaemia cells internal phosphoproteomic environment in response to treatment with an inhibitor by would complement any alterations identified in the genomic approach. The combined system biological approach would add significant data to our understanding of childhood ALL. Preliminary experiments to assess changes in tyrosine phosphorylation in ALL cell lines have been undertaken and significant alterations in phosphorylation signals in cell lines treated with foretinib 1 μ M were identified (fig 6.1).

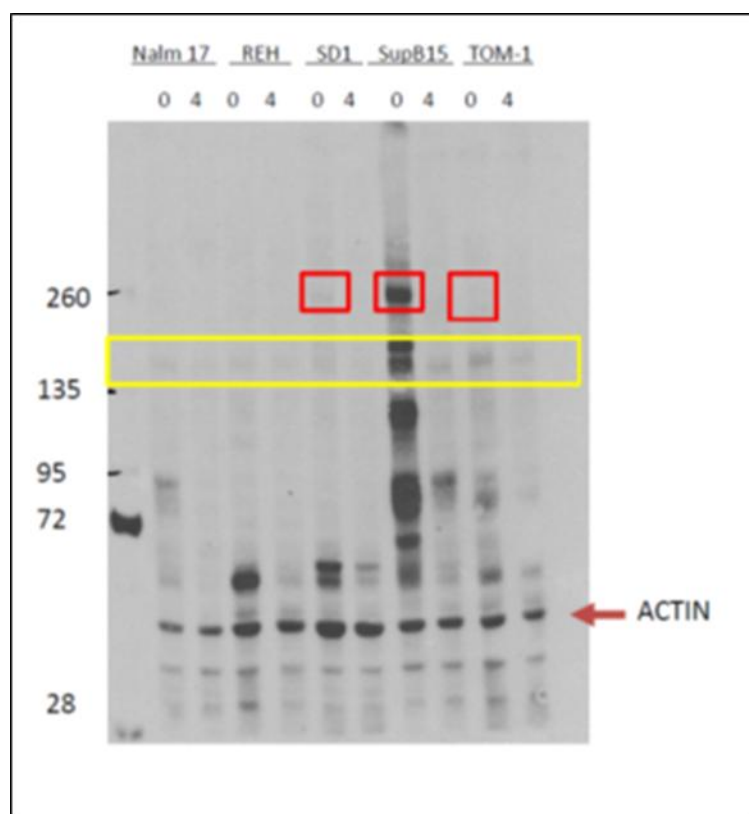


Figure 6.1: Preliminary experiments in pre – B ALL cell lines reveal altered phosphorylation signals in response to incubation with foretinib. 5 ALL cell lines were incubated with 1 μ M foretinib for 4 hours. Western blotting with pan – phospho – tyrosine antibody revealed reduction in signal in regions.

The dominant changes were visible in the consistent the region containing RTKs, MW 130 – 260kDa. To investigate the putative targets in the region between 130 – 260kDa,

immunoprecipitation of cell lysates with a pan – phospho – tyrosine antibodies followed by liquid chromatography and tandem mass spectrometry (LC – MS/MS) – based proteomic approaches may delineate multiple constitutively phosphorylated RTKs and the associated activated cellular pathways.

To help generate protein target hypotheses, the quantitative changes in phosphopeptides in response to treatment could be assessed by stable isotope labelling amino acids in cell culture (SILAC), this reproducible technique is able to compare the proteomic profile of 2 cell populations. The incorporation of a labelled amino acid analogue into proteins synthesised by a cell population allows for quantification of alteration of peptide levels after treatment. The labelled cell lines would be incubated with the candidate TKI, samples lysed and immunoprecipitated with a pan – phospho – tyrosine antibody. Phospho – tyrosine enriched peptides would be produced by in – gel digestion. Further enrichment for phosphopeptides using immobilised metal affinity chromatography (IMAC), followed by a second step for phosphotyrosine peptides with the use of titanium dioxide beads (TiO₂). The peptide mixture is separated on liquid chromatography gradient followed by tandem mass – spectrometry. A drawback of this approach is SILAC requires cycling cells, thus this may approach would be limited to cell lines.

A second more complex approach is the compound – centric chemical proteomic approach. To investigate the spectrum of proteins interacting with the inhibitor, the drug is conjugated to a biochemically inert matrix to capture proteins which will interact with the analogue. Detailed structural activity relationships would need undertaking to ensure the functionalised molecule has similar properties to the original; any alteration of the drug's structure to act as "bait" may interfere with the protein binding of the original compound and change its biological activity. The proteins are subsequently eluted and assessed by LC – MS/MS. While more complicated, this technique would be the preferred method for further identifying candidate drug targets because this technique could be used in cell lines and in non – cycling primary ALLs.

The candidate drugs, dovitinib and foretinib, demonstrated significant in vitro activity, but the reasons for lack of activity in the murine model is at present uncertain. The primagraft work in this study does suggest the compounds may be active if the dosing schedules are optimised. Further xenograft work to expand the murine cohort and investigate the possible in vivo ability for foretinib and dovitinib to sensitise dexamethasone – resistant leukaemias to dexamethasone should be pursued:

6.4 Xenograft Modelling:

The most mature paediatric drug testing programme, the NCI PPTP has investigated the multikinase inhibitors in ALL xenografts with limited objective response (407, 410, 443). Each experiment consists of 6 pre – B ALL xenografts and of the TKIs investigated limited objective responses have been described. While no objective response was present in the model in this study, the leukaemia engrafted very rapidly and dosing may have been too late for a realistic chance of treatment effect. Development of a more comprehensive panel of xenografts including a range of different primary ALL samples would facilitate the full assessment the potential activity of both TKIs, as would optimisation of the dosing schedules.

6.4.1 Identification of dexamethasone – resistant primary sample

Dexamethasone revealed the greatest synergistic activity with foretinib and dovitinib in the cell lines and the primary ALL (ALL – 20). The combination of TKI and steroid requires further investigation, not only to explore the clinical potential, but also to elucidate mechanisms of dexamethasone resistance and sensitisation. The identification or establishment of a dexamethasone – resistant primary ALL may enable further assessment whether foretinib and dovitinib can sensitise a dexamethasone – resistant ALL to dexamethasone in vitro. To identify the molecular pathways involved in dexamethasone resistance/sensitisation, microarray analysis of the dexamethasone – resistant primary leukaemia would be performed at baseline, after exposure to sub – IC₅₀ doses of

dexamethasone and TKI and after combination of TKI and steroid to identify the alterations in gene expression profile.

6.4.2 Combination of dexamethasone and foretinib/dovitinib in dexamethasone – resistant murine model

The combination of foretinib/dovitinib with dexamethasone needs further investigation in the in vivo primagraft model. This would enable the comparison of TKI monotherapy, with dexamethasone monotherapy and the combination of the 2 agents. To assess sensitisation to dexamethasone, a suggested experiment would compare cohorts of mice treated with steroid, TKI or in combination. The first cohort of mice would receive dexamethasone at an anti-leukaemic dose reflecting that used in the clinical if possible, while a second cohort would receive the TKI. Both cohorts of mice would receive TKI and dexamethasone at clinically relevant equivalent doses. The third and fourth cohorts would receive reduced (50%) doses of foretinib/dovitinib and reduced (50%) doses of the dexamethasone, respectively at same scheduling. The fifth cohort would receive a combination of 50% TKI and 50% dexamethasone.

The median survival of each cohort would be documented to assess the impact of each treatment. If the combination of the TKI and dexamethasone were to add a survival benefit, differences in the gene expression profiles of leukaemia cells harvested from the murine organs may be able to identify the molecular pathways involved in the sensitisation.

On basis of the work in this thesis, TKIs are worthy of further investigation as the data presented hints at the role of several as potential therapeutic agents, particularly in the context of combination therapy with conventional chemotherapies.

7 References

1. Craft AW. Childhood cancer—mainly curable so where next? *Acta Pædiatrica*. 2000;89(4):386-92.
2. Statistics OoN. Mortality Statistics, England and Wales Accessed 2013
3. Doll R. THE EPIDEMIOLOGY OF CHILDHOOD LEUKEMIA. *J of the Royal Statistical Society Series a-Statistics in Society*. 1989;152:341-51.
4. Parkin DM KE, Draper GJ, Masuyer E, Michaelis J, Neglia J, Qureshi S, Stiller CA. In: *International Incidence of Childhood Cancer, volume II (IARC Scientific Publications No. 144)*. 1998:366.
5. Steliarova-Foucher E SC, Kaatsch P, Berrino F, Coeberg JWW, Lacour B, Parkin M. Geographical patterns and time trends of cancer incidence and survival among children and adolescents in Europe since the 1970s (the ACCIS project): an epidemiological study. . *Lancet*. 2004;364:2097 - 105.
6. McNally RJ Cairns DP, Eden OB, Kelsey AM, Taylor GM, et al. . Examination of temporal trends in the incidence of childhood leukaemias and lymphomas provides aetiological clues. *Leukemia* 2001;12(10):1612 - 8.
7. Spix C, Eletr D, Blettner M, Kaatsch P. Temporal trends in the incidence rate of childhood cancer in Germany 1987–2004. *Int J Cancer*.2008;122(8):1859-67.
8. Hrusák O TJ, Zuna J, Polouková A, Kalina T, Sary J. Acute lymphoblastic leukemia incidence during socioeconomic transition: selective increase in children from 1 to 4 years. *Leukemia* 2002;16(4):720 - 5
9. Azevedo-Silva F, Reis Rde S, de Oliveira Santos M, Raggio Luiz R, Pombo-de-Oliveira MS. Evaluation of childhood acute leukaemia incidence and underreporting in Brazil by capture–recapture methodology. . *Cancer Epidemiology* 2009;33:403 - 5
10. Swerdlow AJ dSSI, Doll R. *Cancer Incidence and Mortality in England and Wales: Trends and Risk Factors*. . Oxford: Oxford Univeristy Press. 2001:181 - 93
11. Harrison CJ, Haas O, Harbott J, Biondi A, Stanulla M, Trka J, et al. Detection of prognostically relevant genetic abnormalities in childhood B-cell precursor acute

- lymphoblastic leukaemia: recommendations from the Biology and Diagnosis Committee of the International Berlin-Frankfurt-Münster study group. *Br J Haematol*.2010;151(2):132-42.
12. van der Does-Van den Berg A, Bartram CR, Basso G, Benoit YCM, Biondi A, Debatin K-M, et al. Minimal requirements for the diagnosis, classification, and evaluation of the treatment of childhood acute lymphoblastic leukemia (ALL) in the "BFM family" cooperative group. *Med Pediatr Oncol*. 1992;20(6):497-505.
 13. Bennett JM Catovsky D, Daniel MT, Flandrin G, Galton DA, et al. Proposals for the classification of the acute leukaemias. French-American-British (FAB) co-operative group. *Br J Haematol*. 1976;33(4):451 - 8
 14. van Dongen JJM LL, Bottcher S, Almeida J, van der Velden VHJ, Flores - Montero J, Rawstron A, et al. EuroFlow antibody panels for standardized n-dimensional flow cytometric immunophenotyping of normal, reactive and malignant leukocytes. *Leukemia* 2012 26(9):1908 - 75
 15. Murphy K, Travers P, Walport M, Janeway C. Janeway's Immunobiology New York Garland Science 2012.
 16. Mastrangelo R, Poplack D, Bleyer A, Riccardi R, Sather H, D'Angio G. Report and recommendations of the rome workshop concerning poor-prognosis acute lymphoblastic leukemia in children: Biologic bases for staging, stratification, and treatment. *Med Pediatr Oncol*. 1986;14(3):191-4.
 17. Smith M, Arthur D, Camitta B, Carroll AJ, Crist W, Gaynon P, et al. Uniform approach to risk classification and treatment assignment for children with acute lymphoblastic leukemia. *J Clin Oncol*.1996;14(1):18-24.
 18. Donadieu J, Auclerc M-F, Baruchel A, Perel Y, Bordigoni P, Landman - Parker, et al. Prognostic study of continuous variables (white blood cell count, peripheral blast cell count, haemoglobin level, platelet count and age) in childhood acute lymphoblastic leukaemia. Analysis of a population of 1545 children treated by the French Acute Lymphoblastic Leukaemia Group (FRALLE. *Br J Cancer*. 2000;83(12):1617 - 22

19. Horibe K, Hara J, Yagi K, Tawa A, Komada Y, Oda M, Nishimura S, et al. . Prognostic Factors in Childhood Acute Lymphoblastic Leukemia in Japan. *Int J Haem* 2000;72:61 - 8
20. Conter V, Schrappe M, Aricó M, Reiter A, Rizzari C, Dördelmann M, et al. Role of cranial radiotherapy for childhood T-cell acute lymphoblastic leukemia with high WBC count and good response to prednisone. *Associazione Italiana Ematologia Oncologia Pediatrica and the Berlin-Frankfurt-Münster groups. J Clin Oncol.*1997;15(8):2786-91.
21. Stock W, La M, Sanford B, Bloomfield CD, Vardiman JW, Gaynon P, et al. What determines the outcomes for adolescents and young adults with acute lymphoblastic leukemia treated on cooperative group protocols? A comparison of Children's Cancer Group and Cancer and Leukemia Group B studies. *Blood.* 2008;112(5):1646-54.
22. Pieters R, Schrappe M, De Lorenzo P, Hann I, De Rossi G, Felice M, et al. A treatment protocol for infants younger than 1 year with acute lymphoblastic leukaemia (Interfant-99): an observational study and a multicentre randomised trial. *Lancet.* 2007;370(9583):240-50.
23. Stanulla M, Schrappe M. Treatment of Childhood Acute Lymphoblastic Leukemia. *Semin Hematol.* 2009;46(1):52-63.
24. Reiter A, Schrappe M, Ludwig W, Hiddemann W, Sauter S, Henze G, et al. Chemotherapy in 998 unselected childhood acute lymphoblastic leukemia patients. Results and conclusions of the multicenter trial ALL-BFM 86. *Blood.* 1994;84(9):3122-33.
25. Schrappe M, Reiter A, Ludwig W-D, Harbott J, Zimmermann M, Hiddemann W, et al. Improved outcome in childhood acute lymphoblastic leukemia despite reduced use of anthracyclines and cranial radiotherapy: results of trial ALL-BFM 90. *Blood.* 2000;95(11):3310-22.
26. Chessells J. THE MANAGEMENT OF HIGH-RISK LYMPHOBLASTIC LEUKAEMIA IN CHILDREN. *Br J Haematol.* 2000;108(2):204-16.
27. Barry E, DeAngelo DJ, Neuberg D, Stevenson K, Loh ML, Asselin BL, et al. Favorable Outcome for Adolescents With Acute Lymphoblastic Leukemia Treated on Dana-Farber

- Cancer Institute Acute Lymphoblastic Leukemia Consortium Protocols. *J Clin Oncol*.2007;25(7):813-9.
28. Möricke A ZM, Reiter A, Gadner H, Odenwald E, Harbott J, Ludwig W-D, Riehm H, Schrappe M. Prognostic Impact of Age in Children and Adolescents with Acute Lymphoblastic Leukemia: Data from the Trials ALL-BFM 86, 90, and 95. *Klin Padiatr* 2005;217(6):310 - 20
 29. Larsen EC, Salzer W, Nachman J, Devidas M, Freyer DR, Raetz EA, et al. TREATMENT Toxicity in Adolescents and Young ADULT (AYA) PATIENTS COMPARED with Younger PATIENTS TREATED for HIGH RISK B-Precursor ACUTE LYMPHOBLASTIC LEUKEMIA (HR-ALL): A REPORT From the CHILDREN'S Oncology GROUP STUDY AALL0232. *ASH Annual Meeting Abstracts*. 2011;118(21):1510.
 30. Stock W. Adolescents and Young Adults with Acute Lymphoblastic Leukemia. *ASH Education Program Book*. 2010;2010(1):21-9.
 31. Mittelman F. The Third International Workshop on Chromosomes in Leukemia. Lund, Sweden, July 21-25, 1980. Introduction. *Cancer Genet Cytogenet*. 1981;4(2):96-8.
 32. Al-Bahar S, Zámečníkova A, Pandita R. Frequency and Type of Chromosomal Abnormalities in Childhood Acute Lymphoblastic Leukemia Patients in Kuwait: A Six-Year Retrospective Study. *Med Princ Pract*. 2010;19(3):176-81.
 33. Moorman AV, Ensor HM, Richards SM, Chilton L, Schwab C, Kinsey SE, et al. Prognostic effect of chromosomal abnormalities in childhood B-cell precursor acute lymphoblastic leukaemia: results from the UK Medical Research Council ALL97/99 randomised trial. *Lancet Oncology*. 2010;11(5):429-38.
 34. Mullighan CG GS, Radtke I, Miller CB, Coustan-Smith E, Dalton JD, Girtman K, et al. Genome-wide analysis of genetic alterations in acute lymphoblastic leukaemia. *Nature* 2007;446(7137):758 - 64
 35. Chessells JM, Swansbury GJ, Reeves B, Bailey CC, Richards SM, on behalf of the Medical Research Council Working Party in Childhood L. Cytogenetics and prognosis in childhood lymphoblastic leukaemia: results of MRC UKALL X. *Br J Haematol*.1997;99(1):93-100.

36. Bloomfield C, Goldman A, Alimena G, Berger R, Borgstrom G, Brandt L, et al. Chromosomal abnormalities identify high-risk and low-risk patients with acute lymphoblastic leukemia. *Blood*. 1986;67(2):415-20.
37. Heerema NA, Raetz EA, Carroll AJ, Borowitz MJ, Devidas M, Gastier-Foster JM, et al. iAMP21 Is Associated with Inferior Outcomes in Children with Acute Lymphoblastic Leukemia (ALL) on Contemporary Children's Oncology Group (COG) Studies. *ASH Annual Meeting Abstracts*. 2011;118(21):739.
38. Schlieben S, Borkhardt A, Reinisch I, Ritterbach J, Janssen JW, Ratei R, Schrappe M, et al. Incidence and clinical outcome of children with BCR/ABL-positive acute lymphoblastic leukemia (ALL). A prospective RT-PCR study based on 673 patients enrolled in the German pediatric multicenter therapy trials ALL-BFM-90 and CoALL-05-92. *Leukemia*. 1996;10(6):957 - 63
39. Gleißner B, Gökbuget N, Bartram CR, Janssen B, Rieder H, Janssen JWG, et al. Leading prognostic relevance of the BCR-ABL translocation in adult acute B-lineage lymphoblastic leukemia: a prospective study of the German Multicenter Trial Group and confirmed polymerase chain reaction analysis. *Blood*. 2002;99(5):1536-43.
40. Nowell P, Hungerford D. A minute chromosome in human chronic granulocytic leukemia. *Science*. 1960;132:1497.
41. Rowley JD. A New Consistent Chromosomal Abnormality in Chronic Myelogenous Leukaemia identified by Quinacrine Fluorescence and Giemsa Staining. *Nature*. 1973;243(5405):290 - 3.
42. Suryanarayan K, Hunger S, Kohler S, Carroll A, Crist W, Link M, et al. Consistent involvement of the bcr gene by 9;22 breakpoints in pediatric acute leukemias. *Blood*. 1991;77(2):324-30.
43. Romana S, Poirol H, Leconiat M, Flexor M, Mauchauffe M, Jonveaux P, et al. High frequency of t(12;21) in childhood B-lineage acute lymphoblastic leukemia. *Blood*. 1995;86(11):4263-9.

44. Golub TR, Barker GF, Bohlander SK, Hiebert SW, Ward DC, Bray-Ward P, et al. Fusion of the TEL gene on 12p13 to the AML1 gene on 21q22 in acute lymphoblastic leukemia. *Proc Natl Acad Sci USA*.1995;92(11):4917-21.
45. Bhojwani D PD, Sandlund JT, Jeha S, Ribeiro RC, Rubnitz JE, Raimondi SC, Shurtleff S, et al. ETV6-RUNX1-positive childhood acute lymphoblastic leukemia: improved outcome with contemporary therapy. *Leukemia*. 2012;26(2):265 - 70.
46. Borkhardt A, Cazzaniga G, Viehmann S, Valsecchi MG, Ludwig WD, Burci L, et al. Incidence and Clinical Relevance of TEL/AML1 Fusion Genes in Children With Acute Lymphoblastic Leukemia Enrolled in the German and Italian Multicenter Therapy Trials. *Blood*. 1997;90(2):571-7.
47. Aguiar RCT, Sohal J, Van Rhee F, Carapeti M, Franklin IM, Goldstone AH, et al. TEL-AML1 fusion in acute lymphoblastic leukaemia of adults. *Br J Haematol*. 1996;95(4):673-7.
48. Hiebert SW, Sun W, Davis JN, Golub T, Shurtleff S, Buijs A, et al. The t(12;21) translocation converts AML-1B from an activator to a repressor of transcription. *Mol Cell Biol*.1996;16(4):1349-55.
49. Devaraj PE FL, Janossy G, Hoffbrand AV, Secker - Walker LM. Expression of the E2A-PBX1 fusion transcripts in t(1;19)(q23;p13) and der(19)t(1;19) at diagnosis and in remission of acute lymphoblastic leukemia with different B lineage immunophenotypes. *Leukemia* 1995;9(5):821 - 5
50. Johansson B MA, Haas OA, Watmoe AE, Cheung KL, Swanton S, Seckler-Walker LM. Hematologic malignancies with t(4;11)(q21;q23)--a cytogenetic, morphologic, immunophenotypic and clinical study of 183 cases. European 11q23 Workshop participants. *Leukemia*. 1998;12(5):779 - 87.
51. Raimondi S, Peiper S, Kitchingman G, Behm F, Williams D, Hancock M, et al. Childhood acute lymphoblastic leukemia with chromosomal breakpoints at 11q23. *Blood*. 1989;73(6):1627-34.

52. Meyer C SB, Jakob S, Strehl S, Attarbaschi A, Schnittger S, Schoch C, Jansen MWJC, van Dongen JJM, et al. The MLL recombinome of acute leukemias. *Leukemia*. 2006;20(5):777 - 84.
53. Taki K, Ida K, Bessho F, Hanada R, Kikuch A, Yamamoto K, Sako M, et al. . Frequency and clinical significance of the MLL gene rearrangements in infant acute leukemia. *Leukemia*. 1996;10(8):1303 - 7.
54. Daniel-Cravioto A, Gonzalez-Bonilla CR, Mejia-Aranquire JM, Perz-Salvidar ML, Fajardo-Gutierrez A, Jimenez-Hernandez E, et al. Genetic rearrangement MLL/AF4 is most frequent in children with acute lymphoblastic leukemias in Mexico City. *Leuk Lymphoma*. 2009;50:8.
55. Perez-Saldivar M, Fajardo-Gutierrez A, Bernaldez-Rios R, Martinez-Avalos A, Medina-Sanson A, Espinosa-Hernandez L, et al. Childhood acute leukemias are frequent in Mexico City: descriptive epidemiology. *BMC Cancer*. 2011;11(1):355.
56. Harewood L RH, Harris R, Al-Obaidi MJ, Jalali GR, Martineau M, Moorman AV, Sumption N, et al. Amplification of AML1 on a duplicated chromosome 21 in acute lymphoblastic leukemia: a study of 20 cases. *Leukemia*. 2003;17(3):547 - 53.
57. Robinson HM BZ, Cheung KL, Harewood L, Harris RL, Jalali GR, Martineau M, Moorman AV, et al. Amplification of AML1 in acute lymphoblastic leukemia is associated with a poor outcome. *Leukemia*. 2003;17(11):2249 - 50
58. Strefford JC, van Delft FW, Robinson HM, Worley H, Yiannikouris O, Selzer R, et al. Complex genomic alterations and gene expression in acute lymphoblastic leukemia with intrachromosomal amplification of chromosome 21. *Proc Natl Acad Sci USA*. 2006;103(21):8167-72.
59. Moorman AV, Richards SM, Robinson HM, Strefford JC, Gibson BES, Kinsey SE, et al. Prognosis of children with acute lymphoblastic leukemia (ALL) and intrachromosomal amplification of chromosome 21 (iAMP21). *Blood*. 2007;109(6):2327-30.
60. Attarbaschi A, Mann G, Panzer-Grümayer R, Röttgers S, Steiner M, König M, et al. Minimal Residual Disease Values Discriminate Between Low and High Relapse Risk in Children With B-Cell Precursor Acute Lymphoblastic Leukemia and an Intrachromosomal

- Amplification of Chromosome 21: The Austrian and German Acute Lymphoblastic Leukemia Berlin-Frankfurt-Münster (ALL-BFM) Trials. *J Clin Oncol.*2008;26(18):3046-50.
61. Soulier J TL, Najfeld V, Lipton JM, Mathew S, Avet-Loiseau H, De Braekeleer M, Salem S, Baruchel A, Raimondi SC, Raynaud SD. Amplification of band q22 of chromosome 21, including AML1, in older children with acute lymphoblastic leukemia: an emerging molecular cytogenetic subgroup. *Leukemia.* 2003;17(8):1679 - 82
 62. Moorman AV, Robinson HM, Richards SM, Schwab C, Mitchell CD, Goulden N, et al. Treatment Intensification Improves Outcome in Children with iAMP21 positive ALL. *ASH Annual Meeting Abstracts.* 2012;120(21):656.
 63. Trueworthy R, Shuster J, Look T, Crist W, Borowitz M, Carroll A, et al. Ploidy of lymphoblasts is the strongest predictor of treatment outcome in B-progenitor cell acute lymphoblastic leukemia of childhood: a Pediatric Oncology Group study. *J Clin Oncol.*1992;10(4):606-13.
 64. Look A, Roberson P, Williams D, Rivera G, Bowman W, Pui C, et al. Prognostic importance of blast cell DNA content in childhood acute lymphoblastic leukemia. *Blood.* 1985;65(5):1079-86.
 65. Heerema NA, Sather HN, Sensel MG, Zhang T, Hutchinson RJ, Nachman JB, et al. Prognostic Impact of Trisomies of Chromosomes 10, 17, and 5 Among Children With Acute Lymphoblastic Leukemia and High Hyperdiploidy (> 50 Chromosomes). *J Clin Oncol.*2000;18(9):1876-87.
 66. Nachman JB, Heerema NA, Sather H, Camitta B, Forestier E, Harrison CJ, et al. Outcome of treatment in children with hypodiploid acute lymphoblastic leukemia. *Blood.* 2007;110(4):1112-5.
 67. Aricò M, Valsecchi MG, Rizzari C, Barisone E, Biondi A, Casale F, et al. Long-Term Results of the AIEOP-ALL-95 Trial for Childhood Acute Lymphoblastic Leukemia: Insight on the Prognostic Value of DNA Index in the Framework of Berlin-Frankfurt-Muenster-Based Chemotherapy. *J Clin Oncol.*2008;26(2):283-9.

68. Mertens F JB, Mitelman F. Dichotomy of hyperdiploid acute lymphoblastic leukemia on the basis of the distribution of gained chromosomes. *Cancer Genet Cytogenet.* 1996;92(1):8 - 10
69. Moorman AV CR, Farrell DM, Hawkins JM, Martineau M, Secker-Walker LM. Probes for hidden hyperdiploidy in acute lymphoblastic leukaemia. *Genes Chromosomes Cancer* 1996;16(1):40 - 5.
70. Raimondi SC PC, Hancock ML, Behm FG, Filatov L, Rivera GK. Heterogeneity of hyperdiploid (51-67) childhood acute lymphoblastic leukemia. *Leukemia.* 1996;10(2):213 - 24.
71. Raimondi SC, Zhou Y, Mathew S, Shurtleff SA, Sandlund JT, Rivera GK, et al. Reassessment of the prognostic significance of hypodiploidy in pediatric patients with acute lymphoblastic leukemia. *Cancer.* 2003;98(12):2715-22.
72. Pui C, Williams D, Raimondi S, Rivera G, Look A, Dodge R, et al. Hypodiploidy is associated with a poor prognosis in childhood acute lymphoblastic leukemia. *Blood.* 1987;70(1):247-53.
73. Holmfeldt WL, Diaz-Flores E, Walsh M, Zhang J, Ding L, Payne-Turner D, Churchman M, et al. The genomic landscape of hypodiploid acute lymphoblastic leukemia. *Nat Genet.* 2013;45(3):242 - 52.
74. Borowitz MJ, Devidas M, Hunger SP, Bowman WP, Carroll AJ, Carroll WL, et al. Clinical significance of minimal residual disease in childhood acute lymphoblastic leukemia and its relationship to other prognostic factors: a Children's Oncology Group study. *Blood.* 2008;111(12):5477-85.
75. Riehm H, Gadner H, Henze G, Kornhuber B, Lampert F, Niethammer D, Reiter A, Schellong G. Results and significance of six randomized trials in four consecutive ALL-BFM studies. *Haematol Blood Transfus.* 1990;33:439 - 50
76. Gaynon PS BW, Steinherz PG, Finklestein JZ, Littman P, Miller DR, Reaman G, Sather H, Hammond GD. Day 7 marrow response and outcome for children with acute lymphoblastic leukemia and unfavorable presenting features. *Med Pediatr Oncol.* 1990;18(4):273 - 9.

77. Miller DR, Coccia PF, Bleyer WA, Lukens JN, Siegel SE, Sather HN, et al. Early response to induction therapy as a predictor of disease-free survival and late recurrence of childhood acute lymphoblastic leukemia: a report from the Childrens Cancer Study Group. *J Clin Oncol.*1989;7(12):1807-15.
78. Nachman J, Sather HN, Gaynon PS, Lukens JN, Wolff L, Trigg ME. Augmented Berlin-Frankfurt-Munster therapy abrogates the adverse prognostic significance of slow early response to induction chemotherapy for children and adolescents with acute lymphoblastic leukemia and unfavorable presenting features: a report from the Children's Cancer Group. *J Clin Oncol.*1997;15(6):2222-30.
79. Nachman J, Sather HN, Cherlow JM, Sensel MG, Gaynon PS, Lukens JN, et al. Response of children with high-risk acute lymphoblastic leukemia treated with and without cranial irradiation: a report from the Children's Cancer Group. *J Clin Oncol.*1998;16(3):920-30.
80. Bradstock KF, Kerr A, Bollum FJ. Antigenic Phenotype of TdT-positive cells in human peripheral blood. *Cell Immunol.* 1985;90(2):590-8.
81. Bradstock KF JG, Hoffbrand AV, Ganeshaguru K, Llewellyn P, Prentice HG, Bollum FJ. Immunofluorescent and biochemical studies of terminal deoxynucleotidyl transferase in treated acute leukaemia. *Br J Haematol.* 1981;47(1):121 - 31.
82. Flohr T SA, Cazzaniga G, Panzer-Grümayer R, van der Velden V, Fischer S, Stanulla M, Basso G, Niggli FK, Schäfer BW, Sutton R, Koehler R, Zimmermann M, Valsecchi MG, Gadner H, Masera G, Schrappe M, van Dongen JJ, Biondi A, Bartram CR. Minimal residual disease-directed risk stratification using real-time quantitative PCR analysis of immunoglobulin and T-cell receptor gene rearrangements in the international multicenter trial AIEOP-BFM ALL 2000 for childhood acute lymphoblastic leukemia. *Leukemia.* 2008;22(4):771 - 82
83. Stow P, Key L, Chen X, Pan Q, Neale GA, Coustan-Smith E, et al. Clinical significance of low levels of minimal residual disease at the end of remission induction therapy in childhood acute lymphoblastic leukemia. *Blood.* 2010;115(23):4657-63.

84. Coustan-Smith E, Sancho J, Hancock ML, Boyett JM, Behm FG, Raimondi SC, et al. Clinical importance of minimal residual disease in childhood acute lymphoblastic leukemia. *Blood*. 2000;96(8):2691-6.
85. Coustan-Smith E, Sancho J, Behm FG, Hancock ML, Razzouk BI, Ribeiro RC, et al. Prognostic importance of measuring early clearance of leukemic cells by flow cytometry in childhood acute lymphoblastic leukemia. *Blood*. 2002;100(1):52-8.
86. Coustan-Smith E, Behm FG, Sanchez J, Boyett JM, Hancock ML, Raimondi SC, et al. Immunological detection of minimal residual disease in children with acute lymphoblastic leukaemia. *Lancet*. 1998;351(9102):550-4.
87. Basso G, Veltroni M, Valsecchi MG, Dworzak MN, Ratei R, Silvestri D, et al. Risk of Relapse of Childhood Acute Lymphoblastic Leukemia Is Predicted By Flow Cytometric Measurement of Residual Disease on Day 15 Bone Marrow. *J Clin Oncol*. 2009;27(31):5168-74.
88. Conter V, Bartram CR, Valsecchi MG, Schrauder A, Panzer-Grumayer R, Moricke A, et al. Molecular response to treatment redefines all prognostic factors in children and adolescents with B-cell precursor acute lymphoblastic leukemia: results in 3184 patients of the AIEOP-BFM ALL 2000 study. *Blood*. 2010;115(16):3206-14.
89. Seegmiller AC, Kroft SH, Karandikar NJ, McKenna RW. Characterization of Immunophenotypic Aberrancies in 200 Cases of B Acute Lymphoblastic Leukemia. *American J of Clinical Pathology*. 2009;132(6):940-9.
90. Campana D. Role of Minimal Residual Disease Monitoring in Adult and Pediatric Acute Lymphoblastic Leukemia. *Hematology/Oncology Clinics of North America*. 2009;23(5):1083-98.
91. Pui C-H, Campana D, Pei D, Bowman WP, Sandlund JT, Kaste SC, et al. Treating Childhood Acute Lymphoblastic Leukemia without Cranial Irradiation. *N Eng J Med*. 2009;360(26):2730-41.
92. van Dongen JJM, Seriu T, Panzer-Grümayer ER, Biondi A, Pongers-Willemse MJ, Corral L, et al. Prognostic value of minimal residual disease in acute lymphoblastic leukaemia in childhood. *Lancet*. 1998;352(9142):1731-8.

93. Brisco MJ, Condon J, Hughes E, Neoh SH, Sykes PJ, Seshadri R, et al. Outcome prediction in childhood acute lymphoblastic leukaemia by molecular quantification of residual disease at the end of induction. *Lancet*. 1994;343(8891):196-200.
94. van dongen JJM, Langerak A, Bruggemann M, Evans PAS, Hummel M, Lavender FL, et al. Design and standardization of PCR primers and protocols for detection of clonal immunoglobulin and T-cell receptor gene recombinations in suspect lymphoproliferations: Report of the BIOMED-2 Concerted Action BMH4-CT98-3936. *Leukemia*. 2003;17(12):2257 - 317
95. Neale GA, Coustan-Smith E, Stow P, Pan Q, Chen X, Pui C-H, Campana D. Comparative analysis of flow cytometry and polymerase chain reaction for the detection of minimal residual disease in childhood acute lymphoblastic leukemia. *Leukemia*. 2004;18(5):934 - 8
96. Irving J, Jesson J, Virgo P, Case M, Minto L, Eyre L, et al. Establishment and validation of a standard protocol for the detection of minimal residual disease in B lineage childhood acute lymphoblastic leukemia by flow cytometry in a multi-center setting. *Haematologica*. 2009;94(6):870-4.
97. Farber S, Diamond LK, Mercer RD, Sylvester RF, Wolff JA. Temporary Remissions in Acute Leukemia in Children Produced by Folic Acid Antagonist, 4-Aminopteroyl-Glutamic Acid (Aminopterin). *N Eng J Med*. 1948;238(23):787-93.
98. George P, Hernandez K, Hustu O, Borella L, Holton C, Pinkel D. A study of "total therapy" of acute lymphocytic leukemia in children. *The J of pediatrics*. 1968;72(3):399-408.
99. Pui C-H, Evans WE. Treatment of Acute Lymphoblastic Leukemia. *N Eng J Med*. 2006;354(2):166-78.
100. Steinherz PG, Gaynon PS, Breneman JC, Cherlow JM, Grossman NJ, Kersey JH, et al. Cyto-reduction and prognosis in acute lymphoblastic leukemia--the importance of early marrow response: report from the Childrens Cancer Group. *J Clin Oncol*. 1996;14(2):389-98.
101. Pinkel D, Hernandez K, Borella L, Holton C, Aur R, Samoy G, et al. Drug dosage and remission duration in childhood lymphocytic leukemia. *Cancer*. 1971;27(2):247-56.

102. Pinkerton CR BA, Holtzel H, Chessells JM. Intensive consolidation chemotherapy for acute lymphoblastic leukaemia (UKALL X pilot study). *Arch Dis Child*. 1987;62(1):12 - 8
103. Chessells JM BC, Richards SM. Intensification of treatment and survival in all children with lymphoblastic leukaemia: results of UK Medical Research Council trial UKALL X. Medical Research Council Working Party on Childhood Leukaemia. *Lancet*. 1995;345(8943):143 - 8
104. George SL, Ochs JJ, Mauer AM, Simone JV. The importance of an isolated central nervous system relapse in children with acute lymphoblastic leukemia. *J Clin Oncol*. 1985;3(6):776-81.
105. Ortega JA, Nesbit ME, Sather HN, Robison LL, D'Angio GJ, Hammond GD. Long-term evaluation of a CNS prophylaxis trial--treatment comparisons and outcome after CNS relapse in childhood ALL: a report from the Childrens Cancer Study Group. *J Clin Oncol*. 1987;5(10):1646-54.
106. Cousens P, Waters B, Said J, Stevens M. COGNITIVE EFFECTS OF CRANIAL IRRADIATION IN LEUKAEMIA: A SURVEY AND META-ANALYSIS. *J of Child Psychology and Psychiatry*. 1988;29(6):839-52.
107. Mulhern RK, Wasserman AL, Fairclough D, Ochs J. Memory function in disease-free survivors of childhood acute lymphocytic leukemia given CNS prophylaxis with or without 1,800 cGy cranial irradiation. *J Clin Oncol*. 1988;6(2):315-20.
108. Mulhern RK, Fairclough D, Ochs J. A prospective comparison of neuropsychologic performance of children surviving leukemia who received 18-Gy, 24-Gy, or no cranial irradiation. *J Clin Oncol*. 1991;9(8):1348-56.
109. Christie D LA, Chessells JM, Vargha-Khadem F. Intellectual performance after presymptomatic cranial radiotherapy for leukaemia: effects of age and sex. *Arch Dis Child*. 1995;73:136 - 40
110. Alves CHBdS, Kuperman H, Dichtchekenian V, Damiani D, Della Manna T, Cristófani LM, et al. Growth and puberty after treatment for acute lymphoblastic leukemia. *Revista do Hospital das Clínicas*. 2004;59:67-70.

111. Löning L, Zimmermann M, Reiter A, Kaatsch P, Henze G, Riehm H, et al. Secondary neoplasms subsequent to Berlin-Frankfurt-Münster therapy of acute lymphoblastic leukemia in childhood: significantly lower risk without cranial radiotherapy. *Blood*. 2000;95(9):2770-5.
112. Kimball Dalton VM, Gelber RD, Li F, Donnelly MJ, Tarbell NJ, Sallan SE. Second malignancies in patients treated for childhood acute lymphoblastic leukemia. *J Clin Oncol*.1998;16(8):2848-53.
113. Bleyer WA, Coccia PF, Sather HN, Level C, Lukens J, Niebrugge DJ, et al. Reduction in central nervous system leukemia with a pharmacokinetically derived intrathecal methotrexate dosage regimen. *J Clin Oncol*.1983;1(5):317-25.
114. Hill FGH, Richards S, Gibson B, Hann I, Lilleyman J, Kinsey S, et al. Successful treatment without cranial radiotherapy of children receiving intensified chemotherapy for acute lymphoblastic leukaemia: results of the risk-stratified randomized central nervous system treatment trial MRC UKALL XI (ISRC TN 16757172). *Br J Haematol*.2004;124(1):33-46.
115. Duration of chemotherapy in childhood acute lymphoblastic leukaemia. The Medical Research Council's Working Party on Leukaemia in Childhood. *Med Pediatr Oncol*. 1982;10(5):511 - 20
116. Möricke A, Reiter A, Zimmermann M, Gadner H, Stanulla M, Dördelmann M, et al. Risk-adjusted therapy of acute lymphoblastic leukemia can decrease treatment burden and improve survival: treatment results of 2169 unselected pediatric and adolescent patients enrolled in the trial ALL-BFM 95. *Blood*. 2008;111(9):4477-89.
117. Moghrabi A, Levy DE, Asselin B, Barr R, Clavell L, Hurwitz C, et al. Results of the Dana-Farber Cancer Institute ALL Consortium Protocol 95-01 for children with acute lymphoblastic leukemia. *Blood*. 2007;109(3):896-904.
118. Schmiegelow K FE, Hellebostad M, Heyman M, Kristinsson J, Söderhäll S, Taskinen M. Long-term results of NOPHO ALL-92 and ALL-2000 studies of childhood acute lymphoblastic leukemia. *Leukemia*. 2010;24(2):345 - 54.

119. Escherich G HM, Zimmermann M, Janka-Schaub GE. Cooperative study group for childhood acute lymphoblastic leukaemia (COALL): long-term results of trials 82,85,89,92 and 97. *Leukemia*. 2009;24(2):298 - 308
120. Gaynon PS AA, Carroll WL, Nachman JB, Trigg ME, Sather HN, Hunger SP, Devidas M. Long-term results of the children's cancer group studies for childhood acute lymphoblastic leukemia 1983-2002: A Children's Oncology Group Report. *Leukemia*. 2009;24(2):285 - 97
121. Vilmer E SS, Ferster A, Bertrand Y, Cavé H, Thyss A, Benoit Y, Dastugue N, Fournier M, Souillet G, Manel AM, Robert A, Nelken B, Millot F, Lutz P, Rialland X, Mechinaud F, Boutard P, Behar C, Chantaine JM, Plouvier E, Laureys G, Brock P, Uyttebroeck A, Margueritte G, Plantaz D, Norton L, Francotte N, Gyselinck J, Waterkeyn C, Solbu G, Philippe N, Otten J. Long-term results of three randomized trials (58831, 58832, 58881) in childhood acute lymphoblastic leukemia: a CLCG-EORTC report. *Children Leukemia Cooperative Group*. *Leukemia*. 2000;14(12):2257 - 66.
122. Conter V, Arico M, Valsecchi M, Rizzari C, Testi A, Miniero R, et al. Intensive BFM chemotherapy for childhood ALL: interim analysis of the AIEOP-ALL 91 study. *Associazione Italiana Ematologia Oncologia Pediatrica*. *Haematologica*. 1998;83(9):791-9.
123. Chessells JM VP, Kempinski H, Henley P, Leiper A, Webb D, Hann IM. Long-term follow-up of relapsed childhood acute lymphoblastic leukaemia. *Br J Haematol*. 2003;123(3):396 - 405
124. Gaynon PS, Qu RP, Chappell RJ, Willoughby MLN, Tubergen DG, Steinherz PG, et al. Survival after relapse in childhood acute lymphoblastic leukemia. *Cancer*. 1998;82(7):1387-95.
125. Nguyen K DM, Cheng S-C, La M, Raetz EA, Carroll WL, Winick NJ, Hunger SP, Gaynon PS, Loh ML. Factors influencing survival after relapse from acute lymphoblastic leukemia: a Children's Oncology Group study. *Leukemia*. 2008;22(12):2142 - 50
126. Lawson, Harrison, Richards, Oakhill, Stevens, Eden, et al. The UK experience in treating relapsed childhood acute lymphoblastic leukaemia: a report on the Medical Research Council UKALLR1 study. *Br J Haematol*. 2000;108(3):531-43.

127. Roy A, Cargill A, Love S, Moorman AV, Stoneham S, Lim A, et al. Outcome after first relapse in childhood acute lymphoblastic leukaemia – lessons from the United Kingdom R2 trial. *Br J Haematol.* 2005;130(1):67-75.
128. Ko RH, Ji L, Barnette P, Bostrom B, Hutchinson R, Raetz E, et al. Outcome of Patients Treated for Relapsed or Refractory Acute Lymphoblastic Leukemia: A Therapeutic Advances in Childhood Leukemia Consortium Study. *J Clin Oncol.* 2010;28(4):648-54.
129. Eckert C FT, Koehler R, Hagedorn N, Moericke A, Stanulla M, Kirschner-Schwabe R, Cario G, et al. Very early/early relapses of acute lymphoblastic leukemia show unexpected changes of clonal markers and high heterogeneity in response to initial and relapse treatment. *Leukemia.* 2011;25(8):1305 - 13
130. Choi S, Henderson MJ, Kwan E, Beesley AH, Sutton R, Bahar AY, et al. Relapse in children with acute lymphoblastic leukemia involving selection of a preexisting drug-resistant subclone. *Blood.* 2007;110(2):632-9.
131. Li A, Zhou J, Zuckerman D, Rue M, Dalton V, Lyons C, et al. Sequence analysis of clonal immunoglobulin and T-cell receptor gene rearrangements in children with acute lymphoblastic leukemia at diagnosis and at relapse: implications for pathogenesis and for the clinical utility of PCR-based methods of minimal residual disease detection. *Blood.* 2003;102(13):4520-6.
132. Klumper E, Pieters R, Veerman A, Huismans D, Loonen A, Hahlen K, et al. In vitro cellular drug resistance in children with relapsed/refractory acute lymphoblastic leukemia. *Blood.* 1995;86(10):3861-8.
133. Houghton PJ HS. mTOR as a target for cancer therapy. *Curr Top Microbiol Immunol.* 2004;279:339 - 59
134. Avellino R, Romano S, Parasole R, Bisogni R, Lamberti A, Poggi V, et al. Rapamycin stimulates apoptosis of childhood acute lymphoblastic leukemia cells. *Blood.* 2005;106(4):1400-6.
135. Jotta PY, Ganazza MA, Silva A, Viana MB, da Silva MJ, Zambaldi LJG, et al. Negative prognostic impact of PTEN mutation in pediatric T-cell acute lymphoblastic leukemia. *Leukemia.* 2009;24(1):239-42.

136. Morishita N, Tsukahara H, Chayama K, Ishida T, Washio K, Miyamura T, et al. Activation of Akt is associated with poor prognosis and chemotherapeutic resistance in pediatric B-precursor acute lymphoblastic leukemia. *Ped Blood Cancer*. 2012;59(1):83-9.
137. Brown VI, Fang J, Alcorn K, Barr R, Kim JM, Wasserman R, et al. Rapamycin is active against B-precursor leukemia in vitro and in vivo, an effect that is modulated by IL-7-mediated signaling. *Proc Natl Acad Sci USA*. 2003;100(25):15113-8.
138. Teachey DT, Obzut DA, Cooperman J, Fang J, Carroll M, Choi JK, et al. The mTOR inhibitor CCI-779 induces apoptosis and inhibits growth in preclinical models of primary adult human ALL. *Blood*. 2006;107(3):1149-55.
139. Teachey DT, Sheen C, Hall J, Ryan T, Brown VI, Fish J, et al. mTOR inhibitors are synergistic with methotrexate: an effective combination to treat acute lymphoblastic leukemia. *Blood*. 2008;112(5):2020-3.
140. Crazzolara R, Cisterne A, Thien M, Hewson J, Baraz R, Bradstock KF, et al. Potentiating effects of RAD001 (Everolimus) on vincristine therapy in childhood acute lymphoblastic leukemia. *Blood*. 2009;113(14):3297-306.
141. Saunders P CA, Weiss J, Bradstock KF, Bendall LJ. The mammalian target of rapamycin inhibitor RAD001 (everolimus) synergizes with chemotherapeutic agents, ionizing radiation and proteasome inhibitors in pre-B acute lymphocytic leukemia. *Haematologica*. 2010 96(1):69 - 77.
142. Wahlstrom J, Ammon K, Esquivel C, Law J, Hermiston ML. Aberrant MAPK and PI3K Signaling Contribute to Chemotherapy Resistance in T Cell Acute Lymphoblastic Leukemia by Altering the Balance of Apoptosis Mediators. *ASH Annual Meeting Abstracts*. 2011;118(21):3490.
143. Gregorj C, Ricciardi MR, Petrucci MT, Scerpa MC, De Cave F, Fazi P, et al. ERK1/2 phosphorylation is an independent predictor of complete remission in newly diagnosed adult acute lymphoblastic leukemia. *Blood*. 2007;109(12):5473-6.
144. Towatari M LH, Tanimoto M, Iwata H, Hamaguchi M, Saito H. Constitutive activation of mitogen-activated protein kinase pathway in acute leukemia cells. *Leukemia*. 1997;11:479 - 84

145. Case M, Matheson E, Minto L, Hassan R, Harrison CJ, Bown N, et al. Mutation of Genes Affecting the RAS Pathway Is Common in Childhood Acute Lymphoblastic Leukemia. *Cancer Res.* 2008;68(16):6803-9.
146. Perentesis JP BS, Boyle E, Shao Y, Shu XI, Stenbuch M, Sather HN, Gaynon P, Kiffmeyer W, et al. RAS oncogene mutations and outcome of therapy for childhood acute lymphoblastic leukemia. *Leukemia.* 2004;18(4):685 - 92
147. Wiemels JL ZY, Chang J, Zheng S, Metayer C, Zhang L, Smith MT, Ma X, et al. RAS mutation is associated with hyperdiploidy and parental characteristics in pediatric acute lymphoblastic leukemia. *Leukemia.* 2005;19(3):415 - 9
148. Wiemels JL, Kang M, Chang JS, Zheng L, Kouyoumji C, Zhang L, et al. Backtracking RAS mutations in high hyperdiploid childhood acute lymphoblastic leukemia. *Blood Cells Mol Dis.* 2010;45(3):186-91.
149. Liang D-C, Shih L-Y, Fu J-F, Li H-Y, Wang H-I, Hung I-J, et al. K-ras mutations and N-ras mutations in childhood acute leukemias with or without mixed-lineage leukemia gene rearrangements. *Cancer.* 2006;106(4):950-6.
150. Tartaglia M, Martinelli S, Cazzaniga G, Cordeddu V, Iavarone I, Spinelli M, et al. Genetic evidence for lineage-related and differentiation stage-related contribution of somatic PTPN11 mutations to leukemogenesis in childhood acute leukemia. *Blood.* 2004;104(2):307-13.
151. Davidsson J LH, Panagopoulos I, Fioretos T, Johansson B. BRAF mutations are very rare in B- and T-cell pediatric acute lymphoblastic leukemias. *Leukemia.* 2008;22(8):1619 - 21.
152. Nicholson L, Knight T, Matheson E, Minto L, Case M, Sanichar M, et al. Casitas B lymphoma mutations in childhood acute lymphoblastic leukemia. *Genes, Chromosomes and Cancer.* 2012;51(3):250-6.
153. Lubbert M, Mirro JJ, Miller C, Kahan J, Isaac G, Kitchingman G, et al. N-ras gene point mutations in childhood acute lymphocytic leukemia correlate with a poor prognosis. *Blood.* 1990;75(5):1163-9.

154. Yokota S NM, Horiike S, Seriu T, Iwai T, Kaneko H, et al. Mutational analysis of the N-ras gene in acute lymphoblastic leukemia: a study of 125 Japanese pediatric cases. *Int J Haem.* 1998;67(4):379 - 87.
155. Hogan LE, Meyer JA, Yang J, Wang J, Wong N, Yang W, et al. Integrated genomic analysis of relapsed childhood acute lymphoblastic leukemia reveals therapeutic strategies. *Blood.* 2011;118(19):5218-26.
156. Rambal AA, Panaquiton Z, Kramer L, Grant S, Harada H. MEK inhibitors potentiate dexamethasone lethality in acute lymphoblastic leukemia cells through the pro-apoptotic molecule BIM. *Leukemia.* 2009;23(10):1744 - 54.
157. Milella M, Precupanu Z, Gregorj C, Ricciardi MR, Petrucci MT, Kornblau SM, Tafuri A, Andreeff A. Beyond Single Pathway Inhibition: MEK Inhibitors as a Platform for the Development of Pharmacological Combinations with Synergistic Anti-Leukemic Effects. *Curr Pharm Design* 2005;11(21):2779 - 95
158. Marston E, Weston V, Jesson J, Maina E, McConville C, Agathangelou A, et al. Stratification of pediatric ALL by in vitro cellular responses to DNA double-strand breaks provides insight into the molecular mechanisms underlying clinical response. *Blood.* 2009;113(1):117-26.
159. Manning G, Whyte DB, Martinez R, Hunter T, Sudarsanam S. The Protein Kinase Complement of the Human Genome. *Science.* 2002;298(5600):1912-34.
160. Vlahovic G, Crawford J. Activation of Tyrosine Kinases in Cancer. *The Oncologist.* 2003;8(6):531-8.
161. Robinson DR WY-M, Li S-F. The protein tyrosine kinase family of the human genome *Oncogene.* 2000;19(49):5548 - 57.
162. Yin T, Yang L, Yang Y. Tyrosine phosphorylation and activation of JAK family tyrosine kinases by interleukin-9 in MO7E cells. *Blood.* 1995;85(11):3101-6.
163. Lemmon MA SJ. Cell Signaling by Receptor Tyrsoine Kinases. *Cell.* 2010;141(7):1117 - 34.

164. Ward CW, Lawrence MC, Streltsov VA, Adams TE, McKern NM. The insulin and EGF receptor structures: new insights into ligand-induced receptor activation. *Trends in Biochemical Sciences*. 2007;32(3):129-37.
165. Wiesmann C FG, Christinger HW, Eigenbrot C, Wells JA, De Vos AM. Crystal structure at 1.7 Å resolution of VEGF in complex with domain 2 of the Flt-1 receptor. *Cell*. 1997;91(5):695 - 704
166. Earp HS, Dawson T, Li X, Yu H. Heterodimerization and functional interaction between EGF receptor family members: a new signaling paradigm with implications for breast Cancer Res. *Breast Cancer Res Tr*. 1995;35(1):115-32.
167. Mueller KL, Hunter LA, Ethier SP, Boerner JL. Met and c-Src Cooperate to Compensate for Loss of Epidermal Growth Factor Receptor Kinase Activity in Breast Cancer Cells. *Cancer Res*. 2008;68(9):3314-22.
168. Sasaki T KP, Clout NJ, Cheburkin Y, Gohring W, Ullrich A, Timml R, hoheneister E. Structural basis for Gas6-Axl signalling. *EMBO J*. 2006;25(1):80 - 7.
169. Liu H CX, Focia PJ, He X. Structural basis for stem cell factor-KIT signaling and activation of class III receptor tyrosine kinases. *EMBO J*. 2007;26(3):891 - 901
170. Lin X. Functions of heparan sulfate proteoglycans in cell signaling during development. *Development*. 2004;131(24):6009-21.
171. Ogiso H, Ishitani R, Nureki O, Fukai S, Yamanaka M, Kim J-H, et al. Crystal Structure of the Complex of Human Epidermal Growth Factor and Receptor Extracellular Domains. *Cell*. 2002;110(6):775-87.
172. Ullrich A SJ. Signal transduction by receptors with tyrosine kinase activity. *Cell*. 1990;2(61):203 - 12.
173. Nolen B, Taylor S, Ghosh G. Regulation of Protein Kinases: Controlling Activity through Activation Segment Conformation. *Mol Cell*. 2004;15(5):661-75.
174. Chen H, Ma J, Li W, Eliseenkova AV, Xu C, Neubert TA, et al. A Molecular Brake in the Kinase Hinge Region Regulates the Activity of Receptor Tyrosine Kinases. *Mol Cell*. 2007;27(5):717-30.

175. Griffith J, Black J, Faerman C, Swenson L, Wynn M, Lu F, et al. The Structural Basis for Autoinhibition of FLT3 by the Juxtamembrane Domain. *Mol Cell*.2004;13(2):169-78.
176. Shewchuk LM, Hassell AM, Ellis B, Holmes WD, Davis R, Horne EL, et al. Structure of the Tie2 RTK Domain: Self-Inhibition by the Nucleotide Binding Loop, Activation Loop, and C-Terminal Tail. *Structure (London, England : 1993)*. 2000;8(11):1105-13.
177. Niu X-L, Peters KG, Kontos CD. Deletion of the Carboxyl Terminus of Tie2 Enhances Kinase Activity, Signaling, and Function: EVIDENCE FOR AN AUTOINHIBITORY MECHANISM. *J Biol Chem*.2002;277(35):31768-73.
178. Schlessinger J. Cell Signaling by Receptor Tyrosine Kinases. *Cell* 2000;103(2):211 - 25.
179. Metz HE, McGarry Houghton A. Insulin Receptor Substrate Regulation of Phosphoinositide 3-Kinase. *Clin Cancer Res*.2011;17(2):206-11.
180. Elchebly M PP, Michaliszyn E, Cromlish W, Collins S, Lao AL, Normandin D, et al. Increased insulin sensitivity and obesity resistance in mice lacking the protein tyrosine phosphatase-1B gene. *Science* 1999;283(5407):1544 - 8
181. Haj FG, Markova B, Klamann LD, Bohmer FD, Neel BG. Regulation of Receptor Tyrosine Kinase Signaling by Protein Tyrosine Phosphatase-1B. *J Biol Chem*.2003;278(2):739-44.
182. Kovalenko M DK, Sandstrom J, Persson C, Gross S, Jandt J, Vilella R, Bohmer F, Ostman A. Site-selective dephosphorylation of the platelet-derived growth factor beta-receptor by the receptor-like protein-tyrosine phosphatase DEP-1. *J Biol Chem*. 2000;275:16219 - 26.
183. Grazia Lampugnani M ZA, Corada M, Takahashi T, Balconi G, Breviario F, Orsenigo F, Cattelino A, Kemler R, Daniel TO, et al. . Contact inhibition of VEGF-induced proliferation requires vascular endothelial cadherin, beta-catenin and phosphatase DEP-1/CD148. *J Cell Biol*. 2003;161:793 - 804.
184. Palka HL PM, Tonks NK. Hepatocyte growth factor receptor tyrosine kinase met is a substrate of the receptor protein-tyrosine phosphatase DEP-1. *J Biol Chem*. 2003;278:5728 - 35.

185. Arora D, Stopp S, Böhmer S-A, Schons J, Godfrey R, Masson K, et al. Protein-tyrosine Phosphatase DEP-1 Controls Receptor Tyrosine Kinase FLT3 Signaling. *J Biol Chem.* 2011;286(13):10918-29.
186. Levkovitz G WH, Zamir E, Kam Z, Oved S, Langdon et al. c-Cbl/Sli-1 regulates endocytic sorting and ubiquitination of the epidermal growth factor receptor. *Genes Dev.* 1998;12:3663 - 74.
187. Lee PS WY, Dominguez MG, Yeung Y-G, Murphy MA, Bowtell DD, et al. The cbl protooncoprotein stimulates CSF-1 receptor multiubiquitination and endocytosis, and attenuates macrophage proliferation, and attenuates macrophage proliferation. *EMBO J.* 1999;18:3616 - 28.
188. Miyake S, Mullane-Robinson KP, Lill NL, Douillard P, Band H. Cbl-mediated Negative Regulation of Platelet-derived Growth Factor Receptor-dependent Cell Proliferation: A CRITICAL ROLE FOR Cbl TYROSINE KINASE-BINDING DOMAIN. *J Biol Chem.* 1999;274(23):16619-28.
189. Duval M, Bédard-Goulet S, Delisle C, Gratton J-P. Vascular Endothelial Growth Factor-dependent Down-regulation of Flk-1/KDR Involves Cbl-mediated Ubiquitination: CONSEQUENCES ON NITRIC OXIDE PRODUCTION FROM ENDOTHELIAL CELLS. *J Biol Chem.* 2003;278(22):20091-7.
190. Peschard P FT, Lamorte L, Naujokas MA, Band H, Langdon WY, et al. . Mutation of the c-Cbl TKB domain binding site on the Met receptor tyrosine kinase converts it into a transforming protein. *Mol Cell.* 2001;8:995 - 1004.
191. Goormachtigh G JZ, Le Goff A, Fafeur V. . Degradation of the GAB1 adaptor by the ubiquitin-proteasome pathway hampers HGF/SF-MET signaling. *Biochem Biophys Res Commun.* 2011;411(4):780 - 5.
192. Peschard P, Park M. Escape from Cbl-mediated downregulation: a recurrent theme for oncogenic deregulation of receptor tyrosine kinases. *Cancer Cell.* 2003;3(6):519-23.
193. Cheng AM RB, Pao W, Hayday A, Bolen JB, Pawson T. Syk tyrosine kinase required for mouse viability and B-cell development. *Nature.* 1995;378(6554):303 - 6

194. Chan VWF MM, Soriano P, DeFranco AL, Lowell CA. Characterisation of the B lymphocyte populations in Lyn deficient mice and the role of Lyn in signal initiation and down-regulation. *Immunity*. 1997;7:69 - 81
195. Khan WN AF, Gerstein RM, Malynn BA, Larsson I, Rathbun G, Davidson L, Müller S, Kantor AB, Herzenberg LA, et al. Defective B cell development and function in Btk-deficient mice. *Immunity* 1995;3(3):283 - 9
196. Meade J, Fernandez C, Turner M. The tyrosine kinase Lyn is required for B cell development beyond the T1 stage in the spleen: rescue by over-expression of Bcl-2. *European J of Immunology*. 2002;32(4):1029-34.
197. Hibbs ML, Stanley E, Maglitta R, Dunn AR. Identification of a duplication of the mouse Lyn gene. *Gene*. 1995;156(2):175-81.
198. Saijo K SC, Su I, Karasuyama H, Lowell CA, Reth M, Adachi T, Patke A, Santana A, Tarakhovsky A. Essential role of Src-family protein tyrosine kinases in NF-[kappa]B activation during B cell development. *Nat Immunol* 2003;4(3).
199. Hibbs ML, Harder KW, Armes J, Kountouri N, Quilici C, Casagrande F, et al. Sustained Activation of Lyn Tyrosine Kinase In Vivo Leads to Autoimmunity. *J Exp Med*. 2002;196(12):1593-604.
200. Yang M KL, Hicks C, Chesterman CN, Chong BH. Identification of PDGF receptors on human megakaryocytes and megakaryocytic cell lines. *Thromb Haemost*. 1997;78(2).
201. Buhring HJ, Seiffert M, Bock TA, Scheduling S, Thiel A, Scheffold A, Kanz L, Brugger W. Expression of Novel Surface Antigens on Early Hematopoietic Cellsa. *Annals of the New York Academy of Sciences*. 1999;872(1):25-39.
202. Labouyrie E, Dubus P, Groppi A, Mahon FX, Ferrer J, Parrens M, et al. Expression of Neurotrophins and their Receptors in Human Bone Marrow. *Am J Path*. 1999;154(2):405-15.
203. Kaebisch A, Brokt S, Seay U, Lohmeyer J, Jaeger U, Pralle H. Expression of the nerve growth factor receptor c-TRK in human myeloid leukaemia cells. *Br J Haematol*. 1996;95(1):102-9.

204. Kaminski WE, Lindahl P, Lin NL, Broudy VC, Crosby JR, Hellström M, et al. Basis of hematopoietic defects in platelet-derived growth factor (PDGF)-B and PDGF β -receptor null mice. *Blood*. 2001;97(7):1990-8.
205. Turner N GR. Fibroblast growth factor signalling: from development to cancer. *Nat Rev Cancer* 2010;10(12):116 - 29
206. Palmer RH VE, Grabbe C, Hallberg B. Anaplastic lymphoma kinase: signalling in development and disease. *Biochem J* 2009;420 (3):345 - 61.
207. Mackarechtschian K, Hardin JD, Moore KA, Boast S, Goff SP, Lemischka IR. Targeted disruption of the *flk2/flt3* gene leads to deficiencies in primitive hematopoietic progenitors. *Immunity*. 1995;3(1):147-61.
208. Waskow C LK, Darrasse-Jeze G, Guermonprez P, Ginhoux F, Merad M, Shengalia T, Yao K, et al. The receptor tyrosine kinase Flt3 is required for dendritic cell development in peripheral lymphoid tissues. *Nat Immunol*. 2008;9(6):676 - 83
209. Lyman SD, Jacobsen SEW. c-kit Ligand and Flt3 Ligand: Stem/Progenitor Cell Factors With Overlapping Yet Distinct Activities. *Blood*. 1998;91(4):1101-34.
210. Selvaggi G, Novello S, Torri V, Leonardo E, De Giuli P, Borasio P, et al. Epidermal growth factor receptor overexpression correlates with a poor prognosis in completely resected non-small-cell lung cancer. *Annals of Oncology*. 2004;15(1):28-32.
211. Sok JC, Coppelli FM, Thomas SM, Lango MN, Xi S, Hunt JL, et al. Mutant Epidermal Growth Factor Receptor (EGFRvIII) Contributes to Head and Neck Cancer Growth and Resistance to EGFR Targeting. *Clin Cancer Res*. 2006;12(17):5064-73.
212. Werner H, Shen-Orr Z, Rauscher FJ, Morris JF, Roberts CT, LeRoith D. Inhibition of cellular proliferation by the Wilms' tumor suppressor WT1 is associated with suppression of insulin-like growth factor I receptor gene expression. *Mol Cell Biol*. 1995;15(7):3516-22.
213. Karnieli E, Werner H, Rauscher FJ, Benjamin LE, LeRoith D. The IGF-I Receptor Gene Promoter Is a Molecular Target for the Ewing's Sarcoma-Wilms' Tumor 1 Fusion Protein. *J Biol Chem*. 1996;271(32):19304-9.

214. Gerald WL, Rosai J, Ladanyi M. Characterization of the genomic breakpoint and chimeric transcripts in the EWS-WT1 gene fusion of desmoplastic small round cell tumor. *Proc Natl Acad Sci USA*.1995;92(4):1028-32.
215. De Brouwer S, De Preter K, Kumps C, Zabrocki P, Porcu M, Westerhout EM, et al. Meta-analysis of Neuroblastomas Reveals a Skewed ALK Mutation Spectrum in Tumors with MYCN Amplification. *Clin Cancer Res*.2010;16(17):4353-62.
216. Murugan AK, Xing M. Anaplastic Thyroid Cancers Harbor Novel Oncogenic Mutations of the ALK Gene. *Cancer Res*. 2011;71(13):4403-11.
217. Chen Y TJ, Choi, YL, Kato M, Ohira Miki, Sanada M, Wang L, Soda M, Kikuchi A, et al. Oncogenic mutations of ALK kinase in neuroblastoma. *Nature*. 2008;455(7215):971 - 4
218. Gu T-L, Tothova Z, Scheijen B, Griffin JD, Gilliland DG, Sternberg DW. NPM-ALK fusion kinase of anaplastic large-cell lymphoma regulates survival and proliferative signaling through modulation of FOXO3a. *Blood*. 2004;103(12):4622-9.
219. Li Y, Li Y, Yang T, Wei S, Wang J, Wang M, et al. Clinical Significance of EML4-ALK Fusion Gene and Association with EGFR and KRAS Gene Mutations in 208 Chinese Patients with Non-Small Cell Lung Cancer. *PLoS ONE*. 2013;8(1):e52093.
220. Yeoh E-J, Ross ME, Shurtleff SA, Williams WK, Patel D, Mahfouz R, et al. Classification, subtype discovery, and prediction of outcome in pediatric acute lymphoblastic leukemia by gene expression profiling. *Cancer Cell*. 2002;1(2):133-43.
221. Armstrong SA SJ, Silverman LB, Pieters R, den Boer M Minden MD, Sallan SE, Lander ES, Golub TR, Korsmeyer SJ. MLL translocations specify a distinct gene expression profile that distinguishes a unique leukemia. *Nat Genet*. 2002;30(1):41 - 7.
222. Mullighan CG, Zhang J, Harvey RC, Collins-Underwood JR, Schulman BA, Phillips LA, et al. JAK mutations in high-risk childhood acute lymphoblastic leukemia. *Proc Natl Acad Sci USA*.2009;106(23):9414-8.
223. Chiaretti S, Li X, Gentleman R, Vitale A, Wang KS, Mandelli F, et al. Gene Expression Profiles of B-lineage Adult Acute Lymphocytic Leukemia Reveal Genetic Patterns that Identify Lineage Derivation and Distinct Mechanisms of Transformation. *Clin Cancer Res*.2005;11(20):7209-19.

224. Van Etten RA. Disease Progression in a Murine Model of bcr/abl Leukemogenesis. *Leukemia & Lymphoma*. 1993;11(s1):239-42.
225. McLaughlin J CE, Witte ON. Alternative forms of the BCR-ABL oncogene have quantitatively different potencies for stimulation of immature lymphoid cells. *Mol Cell Biol* 1989;9(5):1866 - 74.
226. Li S, Ilaria RL, Million RP, Daley GQ, Van Etten RA. The P190, P210, and P230 Forms of the BCR/ABL Oncogene Induce a Similar Chronic Myeloid Leukemia-like Syndrome in Mice but Have Different Lymphoid Leukemogenic Activity. *J Exp Med*.1999;189(9):1399-412.
227. Voncken J, Kaartinen V, Pattengale P, Germeraad W, Groffen J, Heisterkamp N. BCR/ABL P210 and P190 cause distinct leukemia in transgenic mice. *Blood*. 1995;86(12):4603-11.
228. Neshat MS, Raitano AB, Wang H-G, Reed JC, Sawyers CL. The Survival Function of the Bcr-Abl Oncogene Is Mediated by Bad-Dependent and -Independent Pathways: Roles for Phosphatidylinositol 3-Kinase and Raf. *Mol Cell Biol*.2000;20(4):1179-86.
229. Shuai K HJ, Ten Hoeve J, Rao X, Sawyers CL Constitutive activation of STAT5 by the BCR-ABL oncogene in chronic myelogenous leukemia. *Oncogene* 1996;13(2):247 - 54.
230. Puil L LJ, Gish G, Mbamalu G, Bowtell D, Pelicci PG, Arlinghaus R, Pawson T. Bcr-Abl oncoproteins bind directly to activators of the Ras signalling pathway. *EMBO J*. 1994;13(4):764 - 73
231. Skorski T. BCR/ABL regulates response to DNA damage: the role in resistance to genotoxic treatment and in genomic instability. *Oncogene*. 2002;21(56):8591-604.
232. Danial NK RP. JAK-STAT signaling acitvated by Abl oncogenes. *Oncogene*. 2000;19(21):2523 - 31.
233. Vainchenker W DACS. JAKS in pathology: Role of Janus kinases in haematopoietic malignancies and immunodeficiencies. *Semin Cell Dev Biol*. 2008;19:385 - 93.
234. Sulong S CM, Minto M, Wilkins B, Hall A, Irving J. The V617F mutation in Jak2 is not found in childhood acute lymphoblastic leukaemia. *Br J Haematol*. 2005;130:964 - 5.

235. Meydan N GT, Dadi H, Shahar M, Arpaia E, Lapidot Z, Leeder JS, Freedman M, Cohen A, Gazit A, Levitzki A, Roifman CM. Inhibition of acute lymphoblastic leukaemia by a Jak-2 inhibitor. *Nature*. 1996;379(6566):645 - 8
236. Bercovich D, Ganmore I, Scott LM, Wainreb G, Birger Y, Elimelech A, et al. Mutations of JAK2 in acute lymphoblastic leukaemias associated with Down's syndrome. *Lancet*. 372(9648):1484-92.
237. Mullighan CG C-UJ, Phillips LA, Loudin MG, Liu W, Zhang J, Ma J, Coustan-Smith E, Harvey RC, Willman CL, Mikhail FM, Meyer J, Carroll AJ, Williams RT, Cheng J, Heerema NA, Basso G, Pession A, Pui CH, Raimondi SC, Hunger SP, Downing JR, Carroll WL, Rabin KR. Rearrangement of CRLF2 in B-progenitor- and Down syndrome-associated acute lymphoblastic leukemia. *Nat Genet*. 2009;41(11):1243 - 6
238. Hertzberg L, Vendramini E, Ganmore I, Cazzaniga G, Schmitz M, Chalker J, et al. Down syndrome acute lymphoblastic leukemia, a highly heterogeneous disease in which aberrant expression of CRLF2 is associated with mutated JAK2: a report from the International BFM Study Group. *Blood*. 2010;115(5):1006-17.
239. Malinge S, Ben-Abdelali R, Settegrana C, Radford-Weiss I, Debre M, Beldjord K, et al. Novel activating JAK2 mutation in a patient with Down syndrome and B-cell precursor acute lymphoblastic leukemia. *Blood*. 2007;109(5):2202-4.
240. Russell LJ, Capasso M, Vater I, Akasaka T, Bernard OA, Calasanz MJ, et al. Deregulated expression of cytokine receptor gene, CRLF2, is involved in lymphoid transformation in B-cell precursor acute lymphoblastic leukemia. *Blood*. 2009;114(13):2688-98.
241. Harvey RC, Mullighan CG, Chen I-M, Wharton W, Mikhail FM, Carroll AJ, et al. Rearrangement of CRLF2 is associated with mutation of JAK kinases, alteration of IKZF1, Hispanic/Latino ethnicity, and a poor outcome in pediatric B-progenitor acute lymphoblastic leukemia. *Blood*. 2010;115(26):5312-21.
242. Gaikwad A, Rye CL, Devidas M, Heerema NA, Carroll AJ, Izraeli S, et al. Prevalence and clinical correlates of JAK2 mutations in Down syndrome acute lymphoblastic leukaemia. *Br J Haematol*. 2009;144(6):930-2.

243. Yoda A, Yoda Y, Chiaretti S, Bar-Natan M, Mani K, Rodig SJ, et al. Functional screening identifies CRLF2 in precursor B-cell acute lymphoblastic leukemia. *Proc Natl Acad Sci USA*.2010;107(1):252-7.
244. Flex E, Petrangeli V, Stella L, Chiaretti S, Hornakova T, Knoops L, et al. Somaticly acquired JAK1 mutations in adult acute lymphoblastic leukemia. *J Exp Med*.2008;205(4):751-8.
245. Jeong EG, Kim MS, Nam HK, Min CK, Lee S, Chung YJ, et al. Somatic Mutations of JAK1 and JAK3 in Acute Leukemias and Solid Cancers. *Clin Cancer Res*.2008;14(12):3716-21.
246. Asnafi V, Le Noir S, Lhermitte L, Gardin C, Legrand F, Vallantin X, et al. JAK1 mutations are not frequent events in adult T-ALL: a GRAALL study. *Br J Haematol*.2010;148(1):178-9.
247. Dosil M WS, Lemischka IR. Mitogenic signalling and substrate specificity of the Flk2/Flt3 receptor tyrosine kinase in fibroblasts and interleukin 3-dependent hematopoietic cells. *Mol Cell Biol* 1993;13(10):6572 - 85.
248. Marchetto S FE, Beslu N, Aurran-Schleinitz T, Dubreuil P, Borg J-P, Birnbaum D, Rosnet O. SHC and SHIP phosphorylation and interaction in response to activation of the FLT3 receptor. *Leukemia*. 1999;13:1374 - 82
249. Rottapel R TC, Casteran N, Liu X, Birnbaum D, Pawson T, Dubreuil P. Substrate specificities and identification of a putative binding site for PI3K in the carboxy tail of the murine Flt3 receptor tyrosine kinase. *Oncogene*. 1994;9(6):1755 - 65.
250. Paulsson K, Horvat A, Strömbeck B, Nilsson F, Heldrup J, Behrendtz M, et al. Mutations of FLT3, NRAS, KRAS, and PTPN11 are frequent and possibly mutually exclusive in high hyperdiploid childhood acute lymphoblastic leukemia. *Genes, Chromosomes and Cancer*. 2008;47(1):26-33.
251. Nakao M YS, Iwai T, Kaneko H, Horiike S, Kashima K, Sonoda Y, Fujimoto T, Misawa S. Internal tandem duplication of the flt3 gene found in acute myeloid leukemia. *Leukemia*. 1996;10(12):1911 - 8

252. Stam RW, den Boer ML, Schneider P, Meier M, Beverloo HB, Pieters R. D-HPLC analysis of the entire FLT3 gene in MLL rearranged and hyperdiploid acute lymphoblastic leukemia. *Haematologica*. 2007;92(11):1565-8.
253. Weier HUG, Fung J, Lersch RA. Assignment of protooncogene MERTK (a.k.a. c-mer) to human chromosome 2q14.1 by in situ hybridization. *Cytogenet Cell Gen*. 1999;84(1-2):91-2.
254. Graham DK BG, Dawson TL, Stanford WL, Earp HS, Snodgrass HR. Cloning and developmental expression analysis of the murine c-mer tyrosine kinase. *Oncogene*. 1995;10(12):2349 - 59.
255. Graham DK SD, Joanne Kurtzberg et al. Ectopic Expression of the Proto-Oncogene Mer in Pediatric T-Cell Acute Lymphoblastic Leukemia. *Clin Cancer Res*. 2006;12:2662 - 9.
256. Graham DK DT, Mullaney DL, Snodgrass HR and Earp HS. Cloning and mRNA expression analysis of a novel human protooncogene, c-mer. *Cell Growth Differ*. 1994;5:647 - 57.
257. Chen J CK, Godowski PJ. Identification of Gas6 as ligand for Mer, a neural cell adhesion molecule related receptor implicated in cellular transformation. *Oncogene*. 1997;14(17):2033 - 9.
258. Guttridge KL LJ, Dawson TL, et al. Mer receptro tyrosine kinase signaling: Prevention of apoptosis and alteration of cytoskeletal architecture without stimulation or proliferation. *J Biol Chem*. 2002;277(22):24057 - 66.
259. Khan J, Bittner ML, Saal LH, Teichmann U, Azorsa DO, Gooden GC, et al. cDNA microarrays detect activation of a myogenic transcription program by the PAX3-FKHR fusion oncogene. *Proc Natl Acad Sci USA*. 1999;96(23):13264-9.
260. Wu CW LA, Chi CW, Lai CH, Huang CL, Lo SS, Lui WY, Lin WC. Clinical significance of AXL kinase family in gastric cancer. *Anticancer Res* 2002;22(2B):1071 - 8.
261. Linger RMA DD, Brandao L, Saczyn KK, Jacobsen KM, Liang X, Keating AK and Graham DK. Mer receptor tyrosine kinase is a novel therapeutic target in pediatric B-cell acute lymphoblastic leukemia. *Blood*. 2009;114(13):2678 - 87.

262. Keating AK SD, Sather S, Liang X, Nickoloff S, Anwar A, DeRyckere D, Hill K, Joung D, Sawczyn KK, Park J, Curran-Everett D, McGavaran L, Meltesen L, Gore L, Johnson GL and Graham DK. Lymphoblastic leukemia/lymphoma in mice overexpressing the Mer (MerTK) receptor tyrosine kinase. *Oncogene* 2006;25:6092 - 100.
263. Tyner JW, Deininger MW, Loriaux MM, Chang BH, Gotlib JR, Willis SG, et al. RNAi screen for rapid therapeutic target identification in leukemia patients. *Proc Natl Acad Sci USA*.2009;106(21):8695-700.
264. Valent A DG, Bernheim A. Mapping of the tyrosine kinase receptors trkA (NTRK1), trkB (NTRK2) and trkC(NTRK3) to human chromosomes 1q22, 9q22 and 15q25 by fluorescence in situ hybridization. *Eur J Hum Genet*. 1997;5(2):102 - 4.
265. Klein R S-SI, Smeyne RJ, Lira SA, Brambilla R, Bryant S, Zhang L, Snider WD, Barbacid M. Disruption of the neurotrophin-3 receptor gene trkC eliminates la muscle afferents and results in abnormal movements. *Nature* 1994;368(6468):249 - 51.
266. Meyer J RM, Schiedlmeier B, Kustikova O, Rudolph C, Kamino K, Neumann T, Yang M, Wahlers A, Fehse B, Reuther GW, Schlegelberger B, Ganser A, Baum C, Li Z. Remarkable leukemogenic potency and quality of a constitutively active neurotrophin receptor, deltaTrkA. *Leukemia*. 2007;21(10):2171 - 80.
267. Rhein M, Schwarzer A, Yang M, Kaefer V, Brugman M, Meyer J, et al. Leukemias induced by altered TRK-signaling are sensitive to mTOR inhibitors in preclinical models. *Ann Hematol*. 2011;90(3):283-92.
268. Li Z, Beutel G, Rhein M, Meyer J, Koenecke C, Neumann T, et al. High-affinity neurotrophin receptors and ligands promote leukemogenesis. *Blood*. 2009;113(9):2028-37.
269. Cooper CS PM, Blair DG, Tainsky MA, Huebner K, Croce CM, Vande Woude GF. Molecular cloning of a new transforming gene from a chemically transformed human cell line. *Nature*. 1984;311(5981):29-33.
270. Uehara Y, Minowa O, Mori C, Shiota K, Kuno J, Noda T, et al. Placental defect and embryonic lethality in mice lacking hepatocyte growth factor/scatter factor. *Nature*. 1995;373(6516):702-5.

271. Bladt F, Riethmacher D, Isenmann S, Aguzzi A, Birchmeier C. Essential role for the c-met receptor in the migration of myogenic precursor cells into the limb bud. *Nature*.1995;376(6543):768-71.
272. Schmidt C, Bladt F, Goedecke S, Brinkmann V, Zschiesche W, Sharpe M, et al. Scatter factor/hepatocyte growth factor is essential for liver development. *Nature*. 1995;373(6516):699-702.
273. Corso S, Migliore C, Ghiso E, De Rosa G, Comoglio PM, Giordano S. Silencing the MET oncogene leads to regression of experimental tumors and metastases. *Oncogene*. 2007;27(5):684-93.
274. Xiao G-H, Jeffers M, Bellacosa A, Mitsuuchi Y, Vande Woude GF, Testa JR. Anti-apoptotic signaling by hepatocyte growth factor/Met via the phosphatidylinositol 3-kinase/Akt and mitogen-activated protein kinase pathways. *Proc Natl Acad Sci USA*.2001;98(1):247-52.
275. Choi YL, Tsukasaki K, O'Neill MC, Yamada Y, Onimaru Y, Matsumoto K, et al. A genomic analysis of adult T-cell leukemia. *Oncogene*. 2006;26(8):1245-55.
276. Accordi B, Pillozzi S, Dell'Orto MC, Cazzaniga G, Arcangeli A, Kronnie Gt, et al. Hepatocyte Growth Factor Receptor c-MET Is Associated with FAS and When Activated Enhances Drug-induced Apoptosis in Pediatric B Acute Lymphoblastic Leukemia with TEL-AML1 Translocation. *J Biol Chem*.2007;282(40):29384-93.
277. Mullighan CG, Zhang J, Phillips LA, Pui C-H, Downing JR. Identification of Novel Recurring Mutations in Relapsed Acute Lymphoblastic Leukemia. *ASH Annual Meeting Abstracts*. 2009;114(22):703.
278. Zhang J, Mullighan CG, Harvey RC, Wu G, Chen X, Edmonson M, et al. Key pathways are frequently mutated in high-risk childhood acute lymphoblastic leukemia: a report from the Children's Oncology Group. *Blood*. 2011;118(11):3080-7.
279. Graux C, Cools J, Melotte C, Quentmeier H, Ferrando A, Levine R, et al. Fusion of NUP214 to ABL1 on amplified episomes in T-cell acute lymphoblastic leukemia. *Nat Genet*. 2004;36(10):1084-9.

280. Roberts KG, Morin RD, Zhang J, Hirst M, Harvey RC, Kasap C, et al. Novel Chromosomal Rearrangements and Sequence Mutations in High-Risk Ph-Like Acute Lymphoblastic Leukemia. *ASH Annual Meeting Abstracts*. 2011;118(21):67-.
281. Huusko P, Ponciano-Jackson D, Wolf M, Kiefer JA, Azorsa DO, Tuzmen S, et al. Nonsense-mediated decay microarray analysis identifies mutations of EPHB2 in human prostate cancer. *Nat Genet*. 2004;36(9):979-83.
282. Weinstein IB. Disorders in cell circuitry during multistage carcinogenesis: the role of homeostasis. *Carcinogenesis*. 2000;21(5):857-64.
283. Weinstein IB. Addiction to Oncogenes--the Achilles Heal of Cancer. *Science*. 2002;297(5578):63-4.
284. Moody SE, Sarkisian CJ, Hahn KT, Gunther EJ, Pickup S, Dugan KD, et al. Conditional activation of Neu in the mammary epithelium of transgenic mice results in reversible pulmonary metastasis. *Cancer Cell*. 2002;2(6):451-61.
285. Slamon DJ, Leyland-Jones B, Shak S, Fuchs H, Paton V, Bajamonde A, et al. Use of Chemotherapy plus a Monoclonal Antibody against HER2 for Metastatic Breast Cancer That Overexpresses HER2. *N Eng J Med*. 2001;344(11):783-92.
286. Moody SE, Perez D, Pan T-c, Sarkisian CJ, Portocarrero CP, Sterner CJ, et al. The transcriptional repressor Snail promotes mammary tumor recurrence. *Cancer Cell*. 2005;8(3):197-209.
287. Gotink K, Verheul HW. Anti-angiogenic tyrosine kinase inhibitors: what is their mechanism of action? *Angiogenesis*. 2010;13(1):1-14.
288. Zhang J, Yang PL, Gray NS. Targeting cancer with small molecule kinase inhibitors. *Nat Rev Cancer*. 2009;9(1):28-39.
289. Liu Y, Gray NS. Rational design of inhibitors that bind to inactive kinase conformations. *Nat Chem Biol*. 2006;2(7):358-64.
290. Kwak EL, Sordella R, Bell DW, Godin-Heymann N, Okimoto RA, Brannigan BW, et al. Irreversible inhibitors of the EGF receptor may circumvent acquired resistance to gefitinib. *Proc Nat Acad Sci USA*. 2005;102(21):7665-70.

291. Shah NP, Nicoll JM, Nagar B, Gorre ME, Paquette RL, Kuriyan J, et al. Multiple BCR-ABL kinase domain mutations confer polyclonal resistance to the tyrosine kinase inhibitor imatinib (STI571) in chronic phase and blast crisis chronic myeloid leukemia. *Cancer Cell*. 2002;2(2):117-25.
292. Branford S, Rudzki Z, Walsh S, Grigg A, Arthur C, Taylor K, et al. High frequency of point mutations clustered within the adenosine triphosphate-binding region of BCR/ABL in patients with chronic myeloid leukemia or Ph-positive acute lymphoblastic leukemia who develop imatinib (STI571) resistance. *Blood*. 2002;99(9):3472-5.
293. Karapetis CS, Khambata-Ford S, Jonker DJ, O'Callaghan CJ, Tu D, Tebbutt NC, et al. K-ras Mutations and Benefit from Cetuximab in Advanced Colorectal Cancer. *N Eng J Med*. 2008;359(17):1757-65.
294. Stommel JM KA, Ying H, Nabioullin R, Ponugoti AH, Wiedemeyer R, Stegh AH, Bradner JE, Ligon KL, Brennan C, Chin L, DePinho RA. Coactivation of receptor tyrosine kinases affects the response of tumor cells to targeted therapies. *Science*. 2007;318(5848):287 - 90.
295. Xu AM, Huang PH. Receptor Tyrosine Kinase Coactivation Networks in Cancer. *Cancer Res*. 2010;70(10):3857-60.
296. Yakes FM, Chen J, Tan J, Yamaguchi K, Shi Y, Yu P, et al. Cabozantinib (XL184), a Novel MET and VEGFR2 Inhibitor, Simultaneously Suppresses Metastasis, Angiogenesis, and Tumor Growth. *Mol Cancer Ther*. 2011;10(12):2298-308.
297. Qian F, Engst S, Yamaguchi K, Yu P, Won K-A, Mock L, et al. Inhibition of Tumor Cell Growth, Invasion, and Metastasis by EXEL-2880 (XL880, GSK1363089), a Novel Inhibitor of HGF and VEGF Receptor Tyrosine Kinases. *Cancer Res*. 2009;69(20):8009-16.
298. Schultz KR, Bowman WP, Aledo A, Slayton WB, Sather H, Devidas M, et al. Improved Early Event-Free Survival With Imatinib in Philadelphia Chromosome-Positive Acute Lymphoblastic Leukemia: A Children's Oncology Group Study. *J Clin Oncol*. 2009;27(31):5175-81.
299. Biondi A, Schrappe M, Di Lorenzo P, Castor A, Lucchini G, Gandemer V, et al. Efficacy and Safety of Imatinib on Top of BFM-Like Chemotherapy in Pediatric Patients

- with Ph⁺/BCR-ABL⁺ Acute Lymphoblastic Leukemia (Ph⁺ALL). the EsPhALL Study. ASH Annual Meeting Abstracts. 2011;118(21):873.
300. Hurwitz R, Hozier J, Lebien T, Minowada J, Gajl-Peczalska K, Kubonishi I, et al. Characterization of a leukemic cell line of the pre-B phenotype. *Int J Cancer*. 1979;23(2):174-80.
 301. Matsuo Y DH. Establishment and characterization of human B cell precursor-leukemia cell lines. *Leuk Res* 1998;22:567 - 79
 302. Rosenfeld C, Goutner A, Choquet C, Venuat AM, Kayibanda B, Pico JL, et al. Phenotypic characterisation of a unique non-T, non-B acute lymphoblastic leukaemia cell line. *Nature*. 1977;267(5614):841-3.
 303. Dhut S GB, Chaplin T, Young BD. Establishment of a lymphoblastoid cell line, SD-1, expressing the p190 bcr-abl chimaeric protein. *Leukemia*. 1991;5(1):49 - 55.
 304. Naumovski L, Morgan R, Hecht F, Link MP, Glader BE, Smith SD. Philadelphia Chromosome-positive Acute Lymphoblastic Leukemia Cell Lines without Classical Breakpoint Cluster Region Rearrangement. *Cancer Res*. 1988;48(10):2876-9.
 305. Okabe M, Matsushima S, Morioka M, Kobayashi M, Abe S, Sakurada K, et al. Establishment and characterization of a cell line, TOM-1, derived from a patient with Philadelphia chromosome-positive acute lymphocytic leukemia. *Blood*. 1987;69(4):990-8.
 306. Norman MR, Thompson EB. Characterization of a Glucocorticoid-sensitive Human Lymphoid Cell Line. *Cancer Res*. 1977;37(10):3785-91.
 307. Asou H, Tashiro S, Hamamoto K, Otsuji A, Kita K, Kamada N. Establishment of a human acute myeloid leukemia cell line (Kasumi-1) with 8;21 chromosome translocation. *Blood*. 1991;77(9):2031-6.
 308. Gallagher R, Collins S, Trujillo J, McCredie K, Ahearn M, Tsai S, et al. Characterization of the continuous, differentiating myeloid cell line (HL-60) from a patient with acute promyelocytic leukemia. *Blood*. 1979;54(3):713-33.
 309. Lozzio C, Lozzio B. Human chronic myelogenous leukemia cell-line with positive Philadelphia chromosome. *Blood*. 1975;45(3):321-34.

310. Kamesaki H, Fukuhara S, Tatsumi E, Uchino H, Yamabe H, Miwa H, et al. Cytochemical, immunologic, chromosomal, and molecular genetic analysis of a novel cell line derived from Hodgkin's disease. *Blood*. 1986;68(1):285-92.
311. Schaadt M, Diehl M, Stein H, Fonatsch C, Kirchner HH. Two neoplastic cell lines with unique features derived from Hodgkin's disease. *Int J Cancer*. 1980;26(6):723-31.
312. Soule HD, Vazquez J, Long A, Albert S, Brennan M. A Human Cell Line From a Pleural Effusion Derived From a Breast Carcinoma. *J Natl Cancer Inst*. 1973;51(5):1409-16.
313. Bartek J, Bartkova J, Kyprianou N, Lalani EN, Staskova Z, Shearer M, et al. Efficient immortalization of luminal epithelial cells from human mammary gland by introduction of simian virus 40 large tumor antigen with a recombinant retrovirus. *Proc Natl Acad Sci USA*. 1991;88(9):3520-4.
314. Biedler JL, Helson L, Spengler BA. Morphology and Growth, Tumorigenicity, and Cytogenetics of Human Neuroblastoma Cells in Continuous Culture. *Cancer Res*. 1973;33(11):2643-52.
315. Weston VJ, Austen B, Wei W, Marston E, Alvi A, Lawson S, et al. Apoptotic resistance to ionizing radiation in pediatric B-precursor acute lymphoblastic leukemia frequently involves increased NF- κ B survival pathway signaling. *Blood*. 2004;104(5):1465-73.
316. Nielsen M, Kaltoft K, Nordahl M, Röpke C, Geisler C, Mustelin T, et al. Constitutive activation of a slowly migrating isoform of Stat3 in mycosis fungoides: Tyrphostin AG490 inhibits Stat3 activation and growth of mycosis fungoides tumor cell lines. *Proc Natl Acad Sci USA*. 1997;94(13):6764-9.
317. Changelian PS, Moshinsky D, Kuhn CF, Flanagan ME, Munchhof MJ, Harris TM, et al. The specificity of JAK3 kinase inhibitors. *Blood*. 2008;111(4):2155-7.
318. Sabbatini P, Rowand JL, Groy A, Korenchuk S, Liu Q, Atkins C, et al. Antitumor Activity of GSK1904529A, a Small-molecule Inhibitor of the Insulin-like Growth Factor-I Receptor Tyrosine Kinase. *Clin Cancer Res*. 2009;15(9):3058-67.

319. Garcia-Echeverria C, Pearson MA, Marti A, Meyer T, Mestan J, Zimmermann J, et al. In vivo antitumor activity of NVP-AEW541 A novel, potent, and selective inhibitor of the IGF-IR kinase. *Cancer Cell*. 2004;5(3):231-9.
320. Li D, Ambrogio L, Shimamura T, Kubo S, Takahashi M, Chirieac LR, et al. BIBW2992, an irreversible EGFR/HER2 inhibitor highly effective in preclinical lung cancer models. *Oncogene*. 2008;27(34):4702-11.
321. Smaill JB, Rewcastle GW, Loo JA, Greis KD, Chan OH, Reyner EL, et al. Tyrosine Kinase Inhibitors. 17. Irreversible Inhibitors of the Epidermal Growth Factor Receptor: 4-(Phenylamino)quinazoline- and 4-(Phenylamino)pyrido[3,2-d]pyrimidine-6-acrylamides Bearing Additional Solubilizing Functions. *J Med Chem*. 2000;43(7):1380-97.
322. Green TP, Fennell M, Whittaker R, Curwen J, Jacobs V, Allen J, et al. Preclinical anticancer activity of the potent, oral Src inhibitor AZD0530. *Molecular Oncology*. 2009;3(3):248-61.
323. Remsing Rix LL, Rix U, Colinge J, Hantschel O, Bennett KL, Stranzl T, et al. Global target profile of the kinase inhibitor bosutinib in primary chronic myeloid leukemia cells. *Leukemia*. 2008;23(3):477-85.
324. Lombardo LJ, Lee FY, Chen P, Norris D, Barrish JC, Behnia K, et al. Discovery of N-(2-Chloro-6-methyl-phenyl)-2-(6-(4-(2-hydroxyethyl)-piperazin-1-yl)-2-methylpyrimidin-4-ylamino)thiazole-5-carboxamide (BMS-354825), a Dual Src/Abl Kinase Inhibitor with Potent Antitumor Activity in Preclinical Assays. *J Med Chem*. 2004;47(27):6658-61.
325. Rix U, Hantschel O, Dürnberger G, Remsing Rix LL, Planyavsky M, Fernbach NV, et al. Chemical proteomic profiles of the BCR-ABL inhibitors imatinib, nilotinib, and dasatinib reveal novel kinase and nonkinase targets. *Blood*. 2007;110(12):4055-63.
326. Dubreuil P, Letard S, Ciufolini M, Gros L, Humbert M, Castéran N, et al. Masitinib (AB1010), a Potent and Selective Tyrosine Kinase Inhibitor Targeting KIT. *PLoS ONE*. 2009;4(9):e7258.
327. Timofeevski S, McTigue M, Ryan K, Cui J, Zou H, Zhu J, et al. Enzymatic characterization of c-Met receptor tyrosine kinase oncogenic mutants and kinetic studies with aminopyridine and triazolopyrazine inhibitors. *Biochemistry*. 2009;48(23):5339-49.

328. Zou HY, Li Q, Lee JH, Arango ME, McDonnell SR, Yamazaki S, et al. An Orally Available Small-Molecule Inhibitor of c-Met, PF-2341066, Exhibits Cyto-reductive Antitumor Efficacy through Antiproliferative and Antiangiogenic Mechanisms. *Cancer Res.* 2007;67(9):4408-17.
329. Carpinelli P, Ceruti R, Giorgini ML, Cappella P, Gianellini L, Croci V, et al. PHA-739358, a potent inhibitor of Aurora kinases with a selective target inhibition profile relevant to cancer. *Mol Cancer Ther.* 2007;6(12):3158-68.
330. Hodous BL, Geuns-Meyer SD, Hughes PE, Albrecht BK, Bellon S, Bready J, et al. Evolution of a Highly Selective and Potent 2-(Pyridin-2-yl)-1,3,5-triazine Tie-2 Kinase Inhibitor. *J Med Chem.* 2007;50(4):611-26.
331. Hu-Lowe DD, Zou HY, Grazzini ML, Hallin ME, Wickman GR, Amundson K, et al. Nonclinical Antiangiogenesis and Antitumor Activities of Axitinib (AG-013736), an Oral, Potent, and Selective Inhibitor of Vascular Endothelial Growth Factor Receptor Tyrosine Kinases 1, 2, 3. *Clin Cancer Res.* 2008;14(22):7272-83.
332. Cai Z-W, Zhang Y, Borzilleri RM, Qian L, Barbosa S, Wei D, et al. Discovery of Brivanib Alaninate ((S)-((R)-1-(4-(4-Fluoro-2-methyl-1H-indol-5-yloxy)-5-methylpyrrolo[2,1-f][1,2,4]triazin-6-yloxy)propan-2-yl)2-aminopropanoate), A Novel Prodrug of Dual Vascular Endothelial Growth Factor Receptor-2 and Fibroblast Growth Factor Receptor-1 Kinase Inhibitor (BMS-540215). *J Med Chem.* 2008;51(6):1976-80.
333. Wedge SR, Kendrew J, Hennequin LF, Valentine PJ, Barry ST, Brave SR, et al. AZD2171: A Highly Potent, Orally Bioavailable, Vascular Endothelial Growth Factor Receptor-2 Tyrosine Kinase Inhibitor for the Treatment of Cancer. *Cancer Res.* 2005;65(10):4389-400.
334. Polverino A, Coxon A, Starnes C, Diaz Z, DeMelfi T, Wang L, et al. AMG 706, an Oral, Multikinase Inhibitor that Selectively Targets Vascular Endothelial Growth Factor, Platelet-Derived Growth Factor, and Kit Receptors, Potently Inhibits Angiogenesis and Induces Regression in Tumor Xenografts. *Cancer Res.* 2006;66(17):8715-21.
335. Sonpavde G, Hutson T. Pazopanib: A novel multitargeted tyrosine kinase inhibitor. *Curr Oncol Rep.* 2007;9(2):115-9.

336. Carlomagno F, Vitagliano D, Guida T, Ciardiello F, Tortora G, Vecchio G, et al. ZD6474, an Orally Available Inhibitor of KDR Tyrosine Kinase Activity, Efficiently Blocks Oncogenic RET Kinases. *Cancer Res.* 2002;62(24):7284-90.
337. Wood JM, Bold G, Buchdunger E, Cozens R, Ferrari S, Frei J, et al. PTK787/ZK 222584, a Novel and Potent Inhibitor of Vascular Endothelial Growth Factor Receptor Tyrosine Kinases, Impairs Vascular Endothelial Growth Factor-induced Responses and Tumor Growth after Oral Administration. *Cancer Res.* 2000;60(8):2178-89.
338. Shankar DB, Li J, Tapang P, Owen McCall J, Pease LJ, Dai Y, et al. ABT-869, a multitargeted receptor tyrosine kinase inhibitor: inhibition of FLT3 phosphorylation and signaling in acute myeloid leukemia. *Blood.* 2007;109(8):3400-8.
339. Kulimova E, Oelmann E, Bisping G, Kienast J, Mesters RM, Schwäble J, et al. Growth inhibition and induction of apoptosis in acute myeloid leukemia cells by new indolinone derivatives targeting fibroblast growth factor, platelet-derived growth factor, and vascular endothelial growth factor receptors. *Mol Cancer Ther.* 2006;5(12):3105-12.
340. Strock CJ, Park J-I, Rosen M, Dionne C, Ruggeri B, Jones-Bolin S, et al. CEP-701 and CEP-751 Inhibit Constitutively Activated RET Tyrosine Kinase Activity and Block Medullary Thyroid Carcinoma Cell Growth. *Cancer Res.* 2003;63(17):5559-63.
341. Smith BD, Levis M, Beran M, Giles F, Kantarjian H, Berg K, et al. Single-agent CEP-701, a novel FLT3 inhibitor, shows biologic and clinical activity in patients with relapsed or refractory acute myeloid leukemia. *Blood.* 2004;103(10):3669-76.
342. Trudel S, Li ZH, Wei E, Wiesmann M, Chang H, Chen C, et al. CHIR-258, a novel, multitargeted tyrosine kinase inhibitor for the potential treatment of t(4;14) multiple myeloma. *Blood.* 2005;105(7):2941-8.
343. Galnick AV MJ, Kim S, Hood TL, Li N, et al. Identification of NVP-TAE684, a potent, selective, and efficacious inhibitor of NPM-ALK. *Proc Natl Acad Sci U S A.* 2007;104(1):270 - 5.
344. Wilhelm SM, Carter C, Tang L, Wilkie D, McNabola A, Rong H, et al. BAY 43-9006 Exhibits Broad Spectrum Oral Antitumor Activity and Targets the RAF/MEK/ERK Pathway

- and Receptor Tyrosine Kinases Involved in Tumor Progression and Angiogenesis. *Cancer Res.* 2004;64(19):7099-109.
345. Roskoski Jr R. Sunitinib: A VEGF and PDGF receptor protein kinase and angiogenesis inhibitor. *Biochem Biophys Res Commun.* 2007;356(2):323-8.
346. Pandey A, Volkots DL, Seroogy JM, Rose JW, Yu J-C, Lambing JL, et al. Identification of Orally Active, Potent, and Selective 4-Piperazinylquinazolines as Antagonists of the Platelet-Derived Growth Factor Receptor Tyrosine Kinase Family. *J Med Chem.* 2002;45(17):3772-93.
347. Harrington EA BA, Moore J, Rasmussen RK, Ajose-Adeogun AO, Nakayama T, Graham JA, Demur C, et al. VX-680, a potent and selective small-molecule inhibitor of the Aurora kinases, suppresses tumor growth in vivo. *Nat Med* 2004;10(3):262 - 7.
348. Karaman MW, Herrgard S, Treiber DK, Gallant P, Atteridge CE, Campbell BT, et al. A quantitative analysis of kinase inhibitor selectivity. *Nat Biotech.* 2008;26(1):127-32.
349. Severson WE, Shindo N, Sosa M, Fletcher T, White EL, Ananthan S, et al. Development and Validation of a High-Throughput Screen for Inhibitors of SARS CoV and Its Application in Screening of a 100,000-Compound Library. *J Biomol Screen.* 2007;12(1):33-40.
350. Sims J, Plattner R. MTT assays cannot be utilized to study the effects of STI571/Gleevec on the viability of solid tumor cell lines. *Cancer Chemother Pharmacol.* 2009;64(3):629-33.
351. Chou TC, Talalay P. Quantitative analysis of dose-effect relationships: the combined effects of multiple drugs or enzyme inhibitors. *Adv Enzyme Regul* 1984;22:27 - 55.
352. Chou TC. The median-effect principle and the combination index for quantization of synergism and antagonism. In *Synergism and antagonism in chemotherapy* (Chou, T-C and Rideout, DC, eds). 1991:61 - 102
353. Shinomiya T, Li XK, Amemiya H, Suzuki S. An immunosuppressive agent, FTY720, increases intracellular concentration of calcium ion and induces apoptosis in HL-60. *Immunology.* 1997;91(4):594-600.

354. Wyllie AH. Glucocorticoid-induced thymocyte apoptosis is associated with endogenous endonuclease activation. *Nature*. 1980;284(5756):555-6.
355. Koopman G, Reutelingsperger C, Kuijten G, Keehnen R, Pals S, van Oers M. Annexin V for flow cytometric detection of phosphatidylserine expression on B cells undergoing apoptosis. *Blood*. 1994;84(5):1415-20.
356. Odintsova E, Sugiura T, Berditchevski F. Attenuation of EGF receptor signaling by a metastasis suppressor, the tetraspanin CD82/KAI-1. *Current Biology*. 2000;10(16):1009-12.
357. Weston VJ, Stankovic T, McMullan DJ, Drayson M, Ley BE, Lawson S, Hill FGH. An unrelated cytogenetic karyotype and intra-lineage shift at relapse of an aggressive paediatric B-precursor ALL. *Leukemia*. 2002;16(11):2337 - 9
358. Anderson K, Lutz C, van Delft FW, Bateman CM, Guo Y, Colman SM, et al. Genetic variegation of clonal architecture and propagating cells in leukaemia. *Nature*. 2011;469(7330):356-61.
359. Tamborini E, Viridis E, Negri T, Orsenigo M, Brich S, Conca E, et al. Analysis of receptor tyrosine kinases (RTKs) and downstream pathways in chordomas. *Neuro-Oncology*. 2010;12(8):776-89.
360. Ou W-B, Hubert C, Corson JM, Bueno R, Flynn DL, Sugarbaker DJ, Fletcher JA. Targeted Inhibition of Multiple Receptor Tyrosine Kinases in Mesothelioma. *Neoplasia*. 2011;13(1):12 - 22.
361. Dewaele B, Maggiani F, Floris G, Ampe M, Vanspauwen V, Wozniak A, et al. Frequent activation of EGFR in advanced chordomas. *Clinical Sarcoma Research*. 2011;1(1):4.
362. Ter Elst A, Diks SH, Kampen KR, Hoogerbrugge PM, Ruijtenbeek R, Boender PJ, et al. Identification of new possible targets for leukemia treatment by kinase activity profiling. *Leukemia & Lymphoma*. 2010;52(1):122-30.
363. Hong C-C, Lay J-D, Huang J-S, Cheng A-L, Tang J-L, Lin M-T, et al. Receptor tyrosine kinase AXL is induced by chemotherapy drugs and overexpression of AXL confers drug resistance in acute myeloid leukemia. *Cancer letters*. 2008;268(2):314-24.

364. Miyazaki T, Kato H, Fukuchi M, Nakajima M, Kuwano H. EphA2 overexpression correlates with poor prognosis in esophageal squamous cell carcinoma. *Int J Cancer*. 2003;103(5):657-63.
365. Kamat AA, Coffey D, Merritt WM, Nugent E, Urbauer D, Lin YG, et al. EphA2 overexpression is associated with lack of hormone receptor expression and poor outcome in endometrial cancer. *Cancer*. 2009;115(12):2684-92.
366. Halford MM, Armes J, Buchert M, Meskenaite V, Grail D, Hibbs ML, et al. Ryk-deficient mice exhibit craniofacial defects associated with perturbed Eph receptor crosstalk. *Nat Genet*. 2000;25(4):414-8.
367. Henkemeyer M, Orioli D, Henderson JT, Saxton TM, Roder J, Pawson T, et al. Nuk Controls Pathfinding of Commissural Axons in the Mammalian Central Nervous System. *Cell*. 1996;86(1):35-46.
368. Kullander K, Mather NK, Diella F, Dottori M, Boyd AW, Klein R. Kinase-Dependent and Kinase-Independent Functions of EphA4 Receptors in Major Axon Tract Formation In Vivo. *Neuron*. 2001;29(1):73-84.
369. Jubb AM, Zhong F, Bheddah S, Grabsch HI, Frantz GD, Mueller W, et al. EphB2 is a Prognostic Factor in Colorectal Cancer. *Clin Cancer Res*. 2005;11(14):5181-7.
370. Udayakumar D, Zhang G, Ji Z, Njauw CN, Mroz P, Tsao H. EphA2 is a critical oncogene in melanoma. *Oncogene*. 2011;30(50):4921-9.
371. Taketani T, Taki T, Sugita K, Furuichi Y, Ishii E, Hanada R, et al. FLT3 mutations in the activation loop of tyrosine kinase domain are frequently found in infant ALL with MLL rearrangements and pediatric ALL with hyperdiploidy. *Blood*. 2004;103(3):1085-8.
372. Meshinchi S, Stirewalt DL, Alonzo TA, Boggon TJ, Gerbing RB, Rocnik JL, et al. Structural and numerical variation of FLT3/ITD in pediatric AML. *Blood*. 2008;111(10):4930-3.
373. Ross ME, Zhou X, Song G, Shurtleff SA, Girtman K, Williams WK, et al. Classification of pediatric acute lymphoblastic leukemia by gene expression profiling. *Blood*. 2003;102(8):2951-9.

374. Tsai L, White L, Raines E, Ross R, Smith R, Cushley W, et al. Expression of platelet-derived growth factor and its receptors by two pre-B acute lymphocytic leukemia cell lines. *Blood*. 1994;83(1):51-5.
375. O'Brien SG, Guilhot F, Larson RA, Gathmann I, Baccarani M, Cervantes F, et al. Imatinib Compared with Interferon and Low-Dose Cytarabine for Newly Diagnosed Chronic-Phase Chronic Myeloid Leukemia. *N Eng J Med*. 2003;348(11):994-1004.
376. Spiekermann K, Faber F, Voswinckel R, Hiddemann W. The protein tyrosine kinase inhibitor SU5614 inhibits VEGF-induced endothelial cell sprouting and induces growth arrest and apoptosis by inhibition of c-kit in AML cells. *Exp Hematol*. 2002;30(7):767-73.
377. Hu S, Niu H, Minkin P, Orwick S, Shimada A, Inaba H, et al. Comparison of antitumor effects of multitargeted tyrosine kinase inhibitors in acute myelogenous leukemia. *Mol Cancer Ther*. 2008;7(5):1110-20.
378. Savitskiy VP, Shman TV, Potapnev MP. Comparative measurement of spontaneous apoptosis in pediatric acute leukemia by different techniques. *Cytometry Part B: Clinical Cytometry*. 2003;56B(1):16-22.
379. Alley MC, Scudiero DA, Monks A, Hursey ML, Czerwinski MJ, Fine DL, et al. Feasibility of Drug Screening with Panels of Human Tumor Cell Lines Using a Microculture Tetrazolium Assay. *Cancer Res*. 1988;48(3):589-601.
380. Shoemaker RH. The NCI60 human tumour cell line anticancer drug screen. *Nat Rev Cancer*. 2006;6(10):813-23.
381. Messina JP LD. Effects of 2-mercaptoethanol and buthionine sulfoximine on cystine metabolism by and proliferation of mitogen-stimulated human and mouse lymphocytes. *Int J Immunopharm*. 1992;14(7):1221 - 34.
382. Stegmaier K, Corsello SM, Ross KN, Wong JS, DeAngelo DJ, Golub TR. Gefitinib induces myeloid differentiation of acute myeloid leukemia. *Blood*. 2005;106(8):2841-8.
383. Wakeling AE, Guy SP, Woodburn JR, Ashton SE, Curry BJ, Barker AJ, et al. ZD1839 (Iressa): An Orally Active Inhibitor of Epidermal Growth Factor Signaling with Potential for Cancer Therapy. *Cancer Res*. 2002;62(20):5749-54.

384. Wong TW, Lee FY, Yu C, Luo FR, Oppenheimer S, Zhang H, et al. Preclinical Antitumor Activity of BMS-599626, a pan-HER Kinase Inhibitor That Inhibits HER1/HER2 Homodimer and Heterodimer Signaling. *Clin Cancer Res.*2006;12(20):6186-93.
385. Nordigården A, Zetterblad J, Trinks C, Gréen H, Eliasson P, Druid P, et al. Irreversible pan-ERBB inhibitor canertinib elicits anti-leukaemic effects and induces the regression of FLT3-ITD transformed cells in mice. *Br J Haematol.* 2011;155(2):198-208.
386. Trinks C, Djerf EA, Hallbeck A-L, Jönsson J-I, Walz TM. The pan-ErbB receptor tyrosine kinase inhibitor canertinib induces ErbB-independent apoptosis in human leukemia (HL-60 and U-937) cells. *Biochem Biophys Res Commun.*2010;393(1):6-10.
387. Quentmeier H, Eberth S, Romani J, Zaborski M, Drexler H. BCR-ABL1-independent PI3Kinase activation causing imatinib-resistance. *J Hematol Oncol.* 2011;4(1):6.
388. Hu Y, Liu Y, Pelletier S, Buchdunger E, Warmuth M, Fabbro D, et al. Requirement of Src kinases Lyn, Hck and Fgr for BCR-ABL1-induced B-lymphoblastic leukemia but not chronic myeloid leukemia. *Nat Genet.* 2004;36(5):453-61.
389. Hu Y, Swerdlow S, Duffy TM, Weinmann R, Lee FY, Li S. Targeting multiple kinase pathways in leukemic progenitors and stem cells is essential for improved treatment of Ph+ leukemia in mice. *Proc Natl Acad Sci USA.*2006;103(45):16870-5.
390. Kumar R, Knick VB, Rudolph SK, Johnson JH, Crosby RM, Crouthamel M-C, et al. Pharmacokinetic-pharmacodynamic correlation from mouse to human with pazopanib, a multikinase angiogenesis inhibitor with potent antitumor and antiangiogenic activity. *Mol Cancer Ther.*2007;6(7):2012-21.
391. Chevallier P, Robillard N, Wuilleme-Toumi S, Mechinaud F, Harousseau J, Avet-Loiseau H. Overexpression of Her2/neu is observed in one third of adult acute lymphoblastic leukemia patients and is associated with chemoresistance in these patients. *Haematologica.* 2004;89(11):1399-401.
392. Buhring H, Sures I, Jallal B, Weiss F, Busch F, Ludwig W, et al. The receptor tyrosine kinase p185HER2 is expressed on a subset of B- lymphoid blasts from patients with acute lymphoblastic leukemia and chronic myelogenous leukemia. *Blood.* 1995;86(5):1916-23.

393. Stone DJ, Marine S, Majercak J, Ray WJ, Espeseth A, Simon A, et al. High-Throughput Screening by RNA Interference: Control of Two Distinct Types of Variance. *Cell Cycle*. 2007;6(8):898-901.
394. Birg F, Courcoul M, Rosnet O, Bardin F, Pebusque M, Marchetto S, et al. Expression of the FMS/KIT-like gene FLT3 in human acute leukemias of the myeloid and lymphoid lineages. *Blood*. 1992;80(10):2584-93.
395. Carow C, Levenstein M, Kaufmann S, Chen J, Amin S, Rockwell P, et al. Expression of the hematopoietic growth factor receptor FLT3 (STK- 1/Flk2) in human leukemias. *Blood*. 1996;87(3):1089-96.
396. Yamamoto Y, Kiyoi H, Nakano Y, Suzuki R, Kodera Y, Miyawaki S, et al. Activating mutation of D835 within the activation loop of FLT3 in human hematologic malignancies. *Blood*. 2001;97(8):2434-9.
397. Brown P, Levis M, Shurtleff S, Campana D, Downing J, Small D. FLT3 inhibition selectively kills childhood acute lymphoblastic leukemia cells with high levels of FLT3 expression. *Blood*. 2005;105(2):812-20.
398. Stam RW, den Boer ML, Schneider P, Nollau P, Horstmann M, Beverloo HB, et al. Targeting FLT3 in primary MLL-gene-rearranged infant acute lymphoblastic leukemia. *Blood*. 2005;106(7):2484-90.
399. Armstrong SA, Mabon ME, Silverman LB, Li A, Gribben JG, Fox EA, et al. FLT3 mutations in childhood acute lymphoblastic leukemia. *Blood*. 2004;103(9):3544-6.
400. Armstrong SA, Kung AL, Mabon ME, Silverman LB, Stam RW, Den Boer ML, et al. Inhibition of FLT3 in MLL: Validation of a therapeutic target identified by gene expression based classification. *Cancer Cell*. 2003;3(2):173-83.
401. Kelly LM, Yu J-C, Boulton CL, Apatira M, Li J, Sullivan CM, et al. CT53518, a novel selective FLT3 antagonist for the treatment of acute myelogenous leukemia (AML). *Cancer Cell*. 2002;1(5):421-32.
402. Trinks C, Severinsson EA, Holmlund B, Gréen A, Gréen H, Jönsson J-I, et al. The pan-ErbB tyrosine kinase inhibitor canertinib induces caspase-mediated cell death in human T-cell leukemia (Jurkat) cells. *Biochem Biophys Res Commun*. 2011;410(3):422-7.

403. Allen LF, Eiseman IA, Fry DW, Lenehan PF. CI-1033, an irreversible pan-erbB receptor inhibitor and its potential application for the treatment of breast cancer. *Semin Oncol.* 2003;30, Supplement 16(0):65-78.
404. Fabian MA, Biggs WH, Treiber DK, Atteridge CE, Azimioara MD, Benedetti MG, et al. A small molecule-kinase interaction map for clinical kinase inhibitors. *Nat Biotech.* 2005;23(3):329-36.
405. Mourali J, Bénard A, Lourenço FC, Monnet C, Greenland C, Moog-Lutz C, et al. Anaplastic Lymphoma Kinase Is a Dependence Receptor Whose Proapoptotic Functions Are Activated by Caspase Cleavage. *Mol Cell Biol.* 2006;26(16):6209-22.
406. Houghton PJ, Morton CL, Gorlick R, Kolb EA, Keir ST, Reynolds CP, et al. Initial testing of a monoclonal antibody (IMC-A12) against IGF-1R by the pediatric preclinical testing program. *Ped Blood Cancer .* 2010;54(7):921-6.
407. Kolb EA, Gorlick R, Houghton PJ, Morton CL, Lock R, Carol H, et al. Initial testing (stage 1) of a monoclonal antibody (SCH 717454) against the IGF-1 receptor by the pediatric preclinical testing program. *Ped Blood Cancer .* 2008;50(6):1190-7.
408. Medyouf H, Gusscott S, Wang H, Tseng J-C, Wai C, Nemirovsky O, et al. High-level IGF1R expression is required for leukemia-initiating cell activity in T-ALL and is supported by Notch signaling. *J Exp Med.* 2011;208(9):1809-22.
409. Leclerc G, Leclerc G, Fu G, Barredo J. AMPK-induced activation of Akt by AICAR is mediated by IGF-1R dependent and independent mechanisms in acute lymphoblastic leukemia. *J Mol Signal.* 2010;5(1):15.
410. Maris JM, Morton CL, Gorlick R, Kolb EA, Lock R, Carol H, et al. Initial testing of the aurora kinase a inhibitor MLN8237 by the Pediatric Preclinical Testing Program (PPTP). *Ped Blood Cancer .* 2010;55(1):26-34.
411. Sloane DA, Trikić MZ, Chu MLH, Lamers MBAC, Mason CS, Mueller I, et al. Drug-Resistant Aurora A Mutants for Cellular Target Validation of the Small Molecule Kinase Inhibitors MLN8054 and MLN8237. *ACS Chemical Biology.* 2010;5(6):563-76.

412. Angevin E, Lopez-Martin JA, Lin C-C, Gschwend JE, Harzstark A, Castellano D, et al. Phase I Study of Dovitinib (TKI258), an Oral FGFR, VEGFR, and PDGFR Inhibitor, in Advanced or Metastatic Renal Cell Carcinoma. *Clin Cancer Res.*2013;19(5):1257-68.
413. Eder JP, Shapiro GI, Appleman LJ, Zhu AX, Miles D, Keer H, et al. A Phase I Study of Foretinib, a Multi-Targeted Inhibitor of c-Met and Vascular Endothelial Growth Factor Receptor 2. *Clin Cancer Res.*2010;16(13):3507-16.
414. Chen C-T, Kim H, Liska D, Gao S, Christensen JG, Weiser MR. MET Activation Mediates Resistance to Lapatinib Inhibition of HER2-Amplified Gastric Cancer Cells. *Mol Cancer Ther.*2012;11(3):660-9.
415. Lee SH, Lopes de Menezes D, Vora J, Harris A, Ye H, Nordahl L, et al. In vivo Target Modulation and Biological Activity of CHIR-258, a Multitargeted Growth Factor Receptor Kinase Inhibitor, in Colon Cancer Models. *Clin Cancer Res.*2005;11(10):3633-41.
416. Andre F, Bachelot T, Campone M, Dalenc F, Perez-Garcia J, Hurvitz S, et al. A multicenter, open-label phase II trial of dovitinib, an FGFR1 inhibitor, in FGFR1 amplified and non-amplified metastatic breast cancer. *ASCO Meeting Abstracts.* 2011;29:508
417. Kim KB, Chesney J, Robinson D, Gardner H, Shi MM, Kirkwood JM. Phase I/II and Pharmacodynamic Study of Dovitinib (TKI258), an Inhibitor of Fibroblast Growth Factor Receptors and VEGF Receptors, in Patients with Advanced Melanoma. *Clin Cancer Res.*2011;17(23):7451-61.
418. Angevin E, Ravaud A, Castellano D, Lin C, Gschwend J, Harzstark A, et al., editors. A phase II study of dovitinib (TKI258), an FGFR-and VEGFR-inhibitor, in patients with advanced or metastatic renal cell cancer (mRCC)2011.
419. Seiwert T, Sarantopoulos J, Kallender H, McCallum S, Keer H, Blumenschein G, Jr. Phase II trial of single-agent foretinib (GSK1363089) in patients with recurrent or metastatic squamous cell carcinoma of the head and neck. *Invest New Drugs.* 2013;31(2):417-24.
420. Rayson D LS, Chia SKL, Potvin KR, Dent S, et al. A phase II study of foretinib in triple-negative, recurrent/metastatic breast cancer: NCIC CTG trial IND.197 (NCT01147484). *J Clin Oncol (Meeting Abstracts).* 2012;30(15 (May 20 Supplement)).

421. Bentley AM, Normand G, Hoyt J, King RW. Distinct Sequence Elements of Cyclin B1 Promote Localization to Chromatin, Centrosomes, and Kinetochores during Mitosis. *Mol Biol Cell*.2007;18(12):4847-58.
422. Bachmann PS, Gorman R, Papa RA, Bardell JE, Ford J, Kees UR, et al. Divergent Mechanisms of Glucocorticoid Resistance in Experimental Models of Pediatric Acute Lymphoblastic Leukemia. *Cancer Res*. 2007;67(9):4482-90.
423. Liem NLM, Papa RA, Milross CG, Schmid MA, Tajbakhsh M, Choi S, et al. Characterization of childhood acute lymphoblastic leukemia xenograft models for the preclinical evaluation of new therapies. *Blood*. 2004;103(10):3905-14.
424. Houghton PJ, Morton CL, Tucker C, Payne D, Favours E, Cole C, et al. The pediatric preclinical testing program: Description of models and early testing results. *Ped Blood Cancer* . 2007;49(7):928-40.
425. Dufies M, Jacquel A, Robert G, Cluzeau T, Puissant A, Fenouille N, et al. Mechanism of action of the multikinase inhibitor Foretinib. *Cell Cycle*. 2011;10(23):4138-48.
426. Huynh H, Ong R, Soo K. Foretinib demonstrates anti-tumor activity and improves overall survival in preclinical models of hepatocellular carcinoma. *Angiogenesis*. 2012;15(1):59-70.
427. Zillhardt M, Park S-M, Romero IL, Sawada K, Montag A, Krausz T, et al. Foretinib (GSK1363089), an Orally Available Multikinase Inhibitor of c-Met and VEGFR-2, Blocks Proliferation, Induces Anoikis, and Impairs Ovarian Cancer Metastasis. *Clin Cancer Res*.2011;17(12):4042-51.
428. Huynh H, Chow PKH, Tai WM, Choo SP, Chung AYP, Ong HS, et al. Dovitinib demonstrates antitumor and antimetastatic activities in xenograft models of hepatocellular carcinoma. *J Hepatol*. 2012;56(3):595-601.
429. Suzuki M, Hosaka Y, Matsushima H, Goto T, Kitamura T, Kawabe K. Butyrolactone I induces cyclin B1 and causes G2/M arrest and skipping of mitosis in human prostate cell lines. *Cancer letters*. 1999;138(1):121-30.
430. Innocente SA, Abrahamson JLA, Cogswell JP, Lee JM. p53 regulates a G2 checkpoint through cyclin B1. *Proc Natl Acad Sci USA*.1999;96(5):2147-52.

431. Charrier-Savournin FB, Château M-T, Gire V, Sedivy J, Piette J, Dulić V. p21-Mediated Nuclear Retention of Cyclin B1-Cdk1 in Response to Genotoxic Stress. *Mol Biol Cell*. 2004;15(9):3965-76.
432. Azab AK, Azab F, Quang P, Maiso P, Sacco A, Ngo HT, et al. FGFR3 Is Overexpressed Waldenström Macroglobulinemia and Its Inhibition by Dovitinib Induces Apoptosis and Overcomes Stroma-Induced Proliferation. *Clin Cancer Res*. 2011;17(13):4389-99.
433. Odgerel T, Kikuchi J, Wada T, Shimizu R, Futaki K, Kano Y, et al. The FLT3 inhibitor PKC412 exerts differential cell cycle effects on leukemic cells depending on the presence of FLT3 mutations. *Oncogene*. 2007;27(22):3102-10.
434. Lopes de Menezes DE, Peng J, Garrett EN, Louie SG, Lee SH, Wiesmann M, et al. CHIR-258: A Potent Inhibitor of FLT3 Kinase in Experimental Tumor Xenograft Models of Human Acute Myelogenous Leukemia. *Clin Cancer Res*. 2005;11(14):5281-91.
435. Martins AS, Mackintosh C, Martín DH, Campos M, Hernández T, Ordóñez J-L, et al. Insulin-Like Growth Factor I Receptor Pathway Inhibition by ADW742, Alone or in Combination with Imatinib, Doxorubicin, or Vincristine, Is a Novel Therapeutic Approach in Ewing Tumor. *Clin Cancer Res*. 2006;12(11):3532-40.
436. Mitsiades CS, Mitsiades NS, McMullan CJ, Poulaki V, Shringarpure R, Akiyama M, et al. Inhibition of the insulin-like growth factor receptor-1 tyrosine kinase activity as a therapeutic strategy for multiple myeloma, other hematologic malignancies, and solid tumors. *Cancer Cell*. 2004;5(3):221-30.
437. Erlacher M, Michalak EM, Kelly PN, Labi V, Niederegger H, Coultas L, et al. BH3-only proteins Puma and Bim are rate-limiting for γ -radiation- and glucocorticoid-induced apoptosis of lymphoid cells in vivo. *Blood*. 2005;106(13):4131-8.
438. Parker C, Waters R, Leighton C, Hancock J, Sutton R, Moorman AV, et al. Effect of mitoxantrone on outcome of children with first relapse of acute lymphoblastic leukaemia (ALL R3): an open-label randomised trial. *Lancet* 376(9757):2009-17.

439. Yang B, Papoian T. Tyrosine kinase inhibitor (TKI)-induced cardiotoxicity: approaches to narrow the gaps between preclinical safety evaluation and clinical outcome. *J Appl Toxicol*. 2012;32(12):945-51.
440. Brown P, Piloto O, Levis M, Shurtleff S, Campana D, Downing J, et al. FLT3-Targeted Therapy Selectively Kills MLL-Rearranged Infant and Childhood ALL Blasts In Vitro and in Vivo. *ASH Annual Meeting Abstracts*. 2004;104(11):686.
441. Knapper S, Mills KI, Gilkes AF, Austin SJ, Walsh V, Burnett AK. The effects of lestaurtinib (CEP701) and PKC412 on primary AML blasts: the induction of cytotoxicity varies with dependence on FLT3 signaling in both FLT3-mutated and wild-type cases. *Blood*. 2006;108(10):3494-503.
442. Loh ML ZJ, Harvey RC, Roberts K, Payne - Turner D, Huining K, et al. Tyrosine kinome sequencing of pediatric acute lymphoblastic leukemia: a report from the Children's Oncology Group TARGET Project. *Blood*. 2013 121(3):485 - 8.
443. Keir ST, Maris JM, Lock R, Kolb EA, Gorlick R, Carol H, et al. Initial testing (stage 1) of the multi-targeted kinase inhibitor sorafenib by the pediatric preclinical testing program. *Ped Blood Cancer*. 2010;55(6):1126-33.

8.1 Abstract Blood (ASH Annual Meeting Abstracts) 2011; 118

Tyrosine Kinase Inhibitor Screen Identifies the Multikinase Inhibitor, Foretinib, As a Sensitiser of Treatment-resistant B-Precursor ALL to Core Chemotherapeutic Agents

Shaun R Wilson, MBChB, MRCPCH^{*1}, Victoria J Weston, PhD^{*2}, Tatjana Stankovic, MD, PhD^{*2} and Pamela R Kearns, BSc, MBBCh, MRCP, PhD²

¹ Paediatric Oncology, Birmingham Children's Hospital, Birmingham, United Kingdom,

² School of Cancer Sciences, University of Birmingham, Birmingham, United Kingdom

Abstract 1509

Acute lymphoblastic leukaemia (ALL) is the most frequent malignancy in childhood with resistance or relapse occurring in up to 20% of patients. The precise mechanisms of resistance to conventional therapy leading to relapse have not been elucidated. Deregulation of tyrosine kinases (TKs) have been implicated in resistant solid tumours and the of aetiology haemopoietic tumours, Philadelphia – chromosome positive ALL (Ph+ ALL), FLT3 in MLL+ infant ALL and FLT3-ITD subset in acute myeloid leukaemia. The role of TK inhibitors (TKIs) has not been extensively investigated in non-Ph + ALL.

We screened 5 B-cell precursor ALL cell lines and 20 primary samples with a library of 34 TKIs. Nalm 6 (t(5;12)), Nalm 17 (normal karyotype), REH (t(12;21)), SD1 and Sup15 (Ph+ ALL) and primary cells were tested at 1µM and 10µM and alterations in cell viability assessed with the Promega CellTiter-Glo assay. A drug was considered to be effective if it induced >50% reduction in cell viability at 1µM.

While we demonstrated significant heterogeneity in response to many of the TKIs, we observed reduction in viability to lestaurtinib (FLT3/JAK2), dovitinib (FLT3/FGFR/PDGFR/VEGFR) and bosutinib (Abl/Src) in all cell lines. Compared with Nalm 6 and Nalm 17 which only exhibited sensitivity to these 3 TKIs, REH demonstrated additional sensitivity to crizotinib (ALK/Met) and the quinazoline pan-EGFR inhibitors, afatinib and canertinib. The Ph+ cell lines SupB15 and SD1 responded to the highest number of TKIs, 12 and 14 respectively. These included the expected Bcr/Abl and Aurora kinase inhibitors. Activity of the putative PDGFR/VEGFR TKIs axitinib, linifanib, vargatef and also foretinib (MET/VEGFR2/FLT3) appeared limited to Ph+ cell lines.

The cell lines, REH and SD-1, which are resistant to ionizing radiation–induced apoptosis, were selectively inhibited by both the quinazolines. Baseline mRNA expression of the ErbB family was present in all cell lines and therefore did not correlate with response.

TKIs inducing the greatest reduction in cell viability across the cell lines were those that target class III/IV/V RTKs. Although all cell lines expressed FLT3 mRNA, reduction in cell viability was not universally induced by the specific FLT3 inhibitor tandutinib at doses of up to 10µM. As observed in previous studies, the level of mRNA transcript did not predict or directly correlate with the response to TKI.

A panel of 20 primary ALL samples, representative of common biological features, were screened. We found no correlation between cytogenetics, age, white cell count, post – induction MRD status and response to TKI groups or individual inhibitor. Only 5/20 did not respond to any of the tested TKIs. Lestaurtinib, dovitinib and foretinib reduced cell viability in 7/20 primary ALLs. In addition,

canertinib reduced cell viability in 6/20 primary ALL samples, afatinib and TAE684 (ALK/MET) both in 5/20 ALL samples respectively and vargatef in 4/20 samples.

Based on our preliminary screen, the multikinase inhibitor foretinib was selected as one of several promising candidates for further pre-clinical testing. Recent adult phase 1 solid tumor trials have shown limited toxicity and good bioavailability.

Foretinib inhibited leukaemia proliferation with LD₅₀ in nanomolar and low micromolar range; SupB15 (333nM ±49), SD-1 (381nM ±239), Nalm 17 (484nM ±124), REH (689nM ±92) and Nalm 6 (1.84µM ±0.25). Annexin/PI staining, DNA fragmentation and PARP protein cleavage confirmed that the mechanism of cell death was apoptosis.

We next investigated whether foretinib could sensitise ALL cell lines to dexamethasone, cytarabine, methotrexate, doxorubicin or mitoxantrone. Drug interactions were modelled using the Biosoft Calcsyn software package. We found that the addition of foretinib resulted in predominantly synergistic interactions in all cell lines (CI<1). The most striking example of synergism was in the dexamethasone-resistant cell line, REH. Addition of a sub-LD₅₀ dose of foretinib led to >50% reduction in cell viability when combined with 1nM dexamethasone compared with no response at 10µM dexamethasone alone.

Overall these data support further exploration of TKIs as potential therapeutic agents in childhood ALL. Specifically, we are currently investigating the direct anti-leukemic activity of foretinib in childhood ALL and its synergistic activity with dexamethasone *in vivo* using our NOG mouse primograft model for ALL.

Disclosures: No relevant conflicts of interest to declare.

8.2 Abstract Pediatric Blood and Cancer (2012); 59 (6): O136

TYROSINE KINASE INHIBITOR SCREEN OF B – CELL PRECURSOR ALL IDENTIFIES THE MULTIKINASE INHIBITOR, DOVITINIB, AS A CANDIDATE FOR THE SENSITISATION OF TREATMENT-RESISTANT TUMOURS TO CORE CHEMOTHERAPIES

Shaun Wilson^{1,2}, Victoria Weston¹, Tatjana Stankovic¹, Pamela Kearns^{1,2}

¹School of Cancer Sciences, University of Birmingham; ²Paediatric Oncology, Birmingham Children's Hospital, Birmingham, United Kingdom

Purpose: Deregulation of tyrosine kinases (TKs) has been implicated in high risk non-Philadelphia chromosome positive ALL. This project investigated the role of TK inhibitors (TKIs) in childhood ALL.

Methods: We screened 5 pre – B ALL cell lines and a panel of 20 primary samples representative of common biological features for sensitivity to a library of 33 TKIs. Active compounds were defined as reducing cell viability >50% at 1 mM with a concomitant dose - dependent reduction at 10 mM.

Results: Significant heterogeneity in sensitivity was observed in the panel of leukaemia cells. No correlation was evident between response to TKIs and current clinical or biological stratification parameters in the primary cell panel. In both cell lines and primary cells, categories of TKIs were most effective: (i) the FLT3/PDGFR/VEGFR multikinase inhibitors (vargatef, lestaurtinib, dovitinib, foretinib), (ii) the irreversible pan – EGFR quinazoline inhibitors (canertinib, afatinib) and (iii) dual Met/ALK inhibitors (NVPTAE684, crizotinib). As observed in previous studies, the expression of a putative target at mRNA level did not predict or directly correlate with the response to a TKI. Based on our preliminary screen, the multikinase inhibitor dovitinib was selected as one of several promising candidates for further pre-clinical testing. Dovitinib inhibited leukaemia proliferation with IC₅₀ in nanomolar range (0.19–0.84 mM) in cell lines. Cell cycle analysis revealed dovitinib induced cytostasis and cell death in the cell lines. PARP protein cleavage confirmed that the mechanism of cell death was by apoptosis. Co-incubation with dovitinib sensitised ALL cell lines to dexamethasone and doxorubicin, with predominantly synergistic drug interactions.

Conclusion: Overall these data support further exploration of TKIs as potential therapeutic agents in childhood ALL. We are currently investigating the direct anti-leukaemic activity of dovitinib in childhood ALL in vivo using our NOG mouse primograft model for ALL.